INSULAR SHELVES AS A TOOL FOR RECONSTRUCTING THE EVOLUTION OF VOLCANIC ISLANDS

Presentata da: Alessandro Ricchi

Coordinatore Dottorato

Prof. Giulio Viola

Supervisore

Prof.ssa Claudia Romagnoli

Co-supervisori

Dott. Daniele Casalbore

Dott. Rui Quartau

ABSTRACT

The erosion by waves, accomplished at different elevations due to glacio-eustatic sea-level fluctuations and islands' vertical movements, carves the flanks of volcanic islands resulting in the formation of insular shelves, features long known in literature since the early paper of Menard (1983). However, a systematic study of their morphometric parameters and evolution has seldom been carried out. This Ph.D project, based on high-resolution multibeam bathymetric data and seismic reflection profiles collected in the last decades by the University of Bologna, University of Rome "La Sapienza", CNR-IGAG Rome and by the Hydrographic Institute of the Portuguese Navy, explores the geomorphologic and structural features of the shelves surrounding the volcanic islands of Salina, Lipari and Vulcano in the Central Aeolian Archipelago and Santa Maria in the Azores Archipelago, respectively. The main aim is to increment our knowledge regarding the processes that influence the formation and the evolution of insular shelves and how these features might help us to better constraint the volcanic history of such islands. The study of insular shelves helps to improve the evolutionary models of the studied volcanic islands, which were previously developed only from the knowledge of the onshore geology. The information derived from the measured morphometric parameters (mainly the shelf width and the erosive edge depth) were integrated with field studies, allowing to infer, in some cases, the possible location of their earlier evolutionary stages, as well as to improve the overall geological evolution of studied volcanic islands.

In the Central Aeolian sector, we thus document the occurrence of presently submerged and largely dismantled volcanic edifices predating the oldest complexes located onshore. Unlike the youngest volcanic edifices, surrounded by narrow shelves and mostly vertically stable or slightly uplifting, the older complexes experienced subsidence. By using the insular shelves and the raised marine terraces previously found on the flanks of Salina and Lipari as tracers of relative sea-level changes, we then quantified the pattern and rates of vertical movements affecting the islands since their formation. The estimated subsidence rate, active before the Last Interglacial, has been adopted as a relative dating tool, attesting an early emergence of the islands. The shift from subsidence to uplift has been possibly related to a major geodynamic change occurred at regional scale.

At Santa Maria we adopted the same integrated approach to relate the morphologic characteristics of the shelf with the geology onshore. The submerged marine terraces found offshore have been related with those exposed subaerially on the western portion of the island, and we investigated a possible correlation between the formation of the terraces, the known sea-level changes and the islands' vertical mobility. We thus were able to constrain the age of the subaerial and submarine terraces, which was previously unknown, and to better reconstruct the vertical crustal movements affecting the island in the last million years. This study also allowed us to better understand which factors, among the intensity of marine erosion, eustatic and relative sea level changes and the composition and morphology of the shelf, controlled the distribution of the marine terraces. Overall, the findings of this study in different volcanic islands have been compared in order to provide a more detailed picture of how the processes affecting the insular shelves influence their formation and development.

CONTENTS

4

1. INTRODUCTION

1.1 Overview of the research activity

Several authors (Ablay and Hurlimann, 2000; Mitchell et al. 2003, 2012; Chiocci and Orlando, 2004; Le Friant et al., 2004; Llanes et al., 2009; Quartau et al., 2010, 2012, 2014; 2015b; Romagnoli, 2013; Quartau and Mitchell, 2013; Casalbore et al., 2015, 2016a) stressed the importance of studying the submerged portion of volcanic islands, often representing their (almost unknown) early stages of development. Wave erosion shapes their morphology during glacial-interglacial sea-level fluctuations, creating low-gradient erosive surfaces, developed from the coastline down to the shelf edge, known as insular shelves. Their present-day setting is considered the result of a continuous balance between constructive and destructive processes (Menard, 1983; 1986). Insular shelves have been recognized as important tools to reconstruct the evolution and vertical mobility trends of volcanic islands (Quartau et al., 2010, 2014; Romagnoli, 2013). However, the qualitative analysis of the shelf morphology allows only speculating about the possible earlier manifestation of volcanism. To better define the insular shelf development and relate the submerged portion of the island with its onshore portions, we adopted a "quantitative approach", based on the measure of morphometric parameters, such as the shelf width and the erosive shelf edge depth.

This thesis is the result of a Ph.D project carried out at the University of Bologna in collaboration with University of Rome "Sapienza" and CNR-IGAG of Rome and the Hydrographic Institute of the Portuguese Navy. It focuses on the distribution and morphological features of insular shelves in the Aeolian and Azores Archipelagos and the factors that might influence their development. The dataset is based on recently acquired high-resolution seismic profiles and multibeam bathymetry collected in the shallow water portions around Salina, Lipari and Vulcano islands (Central Aeolian archipelago, Tyrrhenian Sea) and Santa Maria island (Azores archipelago, Atlantic Ocean).

1.2 Objectives

The study of the submarine portions of volcanic islands has been integrated with the results of onshore field studies carried out by volcanologists. This integrated approach, already successfully applied in some volcanic ocean islands (e.g., Coombs et al., 2004; Llanes et al., 2009; Masson et al., 2008; Leat et al., 2010; Quartau et al., 2010, 2014; Lebas et al., 2011; Le Friant et al., 2011; Mitchell et al., 2012; Romagnoli, 2013), allowed us to correlate onshore and offshore features wherever possible, and to enlarge the knowledge on the overall evolution of volcanic edifices, with particular regards to their earlier evolutionary stages.

The Central Aeolian archipelago has been investigated in the first part of the work. Its relatively young islands (< 267 Ka, Forni et al., 2013) are surrounded by insular shelves that represent the perfect site to understand the complex relationships between islands vertical movements and sea-level fluctuation during the Late Quaternary. The morphology of their insular shelves were also used to improve the knowledge of the evolution of these islands.

The second part of the thesis is represented by the island of Santa Maria in the Azores Archipelago, which offered the opportunity to investigate the evolution of insular shelves and Plio-Quaternary marine terraces in a different geodynamic/oceanographic setting. Moreover, being the island c. 6 Ma old, a comparison of how the erosive processes act at different time scales has been carried out.

The research activity was carried out pursuing the objectives summarized below:

- Understand how the depth of the insular shelf edge varies around the islands and whether it reflects the sea-level depth during glacial/interglacial periods or it is controlled by local and/or regional vertical movements.
- Compare the shelves morphometric parameters for islands located in different geodynamic and marine settings (Mediterranean Sea and Atlantic Ocean) in order to discriminate among the different controlling factors (wave climate, sedimentation rate, sea-level changes, physiography of the margin, vertical mobility due to volcanic activity, etc.) driving their evolution.
- Better constraint the evolution of volcanic islands and their history of vertical movements, focusing on the earlier stages of development.

1.3 Thesis structure

In order to pursue the proposed objectives, the thesis structure reflects the workflow followed by the research activity:

Chapter 2 provides a general overview of the literature regarding the formation and evolution of insular shelves. The state of the art of the research is presented in 2.1, while the following sections outline the influence of sea-level changes on shelves evolution (2.2) and the mechanism driving the sediments distribution on the shelf (2.3).

Information regarding the acquisition and processing of the dataset used in this study is given in **chapter 3**. Moreover, this chapter introduces the methodology used to measure the morphometric parameters of the shelves and associated uncertainties. A more detailed description of the methods used to calculate the vertical mobility trends is, instead, presented in the manuscripts III and V.

In **chapter 4** the geographical and geodynamic settings of the Aeolian and Azores Archipelagos are briefly introduced and, in particular, the geological history of the Central Aeolian islands and Santa Maria Island are presented, in order to provide a general overview of the study areas.

In **chapter 5** the morphological characteristics of the shelves around Salina Island have been integrated with the onshore geology and used as proxies for reconstructing the development of the several volcanic complexes that compose the island (section 5.1, Manuscript I). By exploiting the same dataset, we provide insights on the relative sea-level changes experienced by Salina in the last 20 ka, on the base of the distribution, depth range and inner geometry of the sedimentary bodies (named "Submarine Depositional Terraces", SDT) lying on the shelf (section 5.2, Manuscript II). The contribution of regional/local uplift/subsidence on the vertical mobility trend of Salina is

6

also computed and discussed (section 5.3, Manuscript III) by comparing the information provided by subaerial (marine terraces and notches) and submerged (shelf edge depth, submerged terraces) markers with published sea-level curves. Moreover, we discussed the possible mechanism driving the subsidence/uplift trend of the island.

In *chapter 6* the approach adopted for Salina was applied to study the morphological characteristics of the insular shelves of Lipari and Vulcano islands, stressing similarities or differences with respect to Salina Island. The information provided in this section will be further developed in the future, and related manuscripts will be submitted to peer reviewed journals. The island of Lipari has similar sea-level markers to Salina, therefore the vertical behavior of the various volcanic complexes forming Lipari is discussed and compared with nearby Salina.

In *chapter 7* the shelf width and the depth of its edge around Santa Maria Island were consistently related with the onshore geology and were used as proxies to update the evolutionary model of the island. Moreover, we investigated the complex interplay between sedimentation, mass-wasting and tectonics. This chapter is part of a manuscript (Manuscript IV) that is going to be submitted for publication.

Chapter 8 concerns the vertical mobility trend of Santa Maria Island through the study of subaerial and submerged marine terraces. In Manuscript V we deal with the complex interplay between glacio-eustatic sea-level fluctuations and the island vertical motion trends. In this fashion, we tried to correlate the formation of different subaerial and submerged terraces with known sea-level stands, with the aim of providing a relative age for the formation of such terraces, understand which factors controlled their formation and preservation and better constraint the island uplift.

Chapter 9 deals with the comparison of studied insular shelves in the Aeolian Archipelago with those on the volcanic island of Santa Maria, in different oceanographic and volcanic settings, discussing how different factors may play a variable role in these contexts.

Finally, *chapter 10* presents the conclusions and a brief overview of possible future research.

The following articles report the results of this work according to the aim and objectives of the Ph.D project:

- Manuscript I
Romagnoli C, Casalbore D, Ricchi A, Lucchi F, Quartau R, Bosman A, Tranne CA, Chiocci FL. 2018. ***Morpho-bathymetric and seismo-stratigraphic analysis of the insular shelf of Salina (Aeolian archipelago) to unveil its Late-Quaternary geological evolution***. Mar. Geol. 395: 133–151. http://dx.doi.org/10.1016/j.margeo.2017.10.003.

- Manuscript II
Casalbore D, Romagnoli C, Adami C, Bosman A, Falese F, Ricchi A, Chiocci FL. 2018. ***Submarine Depositional Terraces at Salina Island (Southern Tyrrhenian Sea) and Implications on the Late-Quaternary Evolution of the Insular Shelf***. Geosciences 2018 8- 20; DOI:10.3390/geosciences 8010020.

- Manuscript III

Lucchi F, Ricchi A, Romagnoli C, Casalbore D, Quartau R. *Late-Quaternary paleo sea-level geomorphological tracers of opposite vertical movements at Salina volcanic island (Aeolian Arc)*. Submitted to Earth Surface Processes and Landforms, under revision.

- Manuscript IV

Ricchi A, Quartau R, Ramalho R, Romagnoli C, Casalbore D. *The interplay between volcanic, erosional, depositional, tectonic and mass-wasting processes: new insights from the study of Santa Maria Island insular shelf.* In preparation.

- Manuscript V

Ricchi A, Quartau R, Ramalho R, Romagnoli C, Casalbore D, Ventura da Cruz J, Fradique C, Vinhas A. 2018. *Marine terrace development on reefless volcanic islands: new insights from high-resolution geophysical data offshore Santa Maria Island (Azores Archipelago).* Mar. Geol. 406: 42-56; https://doi.org/10.1016/j.margeo.2018.09.002.

2. INSULAR SHELVES

2.1 State of the art

Volcanic islands have been defined as "*highly productive sea mounts that have grown above the sea-level*" (Schmidt & Schmincke, 2000) as the early surtseyan volcanic activity changes to more stable strombolian/hawaiian eruption and allows a submarine volcano to emerge above sea level. The growth and decay of volcanic islands is due to a combination of several processes, such as the age of the underline lithosphere (Parsons & Sclater, 1977), surface and subsurface loading (Menard 1973; McNutt & Menard, 1978; Scott & Rotondo, 1983; Schmidt & Schmincke, 2000; Ali et al., 2003), redistribution of volume due to erosion and landsliding (Rees et al., 1993; Filmer et al., 1994; Schmincke, 2004) and hotspot swell dynamics (Menard, 1973; Detrick & Crough, 1978; McNutt, 1988; Sleep, 1990; Morgan et al., 1995).

Although volcanic islands are in the order of some thousands all around the world, the evolutionary stages that leads to their formation are similar and relatively well known. Generally, the early stages of development are characterized by vigorous volcanic activity, during which islands grow above sea level by volcanic construction occurring faster than the effects of destructive geological processes. The latter prevail during long periods of quiescence. However, in the long term, as the island get older, the erosive processes become predominant (Schmincke et al., 1995; Schmincke, 2004).

Among several simultaneous and/or alternating geological processes (including crustal vertical movements and sea-level fluctuations) acting during thousands to millions of years, wave erosion is one of the most important in shaping the present day morphology of islands. It carves useful geomorphic indicators on the flanks of volcanic islands, such as coastal notches, marine terraces and shore platforms in coastal areas, and insular shelves on submerged flanks (Quartau et al., 2010, 2012; Ramalho et al., 2013). In particular, the imprint of these physical processes in shallow water areas may provide valuable information for reconstructing the geologic history of volcanic islands (Fletcher et al., 2008; Kennedy et al., 2002; Mitchell et al., 2008, 2012; Quartau et al., 2010, 2012, 2014; Quartau and Mitchell, 2013; Babonneau et al., 2013; Chiocci et al., 2013; Romagnoli, 2013; Casalbore et al., 2015).

A significant technological advance of multibeam bathymetric and seismic reflection acquisition systems occurred in the last decades. This allowed to obtain high-resolution geophysical data that can be exploited to characterize with very good detail morphological features underwater (Krastel et al., 2001; Bosman et al., 2015). Studies performed worldwide allowed recognizing insular shelves around volcanic islands in various geodynamic settings. In the open sea, researchers have described shelves in Hawaii (Clague and Moore, 2002; Fletcher et al., 2008), Canaries (Ablay & Hurlimann, 2000; Mitchell et al., 2003; Llanes et al., 2009), Azores (Quartau et al., 2010), Surtsey (Romagnoli & Jakobsson, 2015), Montserrat (Le Friant et al., 2004) and South Sandwich islands (Leat et al., 2010). In the Mediterranean Sea, shelves have been described in the Aeolian Islands (Romagnoli, 2013), Pontine Archipelago (Chiocci and Orlando, 2004), Linosa (Romagnoli, 2004) and Pantelleria (Calarco, 2011) islands.

The initiation of an insular shelf starts when the intense volcanic activity that characterizes the early stages of growth of these islands progressively wanes, allowing marine erosion to carve the flanks of the island (Menard 1983). During stillstands wave erosion essentially works at a constant level, carving a shore platform. In response to subsequent glacial-interglacial sea-level oscillations, the mechanical wave erosion operating in the intertidal zone migrates landward and seaward, turning the shore platform into an insular shelf (Trenhaile et al. 1989, 2001; Quartau et al., 2010; Ramalho et al., 2013). Its successive development/evolution is mainly driven by the balance between the processes that progressively enlarge the shelves (mainly wave erosion) and those that dismantle them (mass wasting) and fill the accommodation space (post-erosion volcanic activity and sedimentation) (Menard, 1983). Quartau et al. (2012; 2015b) developed a conceptual model for the morphologic development of insular shelves in volcanic islands (*Fig. 1.1*) using Faial and Pico islands (Azores Archipelago) as case histories. As the shelf becomes wider and more gently sloping, in fact, wave-eroded surfaces trend towards a state of equilibrium because wave attenuation cause erosion rates to decrease through time so that shelves cannot growth indefinitely (Trenhaile, 2001). Generally, where wave erosion dominates and there is not recent volcanic activity, wide shelves occur, possibly covered by thick sedimentary bodies and facing high plunging cliffs (Quartau et al., 2014, 2015b). On the contrary, where the volcanic activity dominates, the shelves tend to be narrow, characterized by widespread rocky outcrops and are covered by relatively thin sediment cover. The latter morphology is caused by post-erosional volcanism that might partially or completely fill the accommodation space left by erosion, reducing the shelf width ("rejuvenated shelves", Quartau et al., 2015b). Related coastal tracts are morphologically immature, composed of low cliffs or even absent due to formation of lava deltas.

It is commonly accepted that the shelf width reflects the effects of wave erosion occurred during several relative sea-level fluctuations. Ablay and Hurlimann (2000), Le Friant et al. (2004), Llanes et al. (2009), Menard (1983), Quartau et al. (2010) and Romagnoli (2013) checked a direct relationship between shelf age and shelf width. Studies focused in the Azores (Quartau et al., 2010, 2012, 2015b, 2016) and Aeolian Islands (Romagnoli, 2013) addressed the shelf width as a useful tool for reconstructing the original extent of the adjacent volcanic edifice prior to wave erosion (on shelf sectors not affected by landslides processes or covered by later volcanic activity). Accordingly, it can be used as a proxy of the relative age of the adjacent subaerial volcanic edifice (i.e. the wider is the shelf, the older is the subaerial edifice). However, other factors may control the shelf width in a specific sector: for instance, Llanes et al. (2009) and Quartau et al. (2010) related shelf sector width to wave exposure. Quartau et al. (2010) checked the shape of the shelves around Faial Island (Azores Archipelago) through modeling and found disparities between the modeled and the present shelf, which were associated to varied resistance to erosion, tectonic movements, unrecognized volcanic progradation and errors in radiometric dates, or to the shape of the coastline. The role of subsidence in shelves evolution has been also quantitatively discussed by Trenhaile et al. (2014) and Quartau et al. (2018b). Using a wave erosional model they evidenced that subsidence exacerbates the effects of wave erosion, promoting the enlargement of the shelves with an almost linear relationship.
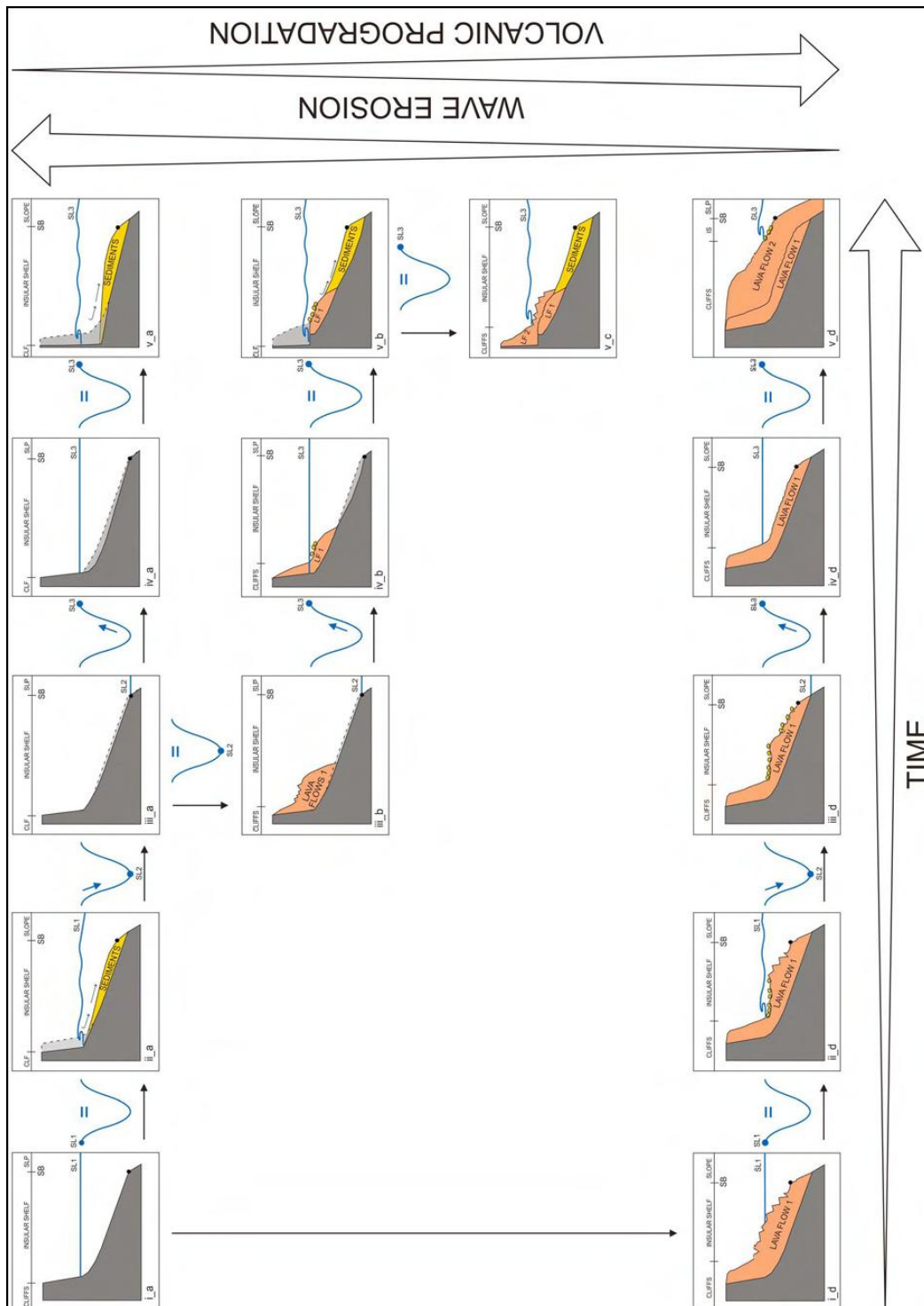
Fig. 1.1 *Conceptual model of the morphologic development of insular shelves in volcanic islands (from Quartau et al. 2012), showing the competition between processes that form them (mainly wave erosion) and processes that fill the erosional spaces (mainly volcanic progradation and sedimentation) during different sea levels. Each box represents a cross-shore profile of the shelf with high vertical exaggeration. The model starts at i_a and develops into the four possible stages v_a, v_b, v_c and v_d. See Quartau et al. (2012) for details on the legend. Note changes in the depth of the shelf edge (black dot).*

2.2 Relative sea-level changes and insular shelves

It is widely accepted that the variations of the eccentricity of the Earth's motion around the sun, and obliquity and precession of the Earth's axis, drive climatic fluctuations (Milankovitch, 1930) being responsible for the alternation of glacial and interglacial periods, especially in the Quaternary. The periodic modification of ice volumes causes variations of the masses and volume of the oceans. These global, "eustatic" sea-level fluctuations (Gornitz, 2005; Miller et al., 2005) led to repeated emergence and submergence of the coastlines. Moreover, due to ice- and water-load variation (Kopp et al., 2015), gravitational attraction (Hay et al., 2014), sediment compaction (Törnqvist et al., 2008; Marriner et al., 2016) and redistribution (Dalca et al., 2013), tectonics (Kelsey & Bockheim, 1994; Vacchi et al., 2012; Dura et al., 2016) and volcanic-related deformations (Lambeck, 2011), landmasses may move vertically, giving their contribute to "relative" sea-level fluctuations. Being regional and/or local in nature, relative sea-level changes may be more important than the global eustatic signal in controlling the emergence or submerged trend of coastal areas (Rovere et al., 2016). The imprint left by relative sea-level fluctuations is commonly evidenced by the occurrence of geological markers and archeological indicators directly connected with former sea-levels (Rovere et al., 2016). Both are widely used to reconstruct paleo sea-level on coastal areas, however only geological indicators may allow to reconstruct relative sea-level fluctuations occurred several ka or Ma ago (Dutton et al., 2015). These markers are represented by fossil remains (Rovere et al., 2015), erosive and depositional features such as beachrocks (Mauz et al., 2015), coastal notches (Ferranti et al., 2006; Trenhaile, 2015), marine terraces (Zazo et al., 2002; Lucchi et al., 2013a, b, Ramalho et al., 2017), insular shelves (Quartau et al., 2010, 2014) and submarine depositional terraces (Casalbore et al., 2014; Pepe et al., 2014). The identification of such markers is fundamental to infer rates of crustal vertical movements and relative sea-level changes. Being volcanic islands commonly subjected to significant vertical movements (De Guidi and Monaco 2009; Ramalho et al., 2013), sea-level markers can often be found both above and below present sea level.

An important geomorphic feature to this purpose is the insular shelf edge or shelf break, a (normally) sharp topographic feature that marks a dramatic increase in slope to greater depths (Southard and Stanley, 1976). Being the result of the wave erosion that occurred during lowstands periods at or close to the water surface (Trenhaile, 2000, 2001), its depth can be adopted to assess subsequent vertical movements undergone by the volcanic edifice or part of it, after its development (Quartau et al., 2014, 2015b, 2016). If the edge of the shelf is shallower than the maximum eustatic sea-level depth during the island growth it means that (i) the island has suffered uplift or (ii) the shelf is more recent than the last lowstand, starting to form after the MIS 2 (20 ka, i.e. the last lowstand). Conversely, if the edge is deeper than -120/125 m (maximum depth reached by the sea with respect to the present level in the past Ma, Bintanja et al., 2005; Miller et al., 2005; Bintanja & Van de Wal, 2008; Raymo et al., 2009; De Boer et al., 2010), the given sector likely subsided (Quartau et al., 2014; 2015b). This may allow to estimate an average subsidence rate affecting the related volcanic edifice which, in turn, can be an important factor in controlling the development of the shelf (Quartau et al., 2018b).

2.3 Sedimentation on insular shelves

Volcanic islands are constantly exposed to degradation and the wind/wave action. Wave erosion strongly influences the shape of the coastline, in particular during the emergent and post-shield island stages and when the volcanic activity wanes (Ramalho et al., 2013), promoting the production of volcaniclastic sediments. On reefless volcanic islands, the island's shape and orientation relative to the trade-winds may also influence the transport and deposition of sediments along the coast. Despite waves being the dominant agent that contribute to shelf sedimentation, other processes like explosive volcanism, lava quenching when entering the sea, fluvial processes (enhanced by rainfall on the windward side of the island) and biological productivity can be also locally important as sediment sources (Menard, 1983, 1986; Quartau et al., 2012; Salvany et al., 2012). The sediments produced by these processes accumulate along the coastline and are transported further down the shelf. In fact, the combination of wave-induced and wind-driven currents can re-suspend the sediments, in particular during more energetic seasons (Calhoun et al., 2002; Ogston et al., 2004; Norcross et al., 2002). As a result, sediment (silt and sand) may be transported along and across the shelf remaining for a short time in the nearshore.

During stormy conditions, waves produce high coastal setup against the shore that is commonly balanced by strong and opposite downwelling bottom currents (Field and Roy, 1984; Hernandez-Molina et al., 2000; Chiocci et al., 2004, Meireles et al., 2013). Based on their observations, Field and Roy (1984), Tsutsui et al. (1987), Hernández-Molina et al. (2000), Chiocci & Romagnoli (2004) and Quartau et al. (2012) suggested that nearshore sediments, suspended by the storm waves-induced turbulence, are efficiently transported onto the shelf by storm-induced downwelling currents. The sediment deposition starts where wave agitation declines towards the threshold of movement, forming more or less thick deposits offshore, having different geometry. These sedimentary wedges are well-recognizable on bathymetry due to their terraced shape, with a marked (depositional) edge corresponding to the topset-foreset rollover depth (commonly in the range of -15/-60 m, depending on the oceanographic setting, Mitchell, 2012) and thickness in the order of tens of metres (Chiocci et al., 2004). Terraced sedimentary bodies, also reported in literature as nearshore sand bodies (i.e. Field and Roy, 1984), infralittoral prograding wedges (i.e. Hernández-Molina et al., 2000) and submarine depositional terraces (SDT in Chiocci et al., 2004 and Casalbore et al., 2017a) will be hereafter referred as SDTs. They have been recognized around several volcanic islands such as in the Azores Islands (Quartau et al., 2010, 2012, 2014, 2015b; Chiocci et al., 2013), the Pontine Archipelago (Chiocci and Orlando, 1996), the Aeolian Islands (Chiocci and Romagnoli, 2004; Casalbore et al., 2010; Romagnoli et al., 2013a, b; Casalbore et al., 2016a) and Linosa island (Romagnoli, 2004). Relationships have been found between the rollover depth, the fetch and exposition of coastal tracts (Chiocci and Romagnoli, 2004; Mitchell et al., 2012) and the local wave regime, evidencing the key role played by storm-wave base level in their formation (Lobo et al., 2005; Bàrcenas et al., 2015; Casalbore et al., 2017). However, despite their wide distribution, the physical parameters driving the formation of SDTs are still partially understood, especially the relationship between their depth, wave energy and sea-level position. In the Aeolian and Pontine Islands, shallow-water clinoforms located in the first 20-35 m depth,

13

have been interpreted as recent to present-day features (Chiocci and Romagnoli, 2004; Casalbore et al., 2016a, b), while terraces found close to the shelf edge have been interpreted as low-stand deposits, which remained relict during sea-level rise (Chiocci & Orlando, 1996; Chiocci et al., 2004; Casalbore et al., 2016a, b). Mid-shelf terraces are generally attributed to stillstands of the relative sea-level during the last transgression (Casalbore et al., 2017a). However, in the Azores, which are much more energetic than the Mediterranean, Quartau et al. (2012, 2014, 2015) found SDTs edges much deeper, down to -60 m, which the authors believe to be present-day features. The edge of the SDTs could be also be used for palaeo-sea level and vertical movement reconstruction if the wave energetic regime in which they were formed is taken into account.

Being insular shelves often prone to submarine mass wasting (Casalbore et al., 2015; Quartau et al., 2018b), the accumulation of sediments within the island shelf is transient, in particular when submarine canyons cut through the shelf edge (Saint-Ange et al., 2011; Sisavath et al., 2011; Romine and Fletcher, 2013) and during sea-level lowstands, when the islands shelves are reduced in size (Ávila et al., 2008a; Quartau et al., 2012). Conversely, the occurrence of a wide shelf during highstand conditions might limit the transport of sediments below the shelf edge, promoting the sediment accumulation on the shelf.

3. DATASET AND METHODS

3.1 Dataset acquisition

This thesis is based on the analysis of single-channel seismic reflection profiles and high-resolution multibeam bathymetric data collected around the Aeolian Archipelago and Santa Maria Island in the last decades.

In the Aeolian Archipelago, data were obtained by the University of Rome "Sapienza", the University of Bologna and the CNR-IGAG (Consiglio Nazionale delle Ricerche, Istituto di Geologia Ambientale e Geoingegneria) of Rome on board the research vessels "Thetis", "Urania" and "Minerva 1". The bathymetric dataset used for our studies (Figure 3.1) was collected using multibeam systems working at frequency range of 50-100 kHz depending on the water depth and recorded using a differential GPS system (see details in Romagnoli et al., 2013). Moreover, shallow water areas (depth < c. 50 m) were surveyed using a small boat equipped with a Teledyne Reson 7125 multibeam system working at a frequency of 400 kHz, and a GPS-RTK (Real Time Kinematics) positioning (see details in Bosman et al., 2015). A grid of 151 high-resolution seismic reflection profiles was acquired in 1993 and 2016 (Figure 3.1). The first dataset was acquired using a Sparker 0.5-1 kJ aboard the catamaran Incaurina Marianna, while the latest one was acquired in 2016 aboard the R/V Minerva1 using a Sparker source working at 0.5-1.5 kJ around the islands of Salina and Lipari (Figure 3.1). Latest data have been collected using a DGPS, while older data were collected using a non-differential GPS periodically calibrated with a ground station. The vertical resolution of the analyzed Sparker profiles can be estimated in the order of 5 m due to the emitted frequency and the ringing effects. Finally, the subaerial Digital Terrain Models (DTMs) of the islands (cell size of 0.4 m) used in the study have been collected by the Italian Ministry for the Environment, Land and Sea Protection, through LiDAR flights.
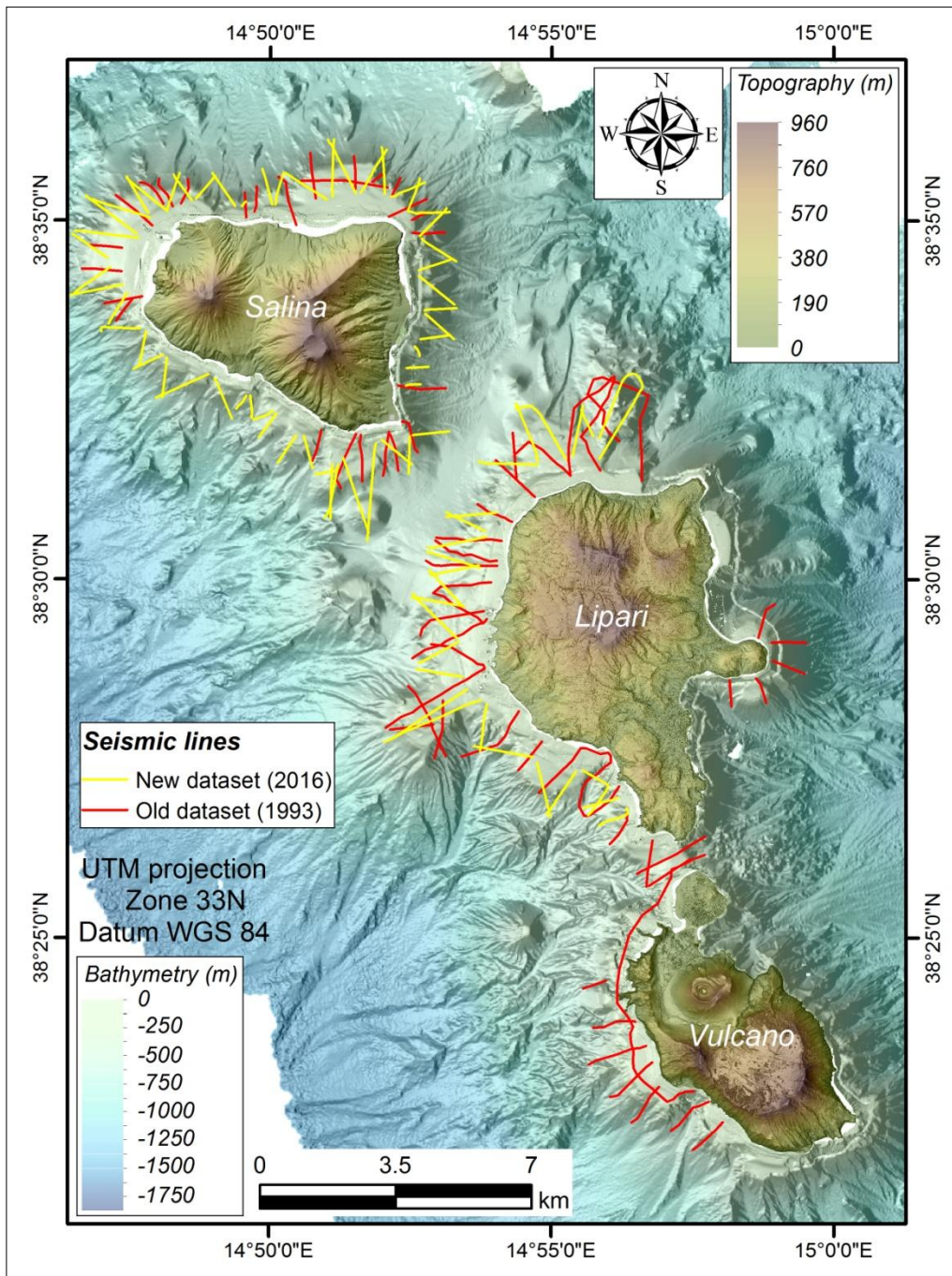
Figure 3.1 *Dataset used to study the insular shelves around the Central Aeolian sector showing the location of the seismic reflection profiles (red and yellow lines) and the multibeam bathymetry.*

The shallow water portions around the island of Santa Maria were, instead, an "unknown territory". Here, high-resolution multibeam bathymetry and seismic reflection data (Figure 3.2) were collected in the scope of PLATMAR project (Development of volcanic island shelves: insights from Sta. Maria Island and implications on hazard assessment, habitat mapping and marine aggregates management) from 24th August to 15th September, 2016 onboard the R/V *Arquipélago*. The multibeam bathymetry was acquired between c. -20 m and c. -250 m mostly parallel to the coastline using a pole mounted Kongsberg EM2040C[TM] system operating at frequencies ranging

from 200 to 400 kHz and angular coverage of 130°. The vessel position relied on DGPS with OMNISTAR corrections. Sound velocity profiles (SVP) were frequently collected during the survey using an AML MinosX Sound Velocity Profiler[TM] to correct variations in sound velocity due to temperature and salinity changes throughout the water column.

A dense network of 614 high-resolution seismic profiles (total of 2008 km, Figure 3.2) was also acquired between -25 m and -300 m using an Applied Acoustic Engineering AA 200 Boomer plate and a receiver array consisted of a single-channel streamer with 8 hydrophones. Most of the seismic profiles were acquired using 100 J or 200 J of output energy, depending on the water depth. Seismic survey lines parallel to bathymetry were made concurrently with the multibeam survey, so line spacing varied along depth (between 20 to 200 m), while seismic lines perpendicular to the coastline were spaced c. 250 m.
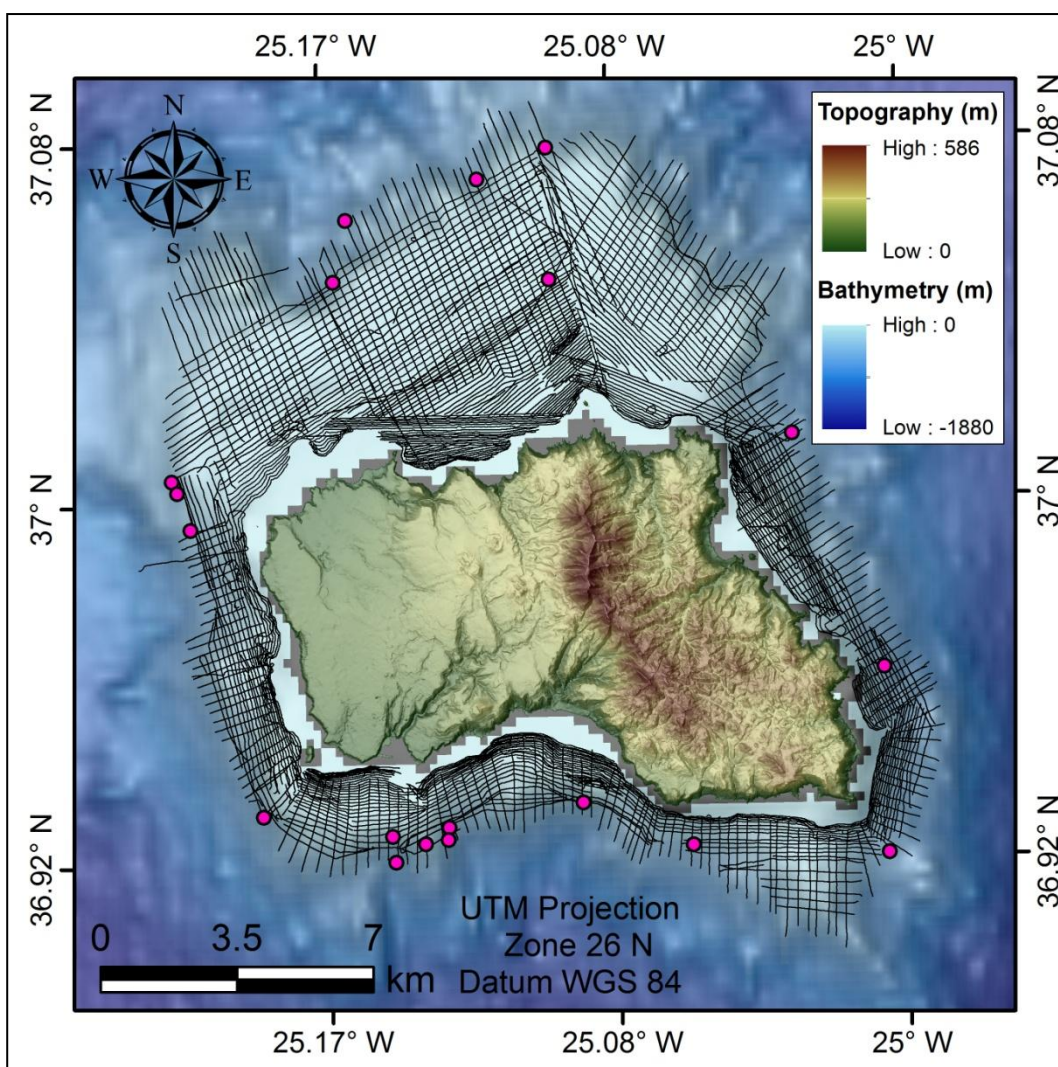
Figure 3.2 *Dataset collected around Santa Maria Island during the PLATMAR 2016 survey. For details see Manuscript V.*

3.2 Dataset processing

In order to create Digital Elevation Models (DEMs), the multibeam data collected around the Aeolian Archipelago were processed using Caris Hips&Sips software by CNR-IGAG. The cell-size varies from 0.1 m to 0.5 m at depths < -50 m, from 0.5 m to 10 m between -50 and -300 m and from 15 m to 25 m at deeper depth (c. -1500 m). The earliest (analogic) dataset of seismic reflection profiles has been digitalized by the University of Rome and successively relocated via homologous matching of features observed on seismic profiles and multibeam bathymetry due to the low accuracy of the adopted GPS system. This work was not necessary for the latest dataset, since data were DGPS-RTK positioned.

The multibeam dataset collected around Santa Maria has been processed by the Hydrographic Institute of Portuguese Navy using Caris Hips&Sips 9.0 software to produce high-resolution DEMs with variable cells size depending on the water depth (1 m for shallow water to 8 m c. 250 m). Seismic reflection profiles were recorded in .TRA format and then converted to SEG-Y to be processed by the IXBLUE DELPH SEISMIC INTERPRETATION software v4.0. Each seismic line was processed applying the following procedures:

a) Layback correction;
b) Bandpass filter between 320 Hz and 5600 Hz, to cut noise outside the signal bandwidth;
c) Time Variant Gain (TVG), in order to recover the signal attenuation with depth;
d) Swell filter to correct the effect of waves;
e) Automatic Gain Control (AGC) that balances out amplitudes across a whole trace;
f) Stacking, in order to improve the signal-to-noise ratio;
g) Water column removal.

To convert from milliseconds to meters, we adopted a sound velocity of 1500 m/s and 1800 m/s depending on the absence/occurrence of sediments on the shelf, respectively.

3.3 Dataset interpretation

The shelf width and erosive edge depth were detailed mapped exploiting bathymetric cross-sections and seismic profiles, while the comparison of offshore and onshore morphologies was realized on subaerial DTMs and submarine DEMs visualized as shaded relief, contour maps, and 3-D surfaces. In the Central Aeolian sector, a detailed and continuous mapping of the erosive shelf edge has been carried out all around the islands through more than 1000 bathy-morphological profiles positioned at 50 m-intervals perpendicularly to the coastline (Figure 3.3), in order to integrate the largely-spaced seismic profiles. The dataset of seismic profiles helped to map the erosive edge depth where sediments (commonly from 10 m to 30 m thick) partially cover the shelf. At Santa Maria, the dense network of seismic profiles collected across the shelf (Figure 3.2) allowed to investigate with high detail the morphological features of the shelf and to map the distribution of the sedimentary cover and to measure its thickness. The uncertainty in the

definition of the erosive shelf edge depth has been estimated in the order of few meters, depending on the resolution of the seismic reflection profiles and the multibeam bathymetry.

Since the shelf in some places is affected by processes responsible for its partial dismantling that are not directly linked with wave action (landslides, canyons, gullies, etc), only the maximum values of shelf width and erosive edge depth for each sector are considered in the analyses. The shelf edge associated to the portion carved by mass wasting process have been named eroded edge, while the edge preserved by erosion have been named erosive shelf edge.

To study the shelf width and the erosive shelf edge depth, the shelf surrounding each island has been divided in sectors, according to their morphological differences and through comparison with the age of the products outcropping onland (see Manuscripts I and IV). Measures were reported in graphs showing the variation of the shelf width and edge depth. An important part of the thesis encompassed an integrated approach with field data of the subaerial portion of the studied volcanic islands. The aim was to better define the links between the onshore/offshore geology and to obtain an integrated estimate of the vertical mobility trend of the islands. To calculate the uplift/subsidence trends we adopted different approaches, which are explained in detail in Manuscripts III and V (included in chapters 5 and 8 respectively).
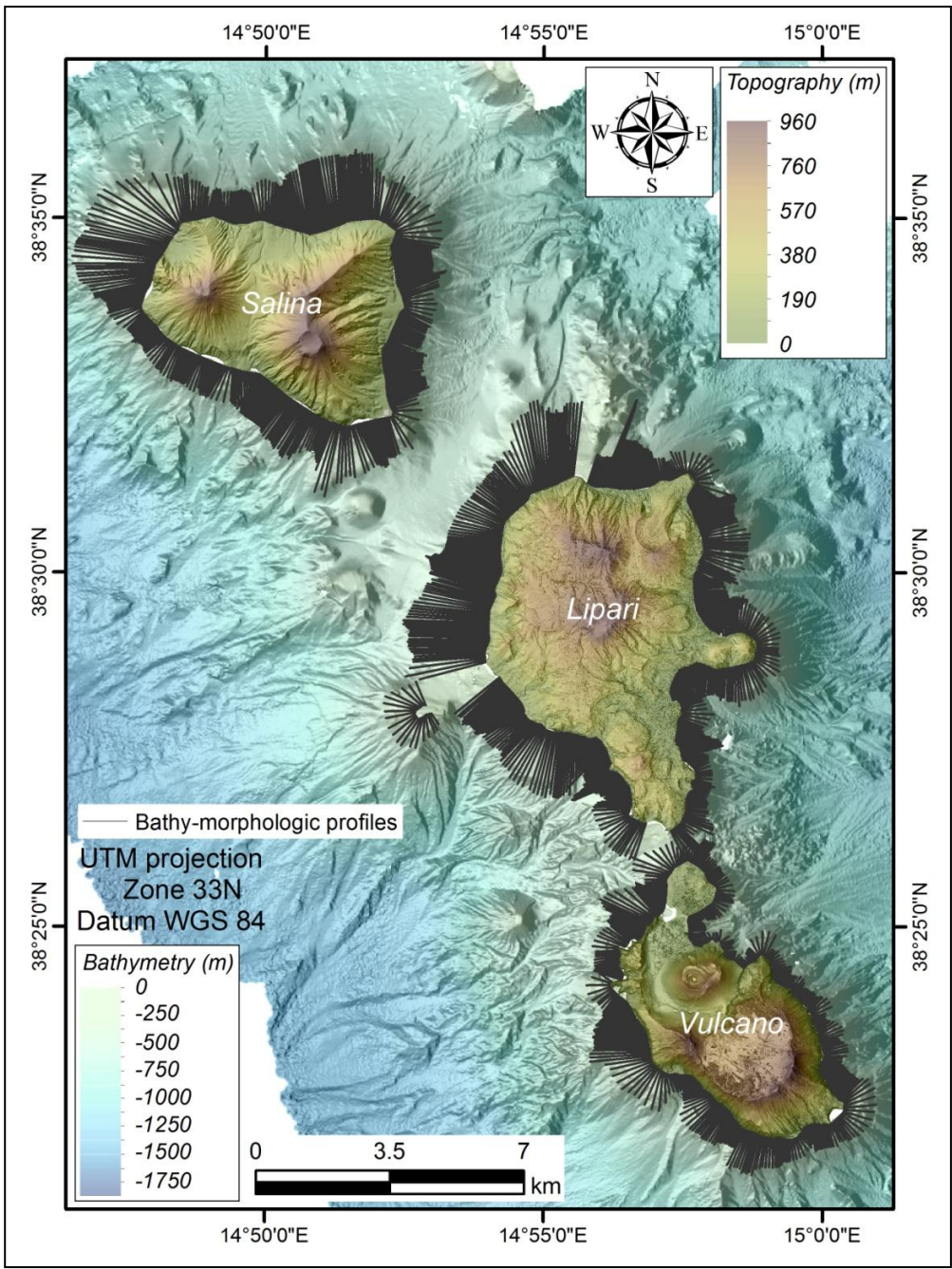
Figure 3.3 *Bathy-morphological profiles (black lines) used to measure the shelf width and the erosive edge depth in the Aeolian Islands.*

4. GEOLOGICAL AND GEOGRAPHICAL SETTING OF THE STUDIED AREAS

4.1 The Aeolian Archipelago – regional setting

The Aeolian Archipelago is an articulated arc-shaped volcanic structure located in the Southern Tyrrhenian Sea, with an overall length of about 200 km. Its seven islands (Alicudi, Filicudi, Salina, Lipari, Vulcano, Panarea and Stromboli, Fig. 4.1) and surrounding seamounts represent the tip of a large volcanic structure emerging from -2000/-2500 m on the northern Sicilian slope (Romagnoli et al., 2013 and reference therein). The formation of the volcanic arc is associated to the roll-back of the NW-directed Ionian subducting slab below Calabria (Faccenna et al., 2001; Serpelloni et al., 2005; Chiarabba et al., 2008). The volcanic activity is mainly controlled by regional fault systems that influence the morpho-structural setting and evolution of the islands (De Astis et al. 2003, 2006b; Ventura 2013). Although a detailed chronostratigraphic framework of the subaerial volcanic activity is well known on the basis of available radiometric ages and regional correlation of marine terraces and tephra layers (Lucchi et al., 2013a), the ages of the submarine portions are still mostly unknown. The volcanic activity is considered to be entirely developed during the Late Quaternary, since the oldest dated rocks, sampled from Sisifo (Beccaluva et al., 1982), Eolo and Enarete seamounts (Beccaluva et al., 1985) were dated at 1.3 Ma and 0.85-0.64 Ma, respectively. The Aeolian Archipelago can be divided in three sectors (i.e. western, central and eastern) on the basis of distinctive structural trends and evolution (De Astis et al., 2003). The westernmost islands (Alicudi and Filicudi) are the oldest and mostly influenced by a WNW-ESE fault system, while the easternmost and youngest islands (Panarea and Stromboli) are aligned along NE-SW striking faults. The central sector (Salina, Lipari and Vulcano islands) lie at the intersection between the Tindari-Letojanni NNW-SSE oriented volcanic belt and the WNW-ENE arc-shaped structure (De Astis et al., 2003) (Figure 4.1).

Information regarding wave and wind conditions in the Aeolian area are scarce, and mostly based on Cicala (2000) for the central and eastern sectors. In the Aeolian Archipelago winds coming from NW and W are predominant, therefore the most energetic waves approach from westerly directions. Storms, mostly coming from the Tyrrhenian Sea, strike the western coastlines with a large fetch (up to 300 nautical miles) and waves up to 6 m height. During autumn and winter, winds from SE provenance also affect the SE and E coastlines. In this thesis particular attention is given to the central Aeolian sector.
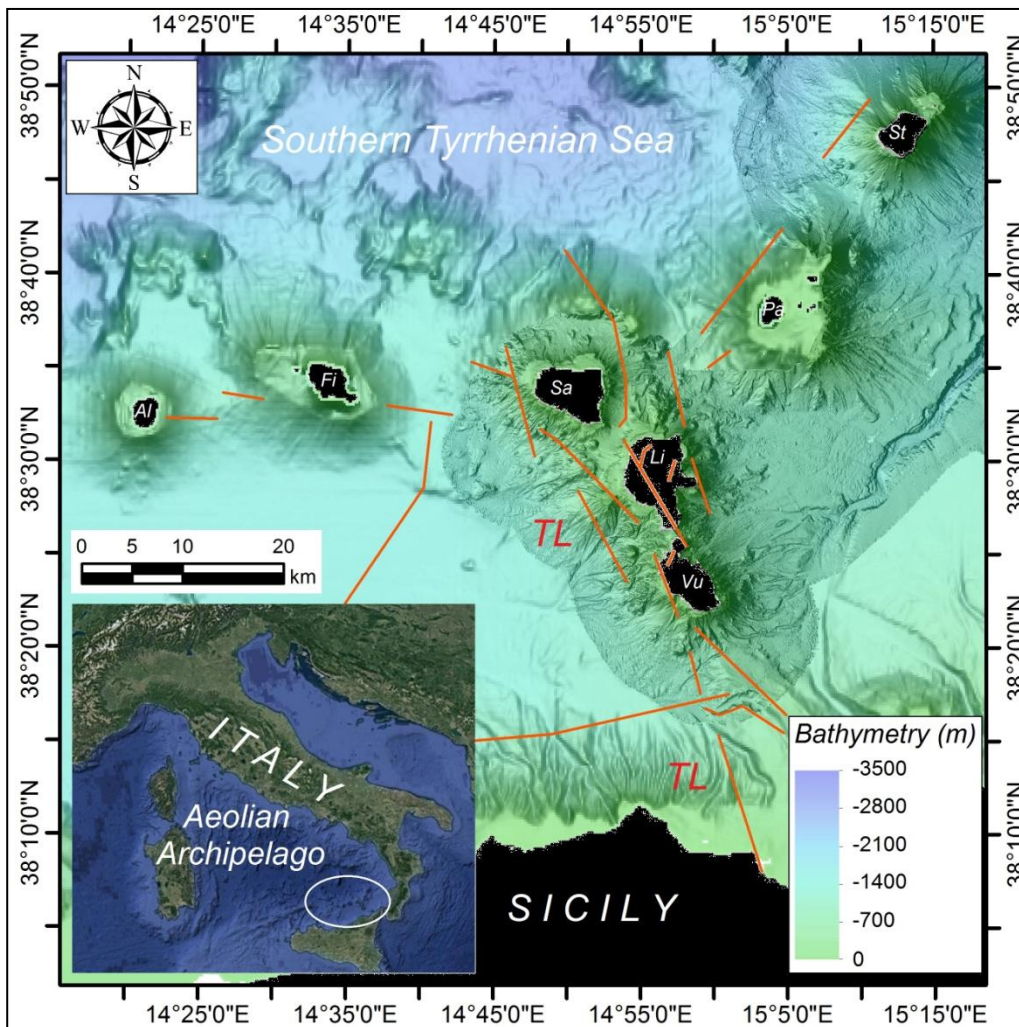
Figure 4.1 *Shaded relief map showing the location of the Aeolian islands in the Southern Tyrrhenian Sea and main structural lineaments (from Barone et al., 1982; Argnani et al., 2007): Alicudi (Al), Filicudi (Fi), Salina (Sa), Lipari (Li), Vulcano (Vu), Panarea (Pa) and Stromboli (St); TL: Tindari-Letojanni fault system.*

4.1.1 CENTRAL AEOLIAN SECTOR

The islands of Salina, Lipari and Vulcano represent the emerged portion of volcanic edifices whose base lies at c. -1700 m (Figure 4.2). A small depositional basin at c. -300 m connects Salina with the nearby Lipari island (SLB, Figure 4.2), while a shallow-water saddle c. 50 m deep in the shallowest point, known as "Bocche di Vulcano" (BV, Figure 4.2), connects Vulcano with Lipari complex.

Romagnoli et al., 2013 and references therein mapped and recognized insular shelves as a characteristic morphological elements of the western, central and eastern islands of the Aeolian archipelago. The shallow water portions around the islands of the central Aeolian sector are, in fact, characterized by gently sloping platforms mostly extended in the first 100-150 m of depth (Romagnoli et al., 2013). The widest shelves are located off the western flanks of Lipari and Vulcano and around the western, south-eastern and north-eastern corners of Salina (Figure 4.2), marking the oldest volcanic edifices of the islands (De Astis et al., 2013; Forni et al., 2013; Lucchi et al., 2013a; Romagnoli et al., 2013). Below the shelf edge, the flanks of the island are steep and commonly carved by gullies exhibiting a sub-radial pattern. The features tend to converge at

deeper depths forming submarine channels (Figure 4.2). Average gradients of the submarine flanks ranges from c. 30° to c. 10° in the first 500 m depth, while approaching greater water depths they decrease down to a few degrees (Romagnoli, 2013).
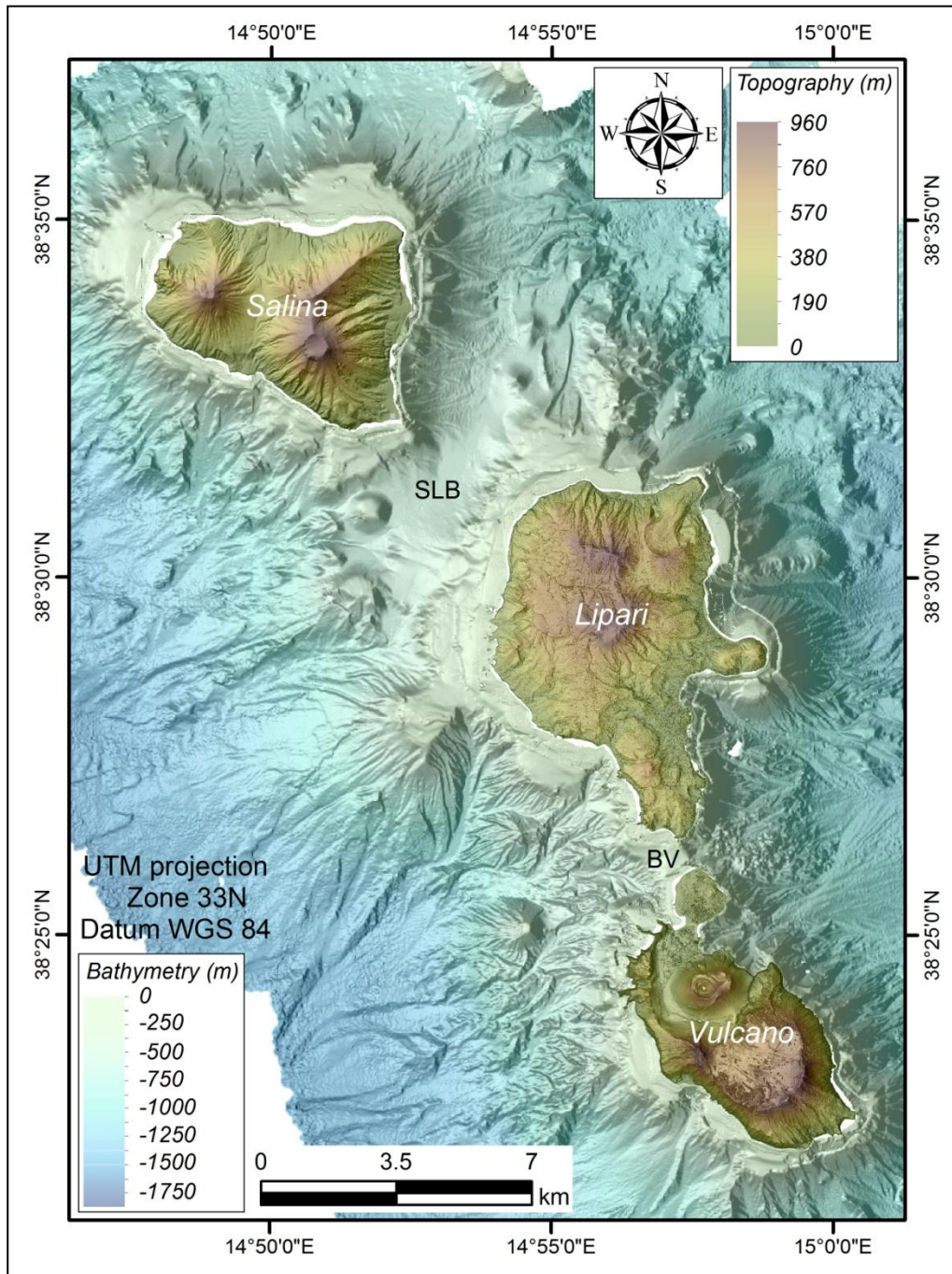
Figure 4.2 *Shaded relief the subaerial and submarine DEM of Salina, Lipari and Vulcano. SLB: Salina-Lipari Basin; BV: Bocche di Vulcano saddle.*

4.1.1.1 Salina

Salina is the highest (962 m a.s.l.) and second largest island (26 km^2) of the Aeolian archipelago. The island is the emerged portion of a volcanic edifice rising from -1300 m (Romagnoli et al., 2013), located at the intersection between the arc-shaped structure of the Aeolian archipelago and the NNW-SSE elongated Salina-Lipari-Vulcano volcanic belt (Figure 4.1).

The subaerial volcanic activity of Salina developed between 244 ka and 15.6 ka through six Eruptive Epochs (EE) (Keller, 1980; Lucchi et al., 2013a)(Figure 4.3). The earliest stage of the island building is represented by the highly eroded Pizzo Corvo edifice (which has an uncertain age and stratigraphic position) and by the products of Pizzo Capo Volcano (EE1, 244-226 ka), located on the W and NE portion of the island, respectively. During the EE3/4 the volcanic activity migrated further south, forming the edifices of Monte Rivi and Monte Fossa delle Felci (160-121 ka). Following a period of volcanic quiescence, a new phase of activity produced the edifice of Monte dei Porri (70-57 ka) on the W side of Salina. The latest volcanic activity (EE6) is located at the Pollara crater (30-15 ka)(Figure 4.3).

A succession of raised Late Quaternary (MIS 5) marine terraces, reflecting the interplay between sea-level fluctuations and long-term vertical movements, crops out along the coastal slopes of Salina. The downstepping arrangement of the different MIS 5 marine terraces (associated to the high sea-level peaks of 5.5, 5.3 and 5.1 by Lucchi et al., 2009), with the oldest located at higher elevation, allowed Lucchi et al. (2013a) to estimate an uplift trend for the archipelago in the order of 0.36 m/ka in the last 124 ka. However, the occurrence of remnant of raised marine terrace of likely MIS 7.3 age below the younger MIS 5 terraces, witnesses the occurrence of possible subsidence before the Last Interglacial (Lucchi et al., 2013a).
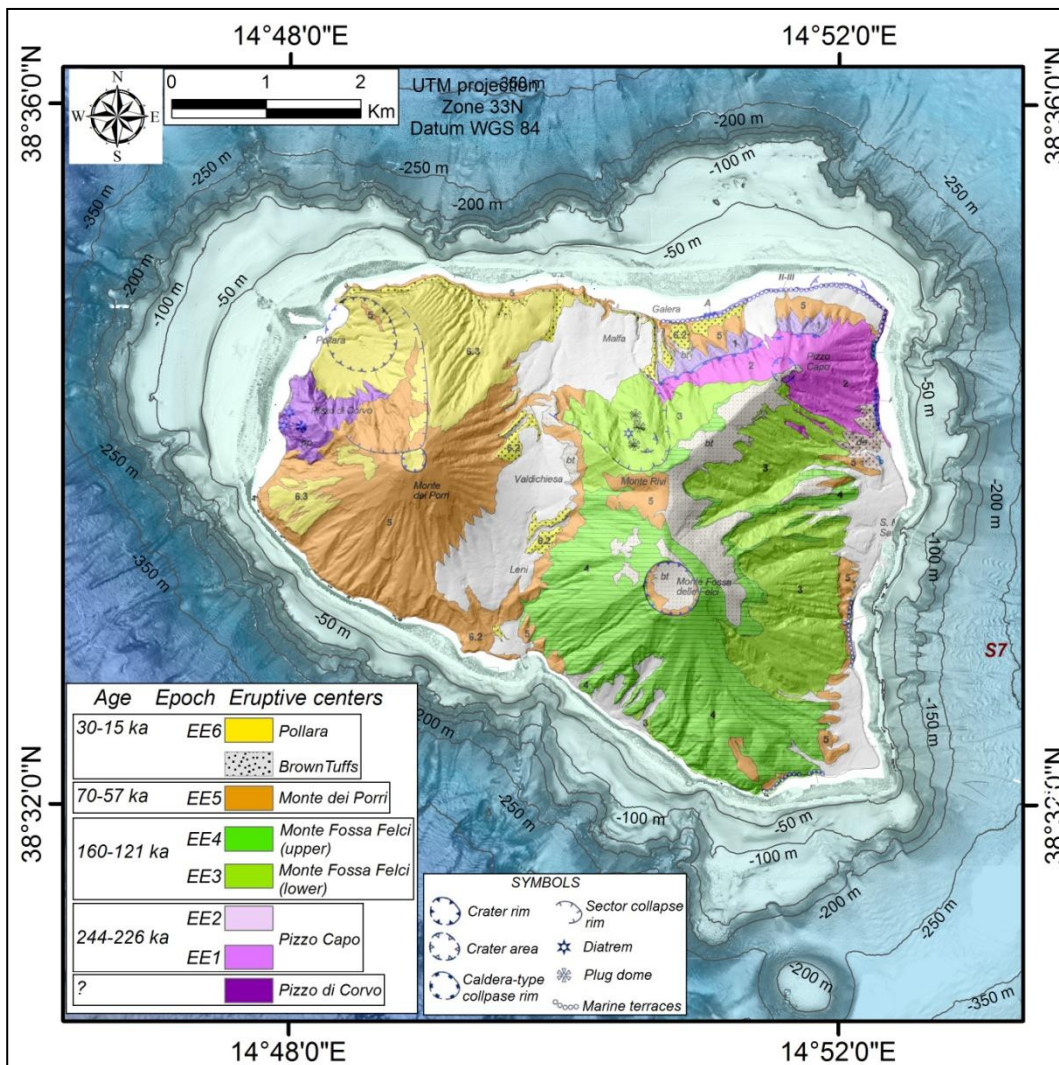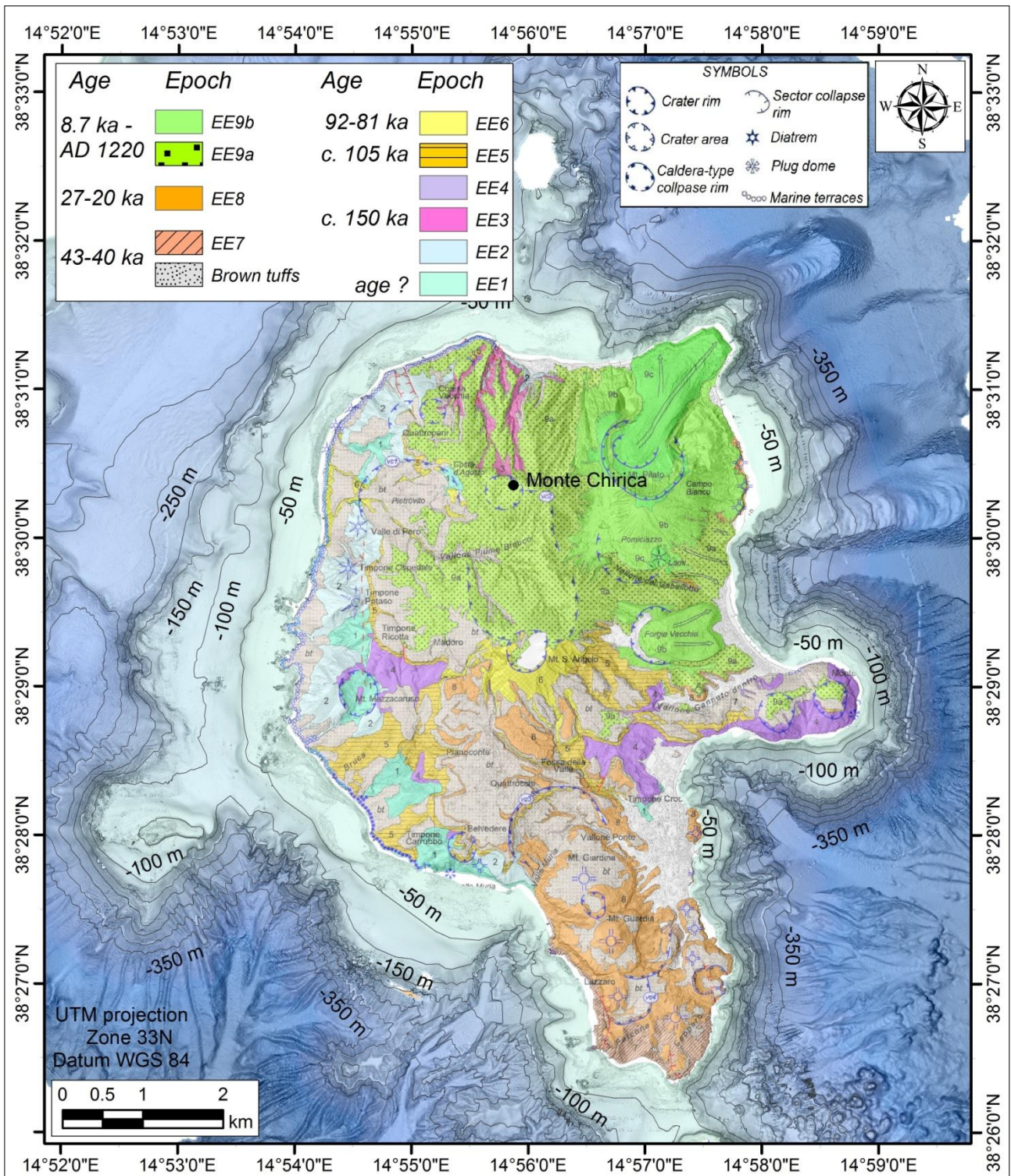
Figure 4.3 *Simplified geological map of Salina (modified after Lucchi et al., 2013) showing the main volcanic centers, eruptive epochs and volcanic features, merged on the DEM of the island and the multibeam bathymetry of the submarine shallow areas.*

4.1.1.2. Lipari

Lipari is the largest island of the Aeolian archipelago (total area of 38 km^2). The present day edifice is characterized by a rugged morphology up to 602 m in elevation (Monte Chirica, Figure 4.4) and represents the culmination of a mainly submerged volcanic complex controlled by the NNW-SSE-oriented Tindari-Letojanni Fault System (Mazzuoli et al., 1995; Ventura, 2013). It emerged from the sea more than 267 ka ago from c. -1700 m. Offshore, wide insular shelves covered by volcaniclastic deposits surround the island all along the western and northwestern side and around the Monterosa promontory in the eastern part, while along the remaining portions these shelves are remarkably narrower (Chiocci & Romagnoli 2004; Romagnoli 2013; Romagnoli et al. 2013), (Figure 4.4). Lipari is characterized by distinct eruptive centers witnessing the complex history of the island. Nine Eruptive Epochs (EE afterwards) interspersed by periods of inactivity and volcano-tectonic collapses, have been identified (Forni et al., 2013). Despite the chronological estimations of the EE1 are incomplete due to the lack of dating, the oldest exposed Paleo-Lipari

volcanic centers (> 267 ka) have been recognized along the west coast and, very subordinately, in the central-eastern sector (Figure 4.4). The EE2 (267-188 ka) records the renewal of volcanism from a number of volcanic centers located along the west coast of Lipari (namely "the western volcanoes", Figure 4.4), distributed along north–south alignments. During the EE3 (c. 150 ka) only M. Chirica renewed its activity. The following prolonged period of volcanic inactivity (c. 30 ka) is recorded by the widespread marine terraces and fossils of palaeoshoreline I, witnessing the first episode of marine ingression (MIS 5e, 124 ka). The onset of the EE4 (119 – 114 ka) led to a significant shift of the vent localization towards the central and eastern sectors of Lipari, as recorded by Monterosa and M. S. Angelo products. The latter, renewed its activity during the EE5 (c. 105 ka) after a major quiescence period. This activity was followed by another c. 10 ka-long period of quiescence that was characterized by further episode of marine ingression and erosion during the interglacial peak of MIS 5c (100 ka), as recorded by the marine terrace deposits of palaeoshoreline II. The EE6 was characterized by renewed activity of M. S. Angelo and M. Chirica, after which the Lipari volcanic complex saw a prolonged period of dormancy covering the 81–43 ka time interval. The episode of marine ingression of MIS 5a (81 ka) occurred during this quiescence period, and it is recorded in the marine terraces of palaeoshoreline III in the south-western coastal sector of Lipari, and subordinately, in the area of Monterosa. Renewal of volcanism occurred from vents located in the southern (collapsed) sector of Lipari under the control of the main NNW–SSE tectonic trend during the EE7 (43-40 ka) and EE8 (27-20 ka). The last activity ranged from c. 8.7 ka to medieval ages and created a dome-field in the north-eastern sector of Lipari, characterized by obsidian flows (Figure 4.4).

A succession of raised marine terraces dated at MIS 5 are interspersed within the volcanic succession along the western and, in a lesser extent, the eastern coastal slopes of the island, at elevation varying between 43-45 m a.s.l. and 12 m a.s.l. (Lucchi, 2009; Calanchi et al. 2002; Lucchi et al. 2004a). On the base of these raised marine terraces, Lucchi et al. (2013b) calculated an average uplift trend of 0.31-0.34 m/ka for the last 124 ka.
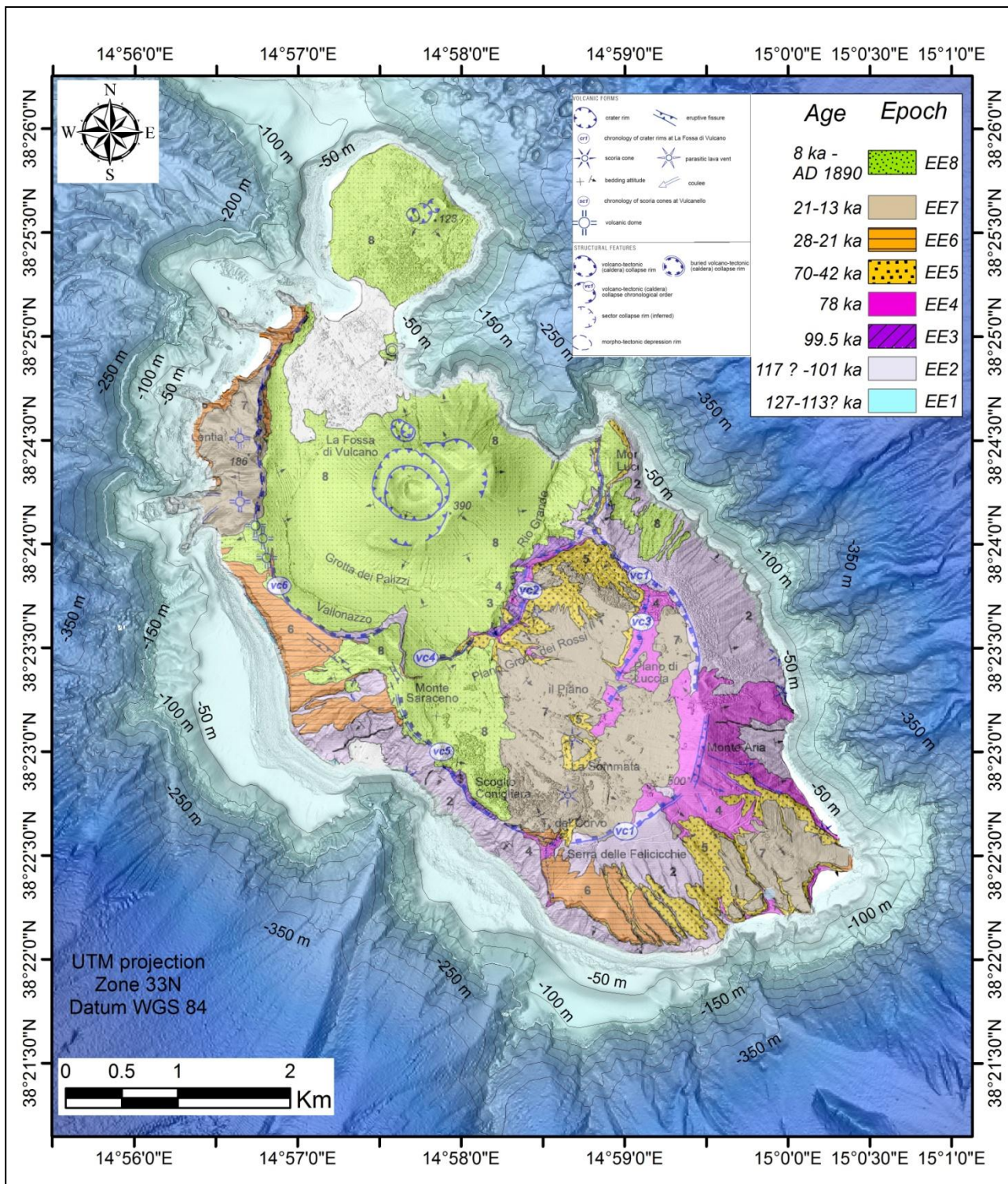
Figure 4.4 *Simplified geological map of Lipari (modified after Forni et al., 2013) showing the main volcanic centers, eruptive epochs and volcanic features, merged on the DEM of the island and the multibeam bathymetry of the submarine shallow areas.*

4.1.1.3. Vulcano

The island of Vulcano (21.2 km^2) is the exposed summit of a volcanic edifice sited in the southern-most sector of the Aeolian archipelago. The edifice rises from the sea floor from c. -1200 m, (Romagnoli, 2013) up to the maximum height of 499 m a.s.l. at Monte Aria (Figure 4.5). The present day subaerial topography is dominated by two intersecting calderas (La Fossa Caldera and Il Piano Caldera), both witnessing a complex history of volcanic and volcano-tectonic events that shaped this volcanic edifice (De Astis et al., 1997, 2006b). Insular shelves surrounding Vulcano are in general less developed with respect to Salina and Lipari, and are mainly located along the western coastal portion (Romagnoli et al., 2012)(Figure 4.5). The geological history of Vulcano is divided in eight successive Eruptive Epochs (EE) in the time interval between c. 127 ka and historical times, separated by intervals of quiescence usually associated with the recurrent volcano-tectonic collapses that produced the multi-stage Il Piano and La Fossa calderas (De Astis et al., 2013).

The oldest product exposed on the island of Vulcano are lava flows that crop out along the steep western coastal cliff in the sector of Capo Secco (EE1, c. 127 − 113 ka, Figure 4.5), a low-sided shield volcano reaching an elevation of c. 150 m above the present sea level. This former cone is presently almost entirely dismantled, as suggested by the occurrence of a wide insular shelf here (Romagnoli, 2013). After a quiescent period, the eastward shifting of the main feeding system gave rise to a large central-conduit stratocone located in the southern sector of the island named "Primordial Vulcano" (EE2, 117-101 ka, Figure 4.5), that reached elevations higher than 700 m. The summit of the original stratocone was truncated by volcanic collapse, followed by the Il Piano caldera collapse likely occurred at c. 100 ka. The renewal of volcanism gave rise to a series of compound lava flows (EE3, 99.5 ka, Figure 4.5) that progressively filled the Il Piano caldera structure. The EE3 was interrupted by a volcanic collapse (occurred between 99.5 ka and 80 ka), inferred to be the earliest phase of the multistage formation of La Fossa caldera. The EE4 (c. 78 ka, Fig. 8) took place after a c. 10-ka-long period of dormancy and erosion. The renewal of activity (EE5, 70-42 ka) was characterized by the shifting of the eruptive vents towards the NNW, along the rims of La Fossa caldera (Monte Rosso, Monte Luccia) and inside its morphologic depression, and within Il Piano caldera. A new collapse resulted in the development of the central-eastern sector of the La Fossa caldera and probably interrupted the activity of the EE5. During the EE6 (28-21 ka, Figure 4.5), magma was erupted from vents and fissures mostly located along the western side of Vulcano Island under the control of the outer rims of Il Piano and La Fossa calderas, attesting for a new shifting of eruptive vents. The EE7 (21-13 ka, Figure 4.5) reported a further shifting of the active vents in the Vulcano history, passing from the western side towards the northern sector of the island, within the multi-phase La Fossa caldera or along its borders, leading to development of the main portion of the Monte Lentia dome field. The whole Monte Lentia dome field was later offset by a collapse fault that formed the current western border of La Fossa caldera. The younger products of Vulcano (EE8, <8 ka, Figure 4.5) were erupted from different vents located along the margins and inside La Fossa caldera. The activity in these new eruptive centers occurred repeatedly at alternating times from c. 5.5 ka up to historical times (youngest products erupted in AD 1739-1890).

Figure 4.5 *Simplified geological map of Vulcano (modified after De Astis et al., 2013) showing the main volcanic centers, eruptive epochs and volcanic features, merged on the DEM of the island and the multibeam bathymetry of the submarine shallow areas.*

4.2 The Azores Archipelago – regional setting

The Azores Archipelago is made of nine islands (Flores, Corvo, Graciosa, Terceira, São Jorge, Pico, Faial, São Miguel and Santa Maria, Figure 4.6) located in mid-North Atlantic on top of the Azores Plateau (Lourenço et al., 1998; Gente et al., 2003; Miranda et al., 2018). This large triangular-shaped area is dissected by the Mid Atlantic Ridge (MAR in Figure 4.6), that separates the North-American plate (to the west) from the Eurasian and Nubian plates (to the east, Figure 4.6). The boundary between these two plates is more diffuse. The Terceira Rift (TR in Figure 4.6) marks the northern border of this area, while to the south the deformation progressively decrease along the line that connects the MAR with the Gloria Fault (GF in Figure 4.6) (Hipolito et al., 2013; Lourenço et al., 1998; Marques et al., 2013). In the past the Nubian-Eurasian border was located at the now inactive East Azores Fault Zone (EAFZ in Figure 4.6) (Laughton and Whitmarsh, 1974; Searle, 1980; Madeira and Ribeiro, 1990; Luís et al., 1994; Luís and Miranda, 2008). In this complex tectonic setting, governed by traction forces and right-lateral transtensional stress, volcanism is tectonically controlled and occurs along faults (fissure volcanic systems) or at fault intersections (central volcanoes) (Madeira et al., 2015; Marques et al., 2013).
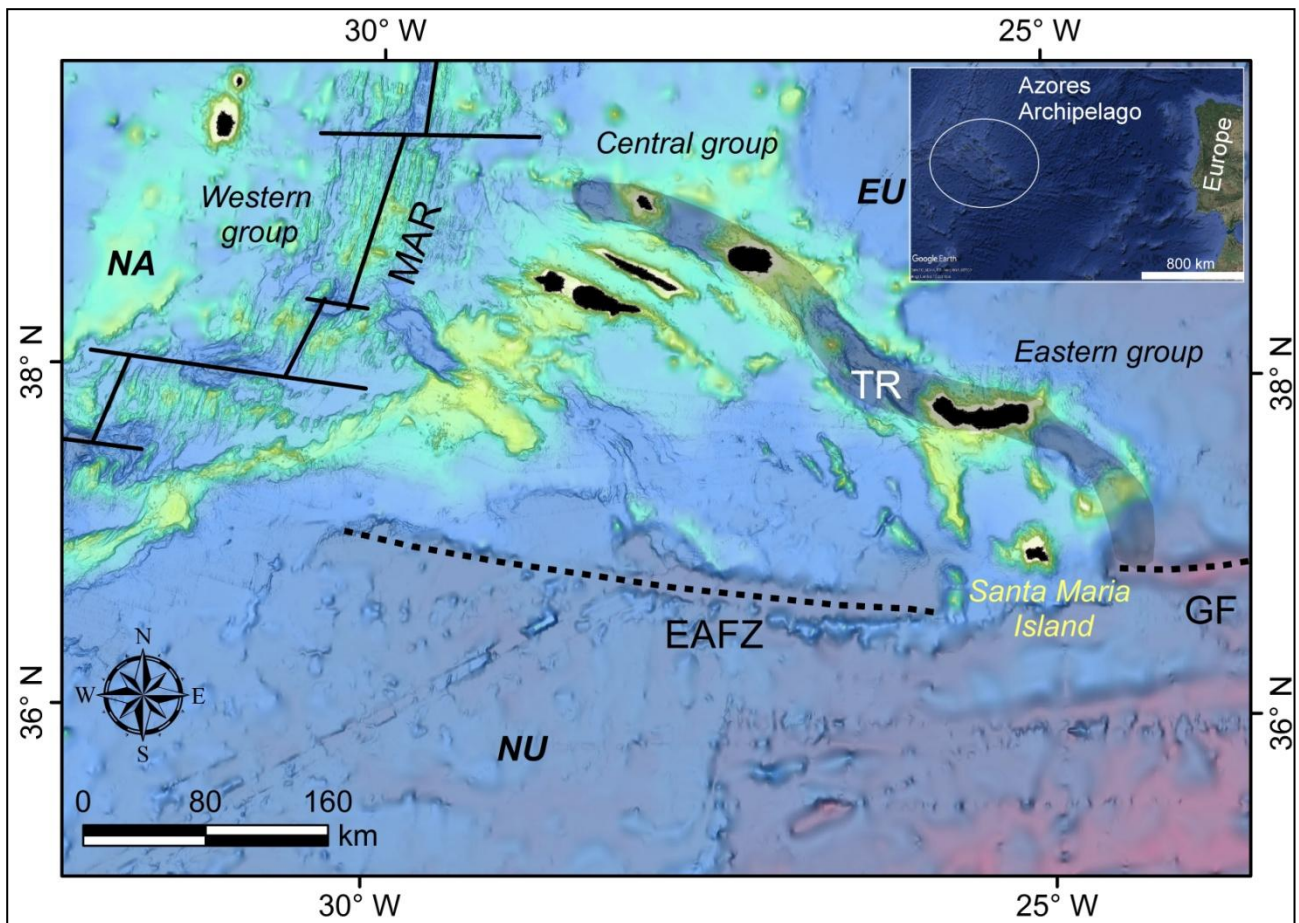

Figure 4.6 *Shaded relief map showing the geodynamic setting of the Azores Archipelago (islands in black).The upper right inset show the location of the Azores Archipelago within the North Atlantic Ocean. MAR: Mid-Atlantic Ridge; TR: Terceira Rift; EAFZ: Eastern Azores Fracture Zone; GF: Gloria Fault; NU: Nubian Plate; EU: European Plate; NA: North American Plate. For details see Manuscript V.*

4.2.1 Santa Maria Island

The island is situated on the eastern edge of the Azores Plateau, at the convergence between the TR, the GF and the EAFZ (Figure 4.6). Santa Maria Island is roughly elongated in E-W direction extending up to 15 km in length and 9 km in width. It is the emerged part of a larger volcanic edifice that rises from 2500 m depth. Its easternmost portion is the most elevated area, reaching 587 m above sea level at Pico Alto and is characterized by a rugged morphology with plunging cliffs up to c. 250 m high (Figure 4.7). On the contrary, the westernmost portion of the island is less steep and exhibits a set of raised marine terraces, giving it a staircase morphology progressively lowering westward (Ramalho et al., 2017, Figure 4.7). The geological evolution of Santa Maria is mostly known from its subaerial edifice, and it is inferred to extend from approximately 6 Ma to 2.8 Ma ago (Ramalho et al., 2017, Figure 4.7).

A complex intermittent volcanic history characterizes the evolution of the island. Products of the surtseyan and strombolian activity crop out on the western side of the island (Cabrestantes and Porto Formations, Figure 4.7), attesting the emergence of the island edifice from the sea. Then, the main building stages occurred between 5.8-5.3 Ma, 4.1-3.5 Ma and 3.2-2.8 Ma. The first stage formed a subaerial shield volcano (Anjos Volcanic Complex, Figure 4.7) that consolidated the island edifice. Then, for c. 1 Ma, erosive processes dominate, causing the partial or complete dismantling of the island edifice. During this period occasional, low-volume submarine volcanism was active in the central and western parts of the island (Touril Volcano-sedimentary Complex, Figure 4.7). Alternating vertical succession of submarine and subaerial volcanic products attests the renewal of the volcanic activity and the re-emergence of the island above sea-level at 4.1 Ma (Ramalho et al., 2017). During this stage, the island growth occurred mainly to the west and to east and culminated in the formation of the Pico Alto Volcanic Complex (Figure 4.7). At 3.5 Ma, the subsidence trend that characterized the island up to this point, reversed into uplift, as attested by the occurrence of raised (on the western side of the island) marine terraces (Ramalho et al., 2017). From 3.5 Ma onwards, the island has been mainly subjected to erosion, although a last stage of volcanism (3.2-2.8 Ma, Figure 4.7) led to the formation of a set of low-volume, monogenetic magmatic and hydromagmatic cones of the Feteiras Formation (Ramalho et al., 2017).
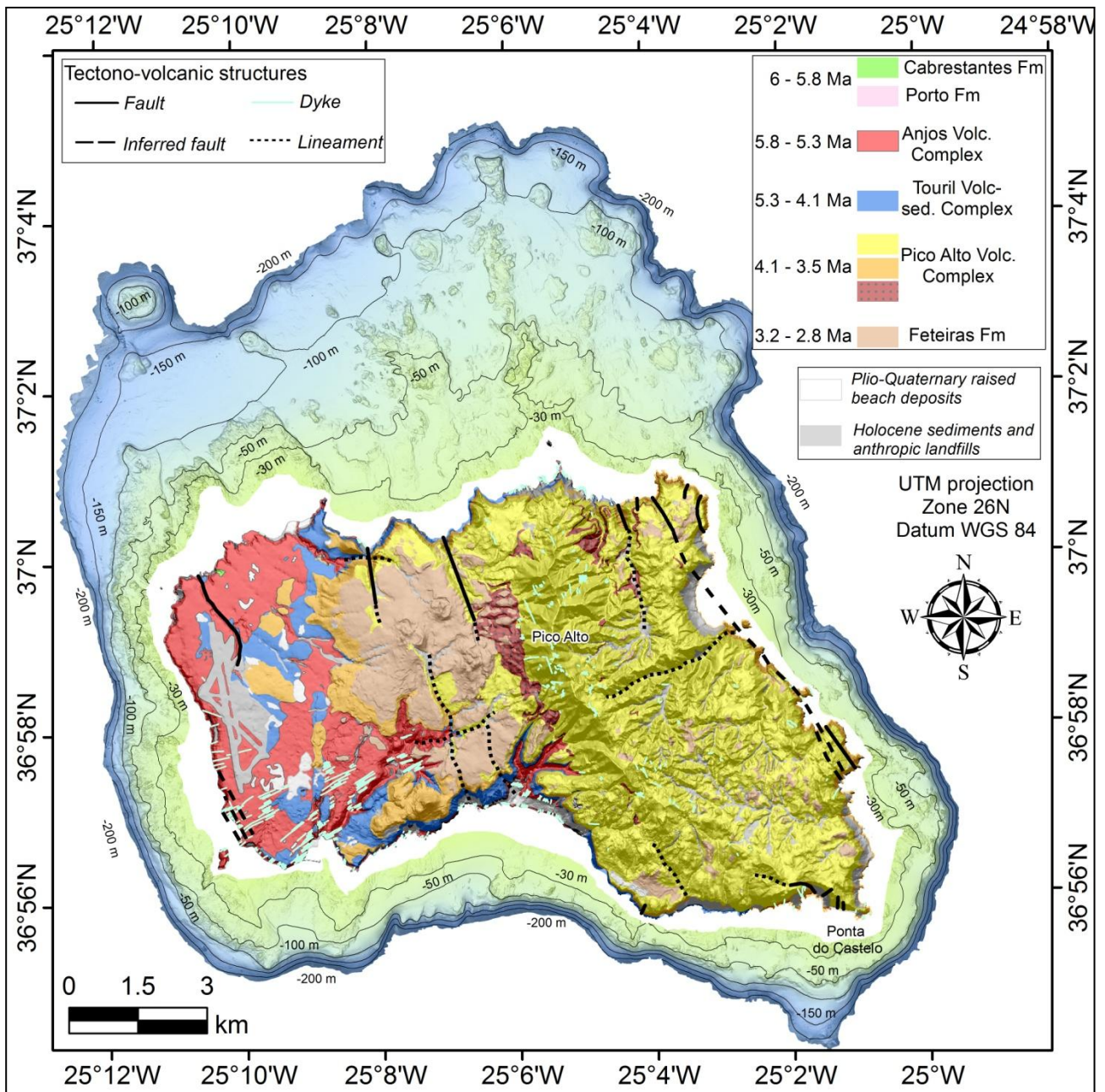
Figure 4.7 *Shaded relief map of the shelf around Santa Maria and geological map, merged on the DEM of the island generated from 1/5000 scale digital altimetric database. Modified after Ramalho et al. (2017).*

5. INSULAR SHELVES IN THE CENTRAL SECTOR OF THE AEOLIAN ARCHIPELAGO: MORPHO-ACOUSTIC CHARACTERIZATION, CONTROLLING FACTORS AND IMPLICATIONS FOR THE GEOLOGICAL EVOLUTION OF SALINA ISLAND

Although largely documented by Romagnoli, 2013 and Casalbore, 2016a, a detailed morphological analysis of the insular shelves around Salina Island has not been carried out before. Furthermore, due to scarce sampling and dating, the age of wide submarine portions of the volcanic edifices remains largely unknown, unlike the emerged portions for which accurate stratigraphic studies are available (Lucchi, 2009; Lucchi et al., 2004a; 2013a). The following manuscript investigates in detail the distribution and morphological differences of insular shelves around Salina and integrates the analysis of the shelf edge depths with the subaerial stratigraphy, in order to infer the relative chronology and development of the submerged portions of the island. The results of this study show that the morphological differences of the shelf surrounding a volcanic island are not simply due to a regular shelf width/age relationship (as suggested by Menard, 1983), but also to other local controlling factors that likely influenced the shelf development. Moreover, the integration of marine geophysical data with onshore field studies allowed investigating a better understanding of the evolution of Salina Island.

My contribution to this manuscript include dataset analysis and interpretation and writing.

5.1 Salina Island - Manuscript I

"Morpho-bathymetric and seismo-stratigraphic analysis of the insular shelf of Salina (Aeolian archipelago) to unveil its Late-Quaternary geological evolution"

Authors:
- Claudia Romagnoli (University of Bologna, Bologna – Italy)
- Daniele Casalbore (University of Rome – "La Sapienza", Rome – Italy)
- Alessandro Ricchi (University of Bologna, Bologna – Italy)
- Federico Lucchi (University of Bologna, Bologna – Italy)
- Rui Quartau (Instituto Dom Luiz, Faculdade de Ciencias, Universidade de Lisboa, Lisbon - Portugal)
- Alessandro Bosman (Instituto di Geologia Ambientale e Geoingegneria, Consiglio Nazione delle Ricerche, Rome - Italy)
- Claudio Antonio Tranne (University of Bologna, Bologna – Italy)
- Francesco Latino Chiocci (University of Rome – "La Sapienza", Rome – Italy)
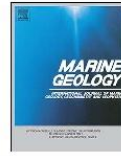
Morpho-bathymetric and seismo-stratigraphic analysis of the insular shelf of Salina (Aeolian archipelago) to unveil its Late-Quaternary geological evolution

C. Romagnoli[a,*], D. Casalbore[b,c], A. Ricchi[a], F. Lucchi[a], R. Quartau[d], A. Bosman[c], C.A. Tranne[a], F.L. Chiocci[b,c]

[a] University of Bologna, Dip. Scienze Biologiche, Geologiche e Ambientali, P.za Porta S. Donato 1, 40126 Bologna, Italy
[b] Sapienza Università di Roma, Dipartimento Scienze della Terra, Roma, Italy
[c] Istituto di Geologia Ambientale e Geoingegneria, Consiglio Nazionale delle Ricerche, Area della Ricerca Roma 1, Montelibretti, Via Salaria Km 29,300, Monterotondo, Roma, Italy
[d] Instituto Dom Luiz, Faculdade de Ciencias, Universidade de Lisboa, Lisboa, Portugal

ARTICLE INFO

ABSTRACT

The distribution and morphological characteristics of the shelves around Salina Island have been analyzed and integrated with observations from onshore geological field studies in order to improve knowledge about its evolution, and to demonstrate how shelf width/depth can be used as proxies for reconstructing the development of the volcanic edifice. Insular shelves form essentially through marine erosion of volcanic centres during stages of reduced or inactive volcanism, and are representative of their original extension. Shelves having larger widths (commonly > 1000 m) and deeper edges (over 125 m depth) experienced wave erosion during successive cycles of sea-level fluctuations and subsidence after their formation, thus being indicative of a relatively older age of the eroded volcanic centres. Accordingly, we document offshore Salina the occurrence of presently submerged and largely dismantled volcanic centres (namely Pizzo Capo North and Fossa delle Felci South) predating the oldest subaerial products exposed on the adjacent coastal sectors. These offshore centres have subsided after their erosion and are no more documented on land. Furthermore, the finding of the largest and deepest shelf around the subaerial remnants of Pizzo di Corvo volcanic edifice allows relating it to an earlier stage of evolution of Salina, shedding light on contradictory radiometric ages on land. Narrower shelves (commonly < 1000 m) indicate a lower evolutionary maturity with respect to the larger ones; they are, in fact, formed along the sectors of the island where younger volcanic products are exposed, such as to the north and south of Monte dei Porri. The depths of the shelf edges, mostly at − 110 m (in the areas not affected by later mass-wasting), suggest that these coastal sectors were relatively stable or even slightly uplifted after erosion during Last Glacial Maximum. Moreover, several interacting factors (such as lithology of volcanic products, fetch and exposure to prevailing storms, degree of submarine erosion, relative sea level changes) have been taken into account to explain the morphological setting of the different shelf and coastal sectors of Salina.

On the whole, our results show the importance of integrated field and marine studies to unravel the geological evolution of insular volcanoes and to obtain inferences on their vertical mobility.

1. Introduction

Salina is the highest (962 m) of the volcanic Aeolian Islands (Southern Tyrrhenian Sea) and represents the emerged culmination (~16% of the total extension) of a larger volcanic edifice that emerges from the seafloor at − 1300 m (Romagnoli et al., 2013; Casalbore et al., 2016a). Its subaerial volcanism developed between ~244 ka and 15.6 ka through the activity of different stratovolcanoes interrupted by

prolonged periods of dormancy and sudden volcano-tectonic collapses. Although its subaerial development is considerably well-constrained (Keller, 1980; Lucchi et al., 2013a), the submarine growth and the older stages of the geological evolution of Salina are still poorly understood.

In this study, the shallow-water and coastal portions of Salina are analyzed and integrated with field studies of the subaerial flanks of the volcanic edifice, in order to improve our knowledge about its evolution. The occurrence of submerged shelves around Salina is documented

---

(Romagnoli, 2013; Casalbore et al., 2016a), but these features were not studied with detail. They are formed by sea level fluctuations and concurrent marine erosion of the volcanic centres, especially during stages of reduced or inactive volcanism, thus playing a potential role for paleo-morphological and relative age reconstructions if integrated with the relative chronology of the products outcropping on land. Submerged shelves commonly surround insular and coastal volcanoes in different geodynamic settings (Ablay and Hurlimann, 2000; Mitchell et al., 2003; Le Friant et al., 2004; Llanes et al., 2009; Quartau et al., 2010). The association of larger and deeper shelves with the older portions of the volcanic edifices is supported by several papers in the literature (among which Menard, 1983; Mitchell et al., 2003; Llanes et al., 2009) and is based on the commonly accepted assumption that shelf width reflects the cumulated erosive action of waves over different relative sea-level fluctuations. A number of case studies (well documented in the Azores islands, see Quartau et al., 2010, 2012, 2015, 2016 and in other Aeolian islands, see also Romagnoli, 2013) proved that, where erosion dominates over volcanism, the shelf width can be used as a proxy of the relative age and original extension of the corresponding subaerial volcanic edifices and allow reconstructing their areal extent prior to marine erosion. Moreover, the depth of erosive shelf break can be related to the paleo sea-level at the moment of its formation as a tool to assess the vertical movements of the corresponding volcanic edifice that have occurred after its erosion (Quartau et al., 2014, 2016).

Salina is considered a good case-study to assess the relative role of different geological and oceanographic factors in controlling the evolution of a volcanic island because its coastal sectors are characterized by different i) overlapping volcanic centres, ii) ages of exposed products on land, iii) dominant lithologies (different ratios of lavas vs pyroclastics) and iv) degree of wave exposure. Therefore, we assessed the role of these local factors on the development and morphology of different coastal and shallow-water sectors of the island, in order to discriminate which of them allow better constraining the evolution of the island.

2. Geological background

Salina Island lies in the centre of the Aeolian Archipelago (Fig. 1, inset), at the intersection between its arc-shaped structure and the NNW–SSE elongated Salina–Lipari–Vulcano volcanic belt that corresponds to the major Tindari–Letojanni strike-slip fault system (see Ventura, 2013 for a review). Salina is dominated by the Monte Fossa delle Felci and Monte dei Porri stratovolcanoes, with the older volcanic edifices of Monte Rivi, Pizzo Capo and Pizzo di Corvo deeply eroded and collapsed (Fig. 1).

The volcanic history of Salina has been described by Lucchi et al. (2013a) relying on the radiometric ages of Keller (1980), Gillot (1987), Calanchi et al. (1987) and Leocat (2011). The subaerial part of the island has grown since ~244 ka through six successive eruptive epochs (EE) interrupted by prolonged periods of volcanic quiescence, subaerial erosion, and by recurrent episodes of sea level ingression leading to the formation of raised marine terraces attributed to the marine oxygen isotope stage (MIS) 7 and 5 (Keller, 1980; Lucchi et al., 2013a, 2013b). The strongly dismantled Pizzo di Corvo stratocone in the western side of the island (Fig. 1) has an uncertain stratigraphic position and radiometric age (Lucchi et al., 2013a). However, it has been generally considered as one of the oldest volcanic centres of Salina based on the high degree of erosion and a basaltic composition similar to the early products of the island (Keller, 1980; Gertisser and Keller, 2000). We follow that assumption based on the above evidence, although recent K/Ar ages of 163–110 ka, with high analytical errors, have been recently proposed by Leocat (2011). The stratigraphically oldest exposed products of Salina are basaltic lava flows and strombolian scoriae of the NE–SW-elongated Pizzo Capo composite volcano (EE1–2, 244–226 ka, Fig. 1) in the NE sector of the island. Marine erosion of the early

volcanic edifices during MIS 7.3 (Lucchi et al., 2013a) is recorded by marine terrace deposits (paleoshoreline A) discontinuously recognized along the northern coastal cliffs (dark blue dots at the coastline in Fig. 1), at elevations varying between 10 m a.s.l. and the present sea level. Renewed activity shifted to the central-southern sector of Salina, where the stratocones of Monte Rivi and Monte Fossa delle Felci were constructed by basaltic to dacitic pyroclastic successions and lava flows (EE3–4, 160–121 ka, Fig. 1). These volcanic edifices, together with the Pizzo Capo volcano, are cut by prominent and laterally-extended terraces (light blue dots at the coastline in Fig. 1) attributed to the Last Interglacial, with inner margins at elevations of c. 50 m (paleoshoreline I, MIS 5e, 124 ka), 25–30 m (paleoshoreline II, MIS 5c, 100 ka) and 10–12 m a.s.l. (paleoshoreline III, MIS 5a, 81 ka). Younger volcanic activity in western Salina built up the basaltic-andesitic to andesitic Monte dei Porri stratovolcano (EE5, 70–57 ka; Fig. 1). The successive period of quiescence was characterized by deposition of thick successions of pyroclastic layers from outside Salina, mostly represented by the Brown Tuffs from Vulcano and the Ischia Tephra (Lucchi et al., 2008, 2013a). These were interlayered with epiclastic horizons derived from erosion and mass-wasting of the existing volcanic edifices, particularly along the northern and eastern coastal areas. The last phase of activity is at the Pollara crater located in the NW corner of Salina along the northern rim of a flank collapse affecting the Monte dei Porri edifice (Fig. 1). This crater produced the andesitic Punta di Perciato lava flows and widespread rhyolitic pumiceous successions (EE6, 30–15 ka).

The raised marine terraces along the coasts of Salina are the result of the interaction between the major Late-Quaternary interglacial high sea-level peaks and long-term vertical crustal movements during the Late Quaternary (Lucchi et al., 2004, 2013a, 2013b). In particular, the MIS 5 terraces are found in a downstepping suite with the older terraces lying at higher elevations, reflecting an uplift of the island at almost constant rates from the Last Interglacial (0.35/0.37 m/ka), comparable to those estimated for Lipari and Filicudi (Lucchi, 2009). Instead, the MIS 7.3 terrace provides evidence of a subsidence affecting the early Salina before the Last Interglacial (Lucchi et al., 2013a).

3. Insular shelves and submarine depositional terraces in the Aeolian Islands

Insular shelves are common features around the Aeolian Islands (Chiocci and Romagnoli, 2004; Romagnoli, 2013). They constitute gently sloping erosive surfaces carved in the volcanic flanks of the islands, extending from the coastline to the shelf break, the latter marking a sharp increase in gradient passing to the submarine slopes of the islands (typically < 12° steep, up to 20° in some cases). In all the islands, the wider shelves are commonly found off sectors where the older volcanic products and centres are located, thus indicating that these coastal sectors experienced extensive wave erosion processes during successive cycles of sea-level fluctuations (Romagnoli, 2013). Consistently, the narrower shelves are found adjacent to sectors where younger volcanic products crop out, thus reflecting the exposure to fewer cycles of marine erosion.

The erosive surfaces of insular shelves are generally covered by volcaniclastic sediments organized in a set of submarine depositional terraces (hereafter named SDTs), with a wedge-shaped geometry and internal prograding structure (Chiocci and Romagnoli, 2004). Different orders of SDTs are recognized on the shelves around the Aeolian Islands, with their depositional edges typically located at depths between −10 m and −120 m. Their formation is due to seaward transport of sand from the surf zone and shoreface during storms, similarly to other sand-rich infralittoral prograding wedges observed on insular and continental shelves (Field and Roy, 1984; Hernandez-Molina et al., 2000; Chiocci et al., 2004; Quartau et al., 2010, 2014, 2015; Mitchell et al., 2012). The shallowest (near-shore) SDT has a depositional edge at depths between −10 m and −25 m, approximately corresponding to the modern, local storm-wave base level (Chiocci and Romagnoli,
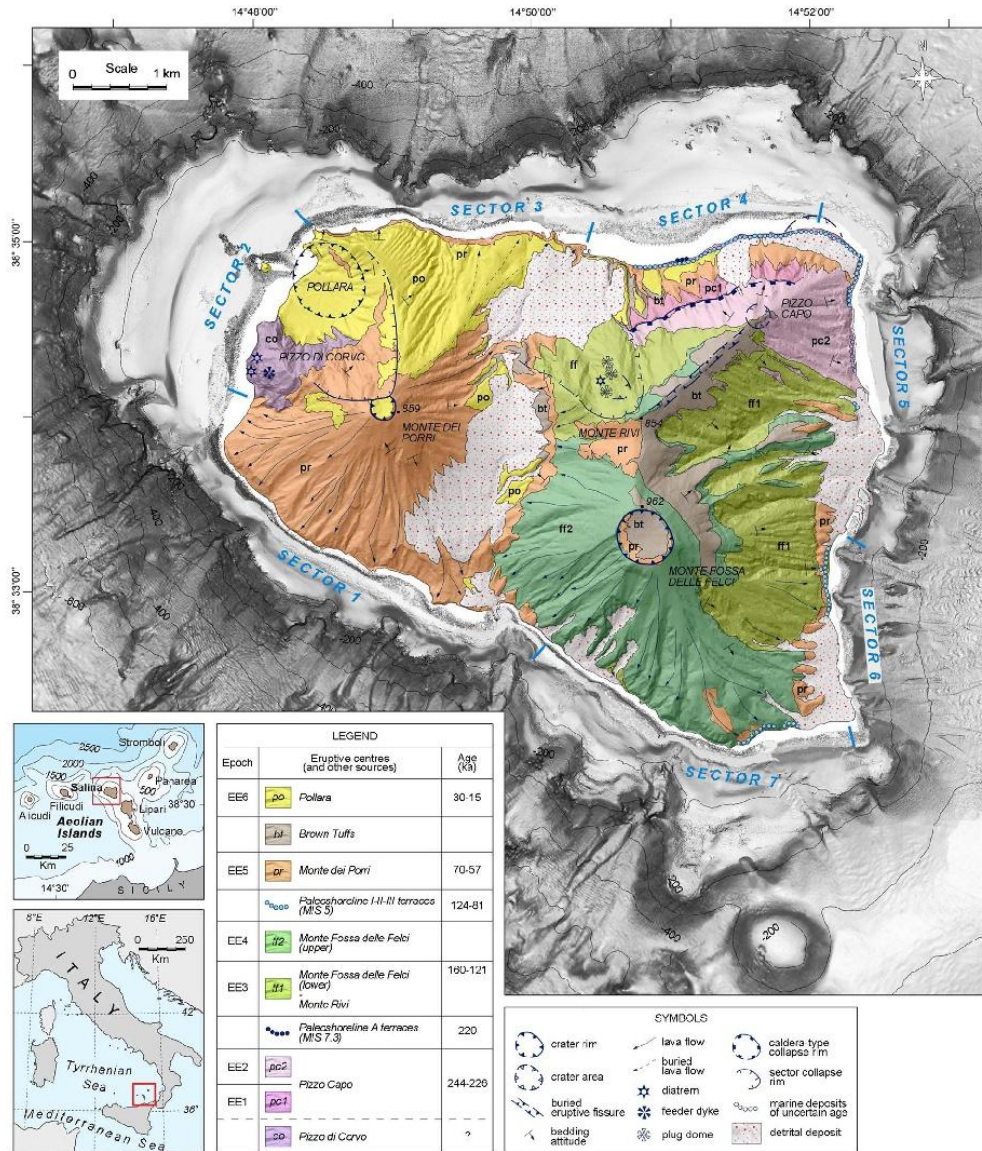
Fig. 1. Simplified geological map of Salina showing main volcanic centres and eruptive epochs, and morpho-structural features, merged on a shaded-relief DEM of the island and submarine shallow-water portions. Elevation is in metres above/below sea-level, respectively. The coastal and shelf areas have been divided into seven sectors, described in the text and represented in the following Figs. 3, 5, 6, 7, 9, 10 and 11. In the lower left panel: location of the Island of Salina in the Aeolian archipelago in the southern Tyrrhenian Sea. (For interpretation of the references to color in this figure, the reader is referred to the web version of this article.)
(Modified from Lucchi et al., 2013a)

2004). The deeper SDTs have the same genesis, but during periods when sea level was stable and lower than the present after Last Glacial Maximum (LGM) (Casalbore et al., 2017b).

The formation of SDTs can be also affected by wave exposition and fetch of related coastal sectors (Casalbore et al., 2017b). The most energetic wave climate approach in the Aeolian Islands is from westerly directions, since prevailing winds are from the NW or the W (Cicala, 2000). The western flank of Salina is exposed to storms coming from the

Tyrrhenian Sea, with a typical fetch of 250–300 nautical miles and waves up to 6 m (Cicala, 2000). Winds from the SE also affect the southeastern and eastern side of the Aeolian Islands, mainly during the autumn and winter. In the case of Salina, however, this effect is reduced in the southwestern sector due to the sheltering effect of the nearby island of Lipari (Fig. 1, inset).

36

4. Data and methodological approach

High-resolution multibeam bathymetric data on the submarine portions of Salina Island have been acquired since 2001 by CNR-IGAG (Consiglio Nazionale delle Ricerche, Istituto di Geologia Ambientale e Geoingegneria), University of Rome (Sapienza) and University of Bologna. Surveys were carried out mainly aboard the R/V *Urania* and *Thetis* (CNR), using multibeam systems working at frequency from 50 to 100 kHz according to the surveyed bathymetric range, using a differential GPS position system. A small boat has been used to survey the shallow-water areas with Teledyne Reson 7125 (400 kHz) multibeam system, using GPS-RTK positioning (see details in Bosman et al., 2015) and a local tide gauge station referenced to the Italian national tide gauge network (www.mareografico.it) for depth correction. Sound velocity probe correction and patch test in areas close to the survey area were daily acquired on flat and steep targets to increase the accuracy of the depth measurements. Multibeam data were processed using Caris Hips & Sips to produce high-resolution Digital Elevations Models (DEMs) in the UTM projection, zone 33, WGS84. The cell-size varies from 0.5 m in shallow water (< −100 m) to 25 m (at over −1300 m). The vertical accuracy of the DEMs in shallow water is 0.1 m, while for the deeper data the accuracy is about 0.5 m. The DEM of the island (0.4 m-cell size) was obtained through LiDAR flights data of Italian Ministry for the Environment, Land and Sea.

The shelf width and depth of the shelf break in each sector were determined from the bathymetric data using Global Mapper 15 software (Blue Marble Geographics), along 400 transects plotted at 50 m intervals from the shoreline to the shelf edge, as perpendicularly as possible to these features (Fig. 1 in Electronic Supplementary Material, ESM). Fig. 2 shows selected topo-bathymetric sections for each of the studied sectors, with indication of main morphological features.

Bathy-morphological data are integrated with a grid of 80 high-resolution seismic profiles transversal to the shelf interpreted with the software Kingdom 8.8 (HIS Kingdom Geophysics). Seismic profiles provide information on the morpho-structural setting of the shelf and the position and depth of the erosive shelf edge. This information is particularly relevant because deposits younger than the LGM frequently cover the erosive shelf surface. A sound velocity of 1500 m/s has been adopted for the conversion from milliseconds to metres in the seismic profiles. Seismic data were acquired in different stages: a specifically-planned survey on board the catamaran *Incaurina Marianna* was carried out in 1993 through a Sparker 0.5–1 kJ; positioning was obtained using a non-differential GPS, periodically calibrated from a ground-base station. A more accurate relocation of seismic profiles was obtained through the homologous matching of features observed on seismic profiles and multibeam bathymetry. A recent acquisition of new seismic profiles (Sparker 0.5–1.5 kJ) around Salina Island has been performed in 2016 aboard the R/V *Minerva1* (CNR), where data were positioned using a differential GPS. The vertical resolution of Sparker profiles is in the order of few metres due to the emitted frequency and to the ringing
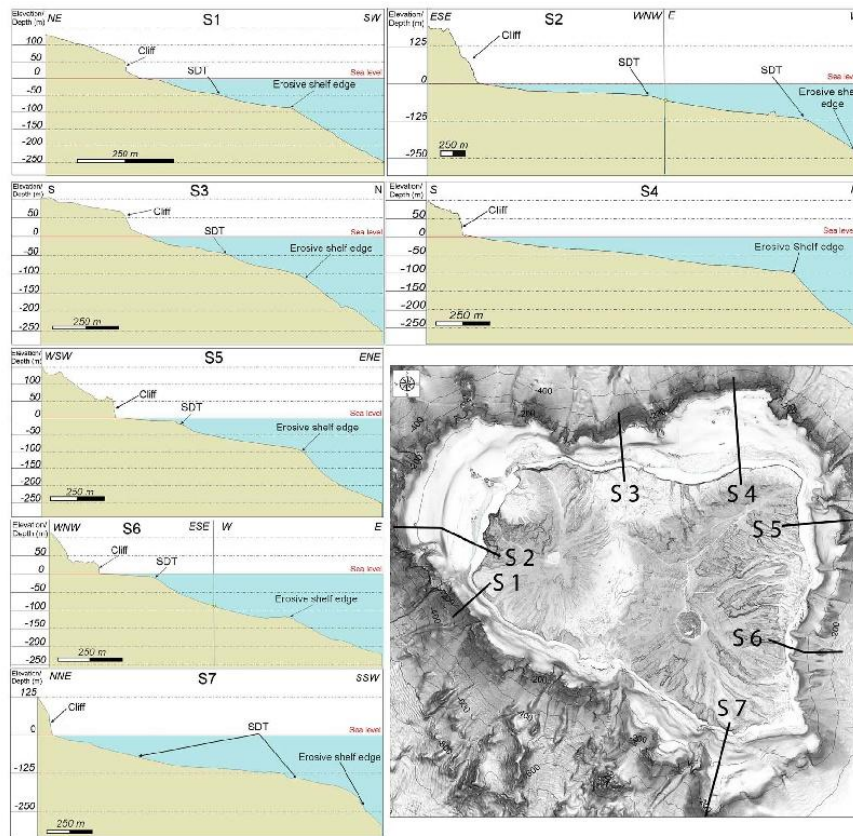

Fig. 2. Topo-bathymetric cross sections across the sub-aerial and submerged flanks of Salina in the different sectors (S1, S2, S3, S4, S5, S6 and S7). Location of cross sections in the lower right shaded-relief DEM map as black lines.

Table 1
Maximum shelf width, depth of the edge and cliff height in the different sectors identified at Salina Island. Shelf measurements (in metres) refer only to areas not affected by erosion.

	Sector 1	Sector 2	Sector 3	Sector 4	Sector 5	Sector 6	Sector 7
Shelf width	1111	2048	963	1730	895	721	1691
Depth of the edge	123	226	125	147	127	127	212
Cliff height	87	143	69	91.5	65	26	89
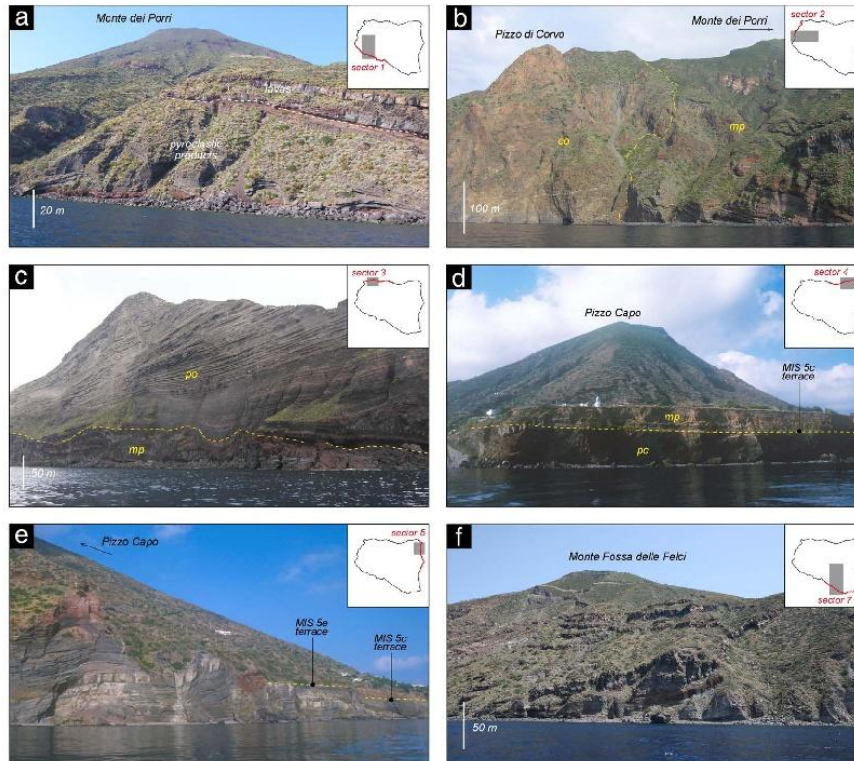
Fig. 3. Outcrop photographs of the sea cliffs in different sectors of Salina Island (see location in the upper right insets): a) sea cliff cut into lavas and pyroclastic products along the southern flank of the Monte dei Porri stratocone (Sector 1); b) panoramic view of the steep cliff cutting the remnants of the Pizzo di Corvo volcano (co) in southern Sector 2. Pizzo di Corvo is unconformably covered by lavas and pyroclastics of Monte dei Porri (mp); c) steep cliff carved into the Monte dei Porri lavas (mp) and overlaid by Pollara pyroclastic products (po) in western Sector 3. A clear gradient change is induced by the different erosion degree due to different lithology and age of the volcanic products; d) subvertical and rectilinear cliff cutting the Pizzo Capo volcanic products (pc) in Sector 4, northern coast of Salina. These products are truncated by the raised (subhorizontal) marine terrace attributed to MIS 5c (paleosealevel ~ 25–30 m), which is sealed by a thick volcaniclastic succession consisting of Monte dei Porri primary and reworked deposits (mp); e) steep irregular cliff cutting the (scoriaceous) pyroclastic products of Pizzo Capo in Sector 5, northeastern coast. These are cut by terraces attributed to MIS 5c (paleosealevel ~ 25–30 m) and MIS 5e (paleosealevel ~ 50 m); f) sea cliff carved into the lavas and (minor) pyroclastic products of the southern flank of Monte Fossa delle Felci (Sector 7).

effects. The uncertainty in the definition of the shelf edge depth through the integration of bathymetric and seismic data can be estimated in the order of some metres. Graphs and a table (Table 1) with measured values are given for the different coastal sectors. We always take into account the maximum values of shelf widths (measured from the coastline to the shelf break) and shelf edge depths in our interpretation. We use this approach because later retrogressive erosion can shift the insular shelf edge coastward, resulting in narrower shelves and depths up to tens of metres shallower than on uneroded areas.

The coastline morphology is concurrently analyzed for each sector of Salina Island, so the height of the marine cliff (when preserved) is measured along the plotted transects (Fig. 1 in ESM). In case of composite cliffs, formed by both marine and subaerial erosion, we considered only the height of the lower part of the cliff, actively shaped by marine processes, which is generally defined by a gradient change

above the marine-eroded part of the cliff top (Figs. 2 and 3).

5. Results

The insular shelves around Salina Island have variable widths and edge depths (Figs. 1 and 2 and Table 1). These morphological differences (and the relative age of the adjacent onshore volcanic products) were used to divide the coastal and shelf areas into seven main sectors, numbered in clockwise direction starting arbitrarily from the southern flank of Monte dei Porri (Fig. 1). Description of the morpho-structural features of each sector is provided below, together with the available information on the stratigraphy and age of the facing subaerial flanks of the island.
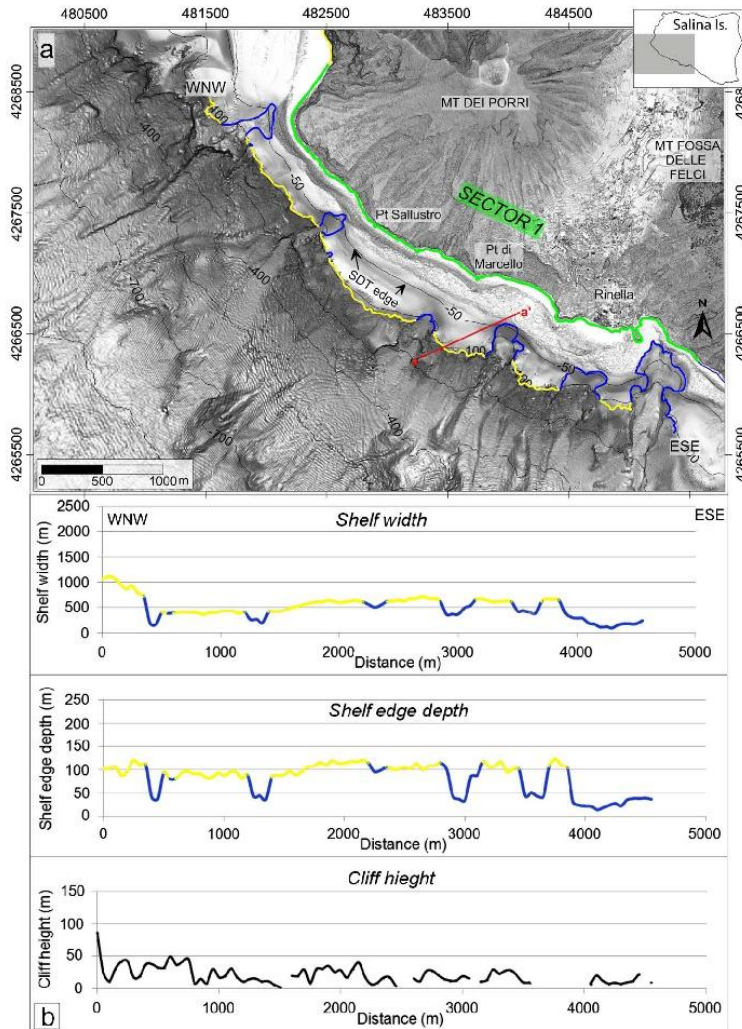
Fig. 4. Map of shelf Sector 1 (a) and graph of shelf width, shelf edge depth and cliff height measurements (b). In (a), the red line shows the location of the seismic profile aa′ in Fig. 5. The yellow line in (b) represents the shelf edge preserved by erosion, the blue line corresponds to areas where the shelf edge has been eroded by canyon heads or slides scars. MT: Monte. (For interpretation of the references to color in this figure legend, the reader is referred to the web version of this article.)

5.1. Sector 1

This sector runs aside the SW part of the island to the south of Monte dei Porri stratocone (EE5), which is constituted by a succession of andesite blocky lava flows and pyroclastic deposits dated as 70–57 ka (Fig. 1). The coastline is irregular in plan-view and conditioned by the morphology of the lava flows descending along the slopes of Monte dei Porri, especially around Rinella (Fig. 4a). Some sea cliffs are higher and heavily carved in the more erodible pyroclastic successions around Punta di Marcello (Fig. 3a). The coastline becomes more regular to the NW, where high cliffs (commonly > 40 m, up to > 80 m high, see Fig. 3a and Table 1) follow the tongue-like morphology of the youngest lava flows coming from the summit of the edifice.

The shelf is WNW-ESE oriented parallel to the coast (Fig. 4a). Its width is constantly between 400 and 650 m (S1 in Fig. 2), except for a sharp increase at the northwestern side passing to Sector 2 (up to a maximum value of 1111 m; see Table 1). The shelf edge is generally located at depths lower than −125 m, mostly around −110/115 m

(Figs. 4b and 5, profile aa′; Table 1). There is a good correspondence between the trend of shelf width and edge depth. The narrower shelf areas normally correspond to shallower edges, which are the result of erosive landslide scars and canyon heads. A major submarine canyon head delimits the southeastern border of Sector 1, in front of Rinella, as the continuation below sea level of the valley representing the morphological limit between Monte dei Porri and the adjacent (older) Monte Fossa delle Felci stratocone (Fig. 4a). Also the other subaerial erosive gullies along the southern flank of Monte dei Porri are mostly aligned with the canyon heads offshore, although nearshore deposits probably hide their natural prolongation. The erosive shelf is quite flat in this area and is covered by sediments organized in a single SDT, having a depositional edge at depths between −40 m and −55 m (S1 in Fig. 2; Fig. 4a and profile aa′ in Fig. 5). This sedimentary wedge tapers seaward, where the edge of the erosive shelf just corresponds to the break-in-slope recognizable on the bathymetry.
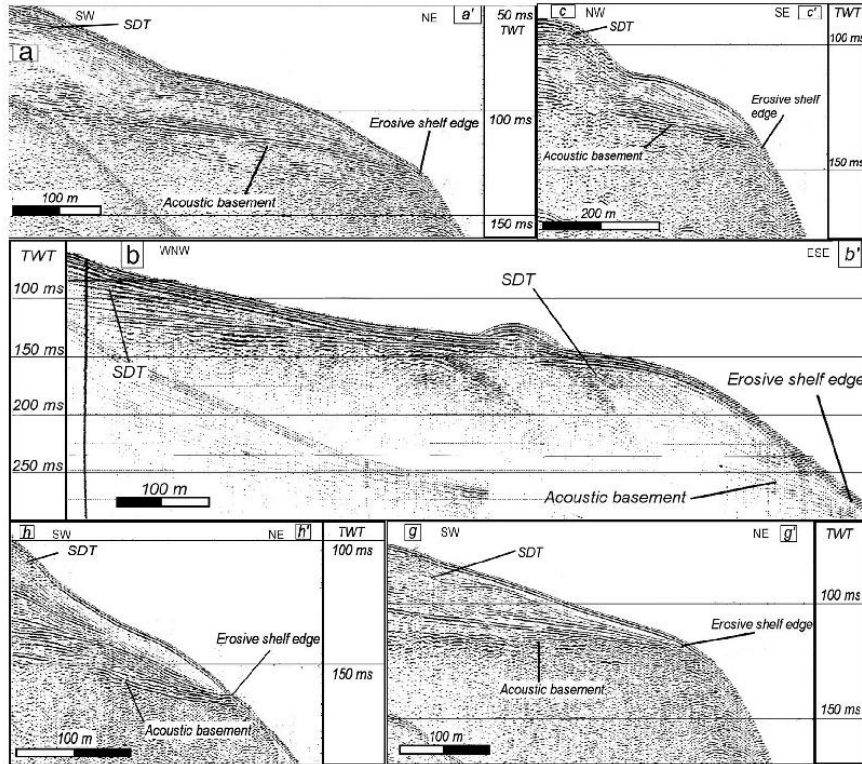
Fig. 5. Seismic (0.5 kj Sparker) profiles, showing the erosive shelf edge and one or more SDT lying above the acoustic basement. aa′: from shelf Sector 1, location in Fig. 4; bb′: from shelf Sector 2, location in Fig. 6; cc′: from shelf Sector 3, location in Fig. 7; gg′: from shelf Sector 5, location in Fig. 10; hh′: from shelf Sector 6, location in Fig. 11.

5.2. Sector 2

This sector runs aside the NW side of the island (Fig. 6a), offshore the Pizzo di Corvo edifice and Pollara crater. The coastline is irregular and roughly NNE-SSW oriented, with cliffs ranging from a few metres to 143 m (Table 1). The highest cliffs are observed in the southern part of this sector carved in the basalt lavas and dykes of the Pizzo di Corvo stratocone and exposing its deeply eroded inner portion (S2 in Fig. 2, Figs. 3b, 6a and b). This largely dismantled stratocone is considered one of the oldest volcanic centres onshore (Section 2). In the rest of Sector 2, the cliffs are carved into the andesite to rhyolite pyroclastic successions of the Pollara crater, the youngest centre in the history of Salina (EE 6, age 30–15.6 ka, Fig. 1; Lucchi et al., 2013a). Particularly, there is an up to 70–80 m high subvertical cliff carved into reworked Pollara products, which is cut by some hanging valleys.

The submerged shelf has a semicircular shape running parallel to the coastline. Its width is fairly constant at values > 1500 m (up to ca. 2050 m) in most of Sector 2 (S2 in Fig. 2, Fig. 6b), becoming narrower towards the NE and SW borders. To the SW, the shelf width decreases down to < 1000 m due to erosion along a wide submarine canyon affecting the outer shelf up to its head at depths of −85 m. Although covered by shallower SDT deposits, this submarine canyon is assumed as the offshore continuation of the large valley found between the Pizzo di Corvo edifice and the stratigraphically-younger Monte dei Porri stratocone. Apart from the eroded areas, the erosive shelf edge is invariably found at high depths, ranging from −141 m down to a maximum of −226 m (the deepest around the entire Salina Island) right in front of the eroded Pizzo di Corvo edifice (Fig. 6b and Table 1). The

entire geometry of the erosive shelf is difficult to reconstruct based on the available seismic profiles, because of the thick and continuous sedimentary cover (profile b–b′ in Fig. 5). This latter is organized in two partially juxtaposed SDTs, with depositional edges located roughly at −45 m and −120 m (Fig. 6a). The edge of the shallower SDT is well recognizable all along the Sector 2, except for the submarine ridge emerging in the Scoglio Faraglione rock, representing the marine continuation of the Punta di Perciato lava flows (PP lava flow in Fig. 6a) related to the early Pollara activity. The edge of the deepest SDT is mainly recognizable in the southern part of the sector, where the seismic profile bb′ (Fig. 5) shows clearly the prograding geometry of this sedimentary wedge. Differently, the thickness and preservation of the deepest SDT is smaller in the northern part of the sector, where it is largely affected by later mass-wasting processes (blue lines in Fig. 6a).

5.3. Sector 3

This sector runs aside the northern side of Salina to the west of Malfa (Fig. 7a), off the northern slopes of Monte dei Porri stratocone (Fig. 1). The coastline is irregular and roughly W-E oriented, mostly following the morphology of the main lava flows originated from the summit crater of Monte dei Porri. The marine cliffs are generally carved in the Monte dei Porri lavas with variable heights from 11 m to 69 m (S3 in Fig. 2, Fig. 7b) and are overlaid by the Pollara pyroclastic successions emplaced above the Monte dei Porri lava flows and affected by intense subaerial erosion (Fig. 3c).

The shelf is very irregular, roughly following a W-E trend around the coastline. It is wider in the eastern (in front of Guardiano del Porto)
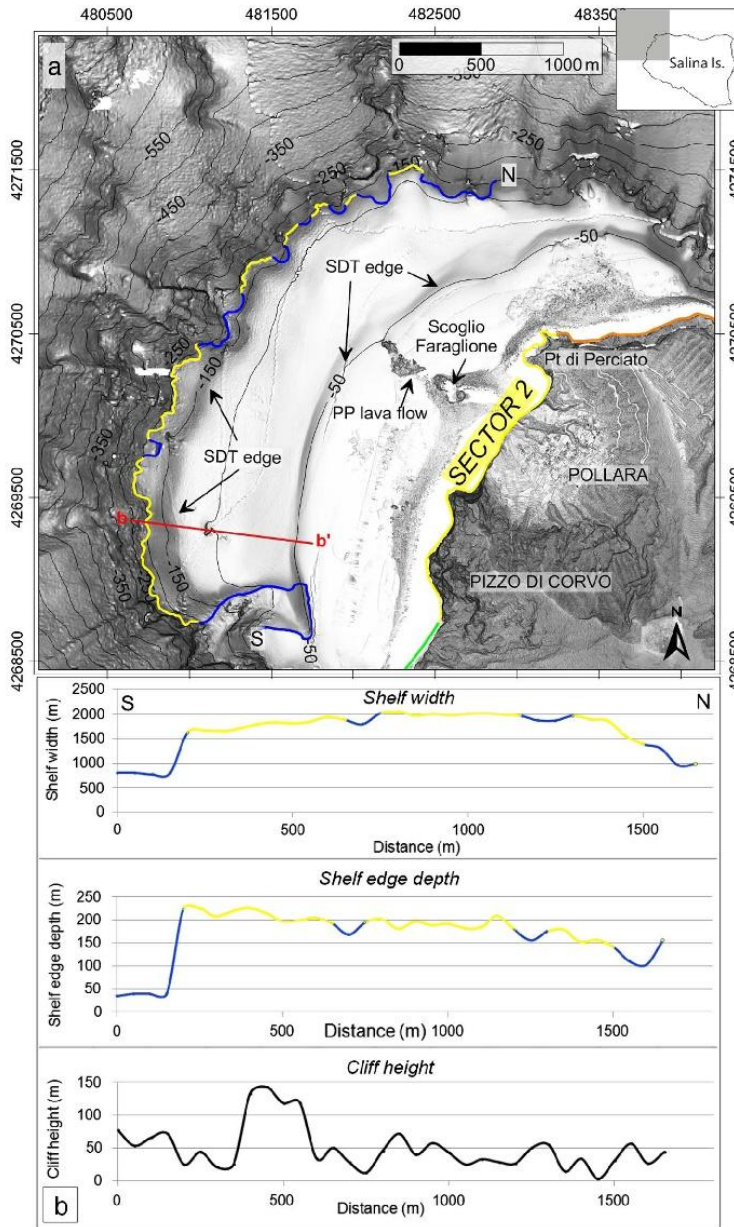
Fig. 6. Map of shelf Sector 2 (a) and graph of shelf width, shelf edge depth and cliff height measurements (b). In (a), the red line shows the location of the seismic profile bb′ in Fig. 5. The yellow line in (b) represents the shelf edge preserved by erosion, the blue line corresponds to areas where the shelf edge has been eroded by canyon heads or slides scars. Pt: Punta; PP: Punta Perciato. (For interpretation of the references to color in this figure legend, the reader is referred to the web version of this article.)

and western (to the west of Punta Fontanelle) portions of Sector 3, up to maximum values of ~960 m (Fig. 7b and Table 1). In contrast, the shelf narrows in the central portion (from Punta Fontanelle to Guardiano del Porto) with values mostly around 500 m down to a minimum of 372 m in the areas where the shelf edge was eroded by canyon heads (Fig. 7b and Table 1). The shelf edge is, in fact, affected by erosive features that dismantled part of the shelf reducing its width, especially in front of Punta Fontanelle (Fig. 7a). There are no clear relationships between the submarine erosive features and morphological lineaments onshore. The depth of the shelf edge is in the range of − 95/− 125 m, mostly around − 110/− 115 m (Fig. 7b). Similarly to Sector 1, seismic profiles allow to define the geometry of the erosive shelf, covered by a main SDT with depositional edge between depths of − 35 and − 50 m (Fig. 7a and profile cc′ in Fig. 5). This sedimentary cover tapers seaward, where the edge of the erosive shelf just corresponds to the break-in-slope recognizable on the bathymetry.
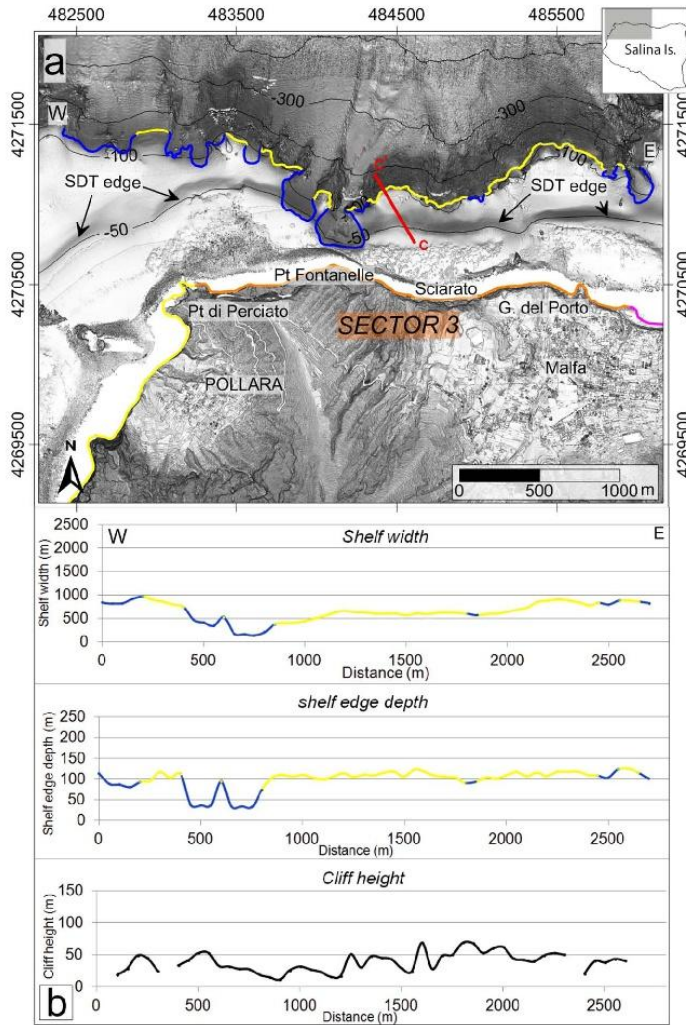
5.4. Sector 4

This sector runs along the northern coast of Salina, to the north of the Pizzo Capo composite volcano (Fig. 8a). This is a NE–SW-elongated volcano constructed by basaltic lava flows and strombolian scoriae dated to 244–226 ka (EE1–2, Fig. 1), interlayered with the marine terraces attributed to MIS 7 and MIS 5. The coastline has a regular, roughly E-W oriented profile shaped by marine erosion. The sea cliff is steep and sub-vertical (up to 91 m), carved into the Pizzo Capo products; these latter are cut by the marine terrace deposits of paleoshorelines II (MIS 5c, 100 ka) and III terrace (MIS 5a, 81 ka) cropping out at elevations from ~25 m down to the present sea level (Fig. 3d). Above the terrace, a ten-of-metres thick volcaniclastic succession of primary and reworked products of Monte dei Porri is affected by intense sub-aerial erosion processes cutting some hanging valleys perpendicular to the coast. In the western part of Sector 4, between Galera and Quartarolo (Fig. 8a), the older marine terrace deposits of MIS 7.3

(paleoshoreline A, 220 ka, Fig. 1) are visible at elevation of 0–5 m a.s.l., cut into brecciated lavas of the Pizzo Capo volcano and stratigraphically located below the MIS 5a terrace, with interlayered lavas and reworked deposits.

The shelf in this sector has a roughly semicircular shape and is mostly wider than 1500 m wide (S4 in Fig. 2), becoming narrower at both sides where it is indented by landslide scars (Fig. 8a). The maximum shelf width up to 1730 m is located where a submerged rocky outcrop appears off Quartarolo (see Table 1). In this area the depth of the shelf edge reaches a maximum value of −147 m (Table 1; Fig. 8b, profile d–d′ in Fig. 9). It is deeper than −120 m in the western part of the sector and becomes shallower to the east, reaching depths of −95/−100 m off Torricella (section S4 in Fig. 2 and profile e–e′ in Fig. 9). In the western portion, the shelf erosive surface is overlaid by a thick sedimentary cover (profiles dd′ and ff′ in Fig. 9), organized in a single SDT having its depositional edge at ca. −40 m. The sedimentary cover sharply disappears in the area of the above mentioned rocky outcrop
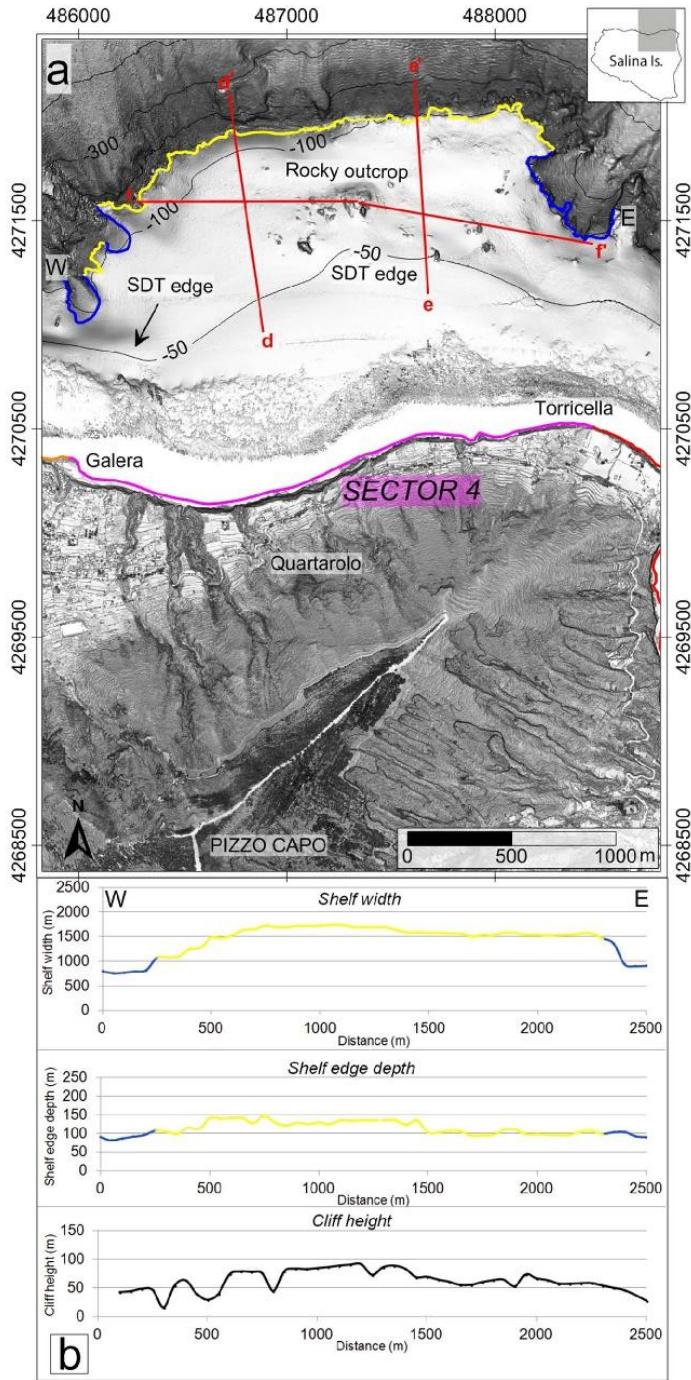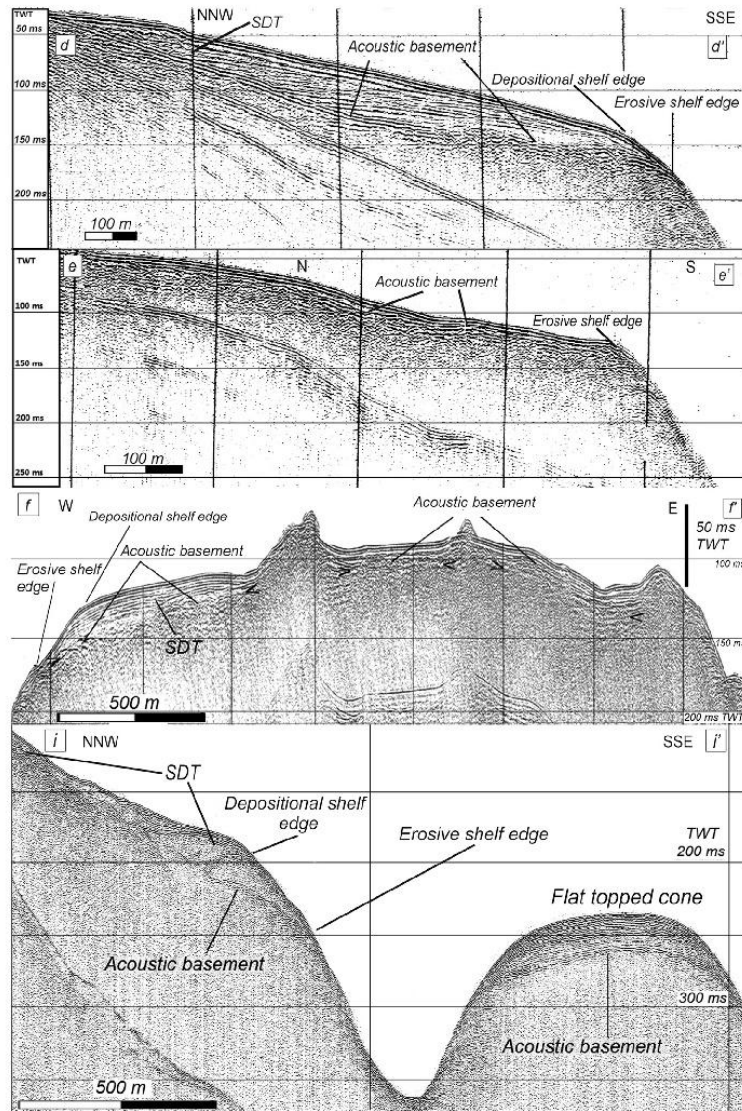
43

Fig. 9. Seismic (0.5 kj Sparker) profiles from shelf Sector 4 (location in Fig. 8), showing the erosive shelf edge and: dd′) a thick sedimentary body (SDT) on top of the acoustic basement; ee′) the lack of sedimentary cover on the acoustic basement; ff′) a transversal section intersecting the two previous seismic lines, showing the sedimentary cover (SDT) that progressively thins out towards the east. Profile ii′ (location in Fig. 12) shows the setting of the shelf in Sector 7 and a small seamount nearby, with flattened top and covered by sediment.

located in the middle of the shelf (Fig. 8a). To the E of this rocky outcrop, a sediment-starved shelf is observed, with only thinner sedimentary bodies (profiles ee′ and ff′ in Fig. 9).

5.5. Sector 5

This sector runs along the eastern coast of Salina to the north of Santa Marina Salina (Fig. 10a), to the east of the Pizzo Capo composite volcano. The coastline is quite regular and roughly N-S oriented, with steep and sub-vertical sea cliffs. These have variable heights up to 65 m (S5 in Fig. 2), progressively decreasing to the south, and are carved into the younger Pizzo Capo products here represented by thick successions of strombolian scoriae (Fig. 3e). The height of the cliff is locally much

higher due to intense subaerial erosion of these easily erodible volcaniclastic products. Raised marine terraces related to MIS 5 are recognized in the northern portion of Sector 5 (Fig. 1), cutting the Pizzo Capo scoriae and a minor lava flow. The terraces have elevations varying between 25 and 50 m a.s.l., with distinctive inner margins recognized at elevations of ~30 m (paleoshoreline II, MIS 5c, 100 ka) and ~50 m (paleoshoreline I, MIS 5e, 124 ka). The present sea cliff exposes a cross-section of these terraces, with a progressive northwards decrease in elevation that is consistent with a different direction of the paleo-coastline during the Last-Interglacial compared with the current one. The terraces are sealed by a volcaniclastic succession mostly consisting of products from the Monte dei Porri stratocone. In the central part of Sector 5, around Passo di Megna (Fig. 10a), the sea cliff
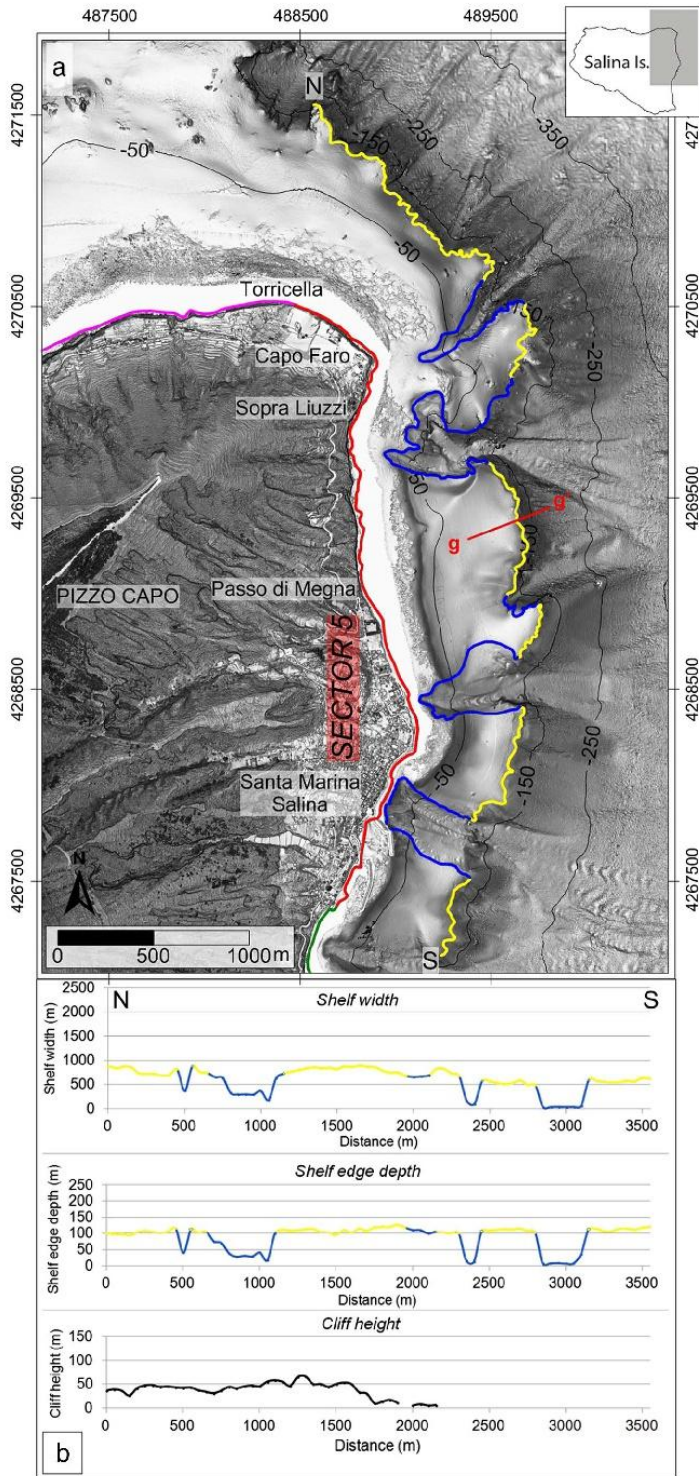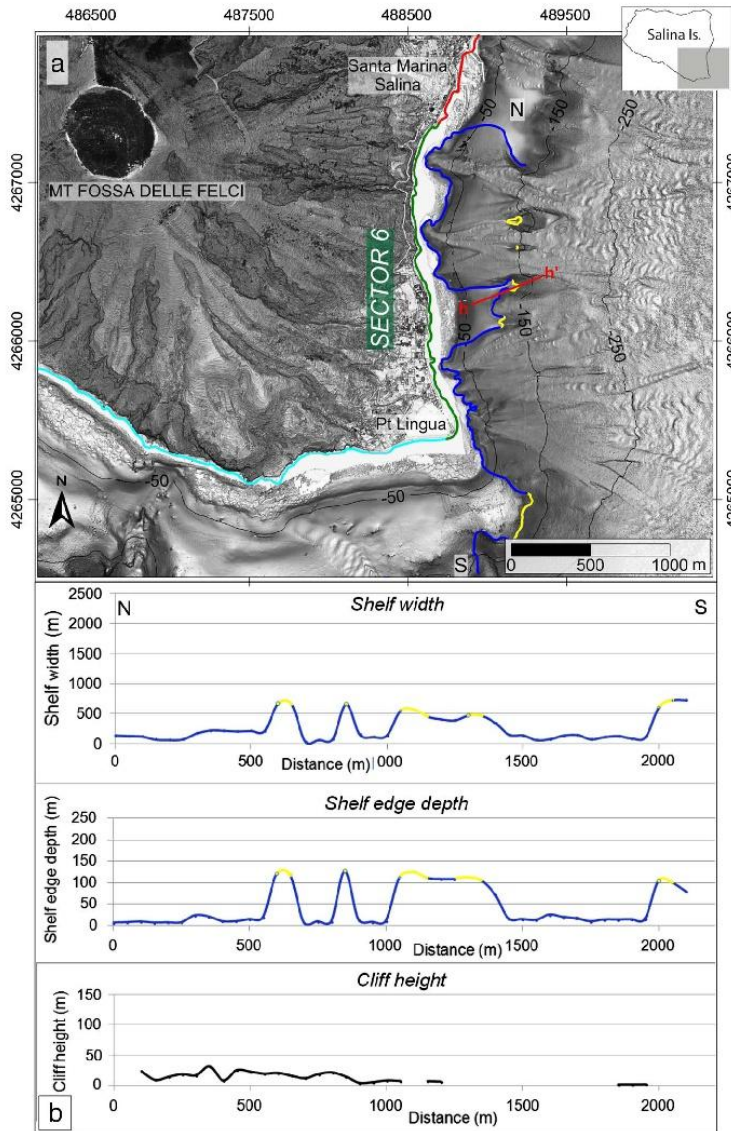
Fig. 10. Map of shelf Sector 5 (a) and graph of shelf width, shelf edge depth and cliff height measurements (b). In (a), the red line shows the location of the seismic profile gg' in Fig. 5. The yellow line in (b) represents the shelf edge preserved by erosion, the blue line corresponds to areas where the shelf edge has been eroded by canyon heads or slides scars. (For interpretation of the references to color in this figure legend, the reader is referred to the web version of this article.)

Fig. 11. Map of shelf Sector 6 (a) and graph of shelf width, shelf edge depth and cliff height measurements (b). In (a), the red line shows the location of the seismic profile hh′ in Fig. 5. The yellow line in (b) represents the shelf edge preserved by erosion, the blue line corresponds to areas where the shelf edge has been eroded by canyon heads or slides scars. Pt: Punta. (For interpretation of the references to color in this figure legend, the reader is referred to the web version of this article.)

allows exposure of a terrace deposit at elevations gradually decreasing southwards from ~25 m down to the present sea level. This terrace has an uncertain age, although Lucchi (2009) proposed its attribution to an interglacial peak older than MIS 5.

The shelf in Sector 5 is generally parallel to the coastline, and is deeply dissected by several canyon heads that influence its morphology (Fig. 10a). The shelf width is lower than in Sector 4, being narrower than 900 m also in the non-eroded areas (Fig. 10b and Table 1, section S5 in Fig. 2). The depth of the shelf edge, measured in areas not affected by erosion, is almost constantly around −100/−110 m, in places reaching depths of −127 m (Fig. 10b and Table 1). The geometry of the erosive shelf is well imaged in the seismic profile gg′ (Fig. 5) and covered by a sedimentary cover tapering seaward, where the erosive shelf edge just corresponds to the break-in-slope recognizable on

bathymetry, similarly to what observed for Sectors 1 and 3.

5.6. Sector 6

This sector runs aside the eastern coast of Salina to the south of Santa Marina Salina (Fig. 11a), offshore the Monte Fossa delle Felci stratovolcano (EE3–4, age 160–131 ka, Fig. 1). This is composed of a very thick strombolian scoriaceous succession with a few interlayered massive lava flows, whereas lava flows descending from the summit of the volcano become dominant in the southern portion towards Punta Lingua. The coastline is quite regular and roughly N-S aligned. Sea cliffs are relatively lower (< 26 m, S6 in Fig. 2 and Table 1) and mostly engraved in the scoriaceous products (and minor) lava flows of Monte Fossa delle Felci (Fig. 1). A much higher cliff, in a backward position

compared to the current one, represent the paleocliff and landward inner margin of the Last-Interglacial marine terraces presently exposed along the coast (Lucchi et al., 2013a). Sea cliffs are absent in the southern portion of Sector 6 due to the occurrence of voluminous detrital slope cones at the foot of the slope of Monte Fossa delle Felci (Fig. 11a). The MIS 5 marine terraces are documented in the central portion by a conglomerate lag horizon cropping out at elevations varying between the present sea level and ~ 12 m a.s.l. It represents the section of a paleoshoreline III terrace related to MIS 5a (81 ka). The older paleoshoreline I (MIS 5e, 124 ka) and II terraces (MIS 5c, 100 ka) are not directly exposed in this coastal sector due to the uniform cover of more recent pyroclastic products originated from the (younger) Monte dei Porri.

The shelf is largely dismantled by marine erosive processes recorded in several landslide scars and canyon heads that allow the preservation of a few shelf edge pieces (Fig. 11a). In the few areas preserved from erosion, the shelf is nevertheless quite narrow, commonly only slightly higher than 500 m (S6 in Fig. 2), with a maximum of ca. 720 m to the south of Punta Lingua (Fig. 11b and Table 1). The depth of the shelf edge is commonly around − 100/−120 m (S6 in Fig. 2, Fig. 11b) where there is no substantial erosion of the shelf. To the north, the shelf is covered by only a thin layer of sediments, whereas a single SDT is locally visible above the shelf to the south (S6 in Fig. 2 and seismic profile hh′ in Fig. 5). The geometry of the erosive shelf (where preserved) is similar to what observed for Sectors 1 and 3, with its edge just corresponding to the break-in-slope on the bathymetry.

5.7. Sector 7

This sector runs aside the southeastern coast of Salina (Fig. 12a), offshore the southern flanks of the Monte Fossa delle Felci stratovolcano. These are constituted by a succession of thick, andesite to dacite, massive to blocky lava flows and minor pyroclastic deposits related to the younger steps of construction of the stratocone during EE4 (ca. 147–121 ka, Fig. 1). The coastline is uneven and oriented NW-SE to W-E. Sea cliffs show variable heights ranging from a few metres to ~90 m (S7 in Fig. 2, Fig. 12b and Table 1), with the highest cliffs recognized around Punta Grottazza of a thick sequence of massive lava flows (Fig. 3f). To the east of Punta Grottazza a marine terrace deposits related to paleoshoreline III (MIS 5a, 81 ka) is visible at elevations varying from 2 m to 12 m a.s.l., cutting the products of Monte Fossa delle Felci and covered by the pyroclastic products of Monte dei Porri.

The shelf has a roughly polygonal shape, with some sub-rounded areas interrupted by erosive canyon heads and landslide scars (Fig. 12a). The shelf width has maximum values of 1700 m south of Punta Grottazza, where the shelf edge configuration is sub-rounded (S7 in Fig. 2). The shelf is generally narrower in other sub-rounded areas, with values commonly higher than 1000 m, and it is substantially narrower in the areas affected by erosion. In particular, a deep canyon head cuts the inner shelf and its sedimentary cover in the central part of the sector (off Punta delle Tre Pietre, Fig. 12a and b). This canyon is likely the seaward continuation of an erosive lineament on land (Fig. 12a). From Punta delle Tre Pietre to the west, the shelf gradually narrows, with another erosive scar causing the shelf retreat, although not affecting the inner shelf (Fig. 12a). In the areas preserved from erosion the shelf edge is always at depths greater than − 125 m, with a maximum value of − 212 m corresponding to the southernmost sub-rounded area (S7 in Fig. 2, Fig. 12b and Table 1). The shelf erosive surface is covered by sedimentary deposits organized in a series of SDTs (profile ii′ in Fig. 9), having depositional edges at depths of ca. − 40, − 70 and − 120 m (Fig. 12a). Seaward, the seismic profile ii′ cuts a flat-topped cone (Fig. 12a), where it is well recognizable a relatively flat erosive shelf, with edges at depths around − 220 m and covered by ca. 25 m of sedimentary cover.

6. Discussion

The bathy-morphological analysis of the coastal and shelf sectors of Salina, combined with the knowledge on the exposed volcanic products, allowed identifying the controlling factors of shelf development (Section 6.1) and better constraining the geological evolution of the island, especially for the early stages of growth of the volcanic edifice that are poorly documented onshore (Section 6.2).

6.1. Controlling factors of shelf development

The insular shelves around Salina Island are considered as dominantly formed by wave erosion of the existing volcanic products during the late-Quaternary sea-level fluctuations. This is outlined by the main features of Salina's shelves, which are: a) relatively wide, with erosive surfaces forming a sharp change in gradient with respect to the deeper submarine flanks (Fig. 2), b) commonly backed up by well-formed sea-cliffs (Fig. 3), c) generally covered by widespread and thick volcaniclastic deposits (Figs. 5 and 9). Moreover, there is no clear evidence of episodes of (recent) lava progradation on the shelf surface.

In general terms, we observe a good correspondence between the trend of the shelf width and depth of the shelf edge (Figs. 4, 6, 7, 8, 10, 11 and 12). A specific check on this relationship has been carried out through a Spearman correlation matrix, obtaining a value of about 0.6 for the entire dataset excluding the areas largely affected by later erosive processes (blue areas in the graphs of Figs. 4, 6, 8, 10, 11 and 12); such correlation is also recognizable on the scatter plot of Fig. 13. This can be explained by the fact that the sectors with a larger shelf and deeper shelf edge face the older volcanic units recognizable on Salina Island (see Section 6.2 for details). In this regard, shelf width has been commonly related to the amount of time that a coastal sector was exposed to waves (including the accumulated erosive action of waves over many similar glacial stages), so that it commonly increases with the edifice age (Menard, 1983; Llanes et al., 2009; Quartau et al., 2010). These larger shelves are covered by thicker volcaniclastic sequences organized in more than one order of STDs lying at different depths, formed through the reworking of eroded material at different relative sea-levels since the LGM (Casalbore et al., 2017b; see Section 3).

Furthermore, the depth of the shelf edges can provide insights on the vertical movements experienced by the shelves after their formation. Starting from the assumption that the sea level reached maximum depths of − 127 m in the last 450 ka (Bintanja et al., 2005), the erosional shelf edges presently lying below those depths are indicative of subsidence processes affecting the corresponding coastal sectors after the formation of the shelves. At Salina this subsidence should have occurred during the early stages of development before the Last Interglacial, because the recognition of raised MIS 5 marine terraces up to elevations of 50 m indicates a general uplift of the area since then (Lucchi et al., 2013a). Differently, the identification of a MIS 7 terrace at a lower elevation with respect to MIS 5 terraces along the northern coast of Salina is likely indicative of subsidence processes before the Last Interglacial period (Lucchi, 2009). This further supports our inference that the deeper shelf edges are associated to the older sectors, even if we are aware that in active volcanic areas vertical movements occur not necessarily at constant rates and can rapidly change in space and time (e.g., Di Vito et al., 1999; De Guidi and Monaco, 2009; Ramalho et al., 2017). The recognition of MIS 5 raised marine terraces at constant elevations on several Aeolian Islands is indicative of a long-term regional uplift affecting the sub-volcanic basement on most of the archipelago, with localized movements at different rates eventually affecting individual volcanic centres in some of the islands (Lucchi et al., 2007; Lucchi, 2009). A more detailed discussion of vertical movements affecting Salina is far from the focus of this paper and will be discussed in a following one.

Besides the age of coastal sectors, the different wave regime and wave energy exposure due to dominant winds have been also claimed
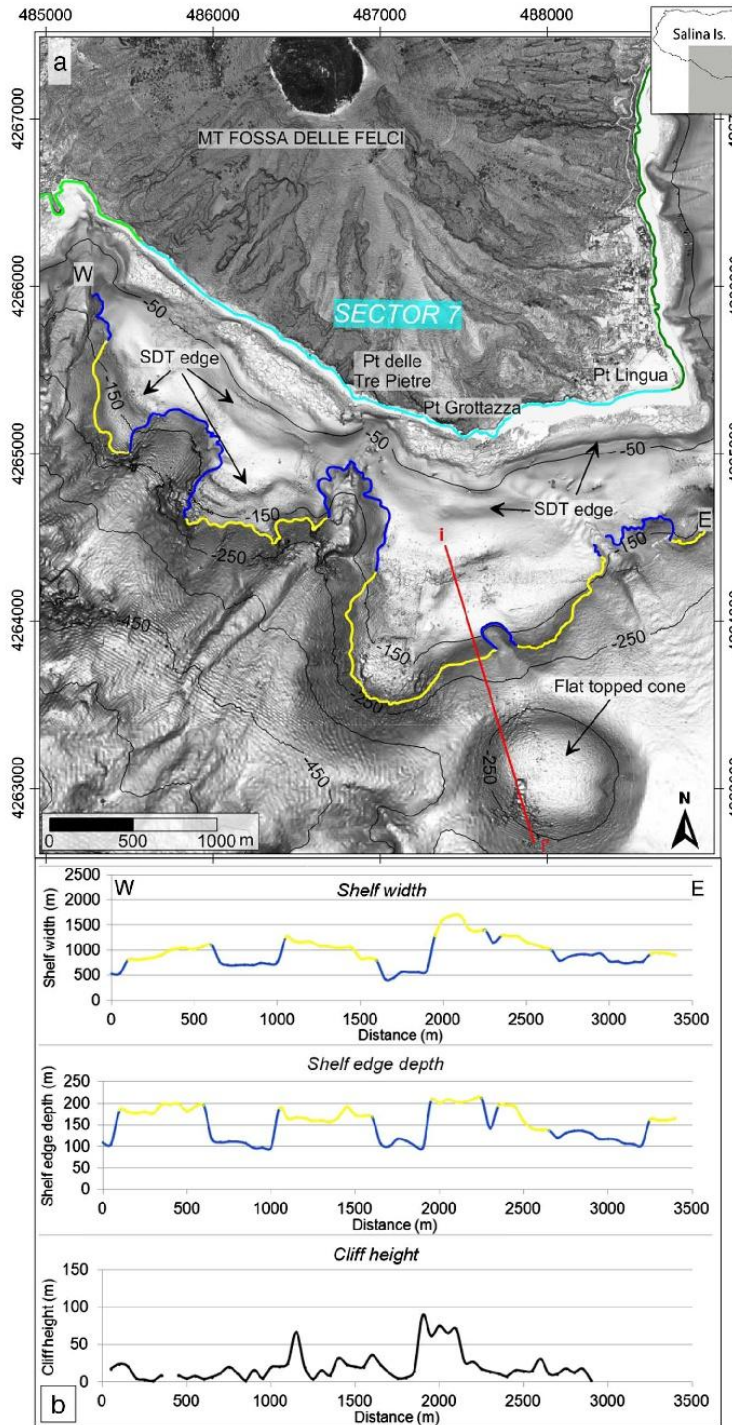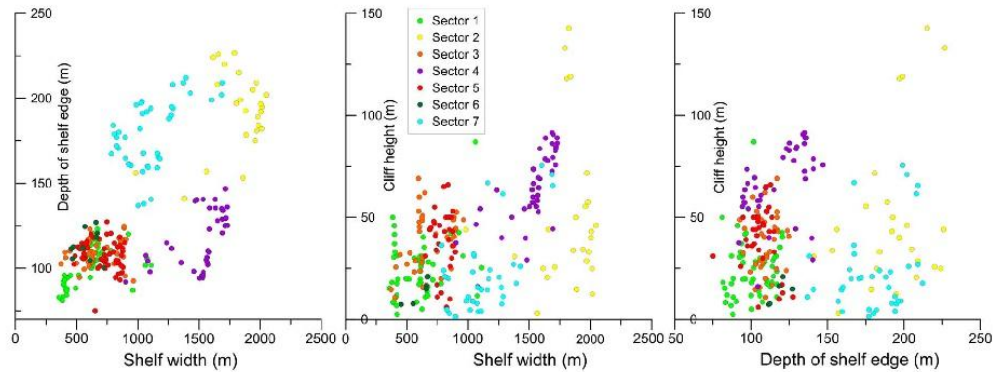
48

Fig. 13. Scatter plots of relationships between shelf width, depth of the shelf edge and cliff height for the different sectors. Note that only the values in areas not largely affected by later mass-wasting processes were considered for the analysis.

to represent important factors controlling the extension of submerged shelves (Llanes et al., 2009; Quartau et al., 2010). This appears as playing a role for the shelf (Sectors 4 and 5) developed around the Pizzo Capo edifice, which comprises the oldest volcanic units found on Salina. The larger shelf in Sector 4 with respect to Sector 5 (Figs. 8 and 10; Table 1) can be related to the fact that the former is more exposed to the dominant storms from the W and NW (Cicala, 2000), and it is also characterized by a markedly larger fetch (800 km from the NW, with respect to maximum 100 km from the E). However, the remarkable difference in width between these two sectors can be also partially accounted for the different age derived by the study of the offshore portions between the two sectors (see Section 6.2 for details). The same effect of exposure is also outlined when comparing shelf Sector 1 with shelf Sector 3. Sharing the same age of development, Sector 3 is wider than Sector 1 due to predominant wave exposure from the NW.

The different meteo-marine regime around the island also plays a role in modeling the cliff height, with particular reference to the cliff height (Trenhaile, 1987; Sunamura, 1992). The latter is commonly considered as mainly dependent on lithology of the facing products onshore and their varied resistance to erosion. Nevertheless, by comparing rates of cliff recession at different time scales from a number of recently active surtseyan-type volcanoes, Romagnoli and Jakobsson (2015) found that estimated rates appear strongly dependent on the period of detection time scales. In our study, the value of the Spearman correlation matrix (about 0.5) for the entire dataset indicates a possible relationship between cliff height and shelf width (Fig. 13), and consequently on the temporal scale of shelf development. However, we are aware that there is a large variability in cliff height among the different coastal sectors, also depending on the degree of marine vs subaerial erosion and lithology (e.g. cliffs on lavas vs those on pyroclastic units in Fig. 3) and on the fact that cliff erosion also operates through continuous renewal. No correlation (value of ca. 0) is instead observed between the cliff height and depth of the shelf edge (Fig. 13), because the latter is more likely associated to submarine mass-wasting processes. Finally, we cannot exclude the role of localized tectonic activity on the morphology of sea cliffs in some sectors of the island.

6.2. Geological implications

The distribution and morphology of the insular shelves around Salina reflect the original extent and paleo-morphology of different volcanic centres, and provides information about their relative age. As mentioned in the previous section, an overall increase of shelf width with age of corresponding eruptive centres onshore is recognizable in Fig. 13 (even if some values move out from the general trend), similarly to what reported in other volcanic islands (Llanes et al., 2009; Quartau

et al., 2010). On the other side, ages assumed for shelf areas, where earlier volcanic activity was presumably located, are basically unconstrained, also due to difficulty in sampling of the few rocky outcrops observed on the shelves. At Salina, we generally recognize two main types of shelves according to their width and depth of the shelf edge. Wider (up to 1700–2000 m) and deeper shelves (depths of shelf edge > − 127 m) are found in Sectors 2, 4 and 7 (Figs. 6, 8, 12), whereas Sectors 1, 3 and 6 are characterized by narrower shelves (up to 700–1000 m) and shallower shelf edges (not deeper than − 127 m, mostly around − 110/115 m; see Figs. 4, 7, 11).

In Sectors 1 and 3, the narrow shelves are in accordance with the young age (70–57 ka) of the Monte dei Porri volcanic products cropping out onshore. Moreover, the shelf edge is mostly at depths of − 100/ 115 m, suggesting that the shelf was tectonically stable or has slightly uplifted since the LGM, in agreement with the tectonic uplift derived from the study of raised MIS 5 marine terraces since the Last Interglacial (Lucchi, 2009). Differently, Sector 6 has a poorly preserved shelf, and its width is narrower than expected from the general trend according to the relatively old age of Monte Fossa delle Felci volcanic products exposed onshore (160–121 ka) (Fig. 14). This is probably because a large number of active submarine erosive features affected the shelf (Fig. 11a) decreasing its original width. These shelf dismantling processes through multiple small- and medium-scale slope failures (Casalbore et al., 2016a, 2016b, 2017a, 2017b) can be related to the existence of drainage system cutting the eastern flank of Monte Fossa delle Felci volcano that is present both onshore and offshore.

The shelf width-age relationship (Fig. 14) is still more controversial if we compare Sectors 6 and 7. The latter shows a markedly larger (up to 1691 m), deeper (shelf edge down to − 212 m) and better-preserved shelf than in Sector 6, even if both sectors run aside the flanks of Monte
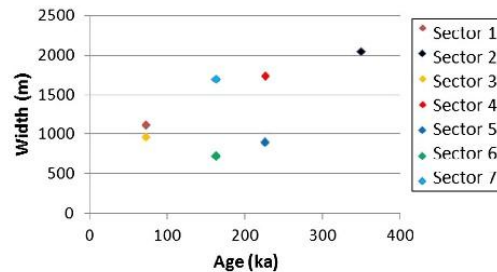

Fig. 14. Maximum shelf width in the different sector of Salina plotted against the age of the adjacent coastal sectors (see text for references).

Mainly Constructional Stages
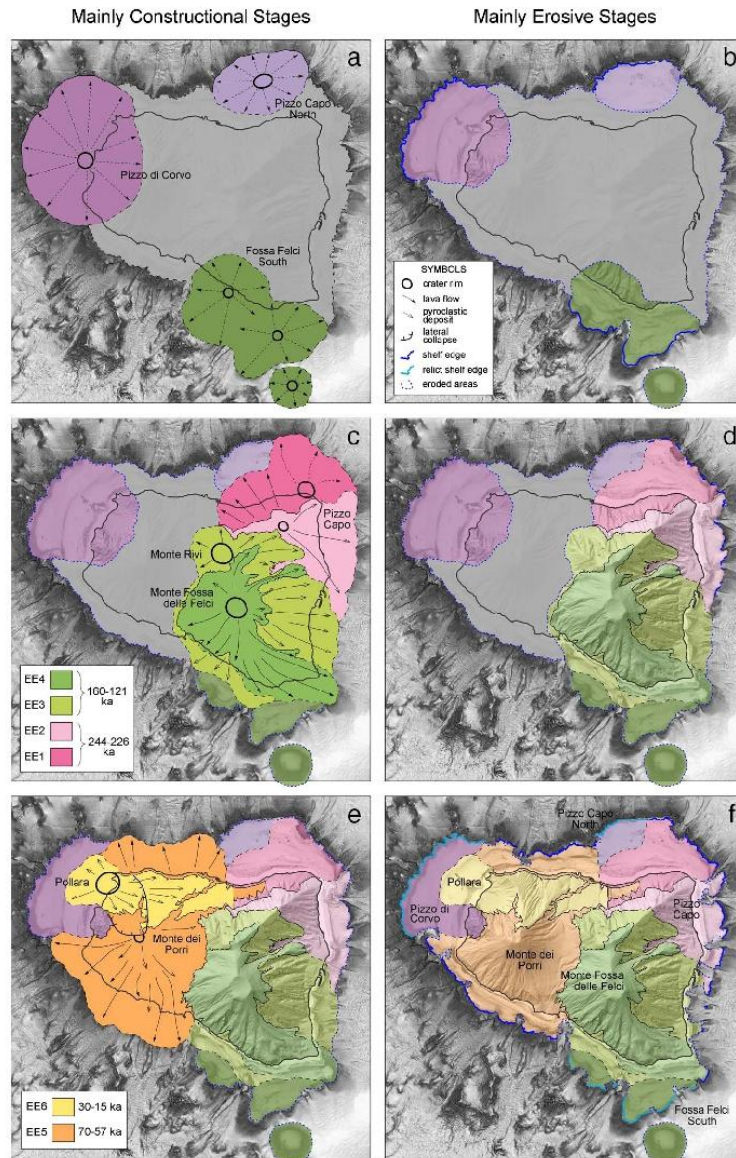
Mainly Erosive Stages

Fig. 15. Schematic sketch of the evolution of Salina, showing how, during the whole evolution of Salina, volcanic activity alternated with erosion and reworking of the successive volcanic centres. The distribution of volcanic products during the successive eruptive stages ("Mainly constructional stages") is schematically outlined in figures a, c and e. "Mainly erosive stages" (during phases of reduced or inactive volcanism) and shelves formation are represented in figures b, d and f.

Fossa delle Felci. The explanation to this fact can be found offshore, where the shelf in Sector 7 shows an articulated morphology, interpreted as derived from the remnants of a series of small volcanic centres, named "Fossa delle Felci South" (Fig. 15a), which are presently largely dismantled and not documented on land. In our interpretation the volcanic activity of these centres predates the growth of Monte Fossa delle Felci. These older offshore centres likely comprise another small, submerged volcanic centre with flattened top and a relevant sedimentary cover, located to the south (Fig. 12a, profile ii' in Fig. 8). The deep shelf edge observed in Sector 7 indicates that these early centres have experienced substantial subsidence after the formation of their shelves. This is also supported by the occurrence of different

orders of STDs, lying at different depths onto the shelf.

Sector 2 has the widest (max. 2048 m) and the deepest shelf (edge depth up to > − 220 m) at Salina, thus providing information on an old age of the eroded volcanic products. The shelf runs aside the remnants of the Pizzo di Corvo volcano, which has an uncertain stratigraphic position and age. We can use the information derived from the shelf width-age model to support the assumption that the Pizzo di Corvo volcano was constructed during the early stages of development of Salina. An old age of this volcano is also in agreement with the high degrees of erosion that contribute to the development of a > 100 m-high coastal cliff exposing the inner core of the edifice (Keller, 1980). The sub-rounded shape of the shelf offshore Pizzo di Corvo is

considered to represent the paleo-morphology of the volcanic edifice before erosion, indicating that the volcano was originally much larger than conceivable on the basis of its current subaerial outcrops (Fig. 15a). Consistently, the edge of Pizzo di Corvo shelf is always below depths of − 141 m (Fig. 6b), suggesting that this coastal sector has experienced substantial subsidence processes after the formation of the shelf.

Following this approach, we propose that the marked difference in width (1730 m vs 900 m) and depth of the shelf edge (− 147 m vs − 115 m) between Sectors 4 and 5, both running aside the Pizzo Capo edifice, also reflects a different age of formation (besides different wave exposure). We interpret the occurrence of a wider and (mainly) deeper shelf in the western portion of Sector 4 as related to a volcanic centre located off the northern coast of Salina, older than the subaerial Pizzo Capo volcano and not documented on land. This submerged centre, named Pizzo Capo North (Fig. 14a), is presently largely dismantled by marine erosion processes, with its remnants possibly represented by the rocky outcrops recognized in the middle of the shelf (Fig. 8a). The occurrence of an eruptive centre in the same position was already hypothesized by De Ritis et al. (2007) on the basis of the aeromagnetic anomaly pattern. This hypothesis might be confirmed by future dredging of the volcanic outcrops. Based on the present depth of shelf edge, the Pizzo Capo North volcano is assumed to have experienced subsidence processes after the formation of the shelf, differently from the rest of the shelf in Sector 4 (commonly lying above − 125 m).

Based on the previous inferences, we consider the wider and deeper shelves offshore W Salina (Pizzo di Corvo volcano), N Salina (Pizzo Capo North volcano) and SE Salina (Fossa delle Felci south) as the eroded remnants of volcanic centres formed in the early stages of development of Salina, before the island assumed its present morpho-structural setting (Fig. 15). Unfortunately there is no direct age information on these (mostly) submerged centres, although it should be important for cross-checking our model. However, according to the assumption of a homogeneous subsidence process in the investigated time period (before the Last Interglacial), it can be hypothesized that Pizzo di Corvo and Fossa delle Felci South (depths > − 200 m) are probably older than Pizzo Capo North (depth < − 147 m). A further implication of this reconstruction is that the Fossa Felci South volcanic centres (and the nearby flat-topped cone), together with a number of small submerged volcanic centres located along the western flank of Lipari and Vulcano edifices (Romagnoli et al., 1989, 2013; Casalbore et al., 2016b), can be considered expression of a large, NNW-SSE elongated volcanic belt active since the early phases of development of the central Aeolian archipelago (Romagnoli et al., 1989).

7. Conclusions

New constraints and hints on the geological evolution of Salina (Fig. 15) have been obtained from the morpho-bathymetric and seismo-stratigraphic setting of insular shelves around the island, integrated with on land geologic observations from field studies. The history of earlier stages of growth of Salina, less documented on land, is now better constrained. Particularly, we have documented the occurrence of three mostly submerged volcanic centres located off the coasts of the island (Pizzo di Corvo, Pizzo Capo North, Fossa Felci South) that pre-date the older volcanic products exposed onshore (220–240 ka). Evidence of substantial subsidence before the Last Interglacial is observed in all these sectors, indicating that this process likely affected the whole Salina volcanic complex. Later uplift of Salina (since the Last Interglacial) is also suggested by integrating the analysis of the depths of the shelves edges and raised marine terraces. These inferences have significant implications on the vertical mobility at the scale of the whole Aeolian Archipelago.

These results show that shelf width-shelf age or shelf depth-shelf age relationships can represent a useful tool to unravel the geological evolution of insular volcanoes, but it is important to highlight that in some sectors these relationships are not straightforwardly direct. Morphological differences observed among nearby shelf sectors of Salina, in fact, may also be due to other factors than the shelf width/age "basic" model commonly adopted for oceanic islands (Menard, 1983) in controlling the characteristics of insular shelves. This can be associated to the interaction between relative sea level changes (that also include vertical crustal movements) and local factors such as:

1) older ages of the volcanism in some sectors, not reported onshore, resulting in abnormally wider shelves;
2) different wave exposures, resulting in wider shelves of the sectors of the same age that are more exposed;
3) different submarine erosion of the shelf edges, resulting in abnormal narrow shelves in sectors that are more indented by submarine canyons.

Supplementary data to this article can be found online at https://doi.org/10.1016/j.margeo.2017.10.003.

References

Ablay, G., Hurlimann, M., 2000. Evolution of the north flank of Tenerife by recurrent giant landslides. J. Volcanol. Geotherm. Res. 103, 135–159.

Bintanja, R., van de Wal, R.S.W., Oerlemans, J., 2005. Modelled atmospheric temperatures and global sea levels the past million years. Nature 437, 125–128.

Bosman, A., Casalbore, D., Anzidei, M., Muccini, F., Carmisciano, C., Chiocci, F.L., 2015. The first ultra-high resolution digital Terrain model of the shallow-water sector around Lipari Island (Aeolian Islands, Italy). Ann. Geophys. 58 (2). http://dx.doi.org/10.4401/ag-6746.

Calanchi, N., De Rosa, R., Mazzuoli, R., Ricci Lucchi, F., Rossi, P.L., Santacroce, R., 1987. L'attività del centro di Pollara (Salina, Isole Eolie). Bol. GNV 187–213.

Casalbore, D., Bosman, A., Romagnoli, C., Chiocci, F.L., 2016a. Morphological map of Salina offshore (Southern Tyrrhenian Sea). J. Maps 12 (5), 725–730. http://dx.doi.org/10.1080/17445647.2015.1070300.

Casalbore, D., Bosman, A., Romagnoli, C., Di Filippo, M., Chiocci, F.L., 2016b. Morphological map of Lipari offshore (Southern Tyrrhenian Sea). J. Maps 12 (81), 77–86. http://dx.doi.org/10.1080/17445647.2014.980858.

Casalbore, D., Falese, F., Martorelli, E., Romagnoli, C., Chiocci, F.L., 2017a. Submarine depositional terraces in the Tyrrhenian Sea as a proxy for paleo-sea level reconstruction: Problems and perspective. Quat. Int. 439, 169–180. 10.1016/j.quaint.2016.07.051.

Casalbore, D., Bosman, A., Romagnoli, C., Chiocci, F.L., 2017b. Small-scale bedforms generated by gravity flows in the Aeolian Islands. In: Guillen, J., Acosta, J., Bernè, S., Chiocci, F., Palanques, A. (Eds.), Atlas of Bedforms in the Western Mediterranean. 44. Springer International Publishing, Switzerland, pp. 287–292. http://dx.doi.org/10.1007/978-3-319-33940-5.

Chiocci, F.L., Romagnoli, C., 2004. Terrazzi depositionali sommersi nelle Isole Eolie. In: Chiocci, F.L., D'Angelo, S., Romagnoli, C. (Eds.), Atlante dei Terrazzi Depositionali Sommersi Lungo le Coste Italiane. Memorie Descrittive della Carta Geologica d'Italia 58. pp. 81–114.

Chiocci, F.L., D'Angelo, S., Romagnoli, C., 2004. In: Chiocci, F.L., D'Angelo, S., Romagnoli, C. (Eds.), Atlante dei Terrazzi Depositionali Sommersi Lungo le Coste Italiane (Atlas of Submerged Depositional Terraces Along the Italian Coasts). Memorie Descrittive della Carta Geologica d'Italia 58.

Cicala, A., 2000. Guida alla meteorologia delle Isole Eolie. In: Natali, A. (Ed.), Comune di Lipari, Lipari, Italy.

De Guidi, G., Monaco, C., 2009. Late Holocene vertical deformation along the coast of Pantelleria Island (Sicily Channel, Italy). Quat. Int. 206, 158–165.

De Ritis, R., Ventura, G., Chiappini, M., 2007. Aeromagnetic anomalies reveal hidden tectonic and volcanic structures in the central sector of the Aeolian Islands, southern Tyrrhenian Sea, Italy. J. Geophys. Res. 112, 1–13. (B10105). https://doi.org/10.1029/2006JB004639.

Di Vito, M.A., Isaia, R., Orsi, G., Southon, J., de Vita, S., D'Antonio, M., Pappalardo, L., Piochi, M., 1999. Volcanic and deformational history of the Campi Flegrei caldera in the past 12 ka. J. Volcanol. Geotherm. Res. 91, 221–246.

Field, M.E., Roy, P.S., 1984. Offshore transport and sand-body formation evidence from a steep, high-energy shoreface, southeastern Australia. J. Sediment. Petrol. 54, 1292–1302.

Gertisser, R., Keller, J., 2000. From basalt to dacite: origin and evolution of the calc-alkaline series of Salina, Aeolian Arc, Italy. Contrib. Mineral. Petrol. 139, 607–626.

Gillot, P.Y., 1987. Histoire volcanique des Iles Eoliennes: arc insulaire ou complexe orogénique anulaire? In: Documents et Travaux de l'Institut Géologique Albert de l'Apparent. 11. pp. 35–42.

Hernandez-Molina, F.J., Fernandez-Salas, L.M., Lobo, F.J., Somoza, L., Díaz del Río, V., Alveirinho Días, J.M., 2000. The infralittoral prograding wedge: a new largescale progradational sedimentary body in shallow marine environments. Geo-Mar. Lett. 20, 109–117.

Keller, J., 1980. The island of Salina. Rend. Soc. Ital. Mineral. Petrol. 36, 489–524.

Le Friant, A., Harford, C.L., Deplus, C., Boudon, G., Sparks, R.S.J., Herd, R.A., Komorowski, J.C., 2004. Geomorphological evolution of Montserrat (West Indies): importance of flank collapse and erosional processes. J. Geol. Soc. Lond. 161, 147–160.

Leocat, E., 2011. Histoire eruptive des volcans du secteur occidental des Iles Eoliennes (Sud de la Mer Tyrrhenienne, Italie) et evolution temporelle du magmatisme (PhD thesis). University of Paris, Orsay 11.

Llanes, P., Herrera, R., Gomez, M., Munoz, A., Acosta, J., Uchupi, E., 2009. Geological evolution of the volcanic island La Gomera, Canary Islands, from analysis of its geomorphology. Mar. Geol. 264, 123–139.

Lucchi, F., 2009. Late-Quaternary marine terrace deposits as tools for wide-scale correlation of unconformity-bounded units in the volcanic Aeolian archipelago (southern Italy). Sediment. Geol. 216, 158–178.

Lucchi, F., Tranne, C.A., Calanchi, N., Rossi, P.L., 2004. Late Quaternary fossil shorelines in the Aeolian Islands (Southern Tyrrhenian Sea): evaluation of long-term vertical displacements. In: Antonioli, F., Monaco, C. (Eds.), Contribution From the Study of Ancient Shorelines to Understanding the Recent Vertical Motions. Field Trip Across the Messina Straits Quaternaria Nova, Il Calamo Editore, Roma, Italy, VIII, pp. 115–137.

Lucchi, F., Tranne, C.A., Calanchi, N., Rossi, P.L., 2007. Late Quaternary deformation history of the volcanic edifice of Panarea (Aeolian Arc). Bull. Volcanol. 69, 239–257.

Lucchi, F., Tranne, C.A., De Astis, G., Keller, J., Losito, R., Morche, W., 2008. Stratigraphy and significance of Brown Tuffs on the Aeolian Islands (southern Italy). J. Volcanol. Geotherm. Res. 177, 49–70.

Lucchi, F., Gertisser, R., Keller, J., Forni, F., De Astis, G., Tranne, C.A., 2013a. Eruptive history and magmatic evolution of the island of Salina (central Aeolian archipelago). In: Lucchi, F., Peccerillo, A., Keller, J., Tranne, C.A., Rossi, P.L. (Eds.), The Aeolian Islands Volcanoes. Geological Society, London, Memoirs 37. pp. 155–211.

Lucchi, F., Keller, J., Tranne, C.A., 2013b. Regional stratigraphic correlations across the Aeolian archipelago (southern Italy). In: Lucchi, F., Peccerillo, A., Keller, J., Tranne, C.A., Rossi, P.L. (Eds.), The Aeolian Islands Volcanoes. Geological Society, London, Memoirs 37. pp. 55–81.

Menard, H.W., 1983. Insular erosion, isostasy, and subsidence. Science 220, 913–918.

Mitchell, N.C., Dade, W.B., Masson, D.G., 2003. Erosion of the submarine flanks of the Canary Islands. J. Geophys. Res. 108 (3–1–3–11).

Mitchell, N.C., Masselink, G., Huthnance, J.M., Fernández-Salas, L.M., Lobo, F.J., 2012. Depths of modern coastal sand clinoforms. J. Sediment. Res. 82, 469–481.

Quartau, R., Trenhaile, A.S., Mitchell, N.C., Tempera, F., 2010. Development of volcanic insular shelves: insights from observations and modelling of Faial Island in the Azores Archipelago. Mar. Geol. 275, 66–83.

Quartau, R., Tempera, F., Mitchell, N.C., Pinheiro, L.M., Duarte, H., Brito, P.O., Bates, R., Monteiro, J.H., 2012. Morphology of the Faial Island shelf (Azores): the interplay between volcanic, erosional, depositional, tectonic and mass-wasting processes. Geochem. Geophys. Geosyst. 13, Q04012. http://dx.doi.org/10.1029/2011GC003987.

Quartau, R., Hipolito, A., Romagnoli, C., Casalbore, D., Madeira, J., Tempera, F., Roque, C., Chiocci, F.L., 2014. The morphology of insular shelves as a key for understanding the geological evolution of volcanic islands: insights from Terceira Island (Azores). Geochem. Geophys. Geosyst. 15, 1801–1826.

Quartau, R., Madeira, J., Mitchell, N.C., Tempera, F., Silva, P.F., Brandao, F., 2015. The insular shelves of the Faial-Pico Ridge (Azores archipelago): a morphological record of its evolution. Geochem. Geophys. Geosyst. 16, 1401–1420.

Quartau, R., Madeira, J., Mitchell, N.C., Tempera, F., Silva, P.F., Brandão, F., 2016. Reply to comment by Marques et al. on "the insular shelves of the Faial-Pico Ridge (Azores archipelago): a morphological record of its evolution". Geochem. Geophys. Geosyst. 17, 633–641.

Ramalho, R.S., Heiffrich, G., Madeira, J., Cosca, M., Thomas, C., Quartau, R., Hipolito, A., Rovere, A., Hearthy, P.J., Avila, S.P., 2017. Emergence and evolution of Santa Maria Island (Azores) – the conundrum of uplifted islands revisited. Geol. Soc. Am. Bull. 129 (3–4), 372–390. http://dx.doi.org/10.1130/B31538.1.

Romagnoli, C., 2013. Characteristics and morphological evolution of the Aeolian volcanoes from the study of submarine portions. In: Lucchi, F., Peccerillo, A., Keller, J., Tranne, C.A., Rossi, P.L. (Eds.), The Aeolian Islands Volcanoes. Geological Society, London, Memoirs 37. pp. 13–26.

Romagnoli, C., Jakobsson, S.P., 2015. Post-eruptive morphological evolution of island volcanoes: Surtsey as a modern case study. Geomorphology 250, 384–396. http://dx.doi.org/10.1016/j.geomorph.2015.09.016.

Romagnoli, C., Calanchi, N., Gabbianelli, G., Lanzafame, G., Rossi, P.L., 1989. Contributi delle ricerche di geologia marina alla caratterizzazione morfostrutturale ed evolutiva dei complessi vulcanici di Salina, Lipari e Vulcano (Is. Eolie). Bol. GNV 1989, 971–978.

Romagnoli, C., Casalbore, D., Bortoluzzi, G., Bosman, A., Chiocci, F.L., D'Oriano, F., Gamberi, F., Ligi, M., Marani, M., 2013. Bathy-morphological setting of the Aeolian islands. In: Lucchi, F., Peccerillo, A., Keller, J., Tranne, C.A., Rossi, P.L. (Eds.), The Aeolian Islands Volcanoes. Geological Society, London, Memoirs 37. pp. 27–36.

Sunamura, T., 1992. The Geomorphology of Rock Coasts. Wiley, Chichester.

Trenhaile, A.S., 1987. The Geomorphology of Rocky Coasts. Oxford University Press, Oxford.

Ventura, G., 2013. Kinematics of the Aeolian volcanism (Southern Tyrrhenian Sea) from geophysical and geological data. In: Lucchi, F., Peccerillo, A., Keller, J., Tranne, C.A., Rossi, P.L. (Eds.), The Aeolian Islands Volcanoes. Geological Society, London, Memoirs 37. pp. 3–11.

52

5.2 Salina Island - Manuscript II

This manuscript investigates in detail the distribution of the Submarine Depositional Terraces (SDTs) on the shelf of Salina Island with particular focus on the depositional edge depth. The aim is to highlight the potential of this morphologic parameter as a tool for reconstructing the relative sea-level in the last 20 ka at Salina and on other volcanic islands where SDTs are recognized. As a co-author of this study I provided a critical feedback and I also contributed to drafting of the final version of the paper.

"Submarine Depositional Terraces at Salina Island (Southern Tyrrhenian Sea) and implications on the Late Quaternary evolution of the insular shelf "

Authors:
- Daniele Casalbore (University of Rome – "La Sapienza", Rome – Italy)
  (Istituto di Geologia Ambientale e Geoingegneria, Consiglio Nazione delle Ricerche, Rome – Italy)
- Claudia Romagnoli (University of Bologna, Bologna – Italy)
  (Istituto di Geologia Ambientale e Geoingegneria, Consiglio Nazione delle Ricerche, Rome – Italy)
- Chiara Adami (Istituto di Geologia Ambientale e Geoingegneria, Consiglio Nazione delle Ricerche, Rome - Italy)
- Alessandro Bosman (Istituto di Geologia Ambientale e Geoingegneria, Consiglio Nazione delle Ricerche, Rome - Italy)
- Francesco Falese (Istituto di Geologia Ambientale e Geoingegneria, Consiglio Nazione delle Ricerche, Rome - Italy)
- Alessandro Ricchi (University of Bologna, Bologna – Italy)
- Francesco Latino Chiocci (University of Rome – "La Sapienza", Rome – Italy)
  (Istituto di Geologia Ambientale e Geoingegneria, Consiglio Nazione delle Ricerche, Rome – Italy)

Submarine Depositional Terraces at Salina Island (Southern Tyrrhenian Sea) and Implications on the Late-Quaternary Evolution of the Insular Shelf

Daniele Casalbore [1,2,*], Claudia Romagnoli [2,3], Chiara Adami [2], Alessandro Bosman [2], Francesco Falese [2], Alessandro Ricchi [3] and Francesco Latino Chiocci [1,2]

[1] Dipartimento Scienze della Terra, Sapienza Università di Roma, 00 185 Roma, Italy; francesco.chiocci@uniroma1.it
[2] Istituto di Geologia Ambientale e Geoingegneria, Consiglio Nazionale delle Ricerche, 00 185 Roma, Italy; claudia.romagnoli@unibo.it (C.R.); kiaradami@gmail.com (C.A.); alessandro.bosman@uniroma1.it (A.B.); francesco.falese@uniroma1.it (F.F.)
[3] Dipartimento di Scienze Biologiche, Geologiche ed Ambientali, Università di Bologna, 3340 126 Bologna, Italy; alessandro.ricchi7@unibo.it
*   Correspondence: daniele.casalbore@uniroma1.it

Abstract: The integrated analysis of high-resolution multibeam bathymetry and single-channel seismic profiles around Salina Island allowed us to characterize the stratigraphic architecture of the insular shelf. The shelf is formed by a gently-sloping erosive surface carved on the volcanic bedrock, mostly covered by sediments organized in a suite of terraced bodies, i.e. submarine depositional terraces. Based on their position on the shelf, depth range of their edge and inner geometry, different orders of terraces can be distinguished. The shallowest terrace (near-shore terrace) is a sedimentary prograding wedge, whose formation can be associated to the downward transport of sediments from the surf zone and shoreface during stormy conditions. According to the range depth of the terrace edge (i.e., 10–25 m, compatible with the estimated present-day, local storm-wave base level in the central and western Mediterranean), the formation of this wedge can be attributed to the present-day highstand. By assuming a similar genesis for the deeper terraces, mid-shelf terraces having the edge at depths of 40–50 m and 70–80 m can be attributed to the late and early stages of the Post-LGM transgression, respectively. Finally, the deepest terrace (shelf-edge terrace) has the edge at depths of 130–160 m, being thus referable to the lowstand occurred at ca. 20 ka. Based on the variability of edge depth in the different sectors, we also show how lowstand terraces can be used to provide insights on the recent vertical movements that affected Salina edifice in the last 20 ka, highlighting more generally their possible use for neo-tectonic studies elsewhere. Moreover, being these terraces associated to different paleo-sea levels, they can be used to constrain the relative age of the different erosive stages affecting shallow-water sectors.

Keywords: prograding wedges; coastal areas; paleo sea-level; insular shelf; volcanic islands; multibeam bathymetry

1. Introduction

In the last few decades, recent advances in seafloor imagery systems enabled to extensively map the submarine flanks of volcanic islands in different geodynamic setting, revealing a large variability of landforms due to volcanic, tectonic, and erosive-depositional processes [1–8]. Until now, most of these studies focused on large-scale instability processes affecting volcanic flanks, mainly in relation to their associated tsunamigenic potential and geohazard assessment [9–12]. Only in the

last years, some papers paid attention to the shallow-water areas around volcanic islands, where the morphological characteristics of the shelf (i.e., shelf width and depth of its edge) can be used: (a) to reconstruct the original extension of early volcanic centres in the development of the island, including deeply eroded submarine cones, with respect to subaerial main centres, and (b) to assess the vertical movements of the volcanic edifice that have occurred after the shelf formation due to erosion [13–17]. Regarding this, another geomorphological/stratigraphic marker for relative paleo-sea level reconstruction and assessment of vertical movement is the edge depth of prograding sedimentary wedges, forming morphological terraces (Submarine Depositional Terraces, SDT hereafter, [18–20]). These features are commonly found on insular shelves and tectonically-controlled margins and are made by oblique and/or sigmoidal foresets (with slope angles between 4° and 20°, commonly more than 10°), generally sloping basinward. Their genesis has been associated to the downward transport of sediments from the surf zone and shoreface during stormy conditions [21,22]. A good match has been found between the depth of these terraces (commonly in the range of 15–60 m) and the upper 10-percentile of the local wave height distribution, evidencing the key role played by storm-wave base level in their formation [23].

The aim of this paper is to characterize, through the integration of high-resolution multibeam bathymetry and single-channel seismic profiles, the overall seismo-stratigraphic architecture of the insular shelf surrounding Salina Island, with particular reference to the suite of submarine depositional terraces here present. Specifically, we discuss the relationship between near-shore (edge at water depths of 10–25 m) and shelf-edge terraces (edge at water depths greater than 120 m) and their use as paleo sea-level markers. This, in turn, can provide insights on the recent vertical movements that affected Salina edifice in the last 20 ka, as well as on the timing of the different erosive stages associated to the canyons that carve the steep flanks of the volcanic edifice.

2. Data and Methods

Data used for this research are high-resolution multibeam bathymetry and single-channel seismic profiles acquired since 1993 from the University Sapienza of Rome, University of Bologna and CNR-IGAG. Specifically, the bathymetry is the result of several surveys mainly carried out onboard the R/V *Urania* and *Thetis* (CNR), using multibeam systems working at frequency from 50 to 100 kHz for the different bathymetric range; data has been recorded using a differential GPS system (for details on data acquisition and processing see [4]). Shallow-water areas (approximately in the first 50 m water depths) were surveyed aboard a small boat using a Teledyne Reson 7125 (400 kHz) multibeam system, recorded using a GPS-RTK positioning (for details on data acquisition and processing see [24]). All the processed data were merged and gridded using the kriging algorithm to produce Digital Elevations Models (DEMs), with cell-size ranging from 1 m within 100 m water depth to 25 m at greater depths.

Two sets of seismic profiles, generally acquired radially to the shelf were collected in 1993 and 2016, respectively. The first set was acquired using a Sparker 0.5–1 kJ aboard the catamaran *Incaurina Marianna*, positioned through GPS. Because of the low accuracy of GPS positioning, these profiles were successively relocated via homologous matching of features observed on seismic profiles and multibeam bathymetry. The second set was acquired in 2016 aboard the R/V *Minerva1* using a Sparker source working at 0.5–1.5 kJ; data were georeferenced using a differential GPS. The vertical resolution of Sparker profiles can be estimated in the order of some metres for both sets due to the emitted frequency and to the ringing effects. A sound velocity of 1500 m/s has been adopted for time-depth conversion in the seismic profiles.

3. Geological Setting

Salina is one of the seven islands of the Aeolian Archipelago in the Southern Tyrrhenian Sea (Figure 1 inset). It is 962 m high and represents the uppermost part (~16%) of a large stratovolcano, whose base lies at ca. 1300 m of water depth (Figure 1a).
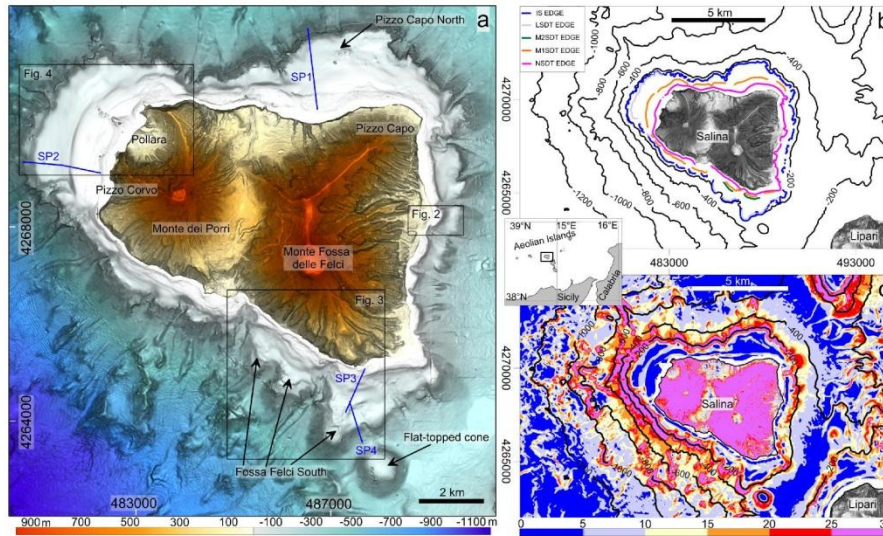
Figure 1. (**a**) Shaded relief of Salina Island and surrounding shelf, showing the location of Figures 2–4 (black boxes) and the trace of seismic profiles (blue lines) shown in Figures 5 and 6. Submarine eccentric centers of Pizzo Capo North and Fossa delle Felci South are also shown (from [17]). (**b**) Bathymetry (isobaths each 200 m) with the mapping of the edge of the insular shelf (IS) and overlying submarine depositional terraces (NSDT: near-shore submarine depositional terrace; M(1/2)SDT: mid-shelf submarine depositional terrace; LSDT: shelf-edge (lowstand) submarine depositional terrace). (**c**) Slope gradient map of the Salina edifice in the southern Tyrrhenian Sea (for location see the inset).

Salina together with Lipari and Vulcano is part of an elongated volcanic belt, whose formation has been related to the occurrence of a main strike-slip NNW–SSE regional fault system, interpreted as the offshore prolongation of the "Tindari-Letojanni" fault, recognized onland in NE Sicily [25]. The volcanological evolution of Salina Island was summarized by [26], encompassing six Eruptive Epochs (EE) between ~244 and 15.6 ka. The products of the oldest EE are found in the NW and NE sectors of Salina, where the deeply eroded volcanic centres of Pizzo di Corvo (uncertain stratigraphic position and radiometric age) and Pizzo Capo (244–226 ka) are found (Figure 1c). Younger EE formed the Monte Fossa delle Felci (160–121 ka) and Monte dei Porri (70–57 ka) stratovolcanoes in the E and W part of the island, respectively (Figure 1c). Activity of the last EE is located at the Pollara crater in the NW part of Salina, where widespread rhyolitic pumiceous successions were emplaced between 30 and 15 ka (Figure 1c). Raised marine terraces are found along the coasts of Salina, indicating an average uplift of 0.36 m/ka for the island since the Last Interglacial [26]. Differently, the occurrence of an older MIS 7.3 terrace at lower elevations than MIS5 terraces was interpreted as the evidence of a subsidence phase affecting the early growth stages of Salina edifice before the Last Interglacial [26].

The submarine deeper flanks of the edifice (Figure 1a) are characterized by a complex seafloor morphology due to the presence of volcanic features (volcanic cones, lava flows, bedrock outcrops, for ~30% of the overall extension) and erosive-depositional features (landslide scars, channels, fan-shaped deposits and waveforms, about ~70%, [27]). The shallower part of the submarine flank is cut by an insular shelf (Figure 1), clearly recognizable on the slope gradient map (Figure 1b), because of its gently declivities (2°–17°, but typically less than 5°), interrupting the morphological continuity between the steeper (>25°) subaerial and submarine flanks of the edifice. It shows variable morphological characteristics; i.e., width and depth of the shelf edge around the island, suggesting indications on the development of the volcanic edifice [17]. The larger and deeper shelves are, in fact,

observed along the W (Pizzo Corvo), NE (Pizzo Capo North) and SE (Fossa Felci South) sectors of the island, where the older volcanic activity is located (Figure 1c). Differently, narrow shelves with a shallower edge are observed around the younger Monte dei Porri edifice (N and SW sectors of the island) as well as along the eastern flank of the island (Monte Fossa delle Felci), where the shelf is strongly dismantled by erosive-depositional processes due to a network of subaerial/submarine channels [27]. The erosive surface of the insular shelf is covered by sediments (mostly volcaniclastic and bioclastic deposits), organized in different orders of submarine depositional terraces [20,22] that are the focus of the present paper.

Despite the commonly accepted influence of meteo-marine conditions in the formation of shelf ad overlying terraces, only few data are available for the Aeolian Islands in order to quantify their effects. On the whole, the most energetic wave climate in this sector is from westerly directions, since prevailing winds are from the NW or the W [17]. The western flank of Salina is struck by storms, with a typical fetch of 250–300 nautical miles and waves up to 6 m [17]. Winds from the SE also affect the south-eastern and eastern side of the Aeolian Islands, especially during the autumn and winter, whereas the southwestern sector is partially sheltered by the nearby Lipari Island.

4. Results

4.1. Overall Morphology and Seismo-Stratigraphic Architecture of the Salina Insular Shelf

The insular shelf around Salina Island is ca. 700–2000 m wide, extending from the coast down to the shelf edge, which is located at water depths ranging from ca. 110 to 225 m (Figure 1c; see also Table 1 of [17]). However, values of shelf width and depth of the shelf edge can be markedly lowered in the sectors affected by mass-wasting processes, as for instance along the eastern flank of the island (Figure 1c). The morphology of the shelf is generally characterized by a relatively smooth and flat surface, apart from the coastal areas where a more rugged morphology is present, as well as by different breaks-in-slope at higher depths, commonly oriented parallel to the contours and corresponding to the edge of submarine depositional terraces (Figures 1–4).
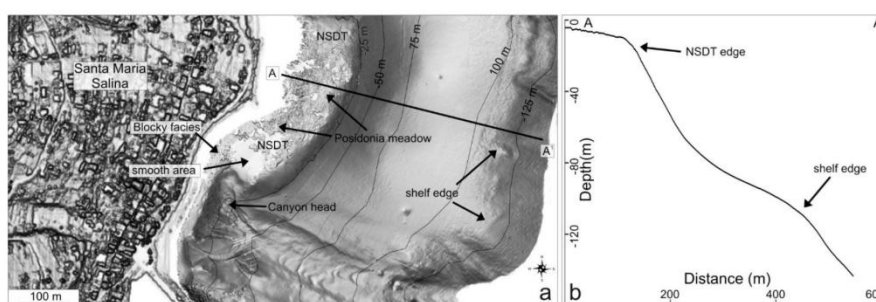
Figure 2. (**a**) Shaded relief map of the area around Santa Maria di Salina village in the eastern part of Salina (location in Figure 1a), where the near-shore submarine depositional terrace (NSDT) is visible in the inner shelf (first 25 m of depth); (**b**) the bathymetric cross-section A–A^1 shows the edge of the insular shelf and overlying NSDT.

The overall seismo-stratigraphic architecture of the shelf, although locally variable in the different sectors of the island, is typically characterized by an aggradational/progradational sedimentary wedge lying upon a relatively flat erosive surface cutting the volcanic bedrock, imaged as having high acoustic impedance and discontinuous echo type, with small diffraction hyperbolae (Figures 5 and 6). Five seismic units were recognized within the sedimentary wedge (Figures 5 and 6): four of these units (units 2–5) can be associated to terraced morphologies on the bathymetry (Section 4.2), whereas the

lowermost unit 1 is rather discontinuous and thin (maximum thickness of 10 m). Unit 1 is commonly found directly above the volcanic bedrock, especially in correspondence of morphological irregularities such as small depressions (SP2 in Figure 5 and SP3 in Figure 6). It is generally characterized by continuous or semi-continuous reflectors, with variable amplitude. The upper four seismic units are described with more detail in the next section, together with the related SDTs.
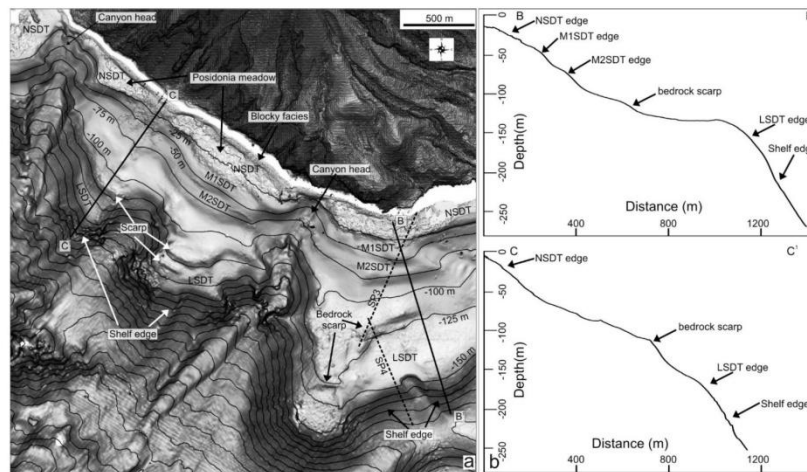
Figure 3. (**a**) Shaded relief map of the SE sector of Salina (location in Figure 1a), where a large shelf with different orders of submarine depositional terraces are present; (**b**) the bathymetric cross sections B–B[1] and C–C[1] evidence the edge depth of the shelf and overlying terraces. Note also the presence of two deeply indenting canyons that cut the shelf in very shallow-water areas, some tens of meters far from the coast. NSDT: near-shore submarine depositional terrace; M(1/2)SDT: mid-shelf submarine depositional terrace; LSDT: shelf-edge (lowstand) submarine depositional terrace. SP3 and 4 are the trace of the Sparker profiles shown in Figure 6.

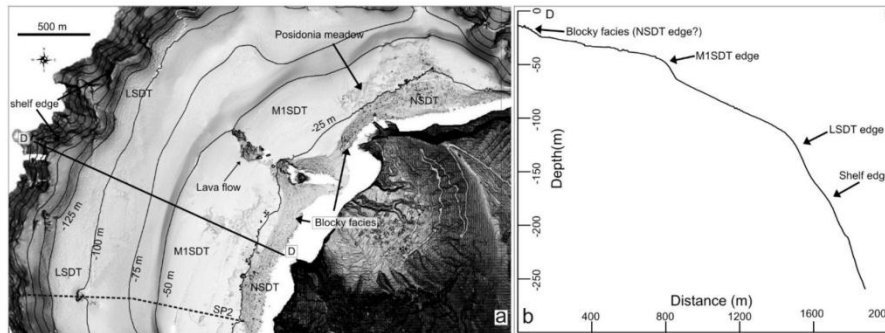### 4.2. Submarine Depositional Terraces

Submarine depositional terraces on the Salina shelf can be grouped in three main orders (near-shore, mid-shelf and shelf-edge terraces) according to their position on the shelf, depth of their edge (rollover depth) and associated seismic unit:

(a) the shallowest terrace (near-shore submarine depositional terrace, NSDT hereafter) has the edge at water depths of ca. 10–25 m (on average 15 m) and is morphologically recognizable all along the island, even if it is more evident in the eastern and south-eastern sectors (NSDT in Figures 2 and 3, respectively). This terrace commonly shows an uneven morphology due to the alternation of smooth areas (corresponding to sandy seafloor with ripples, as deduced from direct check or through backscatter data) and blocky facies (often forming small ridges parallel to the coastline) or *Posidonia Oceanica* meadows (Figures 2–4), widely diffused on the terrace top.

Few seismic profiles cross this terrace because of its shallow depths and proximity to the coastline (tens or few hundreds of meters far from the coastline; Figures 2–4), hindering the manoeuvrability of towed seismic devices. The available profiles for NSDT (see, for instance, SP1 in Figure 5 and SP3 in Figure 6) show an uppermost seismic unit [5] characterized by an inner prograding geometry, with foresets downlap on a high-amplitude reflector, commonly representing the top of the underlying mid-shelf terrace; unit 5 has a maximum thickness of 18 m (10 m on average).

It has to be considered that the geometry of the near-shore terrace is often difficult to define on seismic profiles because its small thickness is partially masked by ringing effects generated by the

Sparker source, and by chaotic echo type/low signal penetration due to occurrence of the blocky facies and *Posidonia Oceanica* meadows (Figures 2–4);


Figure 4. (**a**) Shaded relief map of the NW sector of Salina (location in Figure 1a), where a large shelf with different orders of submarine depositional terraces are present; (**b**) the bathymetric cross section D–D^1 shows the edge depth of the shelf and overlying terraces. In this area, the blocky facies forms a small ridge parallel to the coastline, characterized in cross-section D–D^1 by a convex-upward shape similar to the other submarine depositional terraces, having the edge at water depths around 15 m. NSDT: near-shore submarine depositional terrace; M1SDT: mid-shelf submarine depositional terrace; LSDT: shelf-edge (lowstand) submarine depositional terrace. SP2 is trace of the Sparker profile shown in Figure 5.

(b) the mid-shelf terraces have the outer edge at depths around 40–50 m (M1SDT) and 70–80 m (M2SDT), even if minor and local slope breaks are recognizable on the bathymetry at different depths (always shallower than −120 m). The M1SDT edge is well-recognizable in the N, NW and SE sectors of the island (Figures 1c, 3 and 4), whereas the M2SDT edge is well-recognizable only in the S and SE sector of the island (Figure 3); both edges are not recognizable in the eastern sector (Figure 2).

On seismic profiles, the mid-shelf terraces M1SDT and M2SDT can be associated to the seismic units 4 and 3, respectively (Figures 5 and 6). Despite both seismic units occur on the entire shelf of Salina and are characterized by continuous and medium-high amplitude reflectors, they show a variable inner geometry in the different shelf sectors (Figure 5). Their geometry can vary from prograding (SP2 in Figure 5), with the topsets/foresets rollover forming a marked morphological edge of the terrace on the bathymetry (W sector, Figures 1c and 4), to more tabular, with the occasional recognition of onlapping reflectors on the volcanic bedrock (SP1), where the terrace edge is morphologically less marked (N sector, Figure 1c) or totally absent, such as in the eastern sector of the island (Figures 1c and 2). In a few cases, the morphological expression of a deeper terrace can be masked by the overlying terrace, if the vertical projections of the rollover associated to the two units matches (see SP2 in Figure 5). The thickness of these units is highly variable in the different sector of the shelf, being comprised between 5 and 20 m for the unit 4 and between 10 and 30 m for the unit 3;

(c) the shelf-edge terrace (LSDT in Figures 3 and 4) is recognizable only in the NW and SE sectors of the edifice, with an edge at water depths variable from 130 (cross-section D–D^1 in Figure 4) to 150–160 m (cross sections B–B^1 and C–C^1 in Figure 3).

On seismic profile, this terrace is associated to seismic unit 2, characterized by a marked prograding geometry, with steep foresets (8°–20°) or with weakly transparent facies. Where very steep, these foresets cannot be imaged on seismic profiles since they appear acoustically transparent (see SP4 in Figure 6; see also [28]). This unit mainly lies above the volcanic bedrock, in the sectors where the erosive shelf edge is deeper than 160 m (section B–B′ in Figure 3 and SP2 in Figure 5; section D–D′ in Figure 4 and SP4 in Figure 6c,d). The seismic unit 2 shows a variable thickness, reaching a maximum value of 27 m in the SE sector.
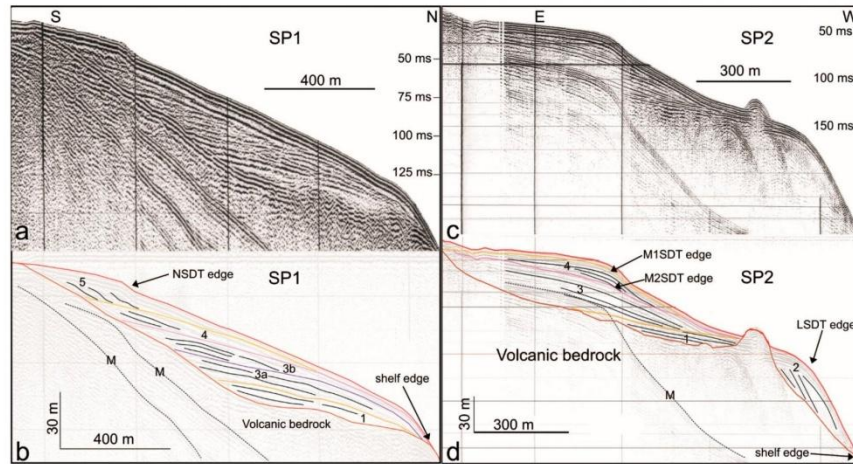
Figure 5. Sparker profiles (**a**,**c**) and associated line drawing (**b**,**d**) showing the stratigraphic architecture of the insular shelf on the northern (SP1) and western (SP2) part of Salina (for location see Figure 1a). The edge of the submarine depositional terraces (i.e., the rollover depth of the associated prograding units) are also shown. A sound velocity of 1500 m/s has been adopted for time-depth conversion. Acronyms as in the previous figure, see text for details.

Finally, it should be considered that each of the above-mentioned terraces and associated seismic units can be locally affected by landslide scars (often representing the head of underlying submarine canyons) that can reduce their width and makes shallower the terrace edge with respect to the surrounding areas (Figures 1c, 2 and 3).
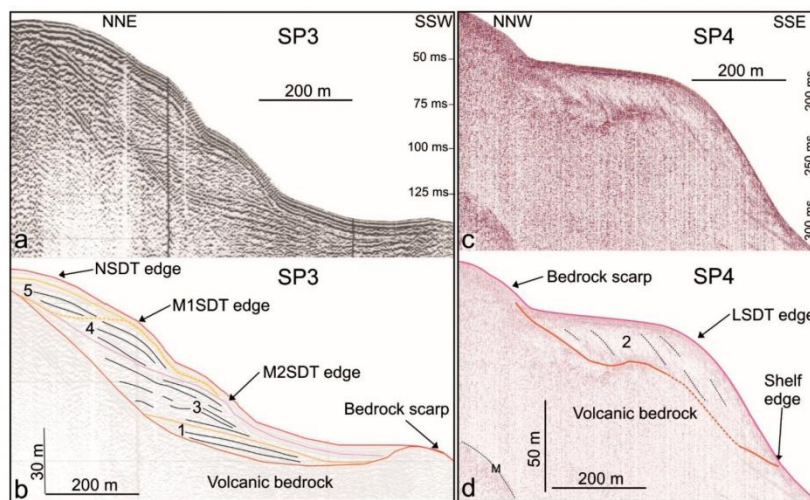
Figure 6. Sparker profiles (**a**,**c**) and associated line drawing (**b**,**d**) showing the stratigraphic architecture of the insular shelf on the south-eastern part of Salina (for location see Figure 1a). The edge of the submarine depositional terraces (i.e., the rollover depth of the associated prograding units) are also shown. A sound velocity of 1500 m/s has been adopted for time-depth conversion. Acronyms as in the previous figure, see text for details.

5. Discussion

5.1. Late-Quaternary Evolution of Insular Shelf and Overlying Submarine Depositional Terrace

The integration of morpho-bathymetric data and single-channel seismic profiles allows us to reconstruct the overall stratigraphic architecture of the shelf surrounding Salina Island, with particular attention to the development of terraced prograding wedges, i.e. submarine depositional terraces. These prograding wedges lie above an erosive surface that was carved on volcanic bedrock (Figures 5 and 6) and interpreted as the result of cumulated marine erosion on the flanks of subaerial/shallow-water volcanic centres during stages of reduced or inactive volcanism over different eustatic cycles [17]. At Salina, the shelf edge is commonly at depths comparable or shallower than the maximum depth of −127 m reached by the sea level in the last 450 ka [29], even if these values are not corrected for glacio-hydro-isostatic effect), in agreement with the regional uplift that characterizes the Aeolian Islands since the Last Interglacial, as witnessed by raised terraces [26]. Differently, the shelf edge is markedly deeper in the older W and SE sectors of the edifice, suggesting that subsidence affected Salina in the early growth stages [17].

The different orders of submarine depositional terraces identified in this study have been presumably formed during the last hemi-eustatic cycle (last 20 ka) that left its imprint over all shelf areas. In detail, the near-shore terrace is very similar in size and depth of its edge to present-day examples of prograding wedges observed on others insular shelves along the Mediterranean area, such as in the other Aeolian Islands [22] and the Pontine Archipelago [18,30] as well as along tectonically-controlled continental margins of Southern Iberia (infralittoral prograding wedge, [31]) and Southern Italy [32]. The depth range (10–25 m) of these edges is, in fact, compatible with the estimated present-day, local storm-wave base level in the central and western Mediterranean [20,21,33], whereas it is markedly lower with respect to the edge of similar features observed around oceanic islands, where the storm-base level is deeper [13,14,23]. Based on such evidences and considering that the present-day level has been attained since ca. 6.5 ka according to the sea level curve of [34], the formation of this terrace has been associated to the present highstand phase and, more generally, can be considered still under formation (Figure 7, [20]).

By applying the same genetic model to the deeper terraces, they can be interpreted as prograding wedges formed during stillstands, when the sea level was lower than the present-day. According to the sea-level curve of [34] and assuming similar meteo-marine conditions also for past sea-level conditions (on average 15 m for the storm-wave base level), the mid-shelf terraces 1 (edge at 40–50 m water depths) and 2 (edge at 70–80 m water depths) could have formed during the final and intermediate part of the transgressive phase (Figure 7). Even if we are aware that meteo-marine conditions could have been different during the Pleistocene and Holocene, as witnessed by some storm-wave deposits in the central and western Mediterranean [35,36], the possible difference in the depth range of ± 10 m is not enough to significantly change their stratigraphic attribution. Finally, the deeper shelf-edge terrace (edge at 130–160 m water depths) could have formed during the last lowstand at around 20 ka (Figure 7), before the sea level rapidly rose. However, the depth variability of its edge is quite large and suggests the possible role of post-depositional vertical movements (discussed in the next section), although a part of this variability could be also due to the different oceanographic regime between the two sectors.

This stratigraphic attribution is also in agreement with a) the observed retrogradational pattern of the SDTs from the shelf edge (LSDT) to the inner shelf (NSDT), and b) the different seismic geometry observed for LSDT and NSDT (prograding geometry, typical of longer stillstand of the sea level, as during the lowstand and highstand phases) with respect to the MSDTs (from prograding to more tabular, with the recognition of onlapping reflectors on the ravinement surface, typical of transgression phase, [22]). Differently, the lowermost unit 1, showing a patchy distribution and small thickness, could be interpreted as composed of regressive deposits, formed during the falling stage before the

LGM and locally preserved on the shelf, in correspondence of morphological steps or local depressions in the bedrock [37].
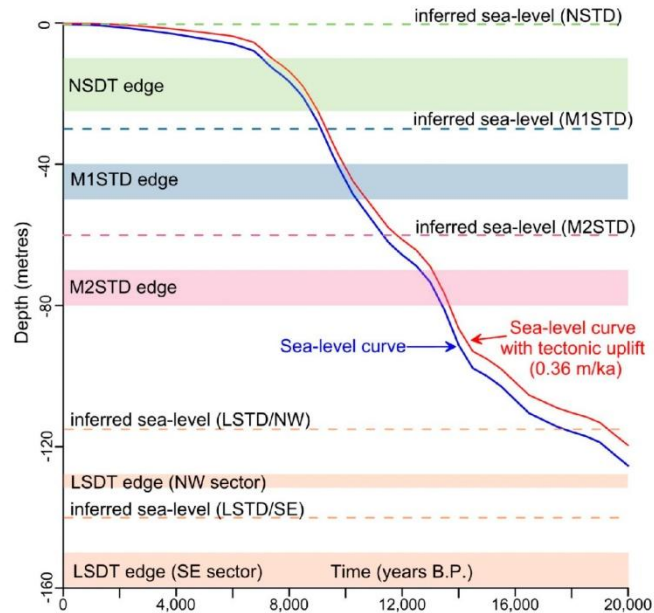
Figure 7. Plot of depth range of the submarine depositional terrace edges observed at Salina, with respect to the sea-level curve isostatically corrected for the last 20 ka (blue line, from [34]) and that (red line) modified for a tectonic uplift of 0.36 m/ka [26]. The inferred paleo sea-level (horizontal dashed lines) corresponding to the different terraces is also shown; this value was obtained by subtracting 15 m (average storm-wave base level at Salina) from the average depth of the terrace's edge. Note that two lines of inferred sea-level are drawn for LSDT in the NW and SE sectors, because of the large difference in depth range between the LSDT edge, suggesting the occurrence of differential vertical movements (see text for details). Acronyms as in the previous figures; B.P. = Before Present.

5.2. Submarine Depositional Terraces as a Tool for the Assessment of Vertical Movements and Relative Dating of Erosive Activity of Canyons

In the previous section, we have inferred that the SDT's edge can be used as a proxy of sea-level position (dashed lines in Figure 7). However, we are aware that this depth is not a direct measure of the sea-level, but it is influenced by different factors, such as the storm-wave base level that varies in response to submarine morphology, coastal physiography and exposition (fetch, winds and wave regime). Moreover, its determination is influenced by mapping procedures (for a review of possible inaccuracies in the estimate, see [20]). By considering the variability of the present-day NSDT edge (10–25 m, on average 15 m), we can roughly estimate an error range in the order of several meters. This means that only larger variations in the edge depths of a SDT could be related to differential vertical movements between two (or more) coastal sectors. This error estimation thus suggests excluding the NSDT for the vertical mobility assessment, because the amount of expected vertical movements in a time span of about 6.5 ka would be small (i.e., some meters at maximum) and, consequently, within the error range. Moreover, the NSDT is considered under formation at present, so possible changes in the depth of its edge due to vertical movements could be "readjusted" by active sedimentary dynamics [20]. Differently, the older M1SDT and M2SDT (the formation of which is roughly corresponding to inferred sea-level around 9 and 12 ka in Figure 7) could be

more promising for such assessment. However, mid-shelf terraces are commonly characterized by a large variability in inner geometry (from prograding to more tabular, with onlapping reflectors) and external shape (Section 4.1, Figures 5 and 6), posing some limits on their comparison among different sectors. The shelf-edge (lowstand) terrace shows instead a constantly, prograding inner geometry and a well-defined morphological edge, thus allowing a comparison at the island scale. On the other hand, where preserved, this terrace shows a larger range of edge depth: in the NW sector of Salina the edge is around 130 m water depth, being 20–30 m shallower than in the SE sector (150–160 m water depth), suggesting the occurrence of differential movements between these two sectors. The depth of LSDT edge in the NW sector is comparable with the predicted depth of the sea level during the last lowstand (Figure 7, around 120 m water depth, with a maximum value of 125 m at the LGM; [34]), also considering the average uplift rate of 0.36 m/ka estimated for the island since the Last Interglacial [26] and accounting for ca. 7 m of vertical displacement in the last 20 ka. Differently, the depth of LSDT edge in the SE sector is deeper than the predicted sea level during the LGM. In particular, even if we subtract a maximum value of 25 m of storm-wave base level (derived from the range depth of the NSDT edge in order to perform a conservative analysis) from the depths of the LSDT edge in the SE sector, we obtain an inferred sea-level value of 130 ± 5 m, indicating a local subsidence of about 10 m occurred in the last 20 ka. This subsidence could be supported by the fact that the LSDT in the SE sector lies above an insular shelf cutting the top of submarine eccentric centers (named Fossa delle Felci South in Figure 1). This subsidence is also testified by the recognition of a nearby flat-topped cone (Figure 1c), characterized by a relatively flat erosive shelf, with edges at depths around -220 m and covered by ca. 25 m of sedimentary cover [17], possibly affected by local vertical movements. These eruptive centres were emplaced close to the Lipari-Salina Channel, separating Salina from Lipari island, where more than 200 m of sediments (mostly with an aggradational pattern) were accumulated in a perched basin (unpublished data), suggesting that this sector has been also affected by a significant subsidence during time. Moreover, local evidence of subsidence, contrasting with the general uplift trend derived by raised marine terraces for the last 127 ka, have been also observed for the last few millennia at Panarea [38] and Lipari [22,39–41], in some coastal and shallow-water sectors.

Besides vertical mobility assessment, submarine depositional terraces can be also used for the relative dating of mass-wasting events affecting the insular shelf, on the basis of the geometrical relationship between them. In general, submarine canyon heads or landslide scars affecting a SDT, and being characterized by a marked morphological freshness, are thought to represent erosive stages occurring after the emplacement of the terrace. In contrast, the low morphological freshness of some canyon head and slide scar could be interpreted as the result of a successive draping or burial from the SDTs, thus indicating an older erosive stage. In this regard, attention should be paid to erosive features affecting the near-shore submarine depositional terrace (see for instance Figures 2 and 3), since the genesis of this latter can be referred to the present high-stand, this can represent a proxy for the occurrence of very recent mass-wasting events. A similar methodological approach has been tentatively applied to other Aeolian edifices (Stromboli and Lipari, [12,42]), and to tectonically-controlled margins [43], providing useful insights for a first geohazard assessment of the facing coastal areas.

6. Final Remarks

In summary, the present study allowed to characterize the complex seismo-stratigraphic architecture of the shelf surrounding Salina Island, that is strongly dependent on the interplay between local physiography, vertical movements, sediment supply, wave regime and sea-level fluctuations. This architecture is mostly made up by a series of terraced features (near-, mid- and shelf-edge terraces) associated to seismic units with an inner prograding geometry (sometimes tabular, with onlapping reflectors for mid-shelf units), whose genesis can be referred to the different sea-level phases (highstand, transgressive and lowstand) developed in the last hemi-eustatic cycle (i.e., post 20 ka).

We suggest that these terraces (specifically, their edge/rollover depth) can be used as proxy for paleo seal-level position, even if affected by significant inaccuracies, that have been estimated in the order of several meters for the Salina case. Despite these inaccuracies, the large depth range of the lowstand submarine depositional terraces edge observed between the NW and the SE sectors of Salina, can be interpreted as the evidence of later vertical displacements (here possibly due to neo-tectonic). Therefore, this study highlights the potential role of SDTs for the assessment of vertical movements in volcanic or tectonically-controlled margins. Furthermore, SDTs can be also used to relatively date the main erosive stages of submarine canyons indenting the insular shelf, through the geometrical relationship between these features. Specifically, the near-shore (highstand) terraces have the potential to evidence the occurrence of (very) recent mass-wasting events affecting shallow-water areas often very close to the coasts, with significant implications on related geohazard assessment.

Author Contributions: Daniele Casalbore coordinated the overall study, and together with Claudia Romagnoli and Francesco Latino Chiocci, developed the main hypotheses regarding the formation of the submarine depositional terraces and their possible use for neo-tectonic studies and to constrain the relative age of the different erosive stages affecting shallow-water sectors. Daniele Casalbore and Claudia Romagnoli wrote the main text. Daniele Casalbore, Claudia Romagnoli, Chiara Adami, Francesco Falese, Alessandro Ricchi, and Alessandro Bosman analyzed the data. Daniele Casalbore together with Chiara Adami prepared the images shown in the text.

Conflicts of Interest: The authors declare no conflict of interest.

References

1.　Mitchell, N.C.; Masson, D.G.; Watts, A.B.; Gee, M.J.R.; Urgeles, R. The morphology of the submarine flanks of volcanic ocean islands. A comparative study of the Canary and Hawaiian hotspot islands. *J. Volcanol. Geothe. Res.* **2002**, *115*, 83–107. [CrossRef]

2.　Coussens, M.; Wall-Palmer, D.; Talling, P.J.; Watt, S.F.L.; Cassidy, M.; Jutzeler, M.; Clare, M.A.; Hunt, J.E.; Manga, M.; Gernon, T.M.; et al. The relationship between eruptive activity, flank collapse, and sea level at volcanic islands: A long-term >1(Ma) record offshore Montserrat, Lesser Antilles. *Geochem. Geophys. Geosyst.* **2016**, *17*, 2591–2611. [CrossRef]

3.　Coombs, M.L.; White, S.M.; Scholl, D.W. Massive edifice failure at Aleutian Arc volcanoes. *Earth Planet. Sci. Lett.* **2007**, *256*, 403–418. [CrossRef]

4.　Romagnoli, C.; Casalbore, D.; Bortoluzzi, G.; Bosman, A.; Chiocci, F.L.; D'Oriano, F.; Gamberi, F.; Ligi, M.; Marani, M. Bathy-morphological setting of the Aeolian Islands. In *The Aeolian Islands Volcanoes*; Geological Society of London: London, UK, 2013; pp. 27–36.

5.　Nomikou, P.; Papanikolaou, D.; Alexandri, M.; Sakellariou, D.; Rousakis, G. Submarine volcanoes along the Aegean volcanic arc. *Tectonophysics* **2013**, *597*, 123–146. [CrossRef]

6.　Bosman, A.; Casalbore, D.; Romagnoli, C.; Chiocci, F.L. Formation of an 'a'ā lava delta: Insights from time-lapse multibeam bathymetry and direct observations during the Stromboli 2007 eruption. *Bull. Volcanol.* **2014**, *76*. [CrossRef]

7.　Casalbore, D.; Romagnoli, C.; Pimentel, A.; Quartau, R.; Casas, D.; Ercilla, G.; Hipolito, A.; Sposato, A.; Chiocci, F.L. Volcanic, tectonic andmass-wasting processes offshore Terceira island (Azores) revealed by high-resolution seafloor mapping. *Bull. Volcanol.* **2015**, *77*. [CrossRef]

8.　Casalbore, D.; Bosman, A.; Romagnoli, C.; Chiocci, F.L. Large-scale seafloor waveforms on the flanks of insular volcanoes (Aeolian Archipelago, Italy), with inferences about their origin. *Mar. Geol.* **2014**, *355*, 318–329. [CrossRef]

9. Urgeles, R.; Canals, M.; Baraza, J.; Alonso, B.; Masson, D. The most recent megalandslides of the Canary Islands: El Golfo debris avalanche and Canary debris flow, west El Hierro Island. *J. Geophys. Res. Solid Earth* **1997**, *102*, 20305–20323. [CrossRef]

10. Oehler, J.F.; Lénat, J.F.; Labazuy, P. Growth and collapse of the Reunion Island volcanoes. *Bull. Volcanol.* **2008**, *70*, 712–742. [CrossRef]

11. Silver, E.; Day, S.; Ward, S.; Hoffmann, G.; Llanes, P.; Driscoll, N.; Appelgate, B.; Saunders, S. Volcano collapse and tsunami generation in the Bismarck Volcanic Arc Papua New Guinea. *J. Volcanol. Geotherm. Res.* **2009**, *186*, 210–222. [CrossRef]

12. Casalbore, D.; Romagnoli, C.; Bosman, A.; Chiocci, F.L. Potential tsunamigenic landslides at Stromboli Volcano (Italy): Insight from marine DEM analysis. *Geomorphology* **2011**, *126*, 42–50. [CrossRef]

13. Quartau, R.; Trenhaile, A.S.; Mitchell, N.C.; Tempera, F. Development of volcanic insular shelves: Insights from observations and modelling of Faial Island in the Azores Archipelago. *Mar. Geol.* **2010**, *275*, 66–83. [CrossRef]

14. Quartau, R.; Hipolito, A.; Romagnoli, C.; Casalbore, D.; Madeira, J.; Tempera, F.; Roque, C.; Chiocci, F.L. The morphology of insular shelves as a key for understanding the geological evolution of volcanic islands: Insights from Terceira Island (Azores). *Geochem. Geophy. Geosyst.* **2014**, *15*, 1801–1826. [CrossRef]

15. Romagnoli, C. Characteristics and morphological evolution of the Aeolian volcanoes from the study of submarine portions. In *The Aeolian Islands Volcanoes*; Geological Society of London: London, UK, 2013; pp. 13–26.

16. Romagnoli, C.; Jakobsson, S.P. Post-eruptive morphological evolution of island volcanoes: Surtsey as a modern case study. *Geomorphology* **2015**, *250*, 384–396. [CrossRef]

17. Romagnoli, C.; Casalbore, D.; Ricchi, A.; Lucchi, F.; Quartau, R.; Bosman, A.; Tranne, C.A.; Chiocci, F.L. Morpho-bathymetric and seismo-stratigraphic analysis of the insular shelf of Salina (Aeolian archipelago) to unveil its Late-Quaternary geological evolution. *Mar. Geol.* **2018**, *395*, 133–151. [CrossRef]

18. Chiocci, F.L.; Orlando, L. Lowstand terraces on Tyrrhenian Sea steep continental slopes. *Mar. Geol.* **1996**, *134*, 127–143. [CrossRef]

19. Pepe, F.; Bertotti, G.; Ferranti, L.; Sacchi, M.; Collura, A.M.; Passaro, S.; Sulli, A. Pattern and rate of post-20 ka vertical tectonic motion around the Capo Vaticano Promontory (W Calabria, Italy) based on offshore geomorphological indicators. *Quat. Int.* **2014**, *322*, 85–98. [CrossRef]

20. Casalbore, D.; Falese, F.; Martorelli, E.; Romagnoli, C.; Chiocci, F.L. Submarine depositional terraces in the Tyrrhenian Sea as a proxy for paleo-sea level reconstruction: Problems and perspective. *Quat. Int.* **2017**, *439*, 169–180. [CrossRef]

21. Lobo, F.J.; Fernandez-Salas, L.M.; Hernandez-Molina, F.J.; Gonzalez, R.; Dias, J.M.A.; Díaz del Río, V.; Somoza, L. Holocene highstand deposits in the Gulf of Cadiz, SW Iberian Peninsula: A high-resolution record of environmental changes. *Mar. Geol.* **2005**, *219*, 119–141. [CrossRef]

22. Chiocci, F.L.; Romagnoli, C. Terrazzi Deposizionali Sommersi Nelle Isole Eolie. Available online: http://www.isprambiente.gov.it/contentfiles/00002400/2434-terrazzi-chiocci3.zip/at_download/file (accessed on 10 December 2017).

23. Mitchell, N.C.; Masselink, G.; Huthnance, J.M.; Fernandez-Salas, L.M.; Lobo, F.J. Depths of modern coastal sand clinoforms. *J. Sediment. Res.* **2012**, *82*, 469–481. [CrossRef]

24. Bosman, A.; Casalbore, D.; Anzidei, M.; Muccini, F.; Carmisciano, C.; Chiocci, F.L. The first ultra-high resolution digital Terrain model of the shallow-water sector around Lipari Island (Aeolian Islands, Italy). *Ann. Geophys.* **2015**, *58*, 771–787.

25. Ventura, G. Kinematics of the Aeolian volcanism (Southern Tyrrhenian Sea) from geophysical and geological data. In *The Aeolian Islands Volcanoes*; Geological Society of London: London, UK, 2013; pp. 3–11.

26. Lucchi, F.; Gertisser, R.; Keller, J.; Forni, F.; De Astis, G.; Tranne, C.A. Eruptive history and magmatic evolution of the island of Salina (central Aeolian archipelago). In *The Aeolian Islands Volcanoes*; Geological Society of London: London, UK, 2013; pp. 155–211.

27. Casalbore, D.; Bosman, A.; Romagnoli, C.; Chiocci, F.L. Morphological map of Salina offshore (Southern Tyrrhenian Sea). *J. Maps* **2016**, *12*, 725–730. [CrossRef]

28. Chiocci, F.L. Distorsioni nella forma dei TDS rilevati dai profili sismici e ripristino delle corrette geometrie (migrazione). In *Atlante dei Terrazzi Deposizionali Sommersi Lungo le Coste Italiane*; Memorie Descrittive della Carta Geologica d'Italia: Roma, Italy, 2004.

29. Bintanja, R.; van de Wal, R.S.W.; Oerlemans, J. Modelled atmospheric temperatures and global sea levels the past million years. *Nature* **2005**, *437*, 125–128. [CrossRef] [PubMed]

30. Casalbore, D.; Bosman, A.; Martorelli, E.; Sposato, A.; Chiocci, F.L. Mass-wasting features on the submarine flanks of Ventotene volcanic edifice (Tyrrhenian Sea, Italy). In *Submarine Mass Movements and Their Consequences, 6th International Symposium*; Springer: Berlin, Germany, 2016.

31. Hernandez-Molina, F.J.; Fernandez-Salas, L.M.; Lobo, F.J.; Somoza, L.; Díaz del Río, V.; Alveirinho Dias, J.M. The infralittoral prograding wedge: A new largescale progradational sedimentary body in shallow marine environments. *Geo-Mar. Lett.* **2000**, *20*, 109–117. [CrossRef]

32. Chiocci, F.L.; Casalbore, D. Unexpected fast rate of morphological evolution of geologically-active continental margins during Quaternary: Examples from selected areas in the Italian seas. *Mar. Pet. Geol.* **2017**, *82*, 154–162. [CrossRef]

33. Bárcenas, P.; Lobo, F.J.; Macías, J.; Fernández-Salas, L.M.; López-González, N.; Díaz del Río, V. Submarine deltaic geometries linked to steep, mountainous drainage basins in the northern shelf of the Alboran Sea: Filling the gaps in the spectrum of deltaic deposition. *Geomorphology* **2015**, *232*, 125–144. [CrossRef]

34. Lambeck, K.; Antonioli, F.; Anzidei, M.; Ferranti, L.; Leoni, G.; Scicchitano, G.; Silenzi, S. Sea level change along the Italian coast during the Holocene and projections for the future. *Quat. Int.* **2011**, *232*, 250–257. [CrossRef]

35. Budillon, F.; Esposito, E.; Iorio, M.; Pelosi, N.; Porfido, S.; Violante, C. The geological record of storm events over the last 1000 years in the Salerno Bay (Southern Tyrrhenian Sea): New proxy evidences. *Adv. Geosci.* **2005**, *2*, 123–130. [CrossRef]

36. Sabatier, P.; Dezileau, L.; Colin, C.; Briqueu, L.; Bouchette, F.; Martinez, P.; Siani, G.; Raynal, O.; Von Grafenstein, U. 7000 years of paleostorm activity in the NW Mediterranean Sea in response to Holocene climate events. *Quat. Res.* **2012**, *77*, 1–11. [CrossRef]

37. Trincardi, F.; Field, M.E. Geometry, lateral variation, and preservation of downlapping regressive shelf deposits: Eastern Tyrrhenian Sea margin, Italy. *J. Sediment. Petrol.* **1991**, *61*, 775–790.

38. Anzidei, M.; Esposito, M.; Benini, M. Evidence of active subsidence at Basiluzzo island (Aeolian islands, southern Italy) inferred from a Roman age wharf. *Quat. Int.* **2014**, *288*, 158–167. [CrossRef]

39. Calanchi, N.; Lucchi, F.; Pirazzoli, P.; Romagnoli, C.; Tranne, C.A.; Radtke, U.; Reyss, J.L.; Rossi, P.L. Late Quaternary relative sea-level changes and vertical movements at Lipari (Aeolian islands). *J. Quat. Sci.* **2002**, *17*, 459–467. [CrossRef]

40. Anzidei, M.; Bosman, A.; Casalbore, D.; Tusa, S.; La Rocca, R. New insights on the subsidence of Lipari island (Aeolian islands, southern Italy) from the submerged Roman age pier at Marina Lunga. *Quat. Int.* **2016**, *401*, 162–173. [CrossRef]

41. Anzidei, M.; Bosman, A.; Carluccio, R.; Casalbore, D.; D'Ajello, C.F.; Esposito, A.; Nicolosi, I.; Pietrantonio, G.; Vecchio, A.; Carmisciano, C.; et al. Flooding scenarios in coastal volcanic areas due to land subsidence and sea level rise: A case study for Lipari Island (Italy). *Terra Nova* **2017**, *29*, 44–51. [CrossRef]

42. Casalbore, D.; Romagnoli, C.; Bosman, A.; Anzidei, M.; Chiocci, F.L. Coastal hazard due to submarine canyons in active insular volcanoes: Examples from Lipari Island (southern Tyrrhenian Sea). *J. Coast. Conserv.* **2017**, *6*, 1–11. [CrossRef]

43. Casalbore, D.; Bosman, A.; Chiocci, F.L. Study of recent small-scale landslides in geologically active marine areas through repeated multibeam surveys: Examples from the Southern Italy. In *Submarine Mass Movement and Their Consequences*; Springer: Berlin, Germany, 2012.

5.3 Salina Island - Manuscript III

In the following manuscript we investigated in detail the vertical behavior of Salina highlighting the potential of a combined study encompassing submerged (insular shelves, submarine depositional terraces) and subaerial (raised marine terraces and notches) markers.

In the Aeolian islands raised fossil shorelines, correlated to (interglacial) high sea-level peaks of the Late-Quaternary eustatic curve, have been widely employed as a means of stratigraphical correlation of volcanic successions on local and inter-island scale (Lucchi, 2009). A long-term continuous uplifting trend since the Last Interglacial (MIS 5, average rate of c. 0.34 m/ka) has been estimated for most of the Aeolian archipelago on the base of marine terraces (Lucchi et al., 2004a). However, marine and subaerial evidences suggested a more irregular pattern for the vertical mobility of Salina (Chiocci and Romagnoli, 2004), suggesting the possible occurrence of subsidence during the middle-late Pleistocene (Lucchi, 2009). In this manuscript we integrated the information derived from the raised marine terraces and the submerged insular shelves to provide a comprehensive picture of the paleo sea-level variations and crustal vertical movements that affected the island since its earlier volcanic evolution. We also discussed the contribution of neo-volcano/tectonic processes at local and regional scale.

In this paper I contributed to conceive the presented idea of investigating the relationship between sea-level changes, insular shelf edge depth and subaerial terraces height. Moreover, I contributed to perform the subsidence calculations and in the writing of the manuscript.

"Late Quaternary paleo sea-level geomorphological tracers of opposite vertical movements at Salina volcanic island (Aeolian Arc)"

Authors:
- **Federico Lucchi** (University of Bologna, Bologna – Italy).
- **Alessandro Ricchi** (University of Bologna, Bologna – Italy).
- **Claudia Romagnoli** (University of Bologna, Bologna – Italy);
  (Istituto di Geologia Ambientale e Geoingegneria, Consiglio Nazione delle Ricerche, Rome – Italy).
- **Daniele Casalbore** (University of Rome – "La Sapienza", Rome – Italy);
  (Istituto di Geologia Ambientale e Geoingegneria, Consiglio Nazione delle Ricerche, Rome – Italy).
- **Rui Quartau** (Instituto Hidrográfico, Divisão de Geologia Marinha);
  (Universidade de Lisboa, Instituto Geofisico Infante Dom Luiz, Instituto Dom Luiz, Faculdade de Ciências da Universidade de Lisboa, Lisbon, Portugal).

Status: submitted to Earth Surface Processes and Landforms

Earth Surface Processes and Landforms

BSG British Society Geomor

Late-Quaternary paleo sea level geomorphological markers of opposite vertical movements at Salina volcanic island (Aeolian Arc)

SCHOLARONE™
Manuscripts

Late-Quaternary paleo sea level geomorphological markers of opposite vertical movements at Salina volcanic island (Aeolian Arc)

F. Lucchi [a], A. Ricchi [a], C. Romagnoli [a], D. Casalbore [b,c], R. Quartau [d,e]

[a] University of Bologna, Dip. Scienze Biologiche, Geologiche e Ambientali, P.za Porta S. Donato 1, 40126 Bologna, Italy

[b] Sapienza Università di Roma, Dipartimento Scienze della Terra, Roma, Italy

[c] Istituto di Geologia Ambientale e Geoingegneria, Consiglio Nazionale delle Ricerche, Area della Ricerca Roma 1, Montelibretti, Via Salaria Km 29,300, Monterotondo, Roma, Italy

[d] Instituto Hidrográfico, Divisão de Geologia Marinha, Lisboa, Portugal

[e] Instituto Dom Luiz, Faculdade de Ciencias, Universidade de Lisboa, Lisboa, Portugal

Abstract

Raised marine terraces and submerged insular shelves are used through an integrated approach as markers of relative sea level changes along the flanks of the Salina volcanic Island (Aeolian Arc, southern Italy) for the purpose of evaluating its crustal vertical deformation pattern through time. Paleo sea level positions are estimated for the terrace inner margins exposed subaerially at different elevations and the erosive shelf edges recognized offshore at different depths. Compared with the eustatic sea levels at the main highstands (for the terraces) and lowstands (for the shelf edges) derived from literature, these paleo sea level markers allowed us to reconstruct the interplay among different processes shaping the flanks of the island and, in particular, to quantify the pattern, magnitudes and rates of vertical movements affecting the different sectors of Salina since the time of their formation. A uniform uplift process at rates of 0.35 m/ka during the Last Interglacial is estimated for Salina (extended to most of the Aeolian Arc) as the evidence of a regional (tectonic) vertical deformation affecting the sub-volcanic basement in a subduction-related geodynamic context. Before, a dominant subsidence at rates of 0.39/0.56 m/ka is instead suggested for the time interval between 465 ka (MIS 12) and the onset of the Last Interglacial (MIS 5.5, 124 ka). By matching the insular shelf edges with the main lowstands of the sea level curve, a relative age

1

attribution is provided for the (mostly) submerged volcanic centres on which the deepest (and oldest) insular shelves were carved, with insights on the chronological development of the older stages of Salina and the early emergence of the island. The shift from subsidence to uplift at the Last Interglacial suggests a major geodynamic change and variation of the stress regime acting on the Aeolian sub-volcanic basement.

1. Introduction

The vertical mobility of coastal sectors is commonly reconstructed on the basis of relative paleo sea level markers that record the interplay between crustal vertical movements and eustatic sea level changes, when corrected for the effect of glacio-hydro-isostatic readjustments (Lambeck et al., 2004). The imprint of relative sea level changes is usually witnessed by the occurrence of raised shore platforms, coastal notches and marine terraces along the emergent coastal areas (e.g. Trenhaile, 2002; Zazo et al., 2002; Kennedy, 2005; Antonioli et al., 2006; Ferranti et al., 2006; Lucchi, 2009; Mauz et al., 2015; Trenhaile, 2015; Ramalho et al., 2017; Antonioli et al., 2015, 2018). In recent years, additional paleo sea level markers, such as archeological proxies, offlap breaks of continental margins, submarine prograding wedges, and the outer edges of insular shelves, have been recognized in submerged areas (Auriemma and Solinas, 2009; Fraccascia et al., 2013; Anzidei et al., 2014; Pepe et al., 2014; Quartau et al., 2014; Quartau et al., 2018; Anzidei et al., 2016; Casalbore et al., 2017a).

On volcanic islands, particularly if recently active, the timing and magnitude of relative sea level changes can be difficult to evaluate due to the complex behavior of crustal vertical deformation, possibly involving alternating, short-term and long-term vertical movements, induced by the interaction between regional and volcano-related deformation processes (Lucchi et al., 2007). The latter are connected to eruptive or volcano-tectonic processes, being usually transitory and active at the scale of an independent volcanic edifice, whereas regional tectonic processes are generally slower and of lower magnitude, affecting on a larger scale the sub-volcanic basement (Lajoie, 1986). Information on mobility trends of volcanic islands recently came from sequences of raised marine terraces (Lucchi et al., 2007; Lucchi, 2009; de Vita and Foresta Martin, 2017; Furlani et al., 2017; Ramalho et al., 2017), which are excellent markers of former sea levels recorded by their inner margins. When terraces are

2

presently found at elevations that are significantly higher than the original sea levels that originated them, uplift has occurred. If corrected for the eustatic (and subordinately glacio-hydro-isostastic) component derived from the predicted sea level curves, the inner margins of datable marine terraces provide information on pattern, magnitude and rates of vertical crustal deformation since the time of their formation. However, the terrace record is often incomplete because of masking by more recent volcanic deposits, erosion and sea cliff dismantling, landslides or lateral collapses, and possible obliteration caused by new terraces formed at lower elevations (Trenhaile, 2014). Furthermore, since most of the insular volcanic edifice usually lays below the present sea level, raised terraces may tell only part of the story of paleo sea level variations and crustal vertical movements.

The submarine flanks of insular volcanoes are commonly cut by shelves that are formed through marine erosion during sea level fluctuations when erosion dominates over volcanism (Ablay and Hurlimann, 2000; Mitchell et al., 2003; Le Friant et al., 2004; Llanes et al., 2009; Quartau et al., 2010). Because the shelf edge forms during lowstand periods in the zone of the most effective wave erosion, at or close to the water surface (Trenhaile, 2000, 2001), the depth of an erosive shelf edge can be adopted as a marker of paleo sea level and used to assess the vertical displacement that have occurred after its development (Quartau et al., 2014, 2015).

In this paper we propose a review and integration of extensive field study of marine terraces onland with high-resolution marine geophysical data from the insular shelf of Salina Island in the active Aeolian Arc, aimed at reconstructing the rates of vertical mobility of this volcanic complex. Compared with the eustatic fluctuations derived from the curve of Rohling et al. (2014), the integration of onshore and offshore paleo sea level markers suggests an articulated deformation history of the Salina volcanic complex over the late Quaternary, characterized by subsidence followed by uplift. The deformation pattern of Salina is then discussed in order to evaluate the possible contribution of active deformation processes resulting from tectonic and/or volcano-related processes at the local and regional scale.

2. Geological background

Salina Island is the second largest of the Aeolian Archipelago (Fig. 1), a tectonically-controlled volcanic arc located in the Southern Tyrrhenian Sea, in a subduction-related

3

geodynamic framework (e.g. Carminati et al., 1998; Faccenna et al., 2001b; De Astis et al., 2003; Ventura, 2013). The island, with an area of ~26.4 km^2, is the culmination of a broad, mainly submarine volcanic complex rising ca. 2000 metres above the sea floor (Casalbore et al., 2016), up to a maximum elevation of 962 m at Monte Fossa delle Felci. Salina is located at the intersection between the main arc-shaped structure of the archipelago and the NNW–SSE elongated Salina–Lipari–Vulcano volcanic alignment, running along the Aeolian-Tindari–Letojanni strike-slip (lithospheric) fault system (Ventura, 2013 and references herein).

2.1. Eruptive history and age constraints

The emergent part of Salina consists of different stratovolcanoes partly overlapping in space and time, which have grown since ~244 ka through six successive Eruptive Epochs (Lucchi et al., 2013a). These are separated by prolonged periods of volcanic quiescence and erosion, at times associated to different caldera and lateral collapses (Fig. 1a). The oldest (undated) volcanic edifices of Pizzo di Corvo, Fossa delle Felci South and Pizzo Capo North (co, ffs and pcn in Fig. 1b) are presently almost entirely submerged and largely dismantled, and recognized through the occurrence of wide and deep submerged shelves (Romagnoli et al., 2018). The early subaerial products of Epochs 1-2 are basaltic lava flows and scoriae erupted at the NE-SW elongated Pizzo Capo composite volcano (244-226 ka; K/Ar ages, Leocat, 2011) located in NE Salina (Fig. 1a). Epochs 3-4 (160-121 ka; K/Ar ages, Leocat, 2011) produced basaltic to dacitic scoriaceous successions and lava flows building up the NNW-SSE aligned Monte Rivi and Monte Fossa delle Felci twin stratovolcanoes in the central-southern part of Salina (Fig. 1a). Epoch 5 activity then shifted to the western sector with the construction of the basaltic-andesitic to dacitic Monte dei Porri stratovolcano (70–57 ka; K/Ar ages, De Rosa et al., 2003 and Leocat, 2011; Fig. 1a). The latest Epoch 6 activity is located at the Pollara crater (30–15.6 ka; K/Ar ages, Gillot, 1987; ^{14}C, Keller, 1980) in the NW edge of Salina, producing andesitic lava flows and basaltic to rhyolitic pumice successions (Fig. 1a). Major, high-energy explosive eruptions are recorded during the younger Epochs of Salina by the Grey Porri Tuffs (70-67 ka; dated through tephrostratigraphy, Lucchi et al., 2008 and references therein), and the Lower (27.5 ka; ^{14}C and tephrostratigraphy, Lucchi et al., 2013b and references therein) and Upper (15.6 ka; ^{14}C, Keller, 1980, calibrated age) Pollara Tuffs. These are repeatedly interlayered with the Brown Tuffs (70-8 ka; ^{14}C and

4

tephrostratigraphy; Lucchi et al., 2013b and references therein) from the island of Vulcano and other tephra layers from the Campanian area (Lucchi et al., 2008), generally constituting a voluminous and widespread pyroclastic succession on most of the island.

2.2. Marine terraces

Raised marine terraces are recognized, interlayered within the volcanic succession, at various elevations along the south-eastern, eastern and northern coastal sectors of Salina (Fig. 1a)(Lucchi et al., 2004; Lucchi, 2009). They are indirectly dated by linking them to the major highstand peaks of Marine Oxygen Isotope (MIS) 5 and MIS 7 on the basis of the reconstructed cross-cutting and stratigraphic relationships with (dated) volcanic deposits onland (Lucchi, 2009; Lucchi et al., 2013a,b). Marine terraces are largely covered by younger volcanic deposits and detrital material, and they are deeply dismantled by erosion processes.

The most prominent terraces are those related to the Last Interglacial (MIS 5). They are carved into the Pizzo Capo (244-226 ka) and Monte Fossa delle Felci (160-121 ka) volcanic deposits, and are uniformly covered by the volcaniclastic succession including the Grey Porri Tuffs and Brown Tuffs (70-8 ka) (Fig. 2a). Within this time-stratigraphic interval, the terrace with inner margin at higher elevations of ~50 m (terrace I) is attributed to the main highstand of MIS 5.5 (124 ka), whereas the terraces II and III, cross-cutting at lower elevations the terrace I, are reasonably attributed to MIS 5.3 (100 ka) and 5.1 (81 ka), respectively (Lucchi, 2009). The MIS 5.5 terrace is the best recorded along the northeastern coastal cliff of Salina (Fig. 2b). Minor marine notches are documented along the southern coastal cliffs of Salina (Lucchi et al., 2004; Lucchi, 2009). One of these notches is recognized at 10-12 m asl and is associated to terrace III.

A stratigraphically older marine terrace (terrace A) discontinuously crops out along the northern coastal cliff of Salina Island (Figs. 2a, c) in a direct vertical stratigraphic succession with the MIS 5 terraces located at higher elevations (Lucchi, 2009). Terrace A is carved into brecciated lavas related to the Pizzo Capo volcano (244-226 ka) and covered by the Monte Rivi volcanic deposits (160-131 ka) (Fig. 2c). According to these ages and stratigraphy, this terrace is attributed to the interglacial sea level peak of MIS 7.3 (Lucchi et al., 2013a), which is the main highstand peak before the Last Interglacial.

5

2.3. Insular shelves

The insular shelves around Salina exhibit a complex morphology, with variable width, morphological setting and depth of the erosive edge, related to the paleo-extension and ages of the different volcanic centres on which they are carved (Romagnoli et al., 2018). These shelves cannot be easily sampled neither directly dated, as it commonly happens in reefless islands. However, relative chronologic information has been obtained by assuming the shelf width as proxy of the age of the eroded bedrock subject to repeated sea level fluctuations (Menard, 1983; Quartau et al., 2010; Romagnoli, 2013). This proxy is compared with the age of the volcanic units outcropping in the coastal sector corresponding to the adjacent shelf. For instance, at Salina the widest (up to 1700–2000 m of extension from the coast to the shelf edge) and deepest shelves are recognized offshore the north, south and west edges of the island (Romagnoli et al., 2018), documenting the occurrence of three presently mostly submerged volcanic edifices (Pizzo di Corvo, Pizzo Capo North, Fossa Felci South) (Fig. 1b). These shelves are substantially wider than those formed around the Pizzo Capo volcano, and are thus assumed to predate the age of its volcanic products exposed onland (244-226 ka, the oldest units recognized on the island). Narrower and shallower shelves (commonly <1000 m) are instead observed offshore the coastal sectors of Salina Island where younger volcanic products are exposed, such as to the north and south of Monte dei Porri and along the eastern sides of Pizzo Capo and Monte Fossa delle Felci (Fig. 1b), thus being younger than the wider and deeper shelves.

The gently-sloping erosive surface of the shelves, carved on the volcanic bedrock, is generally covered by volcaniclastic sediments (Fig. 3a, d, e) organized in a set of prograding submarine depositional terraces (SDTs). At Salina, the SDTs are recognized at different depth ranges with depositional edges (i.e. offlap breaks) typically located between -10 m and -160 m (Casalbore et al., 2018). The shallowest (near-shore) SDT has a depositional edge at depths between -10 m and -25 m that is compatible with the estimated modern, local storm-wave base level, and is thus related to the present-day seaward transportation of sand from the surf zone and shoreface during storms (Chiocci and Romagnoli al., 2004; Quartau et al., 2012; Mitchell et al., 2012). The deeper SDTs have a similar genesis, but they are assumed to have formed during periods when sea level was relatively stable and lower than the present after the Last Glacial Maximum (hereafter LGM) (Casalbore et al., 2017).

6

3. Methodology

We applied a multidisciplinary approach based on the integration of geological fieldwork and interpretation of aerial photographs of the subaerial flanks, morphological analysis of Digital Terrain Models (hereafter DTMs) of the submarine slopes, and interpretation of high-resolution seismic profiles (Sparker 0.5-1 kJ) collected on the insular shelf (see also Romagnoli et al., 2018). In the following sections, we describe the approach adopted to relate the raised marine terraces (onland) and insular shelves (in the shallow-water portions) to different paleo sea level positions associated with major (interglacial and glacial) eustatic peaks (§ 3.1). These paleo sea level markers are used as proxies to evaluate the vertical displacement amounts and rates occurred since the time of formation of marine terraces and insular shelves (§ 3.2), by comparison with a reference eustatic sea level curve (§ 3.3).

3.1. Paleo sea level positions and associated errors

3.1.1. Terrace inner margins

After their first description in Lucchi et al. (2004) and Lucchi (2009), the positions and elevations of relict marine features along the subaerial coastal cliffs of Salina have been carefully checked during field surveys and boat trips. Elevations relative to the present mean sea level were estimated by using a pocket barometric altimeter, regularly calibrated with respect to known elevation points or the present sea level. The measured elevations were repeatedly compared with the contour lines on topographic maps and DTMs. A map at 1:10,000 scale from the Regional Technical Topographic Map of the Regione Sicilia (No. 581020 bis, Isola di Salina 1994) was available, whereas a DTM of the island (0.5 m-cell size) was obtained through LiDAR flights data provided by the Italian Ministry for the Environment and Protection of Land and Sea. The analytical error in the elevation estimate was generally lower than ±2.5 m. An additional error of ±5 m has been introduced for some sites where the precise estimation of the height of the terrace inner margins or notches was hindered by their outcrops at high elevation along a steep coastal cliff.

7

Tidal notches are commonly considered the best morphological markers of former sea levels, particularly when they are formed in carbonate rocks that can be dated (Antonioli et al., 2015). They also form in volcanic rocks (Trenhaile, 2014), but, unfortunately, marine notches recognized on Salina could not be studied in detail because they occur along the cliff at considerable elevations above present sea level, and thus are not considered in the present study.

Raised marine terraces are here adopted as the most significant subaerial markers of paleo sea level positions on Salina. Marine terraces are commonly assumed to form during a highstand (interglacial) sea level peak. They can be preserved by uplift if the rates are high enough to move them above the following highstand, or beyond the reach of cliff retreat during the subsequent lowstand (Trenhaile, 2014). Alternatively, terraces can form during still-stands induced by uplift at rates comparable to sea level rise. Terrace inner margins (Fig. 3a) represent, within a few meters of uncertainty, the paleo sea level position at the time of the corresponding interglacial sea level peak (Rovere et al., 2016), notably in the restricted tidal range (less than 0.5 metres) environment of the Mediterranean Sea (Carobene and Pasini, 1982; Pirazzoli, 1986; Firth et al., 1996; Pirazzoli et al., 1996). The estimated elevation of the corresponding paleo sea level is less accurate if a terrace inner margin is not visible due to the subsequent cover by volcanic and/or detrital deposits or it is locally reshaped due to erosion. In these cases, the paleo sea level position can be also approximately inferred by evaluating the depositional environment of the terrace deposits (e.g. Cantalamessa et al., 2005; Naish et al., 2005; Zecchin et al., 2006; Lucchi, 2009). These deposits are commonly represented on Salina by metre-thick horizons of grain-supported conglomerates composed of well-rounded pebbles to boulders (Ømax=2 m), with heterogeneous clast composition reflecting that of the eroded volcanic lithotypes. They result from reworking and abrasion in a high-energy, shallow-water coastal environment during the progressive landward shift of the shoreface (Lucchi, 2009). We consider a depth of 10 m (±5 m) for the level of effective shore platform abrasion and boulder formation (see § 3.1.2.), which approximately corresponds to the difference in elevation between the terrace inner margin and its outer edge (Fig. 3b). Thus, if the terrace inner margin is not visible, an approximate estimate of the paleo sea level corresponding to a terrace is obtained by adding +10 m to the minimum elevation of the terrace boulder deposits.

3.1.2. Insular shelf edges

Insular shelves and their morphologic parameters were recognized and mapped along the shallow-water flanks of Salina, with systematic measurements of the depths of erosive shelf edges. The depth of the erosive shelf edge is the best marker for paleo sea level estimation, since it records the lowest level of wave erosion during the corresponding glacial stage (Trenhaile, 2001). The analytical error in the depth estimate is generally lower than ±5 m, and is generally associated to imprecise picking of the erosive shelf edge in seismic profiles due to the steepness of the volcanic flanks or the "ringing" effect affecting the vertical resolution of seismic profiles. The shelf edge in rocky surfaces is assumed to form in the zone of most effective wave erosion, corresponding to the intertidal range (Trenhaile, 2000, 2001), which is also dependent on the interplay between the resistance of the bedrock to erosion and local wave conditions. In the present paper we assume a depth of 10 m (±5 m) for the zone of effective wave erosion at the shelf edge, by comparison with the edge of the shore platform carved around the Vulcanello peninsula on Vulcano (southern Aeolian Arc) in the present-day sea level conditions (Romagnoli et al., 2013). We are aware that extrapolating values from the present-day (highstand) conditions to past lowstand stages is not straigthforward, because the shelves formed during lowstands were largely emerged and meteo-marine conditions and oceanographic circulation could have been very different at that time. However, this estimation can be used to roughly assess the maximum erosion level at the outer shelf edge (and its error range) at the time of the corresponding lowstand peak (Fig. 3c). Accordingly, the paleo sea level position corresponding to an erosive shelf edge is approximately estimated by adding +10 m to its current depth. We also assume that a shelf edge was carved in the first lowstand after a main volcanic phase has stopped (Quartau et al., 2014).

Additionally, the depth of the shelf edge can be strongly influenced by other processes, such as subsequent volcanic progradation (Quartau et al., 2015) and/or emplacement of volcaniclastic sediments (Casalbore et al., 2017; Quartau et al., 2012; Romagnoli et al., 2018), as well as by retrogressive erosion related to canyon heads or slide scars that commonly indent the shelf (Casalbore et al., 2015, Quartau et al., 2012; Romagnoli et al., 2012 and 2018; Chiocci and Casalbore, 2017). These processes typically cause an upward and/or landward shift of the shelf edge, resulting in depths up to tens of meters shallower than

9

the originally formed one. The integration of multibeam bathymetry and seismic profiles allows the recognition of the sectors affected by these processes. It also permits distinguishing the erosive shelf edge from the depositional edge when sediments cover the shelf (Fig. 3d, e), enabling to reduce the errors associated to the measurement of (erosive) shelf edge depth. In the present work, we only assumed as a marker of paleo sea level the maximum depth of the erosive shelf edge in the sectors not affected by subsequent volcanic progradation and/or mass-wasting processes.

3.2. Coastal elevation changes

The vertical displacements affecting the different coastal sectors of Salina are estimated by comparing the present elevation of the different paleo sea level markers (terrace inner margins and shelf edges) with the eustatic sea level at the moment they were formed. We adapted the approach of Ramalho et al. (2010c) to take into account both raised terrace inner margins (above present sea level) and submerged erosive shelf edges (below present sea level). The amount of vertical displacement recorded by each of these sea level markers is thus extracted by using the equation:

$$D = h + d - E \qquad (1)$$

where **D** is the vertical displacement, **h** is the present-day elevation or depth of a marker, **d** the estimated depth of effective wave erosion (to infer the paleo sea level at the moment of formation of the marker), and **E** is the coeval eustatic sea level. The vertical displacement (uplift/subsidence) rate corresponding to a given marker is then obtained by dividing the displacement amount for a certain time interval since the highstand or lowstand stage related to its formation. Time-averaged displacement rates are generally estimated by assuming a constant movement and a similar trend between the time of formation of a marker and the present day. This assumption may be faulty and cause an underestimation of not linear or alternating vertical crustal movements, particularly over the short term. In the present paper, we thus estimate partitioned displacement rates resulting from the difference in vertical displacement (uplift or subsidence) affecting two successive paleo sea level markers as a function of the time interval between the corresponding sea level peaks. We extract the

10

vertical displacement between two successive paleo sea level markers (a) and (b), where (a) is younger and (b) is older, by means of the following equation:

$$D_b = h + d - e \tag{2}$$

where **e** is the relative sea level resulting from:

$$e = E + D_a$$

where **E** is the eustatic sea level and D_a is the displacement suffered from the island during the time interval subsequent to the marker (a). Then, we obtain the corresponding partitioned displacement rate by dividing the estimated amount of uplift or subsidence for the time interval between the highstand or lowstand stages relative to markers (a) and (b). This allows to build up a curve of cumulative displacement by plotting the different pulses of uplift/subsidence relative to the corresponding time intervals. We believe this is a valid approach for the definition of long-term crustal vertical movements, particularly if timescales longer than the age of formation of individual terraces or shelves are considered.

3.3. Reference eustatic sea level curve

The described approach to the vertical displacement estimation may suffer from the problem of precisely determining the elevation of eustatic sea levels associated to highstand and lowstand peaks. None of the known Pleistocene eustatic sea level curves can, in fact, be used as a world-wide datum (e.g. Broecker et al., 1968; Chappell and Shackleton, 1986; Bard et al., 1990; Lambeck et al., 2002; Waelbroeck et al., 2002; Bintanja et al., 2005; Miller et al., 2005; Bintanja & Van de Wal, 2008; Raymo et al., 2009; Rohling et al., 2009; Sosdian and Rosenthal, 2009; De Boer et al., 2010; Wang et al., 2010; Grant et al., 2012, 2014; Elderfield et al., 2012; Rohling et al., 2014; Shakun et al., 2015; Spratt and Lisiecki, 2016), as also discussed by Caputo (2007). Moreover, it is well known that regional variations of eustatic sea levels can be caused by glacio-isostatic adjustments (GIA) due to the crust's response to the loading and unloading of the large Northern Hemisphere ice sheets (Lambeck and Johnston, 1995; Pirazzoli, 1998; Lambeck and Bard, 2000; Lambeck et al., 2003). GIA affecting the

11

rising sea level for a few metres have been particularly outlined for the Holocene transgression (Lambeck et al., 2004), the MIS 2 lowstand (Clark et al., 2009) and the MIS 5.5 (Dutton and Lambeck, 2012; Dutton et al., 2015) and MIS 11 (Raymo and Mitrovica, 2012) highstands.

Nevertheless, the adoption of one of the "global" eustatic curves as a reference can allow estimating long-term variations in coastal elevation changes over time spans of hundreds thousand years. To document eustatic sea level fluctuations, we used the sea level curve of Rohling et al. (2014) specifically provided for the Mediterranean. This curve makes available a time-series of GIA-corrected sea level elevations and depths during the glacial–interglacial cycles over the past 550 ka, entirely matching the time period under investigation and being suitable for the purposes of our study. For the eustatic sea level corresponding to the Last Interglacial, i.e. MIS 5.5, we adopt the value of +6 (±3) m estimated in tectonically stable areas of the Mediterranean Sea (Lambeck et al., 2004; Ferranti et al., 2006; Lambeck et al., 2011), which is largely used as the eustatic sea level datum in the region under study along the Southern Tyrrhenian coasts (Antonioli et al., 2018). This sea level datum integrates the Rohling et al. (2014) curve, where there is not a suitable paleo sea level estimation for the MIS 5.5 highstand peak due to the occurrence of a sapropel event.

4. Results

The main results of our geological and morphological analysis along the subaerial and shallow-water flanks of Salina are hereafter presented, particularly referred to the estimation of different paleo sea level positions indicated by (subaerial) marine terraces and (submerged) insular shelf edges (§ 4.1) and the corresponding vertical displacement magnitudes and rates (§ 4.2).

4.1. Paleo sea level markers

4.1.1. Marine terraces

Raised marine terraces crop out along the south-eastern, eastern and northern coastal cliffs of Salina. An elevation of ~50 (±2.5) m for the terrace I inner margin exposed along the

12

eastern and northeastern coastal cliff of Salina (Fig. 2b) is assumed as a representative estimation of the paleo sea level for the MIS 5.5 highstand peak. The MIS 5.3 and MIS 5.1 paleo sea level positions are instead represented at elevations of 25 (±2.5) m and 10 (±5) m asl, corresponding to the terrace inner margins of terraces II and III, respectively.

The MIS 7.3 terrace is assumed as a marker for paleo sea level older than the Last Interglacial, although it has a very discontinuous occurrence along the northern coastal cliff of Salina (Fig. 2c). The sectioned terrace crops out at elevations of 2-6 m asl, but the terrace inner margin is not well established due to erosion and dismantling after its formation, and to covering by subsequent volcanic deposits. The corresponding paleo sea level position is thus only approximately located at ~12 m asl, considering a depth range of 10 m for the minimum present height of the terrace boulder deposits (see § 3.1.1). This is assumed as a safe limit of the paleo-sea level estimate, considering that the present occurrence of the terrace is not necessarily its outer edge. A paleo sea level of ~12 m asl is thus considered representative for the MIS 7.3 highstand peak.

4.1.2. Insular shelves

Insular shelves at various depths are present around Salina, reaching maximum water depths of ~230 m. The shelves have been subdivided into three groups (deep, intermediate and shallow) based on the depths of their erosive edges (Figs. 4-5). Deep shelves have edges at (maximum) depths of -225/-210 m, intermediate shelves at depths of -160/-140 m, and shallow shelves at -125/-110 m (Fig. 4). Each of these erosive shelf edges is assumed to correspond to a paleo sea level located 10 (±5) m higher, based on the estimated depth of effective wave erosion (see § 3.1.2).

Among the deep shelves, the one located in front of the eroded remnants of the Pizzo Corvo volcano (hereafter CO_1), in the western sector of Salina, is the widest and with the deepest edge reaching a maximum value of -225 (±5) m (Fig. 5), which is a marker of a paleo sea level at depth of -215 (±5) m. Another deep edge with a maximum value of -210 (±5) m, corresponding to a paleo sea level of -200 m, is exhibited by the shelf located offshore the SE edge of Salina in correspondence of the Fossa Felci South volcanoes (hereafter FFS_1) (Fig. 5). These edges characterize here the outer portions of a wide shelf that survived erosion, being (locally) deeply dissected by erosive canyon heads (blue lines in Fig. 4).

13

81

Intermediate shelves are recognized to the north of Pizzo di Corvo (hereafter CO_2) and in a small area of the Fossa Felci South volcanoes (hereafter FFS_2), with edges at maximum depths of -140 (±5) m and -160 (±5) m (Fig. 5), corresponding to paleo sea levels of -130 m and -150 m, respectively. Another intermediate shelf with a semicircular shape and shelf edge at maximum depth of -145 (±5) m, referred to a paleo sea level at -135 m, is found off the northern coast of Salina representing the erosion of the Pizzo Capo North submerged volcano (hereafter PCN_W) (Fig. 5).

Shallow shelves are observed offshore the volcanic edifices that presently form the island, i.e. along the southern and northern sides of Monte dei Porri (hereafter PR), and along the eastern sides of Pizzo Capo (hereafter PC) and Monte Fossa delle Felci (hereafter FF), with shelf edges at maximum depths of -125 (±5) m (PR, PC and FF) (Fig. 5), corresponding to a paleo sea level of -115 m. These shelves are narrower than the deep and intermediate ones, and in places poorly preserved due to subsequent erosive processes (blue lines in Fig. 4), as particularly observed in the FF shelf (Fig. 4).

A relatively shallow shelf, with edge at depths of -110 (±5) m, relative to a paleo sea level at -100 m, is also recognized off the northern coast of Salina, on the eastern side of the Pizzo Capo North volcano (hereafter PCN_E) (Figs. 4-5). It has some peculiar morphological characteristics, suggesting a different history with respect to the adjacent intermediate shelf PCN_W (Romagnoli et al., 2018). Therofore, it is not considered in the estimations of vertical displacements (see below).

4.2. Vertical displacement magnitudes and rates

Magnitudes and rates of vertical displacement affecting the different coastal sectors of Salina document a history of vertical movements characterized by a recent uplifting stage (§ 5.1) and an older subsiding stage (§ 5.2).

4.2.1. Uplifting stage

The MIS 5.5 terrace is here adopted as the main marker for paleo sea level because it is consistently widespread along the coasts of Italy and the Southern Tyrrhenian (see Ferranti et al., 2006; Antonioli et al., 2018 for a review). Considering an eustatic sea level of +6 m asl

14

82

at the time of its formation (Lambeck et al., 2004; Ferranti et al., 2006; Antonioli et al., 2018), an uplift of 44 m is derived from the paleo sea level position (50 m asl) corresponding to the terrace I inner margin (Tab. 1 and Fig. 6a). This corresponds to a time-averaged uplift rate of 0.35 m/ka between the MIS 5.5 major highstand peak and today. Uplift rates of the same order of magnitude result by taking into account the terraces II (25 m asl) and III (10 m asl), respectively attributed to MIS 5.3 and MIS 5.1 (Tab. 1 and Fig. 6a). Accordingly, we assume for Salina a similar trend of uplift at fairly constant rates for the whole duration of the Last Interglacial, as supported by the staircased, downstepping suite of raised terraces, with the lower (younger) terraces cross-cutting the (older) ones at higher elevations.

This uplift process is consistent also for the following stages such as the LGM, as indicated by the PC, FF and PR shallow insular shelves. A relative chronological attribution of <70-57 ka (PR), <160-131 ka (FF) and <244-226 ka (PC) is obtained for these shelves from the age of the volcanic deposits exposed onland in the corresponding coastal sectors. Accordingly, we assume that their shelf edges, having the same depths, were carved or reworked during the LGM. These erosive shelf edges are recognized at maximum depths of -125 m, corresponding to a paleo sea level of -115 m (§ 4.1.2). This is approximately in the range of the eustatic sea level for the LGM (MIS 2, -120 m; Rohling et al., 2014), and suggest a limited (average) uplift rate of 0.23 m/ka (Tab. 2 and Fig. 6a), which is in the same order of magnitude of that estimated for the whole duration of the Last Interglacial from the elevation of the subaerial terraces. However, we are aware that such small values are at the limit of the resolution of our methodological approach.

4.2.2. Subsiding stage

A generalized subsidence of Salina, opposite to the above-mentioned uplift trend, is suggested for the time interval before the Last Interglacial by the available paleo sea level markers.

Firstly, the terrace A attributed to MIS 7.3, although cropping out above the present sea level, provides indications of some subsidence, rather than uplift, before the Last Interglacial. Its occurrence at 2-6 m asl is, in fact, referred to a paleo sea level of ~12 m asl (§ 4.1.1). This is not consistent with a presumed relative sea level of 89 m asl ("uplifted sea level" in Fig. 6b) derived by correcting the MIS 7.3 eustatic sea level (12 m asl, Rohling et al., 2014) for the

15

displacement (+77 m) suffered by the terrace if the Last Interglacial uplift rate had been active since MIS 7.3. We thus assume that subsidence occurred before the Last Interglacial. Particularly, by applying equation (2), a net displacement of -44 m (D7.3 in Tab. 1) is obtained if we compare the paleo sea level of MIS 7.3 terrace (h+d) with the relative sea level (e) derived by modifying the eustatic sea level (E) according to the +44 m uplift that occurred since the Last Interglacial (Table 1 and Fig. 6b). This net displacement corresponds to a subsidence rate of 0.45 m/ka that should have occurred in the time interval between MIS 7.3 (221 ka; Rohling et al., 2014) and MIS 5.5 (124 ka) in order to account the present-day elevation of the terrace.

Evidence of subsidence during the early stages of evolution of Salina is also provided by the present elevations of the intermediate (-160/-140 m) and deep insular shelf edges (-225/-210 m), corresponding to paleo sea levels located 10 m higher (§ 4.1.2). These shelf edges have been also likely affected by the general uplift that characterized Salina since MIS 5.5, so that their original shelf depths would be even higher. Considering that the eustatic sea level never reached depths greater than -120 m in the last 550 ka (Rohling et al., 2014), the present elevations of the erosive shelf edges thus clearly indicate that subsidence affected these shelves after their formation. However, a main problem for estimating quantitatively the subsidence magnitudes and rates is the lack of direct ages for the erosive shelf edges, due to obvious difficulties in collecting datable material in these reefless shelves. Relative chronological information can only be derived by assuming the shelf width and depth as a proxy of its age (Romagnoli et al., 2018), which implies that: i) the deep (-225/-210 m) and intermediate (-160/-140 m) shelves around Pizzo di Corvo (CO_1 and CO_2), Fossa Felci South (FFS_1 and FFS_2) and Pizzo Capo North (PCN_W) volcanoes are older than the shallow (-125 m) shelves of Pizzo Capo (PC), Fossa Felci (FF) and Monte dei Porri (PR); ii) the intermediate shelves are younger than the deep shelves; iii) both deep and intermediate and shelves are older than the 244-226 ka age of the onland Pizzo Capo volcanic deposits. An exception is represented by the shelf offshore the north-eastern part of Pizzo Capo edifice (PCN_E in Fig. 4) that has a width similar to the adjacent PCN_W intermediate shelf, suggesting a coeval formation, but it has a markedly shallower shelf edge (-110 m), and thus was not considered as a marker for vertical displacement rates (for details § 5.1).

We attempted to indirectly date the shelves by matching each of the intermediate and deep shelf edges with the main individual lowstands of the sea level curve (Rohling et al.,

16

2014) in the time interval before 244-226 ka (Tab. 2 and Fig. 6c). The considered time interval is extended back to ca. 500 ka that is considered a reliable maximum age for the shallow-water portions of the Salina volcanic island. Accordingly, the initial formation of the intermediate and deep shelves has been tentatively related to MIS 12 (465 ka; Rohling et al., 2014), MIS 10 (356 ka) and MIS 8 (273 ka), which are the main sea level lowstands in the studied time interval (Fig. 6c). Our calculations firstly take into account the CO_1 shelf recognized offshore Pizzo di Corvo, which is the deepest and widest shelf on Salina, and thus the oldest one among those recognized around the island. Its erosive shelf edge presently lies at a depth of -225 m (h) that corresponds to a paleo sea level located 10 m higher (d). By applying equation (2), we obtain a net displacement of -138 m, if the CO_1 shelf is attributed to MIS 12, by comparing the paleo sea level depth (h+d) with the relative sea level (e) of -77 m extracted by correcting the eustatic depth (E) for the vertical displacements occurred between the MIS 7.3 and MIS 5.5 (D7.3) and since MIS 5.5 (D5.5) (Tab. 2 and Fig. 6c). This net displacement corresponds to a time-averaged subsidence rate of 0.56 m/ka for the time interval between MIS 12 (465 ka) and MIS 7.3 (221 ka). Alternatively, if the shelf formation is attributed to MIS 10, we obtain a substantially higher subsidence rate of 1.02 m/ka (Table 2). For the FFS_1 deep shelf, the estimated subsidence rates are of 0.53 m/ka and 0.91 m/ka for MIS 12 and 10, respectively. We then apply a similar approach to the intermediate (younger) shelves of CO_2, FFS_2 and PCN_W. The corresponding subsidence rates are of 0.39 m/ka (CO_2), 0.54 m/ka (FFS_2) and 0.43 m/ka (PCN_W) if the shelves are referred to MIS 10, whereas subsidence rates of 0,79 m/ka (CO_2), 1,17 m/ka (FFS_2) and 0,88 m/ka (PCN_W) are relative to MIS 8 (Table 2). Notably, a fairly uniform subsidence process at constant rates in the range of 0.39/0.56 m/ka for the investigated time interval comes out by attributing the deep shelves (CO_1 and FFS_1) to MIS 12 and the intermediate ones (CO_2, FFS_2 and PCN_W) to MIS 10. These subsidence rates also match the one estimated for the time interval spanning from MIS 5.5 and MIS 7.3 (0.45 m/ka), and is thus assumed as the "best-fit" scenario over the long-term. Instead, the respective attribution of the deep and intermediate shelves to MIS 10 and MIS 8, yielding higher (and variable) subsidence rates (0.79 to 1.17 m/ka), is considered an unlikely vertical behavior. The assumed, most likely scenario with the deep and intermediate shelves attributed to MIS 12 and MIS 10 gives similar subsidence rates (0.42 to 0.53 m/ka) even if calculated over the time interval spanning between MIS 12 and MIS 5.5, which marks the onset of the uplift process on Salina (Tab. 3).

17

5. Discussion

The reconstructed history of vertical movements of Salina Island over the last ~500 ka is hereafter discussed in the direction of providing new relative age constraints on the insular shelves formation and the early development of the island (§ 5.1). We then discuss the long-term uplift and subsidence trends as the result of dominant regional tectonic processes (§ 5.2), with some insights on the geodynamic context in which Salina is situated (§ 5.3).

5.1 Age constraints for insular shelves

By assuming a uniform and constant subsidence rate to match the depths of deep and intermediate shelf edges with MIS 12 and MIS 10 lowstands, respectively, a relative age is inferred for the (mostly) submerged volcanic centres carved by the corresponding insular shelves. This provides information on the chronological development of the older stages of Salina. Specifically, the first emergence of the Salina volcanic complex was mostly limited to the NW (Pizzo di Corvo, PC_1) and SE sectors (Fossa Felci South, FFS_1), as suggested by the occurrence of the deeper insular shelves, and likely started sometime before MIS 12 (465 ka) (Fig. 7). Successive steps of construction of the older portions of the Pizzo di Corvo and Fossa delle Felci volcanic edifices, together with the Pizzo Capo North volcano, occurred since MIS 10 (356 ka) (Fig. 6), as attested by the areal distribution of the intermediate shelf edges (PC_2, FFS_2, PCN_W). A subsequent erosion episode of the deep and intermediate shelves during MIS 8 (273 ka) may have occurred, but it is not witnessed by any of the observed shelf edges. This may be explained by considering that, taking into account the estimated displacement magnitudes and rates, the paleo sea level markers (shelf edge) relative to MIS 8 would have been displaced at depths equal or shallower than the depth range reworked by LGM (Fig. 6c), thus being successively reworked and erased. Nevertheless, our reconstruction shows that the wider and deeper shelves were affected by successive episodes of erosion and reworking during successive, younger sea level cycles, testifying their polycyclic origin, similarly to what proposed by Quartau et al. (2010) at Azores. However, only the occurrence of subsidence of considerable magnitude may allow a shelf edge to be preserved as a relict feature at depths substantially higher than subsequent sea

18

level lowstands (Quartau et al., 2018). At Salina, in fact, the deep and intermediate shelf edges around Pizzo di Corvo, Fossa Felci South and Pizzo Capo North are considered as relict features with respect to the edge of younger, shallow shelves of Monte dei Porri (PR), Pizzo Capo (PC) and Monte Fossa delle Felci (FF), which are mostly related to the LGM (MIS 2, 22 ka) (Fig. 7). The PR shelf was entirely formed during the MIS 2, considering that it is carved on volcanic products dated in the 70-57 ka time interval. Instead, a possible erosion episode of the PC and FF shelves previously occurred during MIS 6 (137 ka) cannot be discounted in light of the available ages of the volcanic products on which the shelves are carved. However, this appears unlikely because, given the estimated subsidence rate, the depth range of MIS 6 is shallower than that of MIS 2 (Fig. 6b). Note that the shallow PR, PC and FF are formed around the volcanic edifices that form the current setting of Salina Island, which have been gradually constructed at 244-226 ka (Pizzo Capo), 160-121 ka (Monte Fossa delle Felci) and Monte dei Porri (70-57 ka), alternating with recurrent episodes of terrace formation during MIS 7.3 and MIS 5 (Fig. 7).

A peculiar case is that represented by the insular shelf recognized offshore the northern flank of the Pizzo Capo volcanic edifice (PCN_E in Figs. 4-5). This shelf has a width similar to the adjacent, intermediate PCN_W shelf (1730 m), but it displays a shelf edge at depth of -110 m that is markedly shallower compared to PCN_W (-145 m) (Fig. 5). This discrepancy outlines that the formation of the two shelves was likely not coeval, as it could be instead suggested by the overall elliptical shape of the Pizzo Capo North submerged centre on which the shelves are carved (Fig. 4). The most plausible hypothesis to explain this anomalous setting is that an early shelf originally developed above the Pizzo Capo North edifice, and its north-eastern portion was successively covered by younger lava flows that partially or completely filled the shelf and made its edge shallower. A similar behavior of shelf "rejuvenation" has been suggested by Quartau et al. (2015) for Pico Island in the Azores. This hypothesis is supported by the different seismo-acoustic characteristics observed between the PCN_E sediment-starved shelf, characterized by an outcropping volcanic bedrock, and the PCN_W shelf, showing a thick sedimentary cover like the other relatively old shelves (Romagnoli et al., 2018). We hypothesize that lava accumulation in this submerged sector was driven by a submarine eruption(s) rather than by lava progradation from the subaerial sectors, consistently with the absence onland in the corresponding coastal sector of evidence

19

87

for volcanic activity more recent than the 244-226 ka Pizzo Capo edifice (Lucchi et al., 2013a).

5.2 Long-term opposite vertical movements

The long-term, opposite vertical movements of Salina during the middle to late Pleistocene are here discussed as the result of the interplay between GIA-corrected eustatic sea level fluctuations (Rohling et al., 2014) and crustal vertical movements. From our results, a roughly uniform trend of uplift at average rates of 0.35 m/ka has occurred at Salina for the whole duration of the Last Interglacial, between the MIS 5.5 major highstand peak and the present day, recorded in the raised subaerial marine terraces I, II and III and coherent with the depth of the shallow shelf edges of PR, FF and PC. This is in agreement with the long-term uplift trend of ~0.34 m/ka during the Last Interglacial previously estimated for most of the Aeolian archipelago (Calanchi et al., 2002; Lucchi et al., 2004c, 2007b; Lucchi, 2009). The long-term uplift of Salina is interpreted to reflect the dominant role played by regional tectonic processes affecting the sub-volcanic basement, as previously discussed for the rest of the Aeolian archipelago (Lucchi et al., 2007b; Lucchi, 2009).

This scenario, however, and unfortunately, cannot be checked against independent evidence provided by Holocene sea level markers. To the present knowledge, Holocene marine notches and terraces are lacking in the whole Aeolian archipelago (Lucchi, 2009), in contrast with a potential net emergence at elevations of +2-4 m *asl* predicted by the estimated rates of uplift. The lack of abrasion notches could be related to the absence of substantial sea level stillstands, at which abrasion notch-forming may occur, during the sea level rise corresponding to the last deglaciation (Lambeck et al., 2004). The Holocene sea level curve of Lambeck et al. (2004) for the area, in fact, predicts rates of sea level rise higher than the estimated long-term uplift rate, resulting in a relative sea level rise that would prevent the emergence of any Holocene markers. This tendency could have been also locally enhanced by the historical to recent subsidence processes witnessed in some sectors of the Aeolian archipelago (Serpelloni et al., 2013; Anzidei et al., 2016). Moreover, tidal notches are typically carved in carbonates in the Mediterranean area (e.g. Rust and Kershaw, 2000; Antonioli et al., 2002; Antonioli et al., 2015), so that it is uncommon to find out them at Salina.

20

Going further back in time, the SDTs recognized above the insular shelves of Salina are associated to relative sea level stillstands during the post-LGM transgressive stage (Casalbore et al., 2017 and 2018), but they cannot be easily matched with specific points of the eustatic curve in absence of reliable age constraints. However, some SDTs associated to the LGM in the south-eastern submarine sector of Salina Island suggest a localized subsidence during the last 20 ka (Casalbore et al., 2018). This subsidence is more likely related to tectonic activity along NE–SW striking normal and transtensive faults forming graben-like structures along the channel separating Salina from the nearby Lipari Island (Ventura et al., 1999), and it thus does not influence the generalized uplift suggested for Salina during the last deglaciation.

Opposite to the Last Interglacial uplift trend, a prolonged subsidence have occurred in the time interval spanning from (at least) ~465 ka (MIS 12) to the onset of the Last Interglacial at ~124 ka (MIS 5.5). Subsidence occurred around the different coastal sectors of Salina Island at nearly constant rates in the range of 0.42/0.53 m/ka for the whole period (0.39/0.56 m/ka if the rates are partitioned by the MIS 7.3 highstand peak). Oceanic volcanic islands are commonly affected by widespread subsidence as the result of either the volcanic load posed on the underlying lithosphere during the early shield building stages (Menard and Ladd, 1963; Watts and ten Brink, 1989) or cooling of the underlying lithospheric plate (Stein and Stein, 1992). These processes are, however, not suitable for a relatively small-scale volcanic arc-island like Salina. Moreover, it is noteworthy that a similar subsidence likely occurred along the northwestern coast of Lipari and in the Lipari-Salina channel, as indicated by the depths of the corresponding insular shelves (Chiocci and Romagnoli, 2004). This means that the outlined subsidence trend involves not only the whole Salina Island but also part of Lipari. Thus, subsidence is more likely considered as the result of regional tectonic processes relative to the central Aeolian sub-volcanic basement.

Our reconstruction indicates that volcano-related deformation due to eruptive or volcano-tectonic processes apparently have not modified the long-term vertical mobility of Salina, as for most of the Aeolian Islands volcanoes (Lucchi et al., 2007b; Lucchi, 2009). The vertical displacement in volcanic areas is, in fact, usually transitory at rates that range up to tens or hundreds of m/ka over time periods of hundreds or thousands of years (e.g. Kilburn et al., 2017, and references therein), and are much higher than those estimated on Salina. The spatial distribution of vertical deformation in volcanic areas is also an important feature to be

21

considered. Large-scale uplift processes in many ocean islands can be induced by cumulative intrusive processes. In the volcanic complexes of the Aeolian Archipelago, instead, vertical movements are more likely localized and record inflation and deflation of individual volcanic edifices in response to their magma chamber filling and draining (Tallarico et al., 2003; Lucchi et al., 2007b), in a spatial range of a few kms from the source (Currenti and Williams, 2014; Browning and Gudmundsson, 2015). This doesn't fit the occurrence of uplift and subsidence processes at similar (constant) rates affecting the different coastal sectors of Salina, where a number of spatially-independent volcanic edifices are recognized. We thus assume that, although strong vertical deformation may have affected individual volcanic edifices in the short-term (on time scales of thousands of years), the long-term vertical behavior of a large polygenetic volcanic complex like Salina was instead more likely dominated by regional tectonic processes affecting the sub-volcanic basement.

5.3 Insights on regional tectonic processes

The occurrence at Salina of opposite long-term trends of uplift and subsidence has possible implications on the large-scale geo-tectonic regime of the region under study. The Aeolian Islands volcanoes are located in the Southern Tyrrhenian Sea at the boundary between the African and Eurasian plates, in a geotectonic context mostly controlled by the northwest dipping subduction of the Ionian slab below the Calabrian Arc (Ventura et al., 2013, and references therein). The volcanoes lie above thinned continental crust belonging to the northwestern margin of the Calabro–Peloritan block, which has undergone a persistent and large-scale uplift at mean rates up to ~1 m/ka since ~0.7 Ma (Hearty et al., 1986; Westaway, 1993; Miyauchi et al., 1994), witnessed by the occurrence of flights of raised marine terraces along most of the southern Tyrrhenian coasts (cfr. Bordoni and Valensise, 1998; Antonioli et al., 2006; Ferranti et al., 2006 for a review). This regional uplift is commonly explained as the result of the isostatic rebound of the upper plate and the Calabrian Arc in response to the southeastward rollback of the subducting Ionian plate (e.g. Westaway, 1993; Hyppolite et al., 1994; Giunchi et al., 1996; Gvirtzman and Nur, 1999, 2001; Doglioni et al., 2001; Neri et al., 2003). The uplift of Salina (and most of the Aeolian Islands volcanoes) during the Last Interglacial is considered reasonable in this regional geotectonic regime that has persisted for hundreds of ka, longer than the age of the individual volcanic edifices. However, the

22

90

subsidence trend previously affecting Salina (and part of Lipari) from at least ~465 ka (MIS 12) to the onset of the Last Interglacial does not fit with the generalized uplift of the Calabrian Arc. The subsidence trend at Salina neither fits with the coeval subsidence processes reported for the peri-Tyrrhenian Gioia basin (Fabbri et al., 1980) and the back-arc Marsili basin (Kastens et al., 1988; Argnani and Savelli, 1999) since the related geotectonic regimes are different. This suggests a more complicated history of vertical movements and regional tectonic processes affecting the Aeolian sub-volcanic basement on a longer time span, ranging from the Middle to the Upper Pleistocene.

Our preferred interpretation is that a major geodynamic change occurred in the Aeolian Islands area and the southern Tyrrhenian before the onset of the Last Interglacial, changing the dominant vertical behavior from subsidence (contemporaneous to uplift in the Calabrian Arc) to prevailing uplift. A change in the stress field (passing from compressional to extensional) some time after the Early Pleistocene has been proposed for the Southern Appennines by Hippolyte et al. (1994), but it is not possible to establish its direct consequences in the adjacent Southern Tyrrhenian continental margin and back-arc basin. Many authors suggest that rollback of the subducting Ionian plate may have ceased or significantly slowed at some point between the Middle and Upper Pleistocene, possibly resulting in a major change in tectonic style and vertical deformation (e.g. Faccenna et al., 2001a; Wortel and Spakman, 2000; Goes et al., 2004; Chiarabba and Palano, 2017). Alternatively, the detachment of the deeper part of subducted plate could be the cause of widespread surface uplift (Wortel and Spakman, 2000; Buiter et al., 2002), whereas a reverse motion (subsidence) during the preceding rollback phase is suggested by Buiter et al. (2002)'s modelling. Chiarabba and Palano (2017) hypothesize that the progressive detachment of the slab took place along the Aeolian-Tindari-Letojanni lithospheric fault system, crossing the Aeolian archipelago in its central sector, thus potentially involving the entire region under study. A more precise definition of the sequence of geotectonic phases leading to the observed vertical movements is beyond the scope of the present work. In any case, the estimated long-term subsidence and uplift magnitudes and rates may represent useful data to implement the models of lithospheric processes governing the geodynamical evolution of the southern Tyrrhenian.

7. Conclusions

23

The magnitudes and rates of vertical deformation affecting Salina Island over the last ~500 ka are estimated by matching the paleo sea level positions recorded in raised subaerial marine terraces and submerged insular shelf edges with the peaks of the eustatic sea level curve. A continuous and constant uplift trend at an average rate of 0.35 m/ka during the last 124 ka (Last Interglacial) is recorded by a staircase of raised marine terraces, indirectly dated by the radiometric ages of volcanic products above and below. This uplift is comparable to that recognized in the whole central-western Aeolian Arc sector and explained with the prevalence of regional tectonic processes in the geodynamic framework of the Southern Tyrrhenian. An opposite, long-term subsidence is instead inferred from the depths of submerged insular shelf edges for the time period before the onset of the Last Interglacial, with a "best-fit" scenario that implies an average, constant displacement rate of -0.42/-0.53 m/ka starting (at least) from the MIS 12 lowstand (465 ka). The estimated subsidence rate provides a useful relative dating tool for the older volcanic edifices that characterize the early stages of development of Salina Island, suggesting its emergence mostly in the 356-465 ka time interval. Moreover, the shift over time from dominant subsidence to uplift of Salina (and most of the Aeolian Islands) likely indicates a possible major geodynamic change, and stress regime variation, affecting the sub-volcanic basement in the region under study in relation to roll-back slowdown or detachment of the Ionian subducting plate.

Acknowledgements

24

the terrestrial LIDAR data. F.L.Chiocci and C.A.Tranne provided useful discussions. We also acnlowledge Ricardo Ramalho and two anonymous reviewers for their insightful feedbacks.

References

Ablay G, Hurlimann M. 2000. Evolution of the north flank of Tenerife by recurrent giant landslides. *Journal of Volcanology and Geothermal Research* 103: 135–159.

Antonioli F, Cremona G, Immordino F, Puglisi C, Romagnoli C, Silenzi S, Valpreda E Verrubbi V. 2002. New data on the holocenic sea level rise in NW Sicily (central Mediterranean sea). *Global and Planetary Change* 34: 121-140.

Antonioli F, Ferranti L, Lambeck S, Kershaw S, Verrubbi V, Dai Pra` G. 2006. Late Pleistocene to Holocene record of changing uplift rates in southern Calabria and northeastern Sicily (southern Italy, central Mediterranean sea). *Tectonophysics* 422: 23–40.

Antonioli F, Ferranti L, Stocchi P, Deiana G, Lo Presti V, Furlani S, Marino C, Orru P, Scicchitano G, Trainito E, Anzidei M, Bonamini M, Sansò P, Mastronuzzi G. 2018. Morphometry and elevation of the last interglacial tidal notches in tectonically stable coasts of the Mediterranean Sea. *Earth-Science Reviews* 185: 600–623.

Antonioli F, Lo Presti V, Rovere A, Ferranti L, Anzidei M, Furlani S, Mastronuzzi G, Orru PE, Scicchitano G, Sannino G, Spampinato CR, Pagliarulo R., Deiana G., de Sabata E, Sansò P, Vacchi M, Vecchio A. 2015. Tidal notches in Mediterranean Sea: a comprehensive analysis. *Quaternary Science Reviews* 119: 66-84.

Anzidei M, Bosman A, Casalbore D, Tusa S, La Rocca R. 2016. New insights on the subsidence of Lipari island (Aeolian islands, southern Italy) from the submerged Roman age pier at Marina Lunga. *Quaternary International* 401: 162-173.

25

Anzidei M, Lambeck K, Antonioli F, Furlani S, Mastronuzzi G, Serpelloni E, Vannucci G. 2014. Coastal structure, sea level changes and vertical motion of the land in the Mediterranean. In: Martini IP, Wanless HR. (eds) Sedimentary coastal zones from high to low Latitudes: similarities and differences. *Geological Society, London, Special Publications* 388, doi10.1144/SP388.20.

Argnani A, Savelli C. 1999. Cenozoic volcanism and tectonics in the southern Tyrrhenian sea: space–time distribution and geodynamic significance. *Geodynamics* 27: 409-432.

Auriemma R, Solinas E. 2009. Archaeological remains as sea level change markers: A review. *Quaternary International* 206: 134–146.

Bintanja R, van de Wal RSW, Oerlemans J. 2005. Modelled atmospheric temperatures and global sea levels the past million years. *Nature* 437: 125–128.

Bintanja R, van de Wal RSW. 2008. North American ice-sheet dynamics and the onset of 100,000-year glacial cycles. *Nature* 454: 869-872.

Bordoni P, Valensise G. 1998. Deformation of the 125 Ka marine terrace in Italy: tectonic implications. In: Stewart IS, Vita-Finzi C. (eds) Coastal Tectonics. *Geological Society, London, Special Publications* 146: 71–110.

Broecker WS, Thurber DL, Goddard J, Ku TL, Matthews RK, Mesolella KJ. 1968. Milankovitch hypothesis supported by precise dating of coral reefs and deep-sea sediments. *Science* 159: 297-300.

Browing J, Gudmundsson A. 2015. Caldera faults capture and deflect inclined sheets: An alternative mechanism of ring-dike formation. *Bulletin of Volcanology* 77(1), DOI:10.1007/s00445-014-0889-4

Buiter SJH, Govers R, Wortel MJR. 2002. Two-dimensional simulations of surface deformation caused by slab detachment. *Tectonophysics* 354: 195– 210.

26

94

Calanchi N, Lucchi F, Pirazzoli PA, Romagnoli C, Tranne CA, Radtke U, Reyss JL, Rossi PL. 2002. Late-Quaternary and recent relative sea level changes and vertical displacements at Lipari (Aeolian Islands). *Journal of Quaternary Science* 17: 459–467.

Cantalamessa G, Di Celma C, Ragaini L. 2005. Sequence stratigraphy of the Punta Ballena Member of the Jama Formation (Early Pleistocene, Ecuador): insights from integrated sedimentologic, taphonomic and paleoecologic analysis of molluscan shell concentrations. *Palaeogeography Palaeoclimatology Palaeoecology* 216: 1–25.

Caputo R. 2007. Sea level curves: Perplexities of an end-user in morphotectonic applications. *Global and Planetary Change* 57(3-4): 417-23.

Carminati E, Wortel MJR, Spakman W, Sabadini R. 1998. The role of slab detachment processes in the opening of the western–central Mediterranean basins: some geological and geophysical evidence. *Earth Planetary and Science Letters* 160: 651-665.

Carobene L, Pasini G. 1982. Contributo alla conoscenza del Pleistocene superiore e dell'Olocene del Golfo di Orosei (Sardegna orientale). *Bollettino della Società Adriatica di Scienze di Trieste* 64: 5-36.

Casalbore D, Romagnoli C, Pimentel A, Quartau R, Casas D, Ercilla G, Hipolito A, Sposato A, Chiocci FL. 2015. Volcanic, tectonic and mass-wasting processes offshore Terceira island (Azores) revealed by high-resolution seafloor mapping. *Bulletin of Volcanology* 77.

Casalbore D, Bosman A, Romagnoli C, Chiocci FL. 2016. Morphological map of Salina offshore (Southern Tyrrhenian Sea). *Journal of Maps* 12 (5): 725–730. http://dx.doi.org/ 10.1080/17445647.2015.1070300.

Casalbore D, Falese F, Martorelli E, Romagnoli C, Chiocci FL. 2017. Submarine depositional terraces in the Tyrrhenian Sea as a proxy for paleo-sea level reconstruction: Problems and perspective. *Quaternary International* 439: 169–180. DOI:10.1016/j.quaint. 2016.07.051.

27

Casalbore D, Romagnoli C, Adami C, Bosman A, Falese F, Ricchi A, Chiocci FL. 2018. Submarine Depositional Terraces at Salina Island (Southern Tyrrhenian Sea) and Implications on the Late-Quaternary Evolution of the Insular Shelf. *Geosciences* 2018 8-20 DOI:10.3390.

Chappell J, Shackleton NJ. 1986. Oxygen isotopes and sea level. *Nature* 324: 137–140.

Chiarabba C, Palano M. 2017. Progressive migration of slab break-off along the southern Tyrrhenianplate boundary: Constraints for the present day kinematics. *Journal of Geodynamics* 105: 51–61.

Chiocci FL, Romagnoli C. 2004. Terrazzi deposizionali sommersi nelle Isole Eolie. In: Chiocci FL, D'Angelo S, Romagnoli C. (eds.). Atlante dei Terrazzi Deposizionali Sommersi Lungo le Coste Italiane. *Memorie Descrittive della Carta Geologica d'Italia* 58: 81–114.

Chiocci FL, Casalbore D. 2017. Unexpected fast rate of morphological evolution of geologically-active continental margins during Quaternary: Examples from selected areas in the Italian seas. *Marine and Petroleum Geology* 82: 154–162.

Currenti G, Williams CA. 2014. Numerical modeling of deformation and stress fields around a magma chamber: Constraints on failure conditions and rheology. *Physics of The Earth and Planetary Interiors* 226: 14-27.

De Astis G, Ventura G, Vilardo G. 2003. Geodynamic significance of the Aeolian volcanism (Southern Tyrrhenian Sea, Italy) in light of structural, seismological and geochemical data. *Tectonics* 22: 1040–1057.

De Boer B, Van De Wal RSW, Bintanja R, Lourens LJ, Tuenter E. 2010. Cenozoic global ice-volume and temperature simulations with 1-D ice-sheet models forced by benthic 18O records. *Annals of Glaciology* 51(55): 23-33.

28

96

De Rosa R, Guillou H, Mazzuoli R, Ventura G. 2003. New unspiked K-Ar ages of volcanic rocks of the central and western sector of the Aeolian Islands: reconstruction of the volcanic stages. *Journal of Volcanology and Geothermal Research* 120: 161–178.

de Vita S, Foresta Martin M. 2017. The palaeogeographic setting and the local environmental impact of the 130 ka Falconiera tuff-cone eruption (Ustica island, Italy). *Annals of Geophysics* 60/2: S0224; doi:10.4401/ag-7113.

Doglioni C, Innocenti G, Mariotti G. 2001. Why Mt. Etna? *Terra Nova* 13: 25-31.

Elderfield H, Ferretti P, Greaves M, Crowhurst SJ, Mc-Cave IN, Hodell DA, Piotrowski AM. 2012. Evolution of ocean temperature and ice volume through the Mid-Pleistocene Climate Transition. *Science* 337, 704–709.

Faccenna C, Becker TW, Lucente FP, Jolivet L, Rossetti F, 2001a. History of subduction and back-arc extension in the central Mediterranean. Geophysical Journal International 145: 809–820.

Faccenna C, Funiciello F, Giardini D, Lucente P. 2001b. Episodic back-arc extension during restricted mantle convection in the central Mediterranean. *Earth Planetary and Science Letters* 187: 105-116.

Ferranti L, Antonioli F, Mauz B, Amorosi A, Dai Pra G, Mastronuzzi G, Monaco C, Orrù P, Pappalardo M, Radtke U, Renda P, Romano P, Sansò P, Verrubbi V. 2006. Markers of the last interglacial sea level high stand along the coast of Italy: tectonic implications. *Quaternary International* 145–146, 30–54.

Firth C, Stewart I, McGuire WJ, Kershaw S, Vita-Finzi C. 1996. Coastal elevation changes in eastern Sicily: implications for volcano instability at Mount Etna. In McGuire WJ, Jones AP, Neuberg J. (eds.). Volcano Instability on the Earth and Other Planets. *Geological Society, London, Special Publications* 80: 57–74.

29

Fraccascia S, Chiocci FL, Scrocca D, Falese F. 2013. Very high-resolution seismic stratigraphy of Pleistocene eustatic minima markers as a tool to reconstruct the tectonic evolution of the northern Latium shelf (Tyrrhenian Sea, Italy). *Geology* 41: 375-378.

Furlani S, Antonioli A, Cavallaro D, Chirco P, Caldareri F, Foresta Martin F, Morticelli MG, Monaco C, Sulli A, Quarta G, Biolchi S, Sannino G, de Vita S, Calcagnile L, Agate M. 2017. Tidal notches, coastal landforms and relative sea level changes during the Late Quaternary at Ustica Island (Tyrrhenian Sea, Italy). *Geomorphology* 299: 94–106.

Gillot PY. 1987. Histoire volcanique des Iles Eoliennes: arc insulaire ou complexe orogenique anulaire? *Documents et Travaux de l'Institut Géologique Albert de l'Apparent* 11: 35–42.

Giunchi C, Sabadini R, Boschi E, Gasperini P. 1996. Dynamic models of subduction: geophysical and geological evidence in the Tyrrhenian Sea. *Geophysical Journal International* 126: 555-578.

Goes S, Giardini D, Jenny S, Hollenstein C, Kahle H-G, Geiger A. 2004. A recent reorganization in the south-central Mediterranean. *Earth Planetary and Science Letters* 226: 335–345.

Grant KM, Rohling EJ, Bar-Matthews M, Ayalon A, Medina-Elizalde M, Bronk Ramsey C, Satow C, Roberts AP. 2012. Rapid coupling between ice volume and polar temperature over the past 150 kyr. *Nature* 491, 744–747.

Grant KM, Rohling EJ, Bronk Ramsey C, Cheng H, Edwards RL, Florindo F, Heslop D, Marra F, Roberts AP, Tamisiea ME, Williams F. 2014. Sea-level variability over five glacial cycles, *Nature Communications* 5, 5076.

Gvirtzman Z, Nur A. 1999. Plate detachment, asthenosphere upwelling, and topography across subduction zones. *Geology* 27(6). DOI: 10.1130/0091-7613(1999).

30

Gvirtzman Z, Nur A. 2001. Residual topography, lithospheric structure and sunken slabs in the central Mediterranean. *Earth and Planetary Science Letters* 187(1-2): 117-130. DOI: 10.1016/S0012-821X(01)00272-2.

Hearty PJ, Miller GH, Stearns CE, Szabo BJ. 1986. Aminostratigraphy of Quaternary shorelines in the Mediterranean basins. *Geological Society of America, Bulletin* 97: 850-858.

Hippolyte JC, Angelier J, Roure F, Casero P. 1994. Piggyback basin development and thrust belt evolution: structural and palaeostress analyses of Plio-Quaternary basins in the Southern Apennines. *Journal of Structural Geology* 16: 159-173.

Kastens K, Mascle J, Auroux C, Bonatti E, Broglia C, Channell J, Curzi P, Emeis KC, Glacon G, Asegawa S, Hieke W, Mascle G, McCoy F, McKenzie J, Mendelson J, Muller C, Réhault JP, Robertson A, Sartori R, Sprovieri R, Tori M. 1988. ODP Leg 107 in the Tyrrhenian Sea: insights into passive margin and back-arc basin evolution. *Geological Society of America, Bulletin* 100: 1140–1156.

Keller J. 1980. The island of Salina. *Rendiconti della Societa` Italiana di Mineralogia e Petrologia* 36: 489–524.

Kennedy DM, Beban JG. 2005. Shore platform morphology on a rapidly uplifting coast, Wellington, New Zealand. *Earth Surface Processes and Landforms* 30: 823–832.

Kilburn CRJ, De Natale G, Carlino S. 2017. Progressive approach to eruption at Campi Flegrei caldera in southern Italy. *Nature Communications* 8. DOI:10.1038/ncomms15312.

Lajoie KR. 1986. Coastal tectonics. In Usselman TM (ed). Studies in Geophysics – Active Tectonics. National Academy Press, Washington DC, 95–124.

Lambeck K, Bard E. 2000. Sea-level change along the French Mediterranean coast since the time of the Last Glacial Maximum. *Earth and Planetary Science Letters* 175 (3–4): 202–222.

31

Lambeck K, Yokoyama Y, Purcell T. 2002. Into and out of the Last Glacial Maximum: sea-level change during Oxygen Isotope Stages 3 and 2. *Quaternary Science Reviews* 21: 343–360.

Lambeck K, Purcell A, Johnston P, Nakada M, Yokoyama Y. 2003. Water-load definition in the glacio-hydro-isostatic sea-level equation. *Quaternary Science Reviews* 22: 309–318.

Lambeck K, Antonioli F, Purcell A, Silenzi S. 2004. Sea level change along the Italian coast for the past 10,000 yrs. *Quaternary Science Reviews* 23: 1567–1598.

Lambeck K, Antonioli F, Anzidei M, Ferranti L, Leoni G, Scicchitano G, Silenzi S. 2011. Sea level change along the Italian coast during the Holocene and projections for the future. *Quaternary International* 232: 250-257.

Le Friant A, Harford CL, Deplus C, Boudon G, Sparks RSJ, Herd RA, Komorowski JC. 2004. Geomorphological evolution of Montserrat (West Indies): importance of flank collapse and erosional processes. *Geological Society, London, Journal* 161: 147–160.

Leocat E. 2011. Histoire eruptive des volcans du secteur occidental des Iles Eoliennes (Sud de la Mer Tyrrhenienne, Italie) et evolution temporelle du magmatisme. PhD thesis, University of Paris, Orsay 11.

Llanes P, Herrera R, Gomez M, Munoz A, Acosta J, Uchupi E. 2009. Geological evolution of the volcanic island La Gomera, Canary Islands, from analysis of its geomorphology. *Marine Geology* 264: 123–139.

Lucchi F. 2009. Late-Quaternary marine terrace deposits as tools for wide-scale correlation of unconformity-bounded units in the volcanic Aeolian archipelago (southern Italy). *Sedimentary Geology* 216: 158–178.

Lucchi F, Tranne CA, Calanchi N, Rossi PL. 2004. Late Quaternary fossil shorelines in the Aeolian Islands (Southern Tyrrhenian Sea): evaluation of long-term vertical displacements. In

32

100

Antonioli F, Monaco C. (eds). Contribution from the study of Ancient Shorelines to Understanding the Recent Vertical Motions. Field trip across the Messina Straits. *Quaternaria Nova* VIII: 115–137.

Lucchi F, Tranne CA, Calanchi N, Rossi PL. 2007. Late Quaternary deformation history of the volcanic edifice of Panarea (Aeolian Arc). *Bulletin of Volcanology* 69: 239–257.

Lucchi F, Tranne CA, De Astis G, Keller J, Losito R, Morche W. 2008. Stratigraphy and significance of Brown Tuffs on the Aeolian Islands (southern Italy). *Journal of Volcanology and Geothermal Research* 177: 49–70.

Lucchi F, Gertisser R, Keller J, Forni F, De Astis G, Tranne CA. 2013a. Eruptive history and magmatic evolution of the island of Salina (central Aeolian archipelago). In Lucchi F, Peccerillo A, Keller J, Tranne CA, Rossi PL. (eds). The Aeolian Islands Volcanoes. *Geological Society, London, Memoirs* 37: 155–211.

Lucchi F, Keller J, Tranne CA. 2013b. Regional stratigraphic correlations across the Aeolian archipelago (southern Italy). In Lucchi F, Peccerillo A, Keller J, Tranne CA, Rossi PL. (eds). The Aeolian Islands Volcanoes. *Geological Society, London, Memoirs* 37: 55–81.

Lucchi F, Peccerillo A, Keller J, Tranne CA, Rossi PL. 2013c (eds). The Aeolian Islands Volcanoes. *Geological Society, London, Memoirs* 37.

Mauz B, Vacchi M, Green A, Hoffmann G, Cooper A. 2015. Beachrock: a tool for reconstructing relative sea level in the far-field. *Marine Geology* 362(0): 1-16. DOI: 10.1016/j.margeo.2015.01.009.

Menard HW, Ladd HS. 1963. Oceanic islands, seamounts, guyots and atolls. In Hill MN (ed). The sea ideas and observations on progress in the study of the seas. New York Interscience Publisher 3. The Earth beneath the sea: 365-385.

Menard HW. 1983. Insular erosion, isostasy, and subsidence. *Science* 220: 913–918.

33

Miller KG, Kominz MA, Browning JV, Wright JD, Mountain GS, Katz ME, Sugarman PJ, Cramer BS, Christie-Blick N, Pekar SF. 2005. The Phanerozoic record of global sea-level change. *Science* 310: 1293–8.

Mitchell NC, Dade WB, Masson DG. 2003. Erosion of the submarine flanks of the Canary Islands. *Journal of Geophysical Research* 108: 3–11.

Mitchell NC, Masselink G, Huthnance JM, Fernández-Salas LM, Lobo FJ. 2012. Depths of modern coastal sand clinoforms. *Journal of Sedimentary Research* 82: 469–481.

Miyauchi T, Dai Pra G, Labini SS. 1994. Geochronoly of Pleistocene marine terraces and regional tectonics in the Tyrrenian coast of South Calabria. *Il Quaternario* 7: 17-34.

Naish TR, Wehland F, Wilson GS, Browne GH, Cook RA, Morgans HEG, Rosenberg M, King, PR, Smale D, Nelson CS, Kamp PJJ, Rickett B. 2005. An integrated sequence stratigraphic, palaeoenvironmental, and chronostratigraphic analysis of the Tangahoe Formation, southern Taranaki coast, with implications for mid-Pliocene (c. 3.4–3.0 Ma) glacio-eustatic sea level changes. *Journal of the Royal Society New Zealand* 35: 151–196.

Neri G, Barberi G, Orecchio B, Mostaccio A. 2003. Seismic strain and seismogenic stress regimes in the crust of the southern Tyrrhenian region. *Earth Planetary and Science Letters* 213: 97-112.

Pepe F, Bertotti G, Ferranti L, Sacchi M, Collura AM, Passaro S, Sulli A. 2014. Pattern and rate of post-20 ka vertical tectonic motion around the Capo Vaticano Promontory (W Calabria, Italy) based on offshore geomorphological indicators. *Quaternary International* 322: 85-98.

Pirazzoli PA. 1986. Marine notches. In: Van de Plassche, O. (Ed.), Sea-level Research: A Manual for the Collection and Evaluation of Data. Geo Books. Norwich: 361–400.

34

Pirazzoli PA. 1998. A Comparison between postglacial isostatic predictions and Late Holocene sea-level field data from Mediterranean and Iranian coastal areas. GeoResearch Forum 3–4: 401–420.

Pirazzoli PA, Laborel J, Stiros SC. 1996. Earthquake clusteringin the eastern Mediterranean duringhistorical times. Journal of Geophysical Research 101: 6083–6097.

Quartau R, Trenhaile AS, Mitchell NC, Tempera F. 2010. Development of volcanic insular shelves: insights from observations and modelling of Faial Island in the Azores Archipelago. *Marine Geology* 275: 66–83.

Quartau, R, Tempera, F, Mitchell, NC, Pinheiro, LM, Duarte, H, Brito, PO, Bates, R, Monteiro, JH. 2012. Morphology of the Faial Island shelf (Azores): The interplay between volcanic, erosional, depositional, tectonic and mass-wasting processes. *Geochemistry Geophysics Geosystems* 13: Q04012, doi:10.1029/2011GC003987.

Quartau R, Hipolito A, Romagnoli C, Casalbore D, Madeira J, Tempera F, Roque C, Chiocci FL. 2014. The morphology of insular shelves as a key for understanding the geological evolution of volcanic islands: insights from Terceira Island (Azores). *Geochemistry Geophysics Geosystems* 15: 1801–1826.

Quartau, R, Madeira, J, Mitchell, NC, Tempera, F, Silva, PF, Brandão, F. 2015. The insular shelves of the Faial-Pico Ridge: a morphological record of its geologic evolution (Azores archipelago). *Geochemistry Geophysics Geosystems* 16: 1401–1420.

Quartau, R, Trenhaile, AS, Ramalho, RS, Mitchell, NC. 2018. The role of subsidence in shelf widening around ocean island volcanoes: Insights from observed morphology and modeling. *Earth and Planetary Science Letters* 498: 408-417.

Ramalho RS, Helffrich G, Cosca M, Vance D, Hoffmann D, Schmidt DN. 2010c. Vertical movements of ocean island volcanoes: Insights from a stationary plate environment. *Marine Geology* 275: 84–95. DOI: 10 .1016 /j .margeo .2010 .04 .009.

35

Ramalho RS, Helffrich G, Madeira J, Cosca M, Thomas C, Quartau R, Hipólito A, Rovere A, Hearty P, Ávila SP. 2017. Emergence and evolution of Santa Maria Island (Azores) – The conundrum of uplifted islands revisited. *Geological Society of America, Bulletin* 129. DOI: 10.1130/B31538.1.

Raymo ME, Hearty P, Conto RD, O'Leary M, Dowsett HJ, Robinson MM. 2009. PLIOMAX: Pliocene maximum sea level project. *PAGES News* 17(2).

Rohling EJ, Grant K, Bolshaw M, Roberts AP, Siddall M, Hemleben C, Kucera M. 2009. Antarctic temperature and global sea level closely coupled over the past five glacial cycles. *Nature Geoscience* 2, 500–504.

Rohling EJ, Foster GL, Grant KM, Marino G, Roberts AP, Tamisiea ME, Williams F. 2014. Sea-level and deep-sea-temperature variability over the past 5.3 million years. *Nature* 508: 477-482.

Romagnoli C. 2013. Characteristics and morphological evolution of the Aeolian volcanoes from the study of submarine portions. In: Lucchi F, Peccerillo A, Keller J, Tranne CA, Rossi PL. (eds). The Aeolian Islands Volcanoes. *Geological Society, London, Memoirs* 37: 13–26.

Romagnoli C, Casalbore D, Chiocci FL. 2012. La Fossa Caldera breaching and submarine erosion (Vulcano island, Italy). *Marine Geology* 303-306: 87-98.

Romagnoli C, Casalbore D, Ricchi A, Lucchi F, Quartau R, Bosman A, Tranne CA, Chiocci FL. 2018. Morpho-bathymetric and seismo-stratigraphic analysis of the insular shelf of Salina (Aeolian archipelago) to unveil its Late-Quaternary geological evolution. *Marine Geology* 395: 133–151.

Rovere A, Raymo ME, Vacchi M, Lorscheid T, Stocchi P, Gómez-Pujol L, Harris DL, Casella E, O'Leary MJ, Hearty PJ. 2016. The analysis of last interglacial (MIS 5e) relative sea-level

36

104

indicators: Reconstructing sea-level in a warmer world. *Earth-Science Reviews* 159: 404–427. DOI: 10 .1016 /j.earscirev .2016 .06 .006.

Rust D, Kershaw S. 2000. Holocene tectonic uplift patterns in north-eastern Sicily: evidence from marine notches in coastal outcrops. *Marine Geology* 167: 105–126.

Serpelloni E, Faccenna C, Spada G, Dong D, Williams SDP. 2013. Vertical GPS ground motion rates in the Euro-Mediterranean region: New evidence of velocity gradients at different spatial scales along the Nubia-Eurasia plate boundary. *Journal of Geophysical Research, Solid Earth* 118, 6003–6024

Shakun JD, Lea DW, Lisiecki LE, Raymo ME. 2015. An 800-kyr record of global surface ocean _18O and implications for ice volume-temperature coupling. *Earth Planetary and Science Letters* 426, 58–68.

Sosdian S, Rosenthal Y. 2009. Deep-Sea Temperature and Ice Volume Changes Across the Pliocene-Pleistocene Climate Transitions. *Science* 325, 306–310.

Spratt RM, Lisiecki LE. 2016. A Late Pleistocene sea level stack. *Climate of the Past* 12, 1079–1092.

Stein CA, Stein S. 1992. A model for the global variation in oceanic depth and heat flow with lithospheric age. *Nature* 359: 123-129. DOI: 10.1038/359123a0.

Tallarico A, Dragoni M, Anzidei M, Esposito A. 2003. Modeling long term ground deformation due to the cooling of a magma chamber: the case of Basiluzzo Island (Aeolian Islands, Italy). *Journal of Geophysical Research* 108(B12): 2568-2585. DOI:10.1029/2002JB002376

Trenhaile AS. 2000. Modeling the development of wave-cut platforms. *Marine Geology* 166: 163–178.

Trenhaile AS. 2001. Modelling the Quaternary evolution of shore platforms and erosional continental shelves. *Earth Surface Processes and Landforms* 26: 1103–1128.

Trenhaile AS. 2002. Modeling the development of marine terraces on tectonically mobile rock coasts. *Marine Geology* 185: 341-61.

Trenhaile AS. 2014. Modelling the effect of Pliocene–Quaternary changes in sea level on stable and tectonically active land masses. *Earth Surface Processes and Landforms* 39: 1221-35. DOI: 10.1002/esp.3574.

Trenhaile AS. 2015. Coastal notches: Their morphology, formation, and function. *Earth-Science Reviews* 150: 285-304. DOI: 10.1016/j.earscirev.2015.08.003.

Ventura G. 2013. Kinematics of the Aeolian volcanism (Southern Tyrrhenian Sea) from geophysical and geological data. In: Lucchi F, Peccerillo A, Keller J, Tranne CA, Rossi PL. (eds). The Aeolian Islands Volcanoes. *Geological Society, London, Memoirs* 37: 3–11.

Ventura G, Vilardo G, Milano G, Pino NA. 1999. Relationships among crustal structure, volcanism and strike-slip tectonics in the Lipari-Vulcano volcanic complex (Aeolian Islands, Southern Tyrrhenian Sea, Italy). *Physics of the Earth and Planetary Interiors* 116 (1-4): 31-52.

Waelbroeck C, Labeyrie L. Michel E, Duplessy JC, McManus JF, Lambeck K, Balbon E, Labracherie M. 2002. Sea-level and deep water temperature changes derived from foraminifera isotopic records. *Quaternary Science Reviews* 21: 295–305.

Wang P, Tian J, Lourens LJ. 2010. Obscuring of long eccentricity cyclicity in Pleistocene oceanic carbon isotope records. *Earth Planetary and Science Letters* 290, 319–330.

Watts AB, ten Brink US. 1989. Crustal structure, flexure and subsidence of the Hawaiian Islands. *Journal of Geophysical Research* 94: 10473-10500.

38

Westaway R. 1993. Quaternary uplift of southern Italy. *Journal of Geophysical Research* DOI.org/10.1029/93JB01566.

Wortel MJR, Spakman W. 2000. Subduction and slab detachment in the Mediterranean-Carpathian Region. *Science* 290: 1917–1920.

Zazo C, Goy JL, Hillaire-Marcel C. Gillot PY, Soler V, González JÁ, Ghaleb B. 2002. Raised marine sequences of Lanzarote and Fuerteventura revisited - A reappraisal of relative sea-level changes and vertical movements in the eastern Canary Islands during the Quaternary. *Quaternary Science Reviews* 21(18–19): 2019–2046. DOI: 10.1016/S0277-3791(02)00009-4.

Zecchin M, Mellere D, Roda C. 2006. Sequence stratigraphy and architectural variability in growth fault-bounded basin "lls: a review of Plio-Pleistocene stratal units of the Crotone Basin, southern Italy. *Geological Society, London, Journal* 163: 471–486.

Figure captions

Fig. 1. (a) Simplified geological map of Salina (organized into distinct Eruptive Epochs), merged on a shaded-relief DEM of the island, and (b) shaded relief map of the submarine shallow-water portions, showing the main volcanic centres and morpho-structural features (modified after Lucchi et al., 2013 and Romagnoli et al., 2018, respectively). Elevation/depth is in metres above/below sea level. In the lower left panel: location of the Island of Salina and the Aeolian Archipelago in the Southern Tyrrhenian Sea.

Fig. 2. Simplified geological section (a) and outcrop photographs (b, c) showing the vertical stacking pattern of marine terraces related to MIS 5 (I, II, III) and MIS 7.3 (A) on Salina, and their stratigraphic relationships with interbedded volcanic rocks. b) Marine terraces I (MIS 5.5) and II (MIS 5.3) and interlayered volcanic deposits, exposed on the coastal cliff along the eastern flank of the Pizzo Capo volcanic edifice. The terraces are notably found in a downstepping suite with the younger terrace II at lower elevations crosscutting the older terrace I. This is in agreement with a context of uplift during the time interval between the

39

107

corresponding sea level highstands. c) Marine deposits of terrace A (MIS 7.3) exposed in the basal portion of the coastal cliff along the northern side of Pizzo Capo: they are found in a direct stratigraphic succession below the terrace III (MIS 5.1), with interlayered volcanic deposits. See the text for age references.

Fig. 3. Illustrative sections showing the morphologic setting and stratigraphic architecture of marine terraces and insular shelves on Salina (a), the development of the main paleo sea level markers (b, terrace inner margin; c, erosive shelf edge) and the volcaniclastic cover (d), organized in submarine depositional terraces (SDT), according to the correlative sea level oscillations. In (e) a seismic reflection profile across the shelf of Salina and its interpretative section show an example of insular shelf carved into the volcanic bedrock and overlaid by the SDT, with the depositional edge shallower than the erosive shelf edge.

Fig. 4. Shaded relief image of the island of Salina and its submarine shallow-water portions showing the areal distribution of the insular shelves and the classification into deep, intermediate and shallow shelves according to the depth range of the erosive shelf edges: CO_1=Pizzo di Corvo 1; CO_2=Pizzo di Corvo 2; PR=Monte dei Porri; PCN_W=Pizzo Capo North West; PCN_E=Pizzo Capo North East; PC=Pizzo Capo; FF=Monte Fossa delle Felci; FFS_1=Fossa Felci South 1; FFS_2=Fossa Felci South 2. PCN_E is indicated apart because of its peculiar features (see text for explanation). Blue lines indicate shelf edge areas eroded by later mass-wasting processes.

Fig. 5. Schematic dip-oriented sections across the coastal and shallow-water portions of Salina, showing the position and maximum depth of the insular shelf edges in the different sectors of the island, and the volcaniclastic cover above the acoustic bedrock (based on information derived from the seismic profiles, see Fig. 2e).

Fig. 6. Coastal elevation changes at Salina, reconstructed from paleo-sea level markers. A curve of cumulative displacement (light blue) is obtained by plotting the amounts of uplift/subsidence recorded by marine terraces and insular shelves as a function of the time intervals between different sea level markers: a) present day-MIS 5.5; b) MIS 5.5-MIS 7.3; c) MIS 7.3-MIS 12. The amounts of uplift/subsidence are calculated as the difference between

40

108

the paleo sea levels corresponding to the terraces/shelves at the moment of their formation and the eustatic sea levels derived from the curve of Rohling et al. (2014). The eustatic sea level defined by Lambeck et al. (2004) is adopted as a reference for MIS 5.5 (in red). Symbols (see also Tabs. 1, 2): h=present depth of the paleo sea level position (terrace inner margin or erosive shelf edge); d=inferred paleo-depth with respect to the mean sea level; E=eustatic sea level; $D_{5.5}$=displacement after MIS 5.5 (uplift of 44m); $D_{7.3}$=displacement between MIS 7.3 and MIS 5.5 (subsidence of 44 m); e=relative sea level ($E+D_{5.5}+D_{7.3}$); D=displacement (h+d-e). In b) the light blue dotted line is the curve of presumed relative sea level derived by displacing the eustatic curve if the Last Interglacial uplift rate had been active since MIS 7.3. The stratigraphic age of marine terraces is derived from dated volcanic deposits onland (Leocat, 2011; Lucchi et al., 2013), whereas the age range of the Pizzo volcanic deposits, the oldest exposed onland, is reported as a stratigraphic marker for the chronological attribution of the insular shelves (Romagnoli et al., 2018). See the text for further explanation.

Fig. 7. Simplified interpretative, WNW-ESE oriented sections showing the main stages of geological evolution of Salina in the time interval from MIS 12 to the present day configuration. The formation of various marine terraces and insular shelves is displayed according to the proposed chronological attribution (see the text for explanation). For each evolutionary step, the active volcanic edifices are displayed (colours as in Fig. 1; in grey, the inactive volcanoes).

Table captions

Tab. 1. Displacement magnitudes and rates relative to the raised marine terraces on Salina

Tab. 2. Displacement magnitudes and rates relative to the insular shelves on Salina

Tab. 3. Displacement magnitudes and rates relative to the insular shelves on Salina by referring to MIS 5.5

41

Fig. 1

185x242mm (300 x 300 DPI)

110

1
2
3
4
5
6
7
8
9
10
11
12
13
14
15
16
17
18
19
20
21
22
23
24
25
26
27
28
29
30
31
32
33
34
35
36
37
38
39
40
41
42
43
44
45
46
47
48
49
50
51
52
53
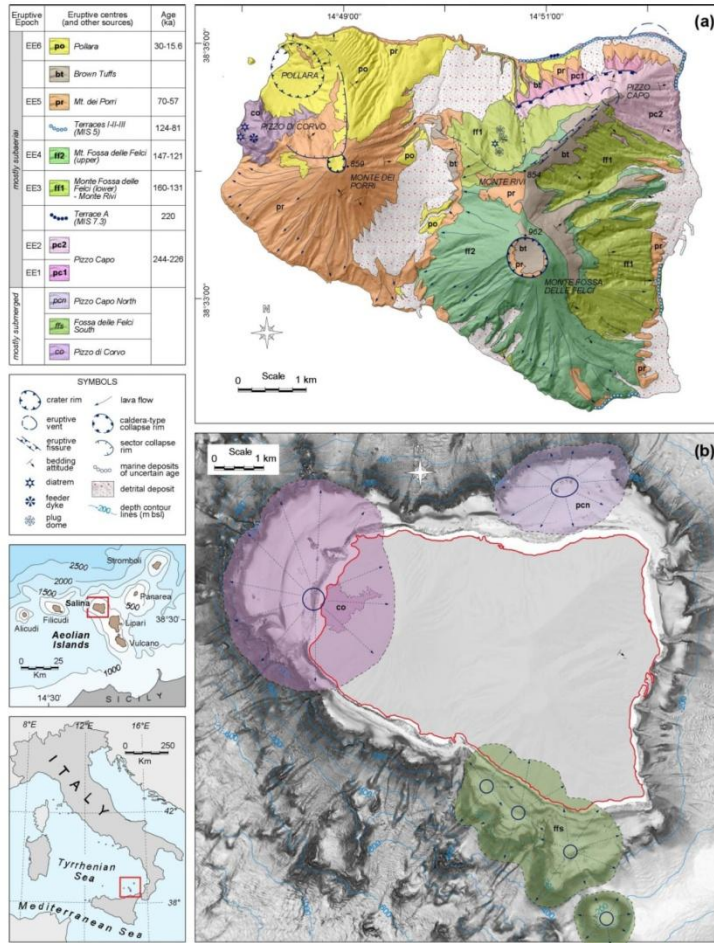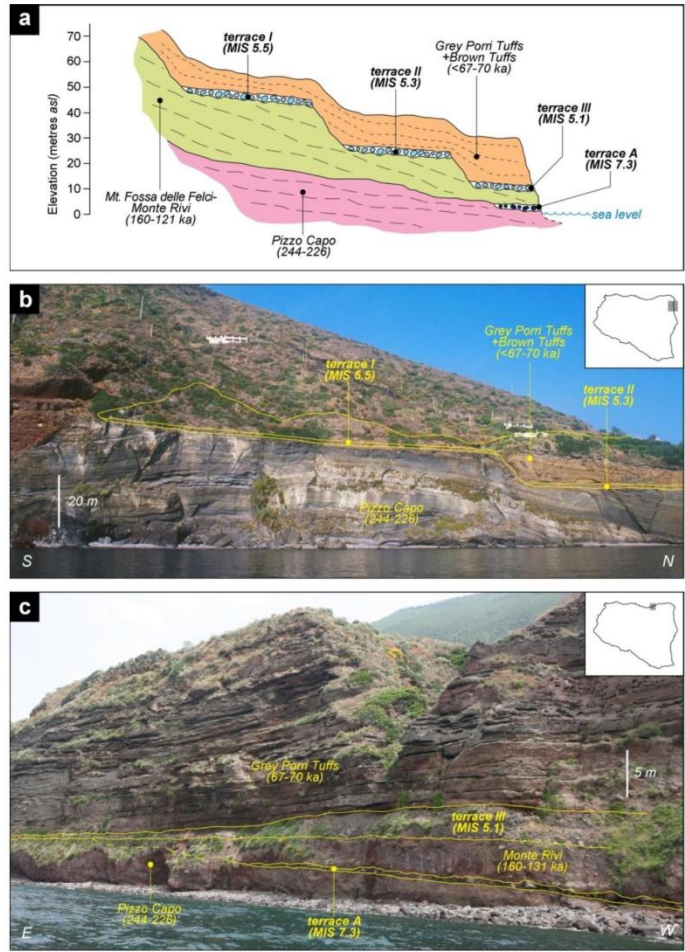54
55
56
57
58
59
60

Fig. 2

123x172mm (300 x 300 DPI)

111
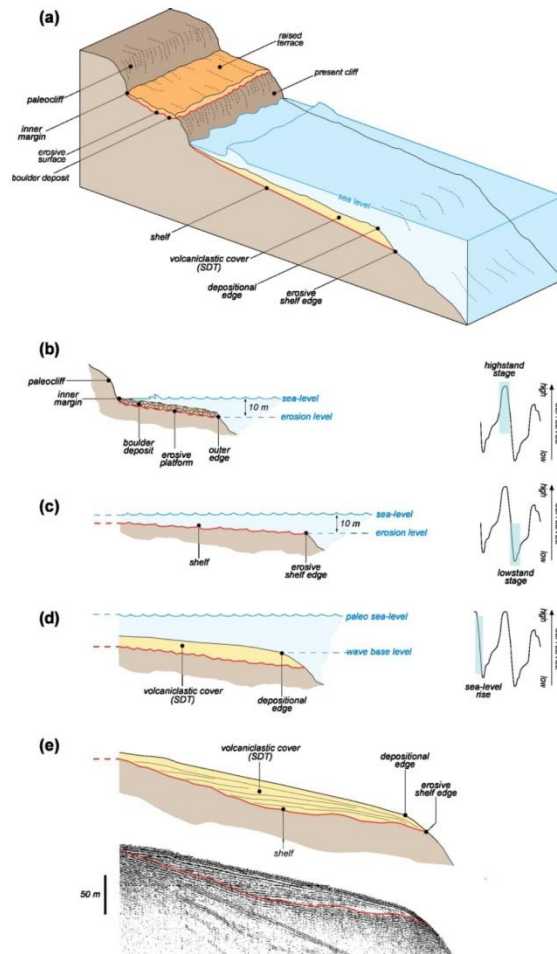
Fig. 3

138x237mm (300 x 300 DPI)

112
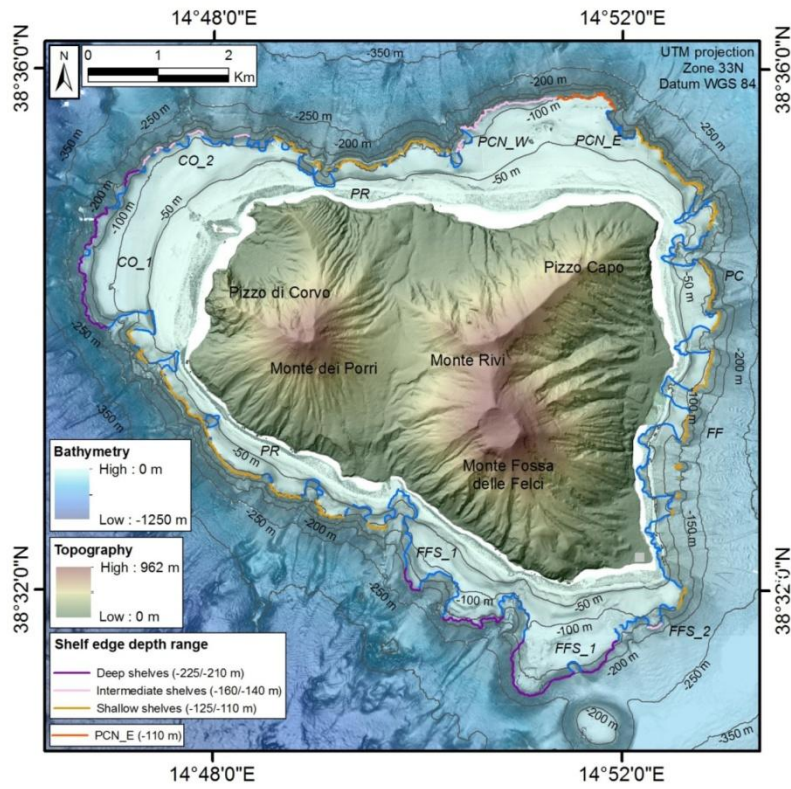
Fig. 4

139x139mm (300 x 300 DPI)
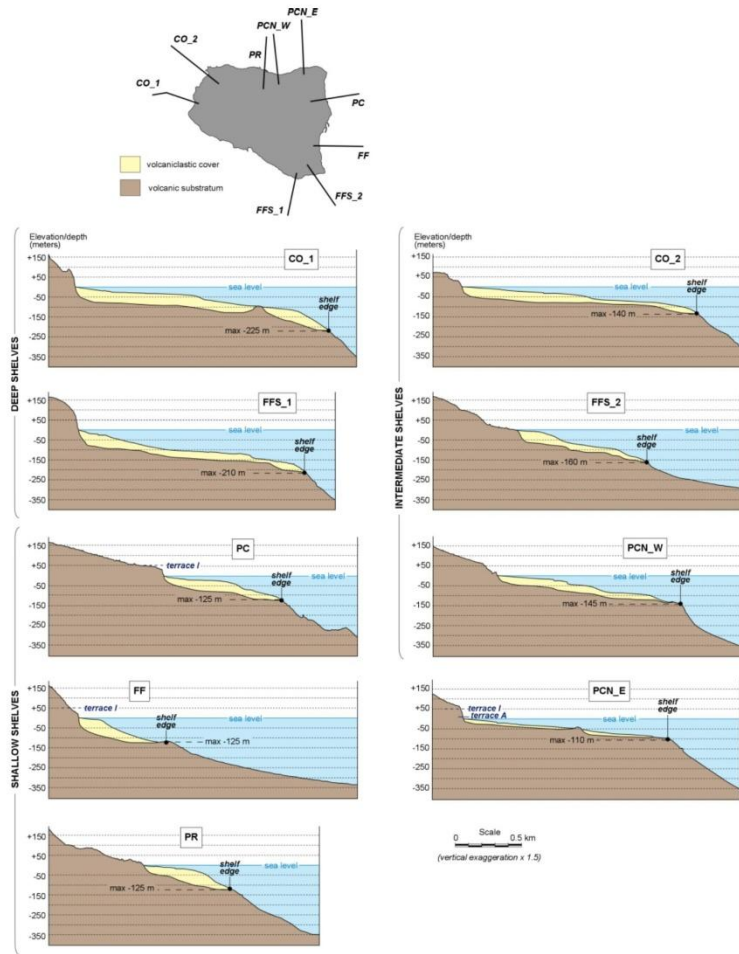
Fig. 5

184x238mm (300 x 300 DPI)
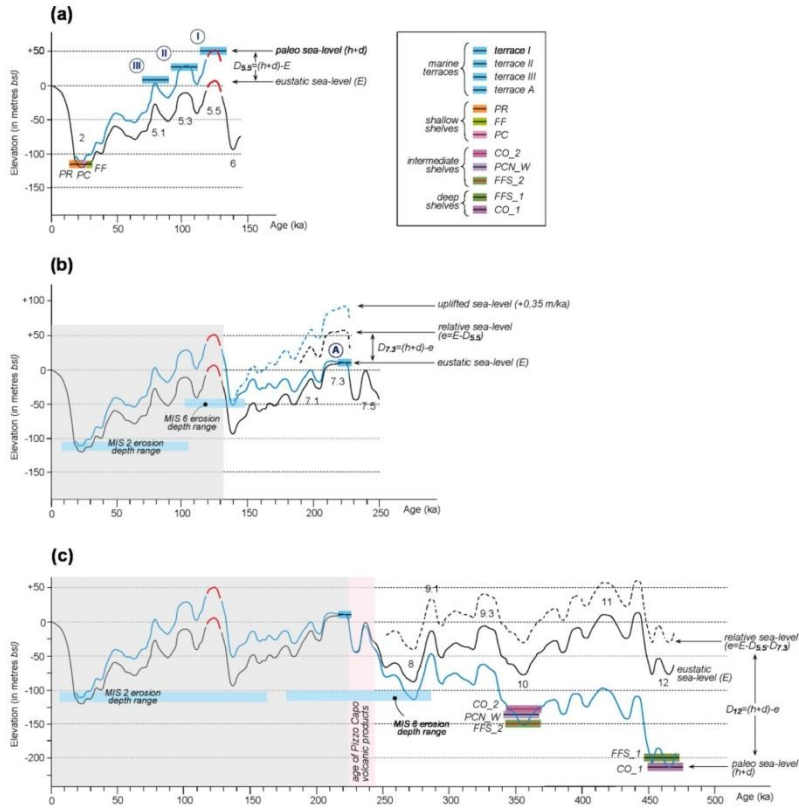
Fig. 6

183x186mm (300 x 300 DPI)

115
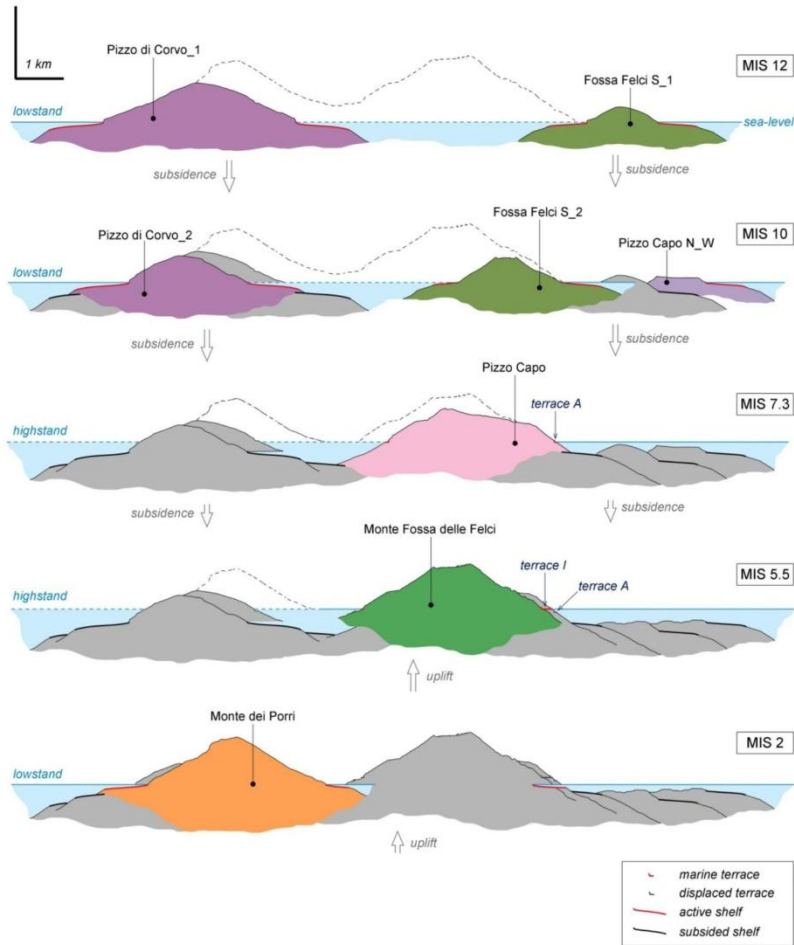
Fig. 7

156x186mm (300 x 300 DPI)

Table 1 - Displacement magnitudes and rates relative to the raised marine terraces on Salina

terrace	stage	age	h	d	E	D h+d-E	D5.5	e E+D5.5	D7.3 h+d-e	stage interval	t	D/t
		(ka)	(m)	(m)	(m)	(m)		(m)			(ka)	(m/ka)
III	MIS 5.1	78	+10	0	-25	+35				0-MIS 5.1	78 (0-78)	0.03
II	MIS 5.3	99	+25	0	-11	+36				0-MIS 5.3	99 (0-99)	0.03
I	MIS 5.5	124	+50 (*)	0	+6	+44	+44			0-MIS 5.5	124 (0-124)	0.35
A	MIS 7.3	221	+2 (**)	+10	+12		+44	+56	-44	MIS 5.5-MIS 7.3	97 (124-221)	-0.45

Labels: h=present elevation (*=inner margin; **=minimum elevation of the terrace bounder deposit); d=inferred paleo-depth with respect to the mean sea-level; E=eustatic sea-level from Rohling et al. 2014 (E=+6 m for MIS 5.5 is from Lambeck et al., 2004); D5.5=displacement after MIS 5.5 from interpretation of the terrace I paleo sea-level; e=relative sea-level (E-D5.5); D7.3=displacement between MIS 7.3 and MIS 5.5 from the interpretation of terrace A paleo sea-level; t=time span between different paleo sea-level tracers; D/t=displacement rate. Notes: the inferred age of terraces by linking with the isotope stages is that derived from the reconstructed stratigraphic relationships and radiometric ages of volcanic products above and below the terraces (Lucchi et al., 2013).

Table 2 - Displacement magnitudes and rates relative to the insular shelves on Salina

insular shelf		stratigraphic age	inferred age	stage	age	h	d	E	D5.5	D7.3	e E+D5.5+D7.3	D h+d-e	stage interval	t	D/t
		(ka)	(ka)		(ka)	(m)	(m)	(m)	(m)	(m)	(m)	(m)		(ka)	(m/ka)
CO_1	Pizzo di Corvo 1	DE	>244-226	MIS 12	465	-225	+10	-77	+44	-44	-77	-138	MIS 7.3-MIS 12	244 (221-465)	-0.56
				MIS 10	356	-225	+10	-77	+44	-44	-77	-138	MIS 7.3-MIS 10	135 (221-356)	-1.02
CO_2	Pizzo di Corvo 2	INT	>244-226 (younger than Pizzo di Corvo 1)	MIS 10	356	-140	+10	-77	+44	-44	-77	-53	MIS 7.3-MIS 10	135 (221-356)	-0.39
				MIS 8	273	-140	+10	-89	+44	-44	-89	-41	MIS 7.3-MIS 8	52 (221-273)	-0.79
FFS_1	Fossa Felci S_1	DE	>244-226	MIS 12	465	-210	+10	-77	+44	-44	-77	-123	MIS 7.3-MIS 12	244 (221-465)	-0.50
				MIS 10	356	-210	+10	-77	+44	-44	-77	-123	MIS 7.3-MIS 10	135 (221-356)	-0.91
FFS_2	Fossa Felci S_2	INT	>244-226 (younger than Fossa Felci S_1)	MIS 10	356	-160	+10	-77	+44	-44	-77	-73	MIS 7.3-MIS 10	135 (221-356)	-0.54
				MIS 8	273	-160	+10	-89	+44	-44	-89	-61	MIS 7.3-MIS 8	52 (221-273)	-1.17
PCN_W	Pizzo Capo N_W	INT	>244-226	MIS 10	356	-145	+10	-77	+44	-44	-77	-58	MIS 7.3-MIS 10	135 (221-356)	-0.43
				MIS 8	273	-145	+10	-89	+44	-44	-89	-46	MIS 7.3-MIS 8	52 (221-273)	-0.88
PC	Pizzo Capo	SHA 244-226		MIS 6	137	-125	+10	-95	+44	-44	-95	-20	MIS 5.5-MIS 6	13 (124-137)	-1.53
				MIS 2	22	-125	+10	-120			-120	+5	0-MIS 2	22 (0-22)	+0.23
FF	Monte Fossa delle Felci	SHA 160-131		MIS 6	137	-125	+10	-95	+44	-44	-95	-20	MIS 5.5-MIS 6	13 (124-137)	-1.53
				MIS 2	22	-125	+10	-120			-120	+5	0-MIS 2	22 (0-22)	+0.23
PR	Monte dei Porri	SHA 70-57		MIS 2	22	-125	+10	-120			-120	+5	0-MIS 2	22 (0-22)	+0.23

Labels: DE=deep, INT=intermediate, SHA=shallow; h=present depth (maximum depth of the erosive shelf edge); d=inferred paleo-depth with respect to the mean sea-level; E=eustatic sea-level Rohling et al., 2005); D5.5=displacement after MIS 5.5 (uplift of +44m in the last 124 ka from interpretation of the terrace I paleo sea-level); D7.3=displacement between MIS 7.3 and MIS 5.5 (subsidence of -44 m between 221 ka and 124 ka from interpretation of terrace A paleo sea-level); e=relative sea-level (E+D5.5+D7.3); D=displacement (h+d-e); t=time span between different paleo sea-level tracers; D/t=displacement rate. Notes: The stratigraphic age is that derived from dated volcanic products onland (Leocat, 2011; Lucchi et al., 2013), and the inferred age is that derived for submerged shelves from a model of increasing shelf width with the age of the eroded volcanic edifice (Romagnoli et al., 2018).

insular shelf		stratigraphic age	inferred age	stage	age	h	d	E	D5.5	e E+D5.5	D h+d-e	stage interval	t	D/t
		(ka)	(ka)		(ka)	(m)	(m)	(m)	(m)	(m)	(m)		(ka)	(m/ka)
CO_1	Pizzo di Corvo 1	DE	>244-226	MIS 12	465	-225	+10	-77	+44	-33	-182	MIS 5.5-MIS 12	341 (124-465)	-0.53
CO_2	Pizzo di Corvo 2	INT	>244-226 (younger than Pizzo di Corvo 1)	MIS 10	356	-140	+10	-77	+44	-33	-97	MIS 5.5-MIS 10	232 (124-356)	-0.42
FFS_1	Fossa Felci S_1	DE	>244-226	MIS 12	465	-210	+10	-77	+44	-33	-167	MIS 5.5-MIS 12	341 (124-465)	-0.49
FFS_2	Fossa Felci S_2	INT	>244-226 (younger than Fossa Felci S_1)	MIS 10	356	-160	+10	-77	+44	-33	-117	MIS 5.5-MIS 10	232 (124-356)	-0.50
PCN_W	Pizzo Capo N_W	INT	>244-226	MIS 10	356	-145	+10	-77	+44	-33	-102	MIS 5.5-MIS 10	232 (124-356)	-0.44

Table 3 - Displacement magnitudes and rates relative to the insular shelves on Salina by referring to MIS 5.5

Labels: DE=deep, INT=intermediate, SHA=shallow; h=present depth (maximum depth of the erosive shelf edge); d=inferred paleo-depth with respect to the mean sea-level; E=eustatic sea-level (Rohling et al., 2014); D5.5=displacement after MIS 5.5 (uplift of +44m in the last 124 ka from interpretation of the terrace I paleo sea-level); e=relative sea-level (E+D5.5); D=displacement (h+d-e); t=time span between different paleo sea-level tracers; D/t=displacement rate. Notes: The stratigraphic age is that derived from dated volcanic products onland (Leocat, 2011; Lucchi et al., 2013), and the inferred age is that derived for submerged shelves from a model of increasing shelf width with the age of the eroded volcanic edifice (Romagnoli et al., 2018).

6. INSULAR SHELVES IN THE CENTRAL SECTOR OF THE AEOLIAN ARCHIPELAGO: MORPHO-ACOUSTIC CHARACTERIZATION, CONTROLLING FACTORS AND IMPLICATIONS FOR THE GEOLOGICAL EVOLUTION OF LIPARI AND VULCANO ISLANDS

The submarine portion of Lipari and Vulcano islands have been studied in the past (see section 4.1.1). However, a detailed integration of the subaerial geology with the submerged, shallow-water portions has never been carried out (apart from some specific sectors as in Romagnoli et al., 2013 and Casalbore et al., 2016). Moreover, a detailed mapping of the shelf width and erosive edge depth all around the island was previously limited to some sectors (Chiocci and Romagnoli, 2004). In this chapter, the detailed analysis of the shelf surrounding Lipari and Vulcano islands is proposed and related to the onshore geology, following the same approach adopted for Salina (see manuscript enclosed in Chapter 5.1) i.e. using the morphologic characteristics of insular shelves to improve our understanding of the evolutionary history of such islands.

At Lipari, we integrated information from subaerial (MIS 5 raised terraces) and submerged (insular shelf edge) palaeo sea-level markers, in order to match their present-day height/depth with the relative sea-level curve and to reconstruct the rates of vertical movements experienced by the volcanic edifice in the last ka. Until now, in fact, most of the efforts for reconstructing the vertical movements of the island have been made by looking at subaerial uplifted sea-level markers, such as MIS 5 (124 ka) raised marine terraces (Lucchi et al., 2013b). However, this method allows to estimate the vertical mobility trend only back to the MIS 5 (124 ka), since, differently from Salina, older terraces were not recognized at Lipari (Lucchi et al., 2004). Marine terraces are not recognized at Vulcano, likely due to its relatively younger age (De Astis et al., 2013).

In the last decade, at Lipari the information provided by marine terraces were integrated by those derived from archeological markers and GPS data, which yielded an historical subsidence trend of up to c. 10-11 mm/yr (Calanchi et al., 2002; Serpelloni et al., 2005; Anzidei et al., 2015, 2016, 2017). However, the sea-level position indicated by such markers can be estimated only at local scale and only for the last 2 ka (archeological markers) or historical times (GPS data).

6.1 INSULAR SHELVES AROUND LIPARI ISLAND

The island of Lipari is surrounded by a shelf that reflects a complex geological evolution, where several volcanic edifices superimposed each other (Forni et al., 2013,). Offshore the youngest portions of the island (corresponding to shelf sectors 1 and 3 in Figure 6.1), formed during EE7 (43-40 ka), 8 (27-20 ka) and 9 (8.7 ka – AD 1220) (see section 4.1.1.2) insular shelves are mostly lacking or are very narrow (Romagnoli, 2013) and are affected by intense erosive processes (Casalbore et al., 2016 and 2017). On the contrary, the oldest volcanic centers (in correspondence with shelf sectors 2 and 4 in Figure 6.1) created during the EE1 (unknown age), 2 (267-188 ka) and 4 (119-114 ka)(see section 4.1.1.2), exhibit wide shelves in their offshore, with edges generally deeper than -

120 m and covered by thick sedimentary bodies (Chiocci and Romagnoli, 2004; Romagnoli, 2013; Casalbore et al., 2016). The shelf sectors are hereafter described according to their different characteristics.
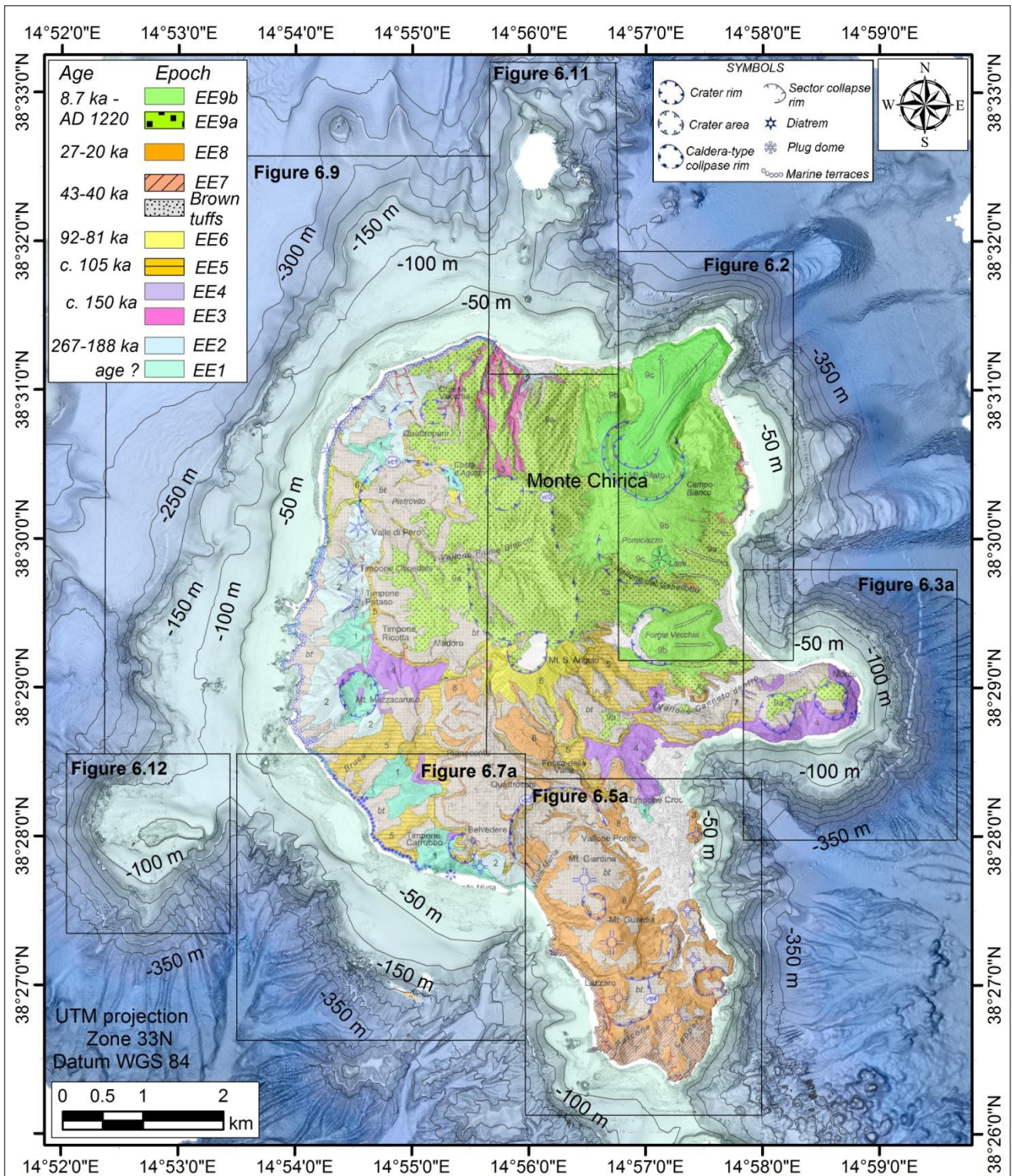
Figure 6.1 *Simplified geological map of Lipari (modified after Forni et al., 2013) merged on the DEM of the island and the multibeam bathymetry of the submarine shallow areas. The black boxes locate the shelf sectors represented in figures 6.2, 6.3a, 6.5a, 6.7a, 6.9, 6.11 and 6.12.*

SECTOR 1

The north-eastern sector of Lipari (from Acquacalda to Canneto, Figure 6.2) is relatively recent (see Figure 6.1); it corresponds to the products of the N-S aligned Capo Rosso domes (EE8b, 24-20 ka), overlapped by the thick pomiceous succession erupted during the EE9. No insular shelf is observed here, but an erosive surface extending to 27 m depth is present from offshore Acquacalda to Punta della Castagna, likely representing the present-day shore platform (Figure 6.2). Offshore the Capo Rosso domes, a wide semicircular portion of the seafloor exhibits a smoother morphology with respect the rest of the sector, being likely represented by a wide depositional terrace (Figure 6.2). No seismic profiles were collected in this area; therefore from bathymetry we can only determine the depositional edge depth, which is comprised between -15 m and -25 m (Figures 6.2). To the south of the Capo Rosso domes, a large erosive scar (head of the Canneto canyon, Casalbore et al., 2016), affects the submerged flank from few meters below the sea-level to c. more than -350 m (Figure 6.2).
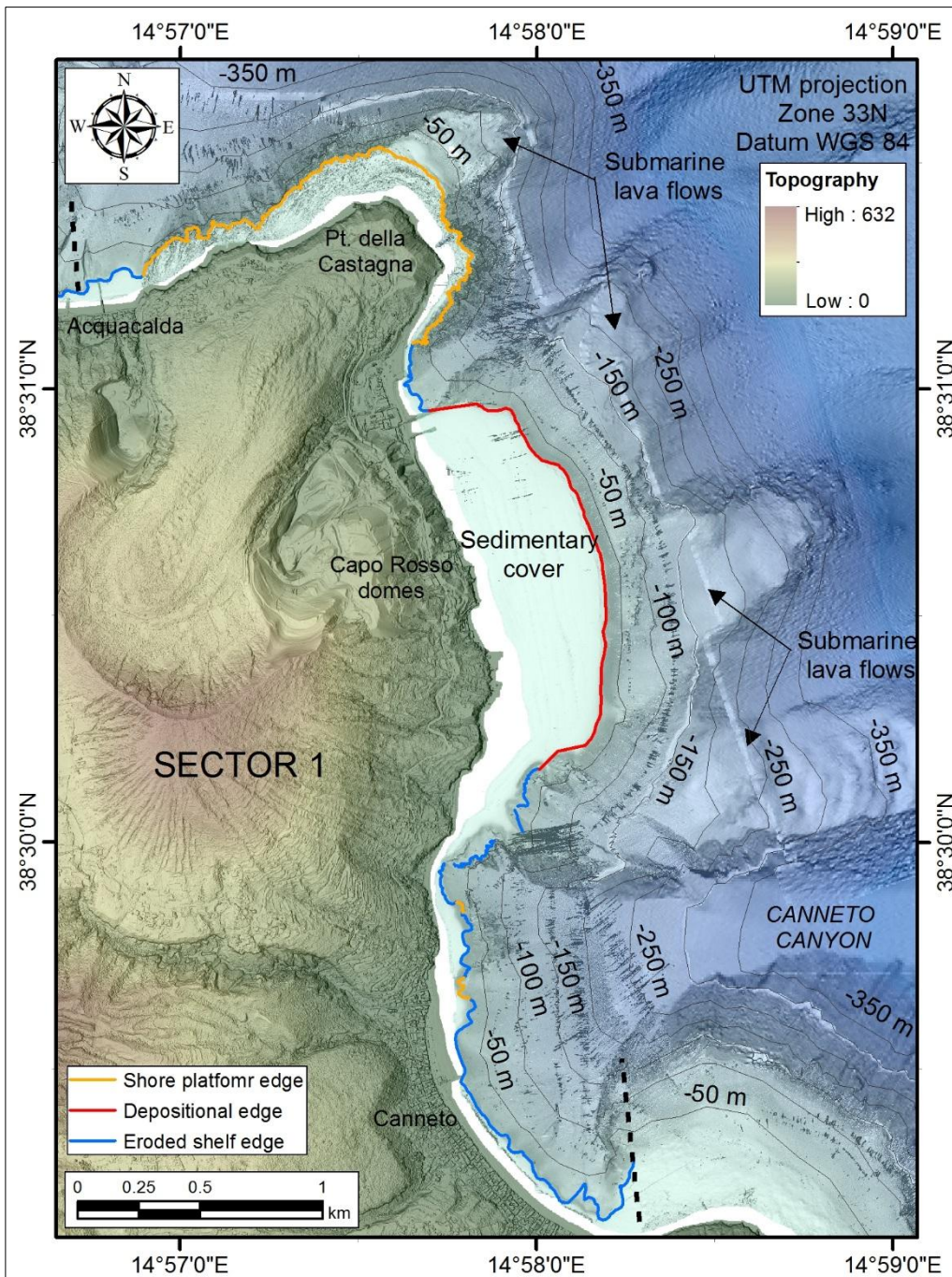
Figure 6.2 *Shaded relief map of the shelf sector 1 (equidistance of isobaths: 50 m). The black dashed lines represent the limit of the shelf sector 1. Pt.: Punta.*

SECTOR 2

This shelf sector runs aside the Monterosa promontory, which is made of two scoria cones belonging to the EE4 (Forni et al., 2013, Figure 6.1). This is the oldest portion of the eastern coast of Lipari, as suggested by the occurrence of marine terrace deposits of the Palaeoshoreline III (MIS 5a, 81 ka, Lucchi et al., 2004). The shelf offshore the northern and eastern flanks of Monterosa mimics, in plan view, the coastline profile, while in the southern flank it is deeply dissected by two evident scars (Figure 6.3a). Overall, the shelf width ranges from c. 400 offshore Sciarra di

Monterosa in the northern part to up to c. 845 m offshore Pignataro di Fuori to the South (Figure 6.3b). The erosive shelf edge is shallower along the northernmost portion (max value -135 m), while offshore the southern coastline of the promontory it locally reaches -169 m (Figures 6.3a, 6.3b, 6.4 and Table 6.1). Lower values of the erosive edge depth are locally observed, in correspondence of scars or gully heads (Figures 6.3a and 6.3b). The sedimentary cover (organized in SDTs) has a depositional edge at roughly -50/-60 m on the northern and eastern shelf sectors, while on the southern shelf sector an additional SDT exhibits an edge at c. -100 m (Figures 6.3a and 6.4). The overall thickness of the sediments tends to increase from north to south around Monterosa promontory.
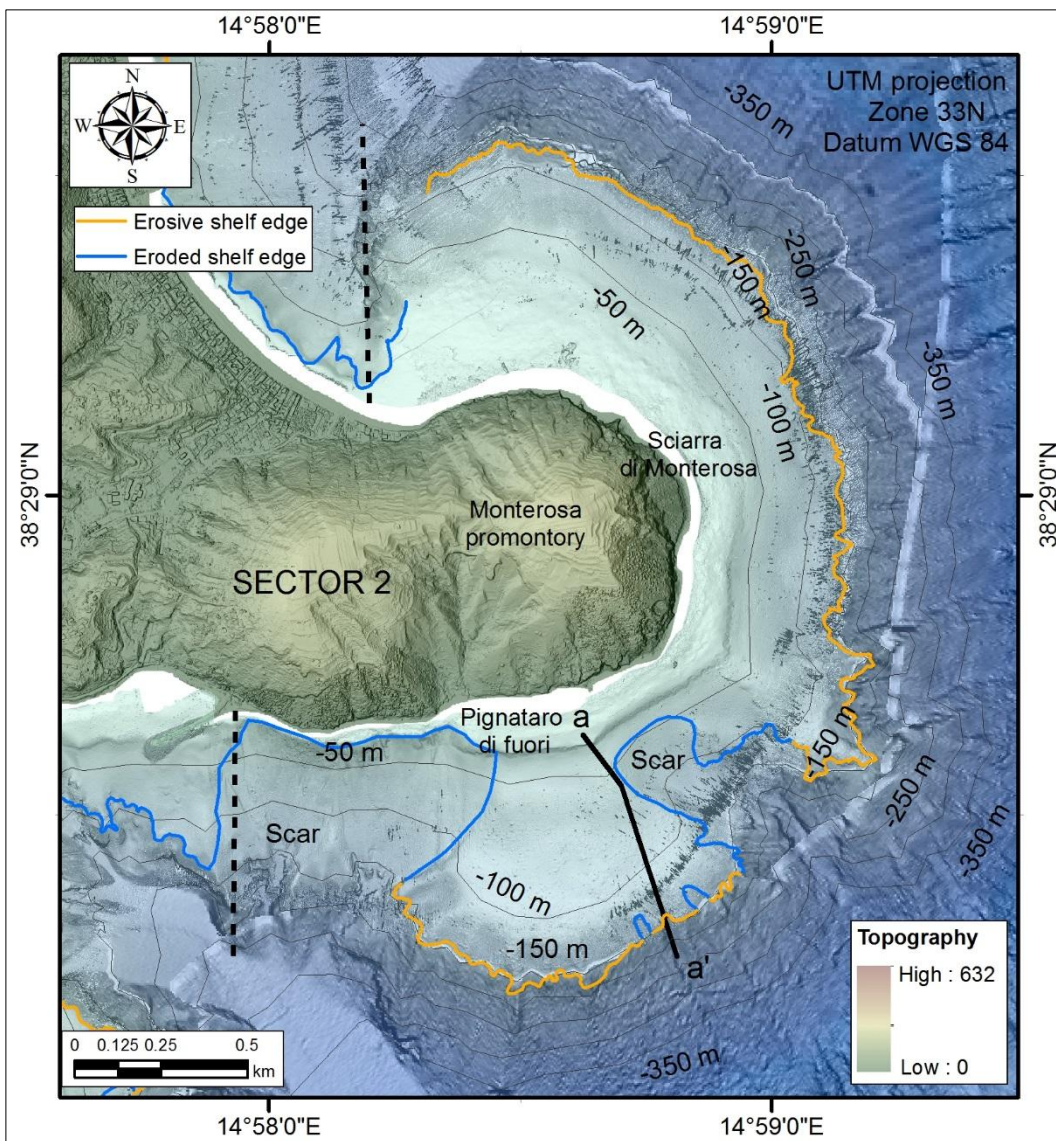
Figure 6.3a *Shaded relief map of the shelf sector 2 (equidistance of isobaths: 50 m).The seismic profile aa' is shown in figure 6.4. The black dashed lines represent the limit of the shelf sector 2.*
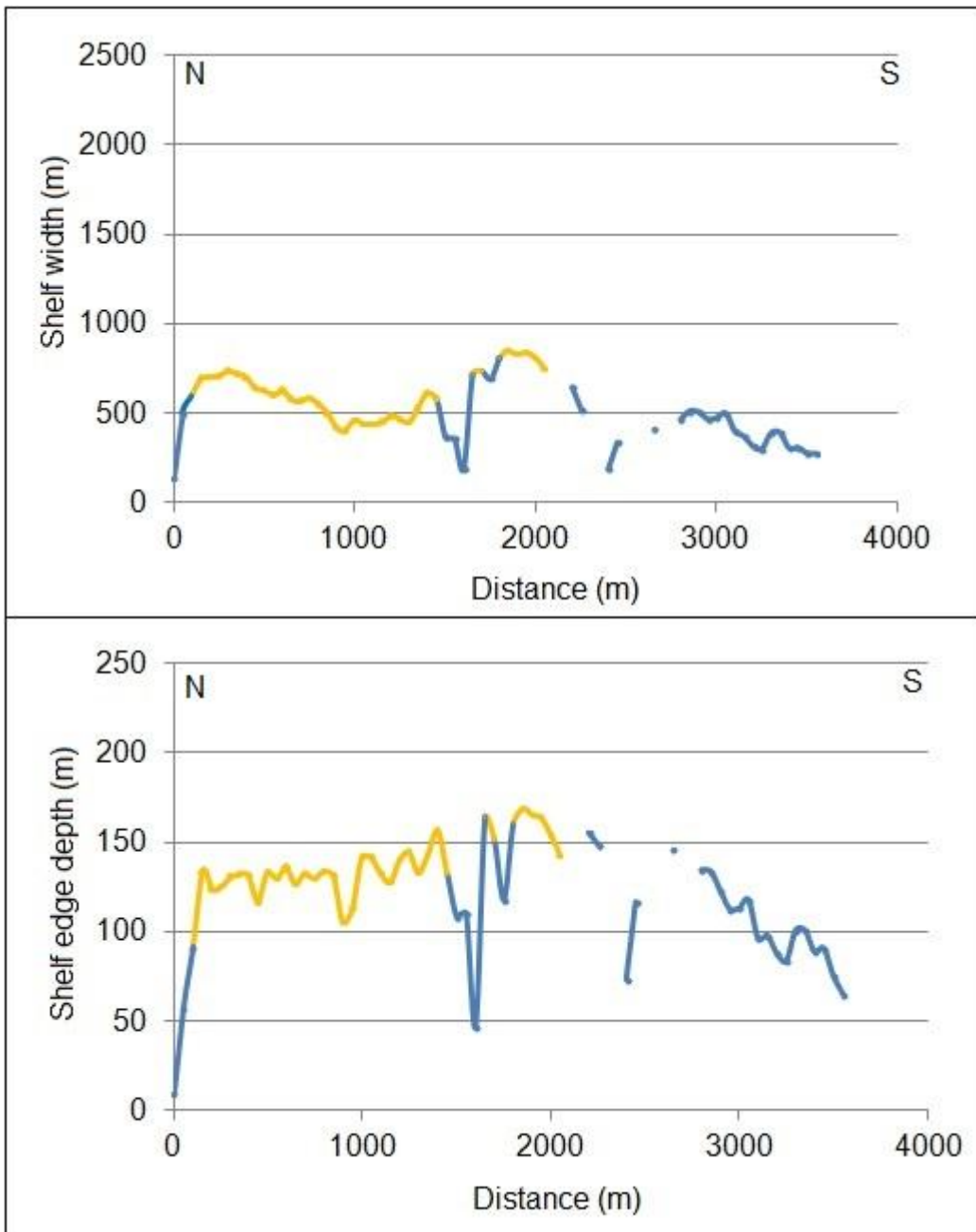
Figure 6.3b *Graphs showing the shelf width and shelf edge depth for shelf sector 2. In yellow: erosive shelf edge; in blue: eroded shelf edge.*
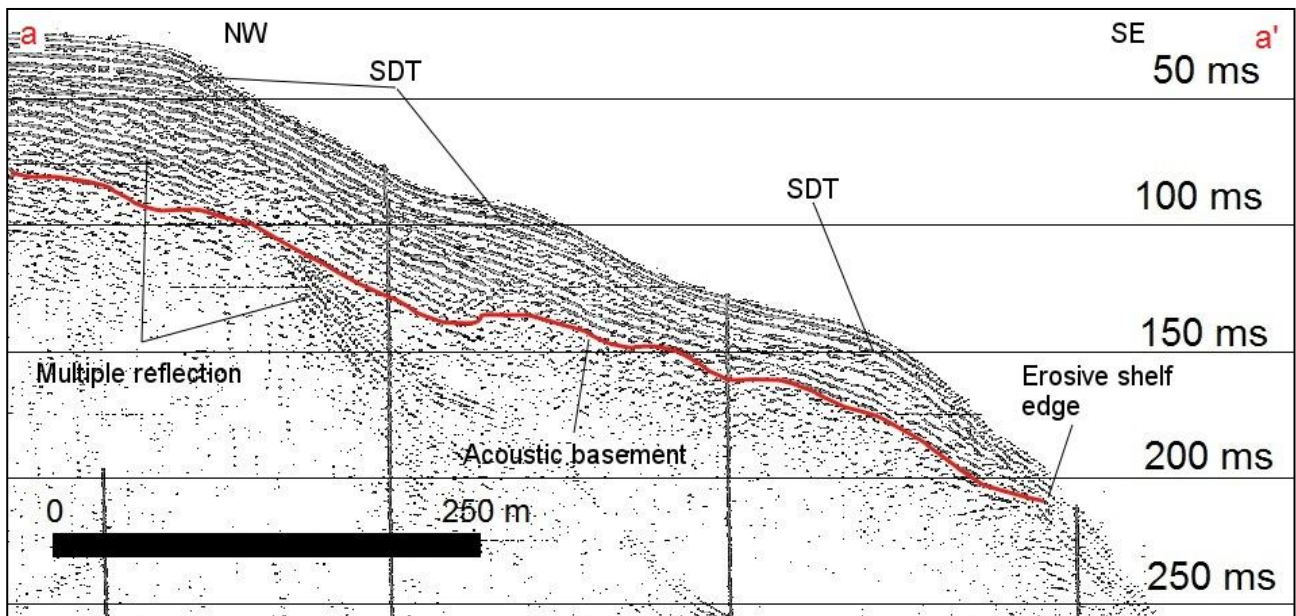
Figure 6.4 *Sparker seismic reflection profile showing the erosive edge and the SDTs lying above the shelf. Location of the seismic profile in figure 6.3a.*

SECTOR 3

This shelf sector includes the south-eastern (from Marina di Porto Salvo to Pt. della Crapazza, Figure 6.5a) and the south-western portions (from Pt. Perciato to Pt. Levante, Figure 6.5a) of Lipari. The south-easternmost portion is mainly made of lava domes belonging to EE7 (43-40 ka), overlapped by the products of the N-S aligned Castello domes (related to the EE8b, 24-20 ka) and the NNW-SSE aligned Pt.S. Giuseppe domes (EE8a, 27-24 ka, Figure 6.1). The shelf, commonly narrow, is locally deeply eroded, and in places is almost absent since erosive scars extend to the shallow water areas (Figures 6.5a and 6.5b). Only small shelf portions, carved in the lava domes of EE7/8 (Falcone and Castello domes), are not affected by mass wasting processes and exhibit a shelf up to c. 460 m wide. It is covered by SDTs in the innermost portion (depositional edge at -25/-30 m, Figure 6.5a). detected on the bathymetric data, since seismic profiles were not available for this portion of the shelf. Likewise, the erosive shelf edge depth (only measured from bathymetric profiles) exhibits sharp variations in this sector. Where the shelf is preserved, the maximum erosive edge depth ranges from c. -95 m (offshore the Castello domes) to -120 m (offshore the Falcone domes, Figures 6.5a and 6.5b).

The sector offshore the southern part of Lipari corresponds to the Bocche di Vulcano area, where an underlying insular shelf is covered by thick STDs (Chiocci and Romagnoli, 2004). Because of the connection with the nearby island of Vulcano (Figure 4.2), the shelf width and the erosive edge depth were not measured here.

The south-western coastline is NNW-SSE oriented and entirely made of the products of Monte Giardina lava domes (EE7, Figure 6.1). Offshore it is characterized by a shelf up to c. 750 m wide (Figure 6.5b), locally covered by up to 15 m-thick sedimentary bodies organized in a thick SDT(Figure 6.5). To the north the shelf is deeply eroded and dissected by landslide scars and gully heads, representing the prolongation of narrow valleys onshore (Figures 6.1 and 6.5a). The erosive

shelf edge depth has been measured only offshore Punta del Perciato, (i.e. where the shelf is preserved) ranging from -110 m to -128 m (Figures 6.5a, 6.5b and 6.6).
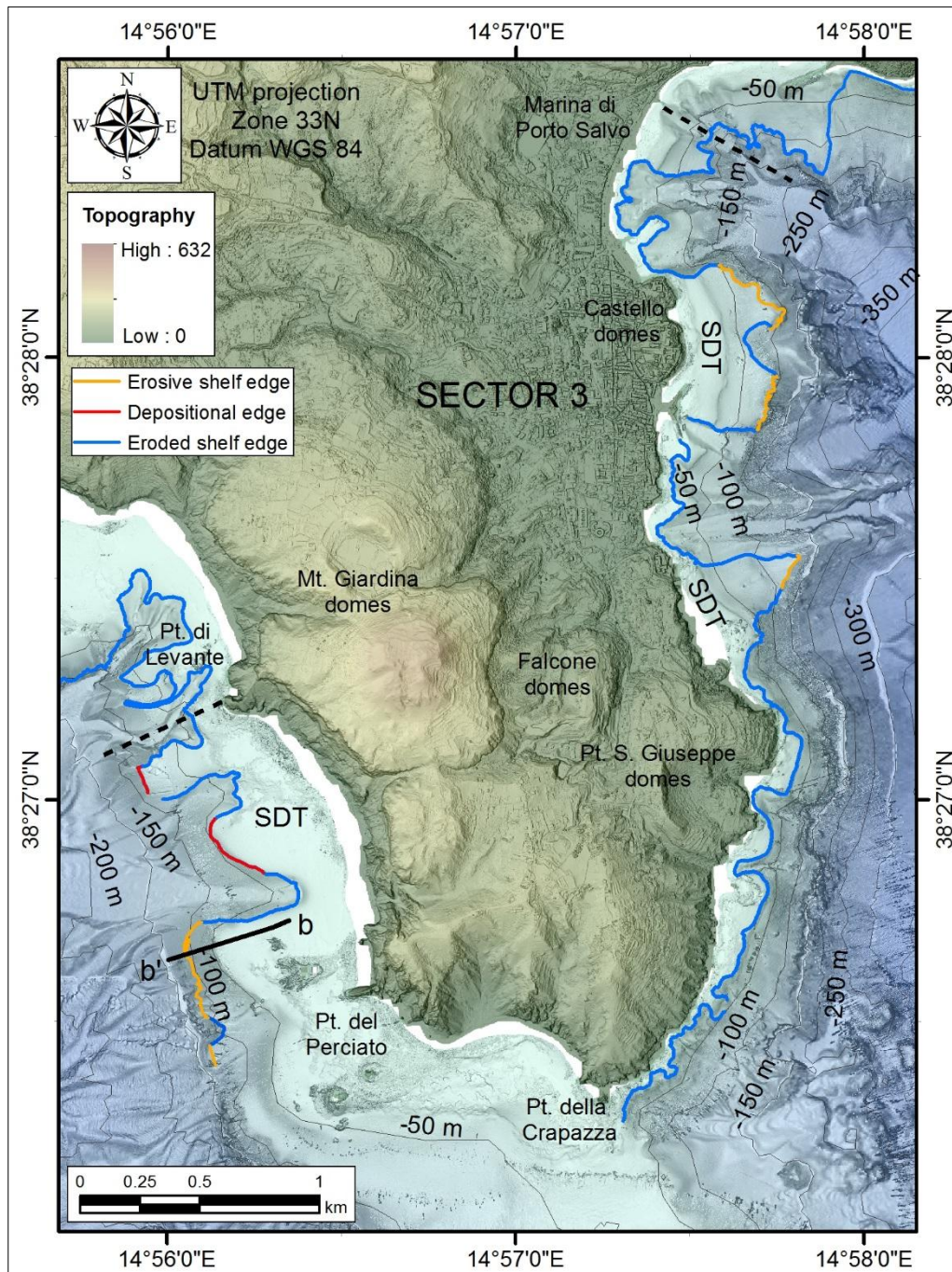
Figure 6.5a *Shaded relief map of the shelf sector 3 (equidistance of isobaths: 50 m).The seismic profile bb' in shown in figure 6.6. The black dashed lines represent the limit of the shelf sector 3. Pt.: Punta; Mt.: Monte.*
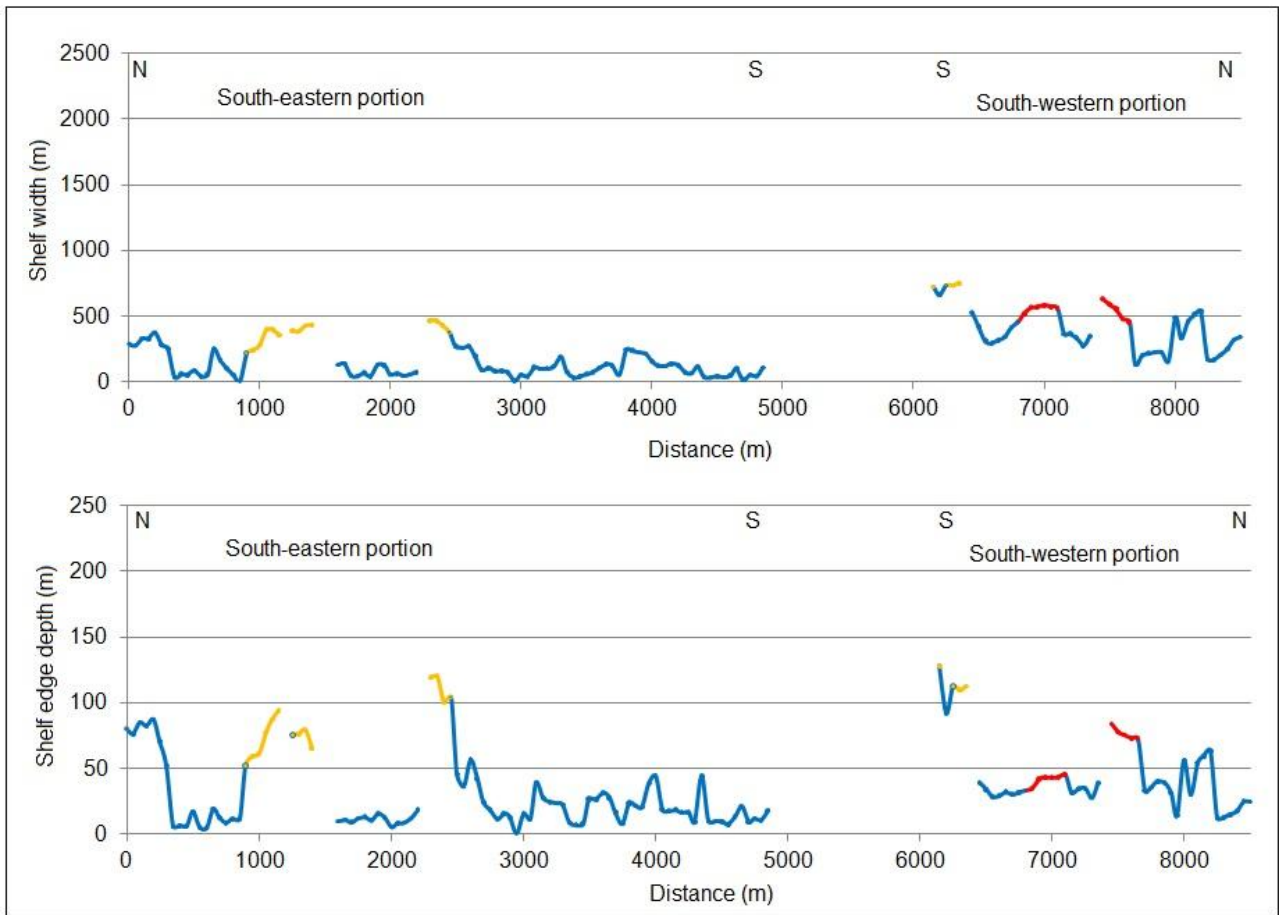
Figure 6.5b *Graphs showing the shelf width and shelf edge depth for shelf sector 3. In yellow: erosive shelf edge; in blue: eroded shelf edge; in red: depositional edge.*
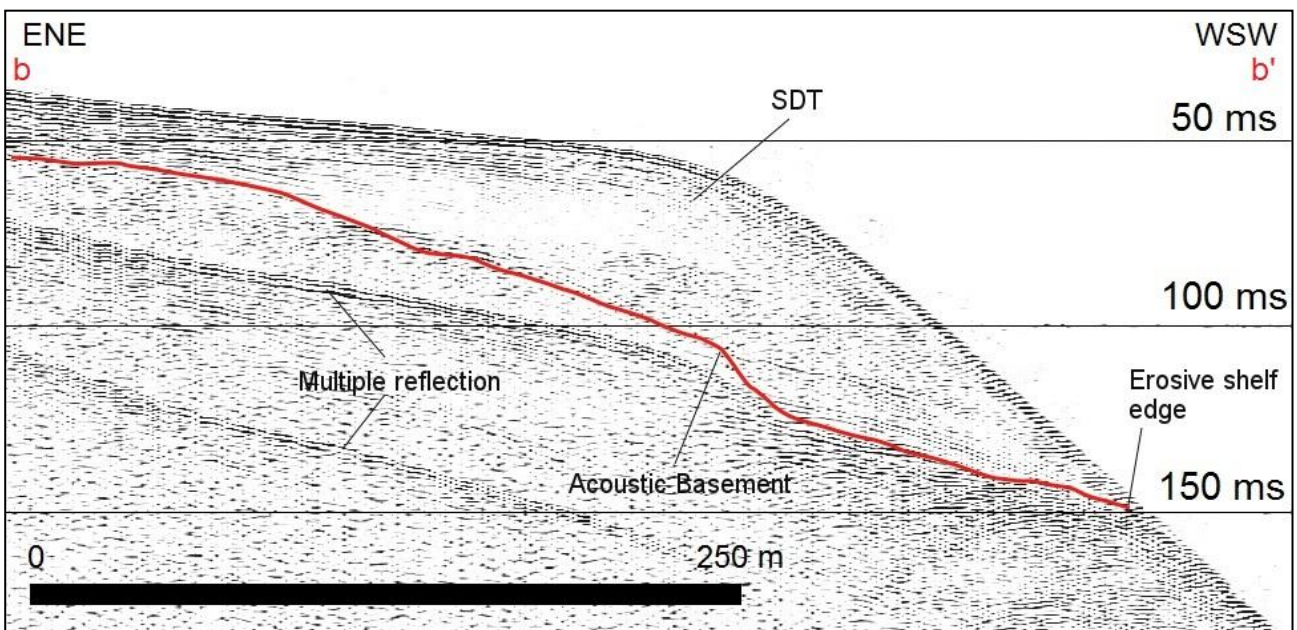
Figure 6.6 *Sparker seismic reflection profile showing the erosive edge and the SDT lying above the shelf. Location of the seismic profile in figure 6.4a.*

SECTOR 4

This sector includes the entire western shelf (apart from Banco del Bagno bank) from Punta di Ponente to Acquacalda (Figures 6.1, 6.7a, 6.9 and 6.11). From the south to the north, the shelf is carved in the products of Timpone Carrubbo (TC) and Monte Mazzacaruso (MM) compound volcanoes, referred as the "older volcanoes" (EE1, Forni et al., 2013), Timpone Ospedale cones (TO), Chiesa Vecchia volcano (CV) and Monte Chirica stratocone (MC), referred as the "western volcanoes" (EE2, Forni et al., 2013).

Starting from the southernmost part of the sector, offshore TC the shelf has a roughly semicircular shape and is mostly over 1000 m wide, up to 1515 m in front of Punta le Grotticelle (Figures 6.7a, 6.7b and Table 6.1). However, offshore Pt. delle Fontanelle, a dense system of gully heads (some of them aligned with structures visible on land) dissects the shelf reducing its width to less than 1000 m (Figures 6.7a and 6.7b). To the north, the width of the shelf progressively increases, being from roughly 1500 m to c. 2100 m offshore Le Puntazze (Figures 6.7b, 6.9 and Table 6.1). The shelf is less than 1500 m wide only offshore Scoglio dell'Immeruta, being 1000 m on average. To the east, offshore Acquacalda, a sub-rounded shelf up to 1.1 km wide is located between two NNE-SSW oriented erosive scars (up to c. 500 wide, Figure 6.11).

The erosive shelf edge depth in this southern portion ranges from -156 m to -178 m offshore TC (Figures 6.7a, 6.7b and 6.8), becoming shallower northwards where the shelf edge is eroded by the scars (c. -110/-125 m offshore Pt. delle Fontanelle, Figures 6.7a and 6.7b). To the north it ranges from -150 m to -182 m offshore Cala Fico, and -214 m offshore Cala Sciabeca (Figures 6.7b and 6.9). From Cala Sciabeca to the north the edge depth decrease being at maximum at -146 m offshore Lo Inzolfato, -156 m offshore Le Puntazze (Figure 6.9) while offshore Acquacalda due to the lack of seismic profiles we identified only the depositional edge of the deeper SDT at c. -105 m (Figure 6.11). The lack of multibeam and seismic data does not allow the measurement of the shelf depth in the area offshore Acquacalda.

In the shelf, different orders of SDTs with variable depositional break depth are observed (see also Chiocci and Romagnoli, 2014), such as offshore Punta le Grotticelle (Figure 6.8) and offshore Le Puntazze, were a threefold staircase of SDTs lies between -20 m and -90 m (Figures 6.9).
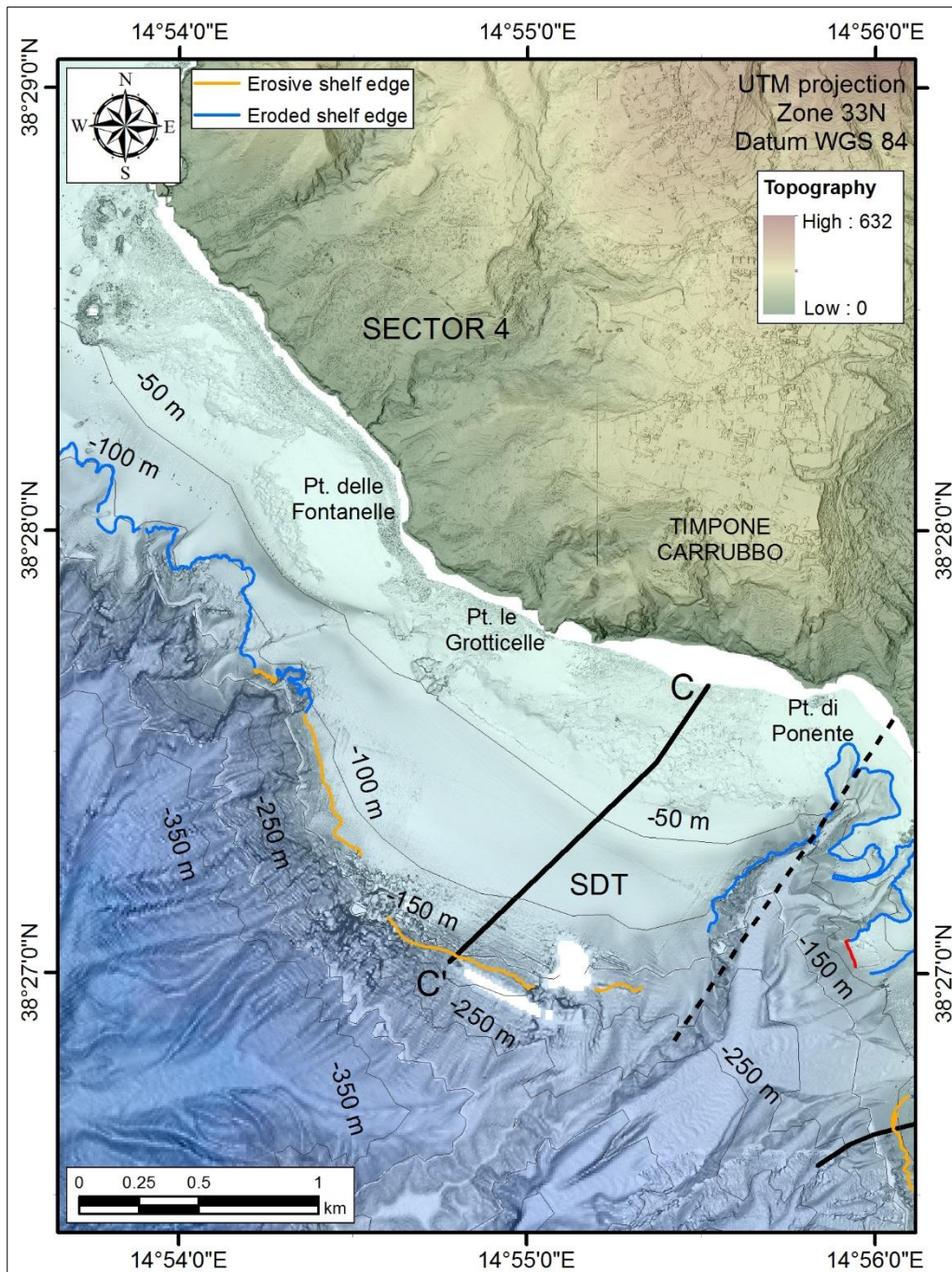
Figure 6.7a *Shaded relief map of the southernmost portion of shelf sector 4 (equidistance of isobaths: 50 m). The seismic profile cc' is shown in figure 6.8. The black dashed line represents the southern limit of the shelf sector 4. Pt.: Punta.*
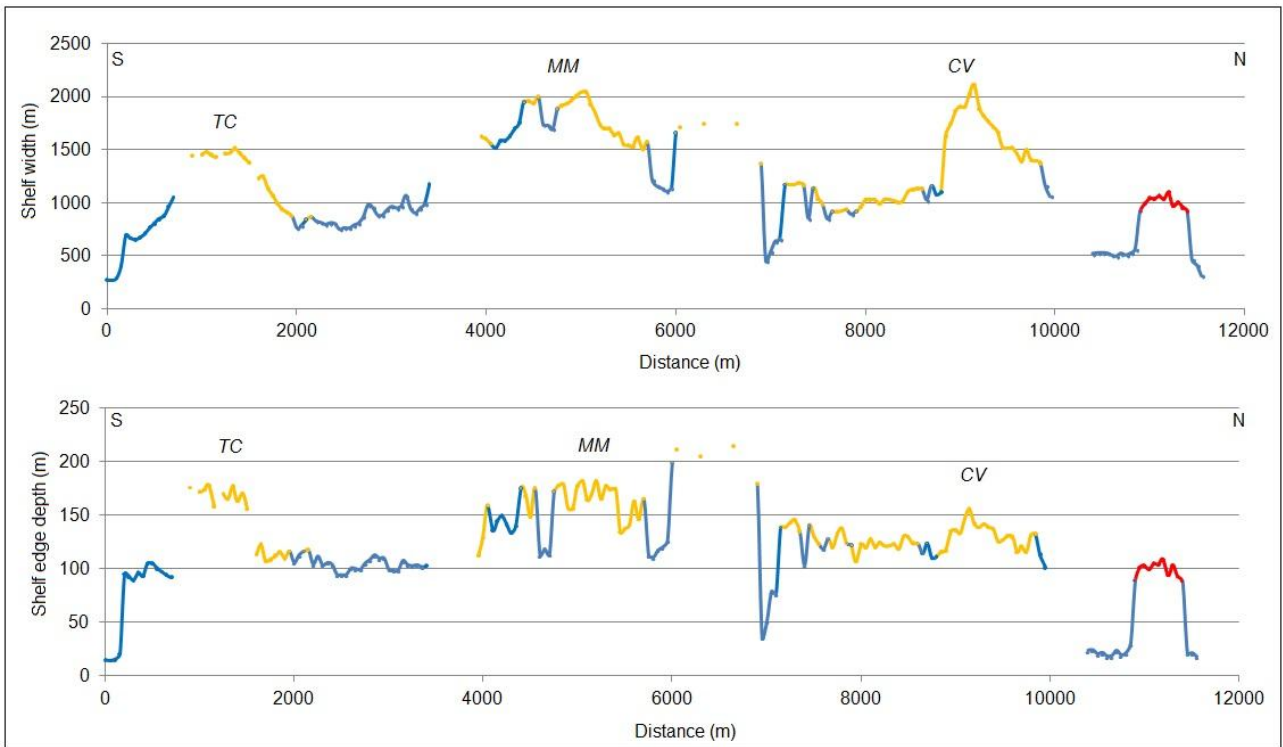
Figure 6.7b *Graphs showing the shelf width and shelf edge depth for shelf sector 4.TC: Timpone Carrubbo; MM: Monte Mazzacaruso; CV: Chiesa Vecchia. In yellow: erosive shelf edge; in blue: eroded shelf edge; in red: depositional edge.*
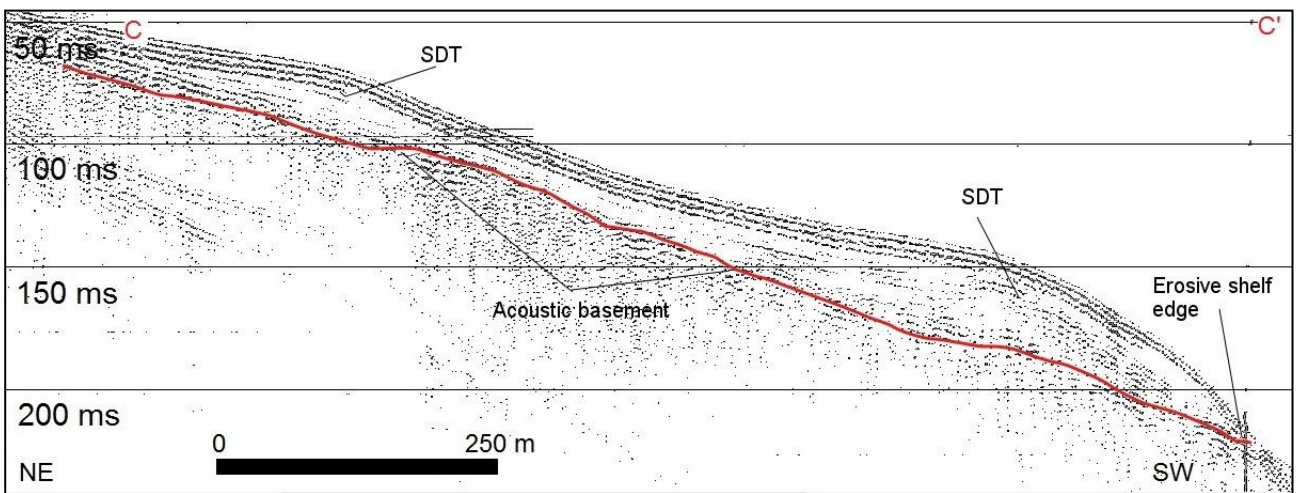
Figure 6.8 *Sparker seismic reflection profile showing the erosive edge and the SDT lying above the shelf. Location of the seismic profile in figure 6.6a.*
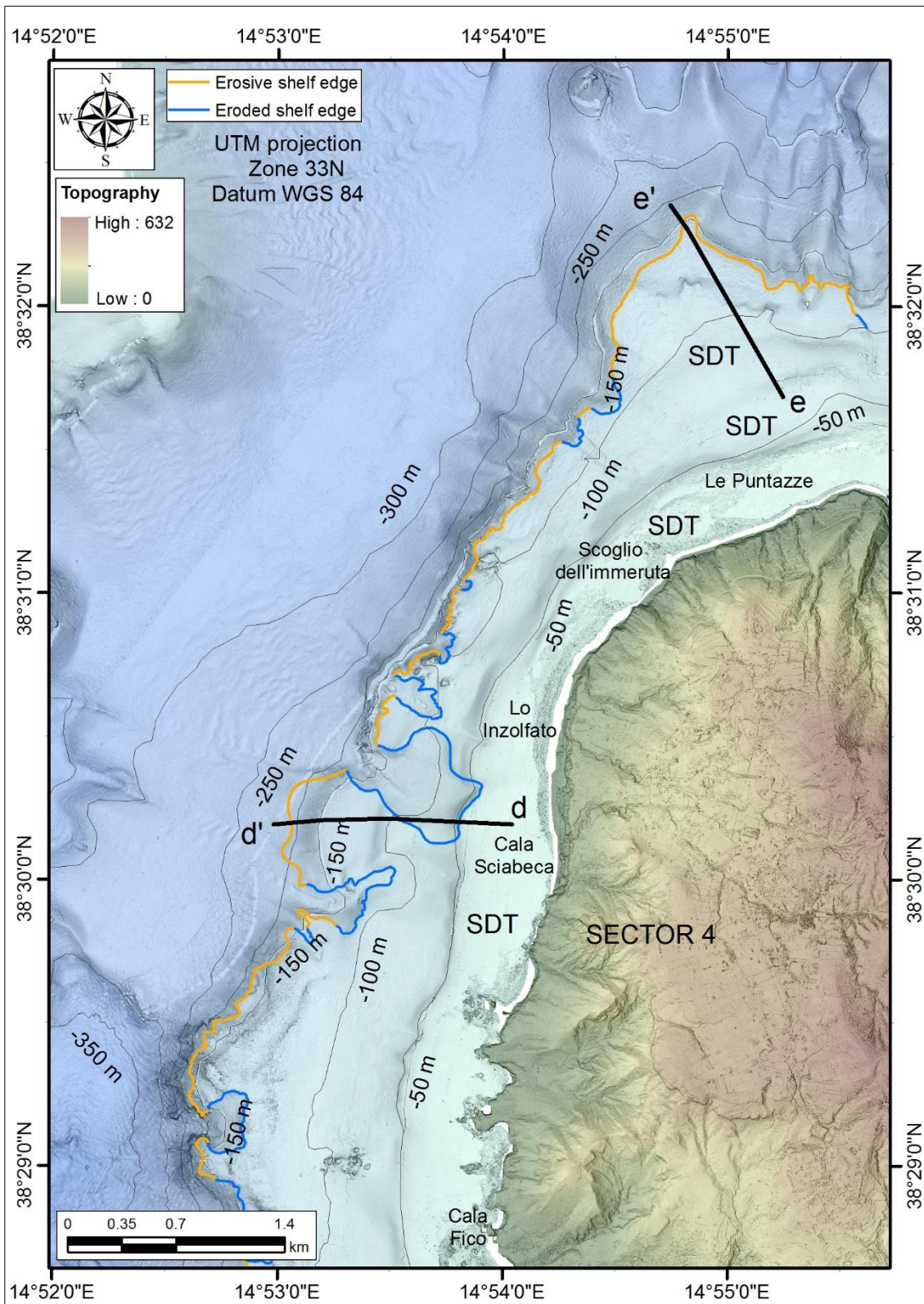
Figure 6.9 *Shaded relief map of the central portion of shelf sector 4 (equidistance of isobaths: 50 m). The seismic profile dd' is shown in figure 6.9. Pt.: Punta.*
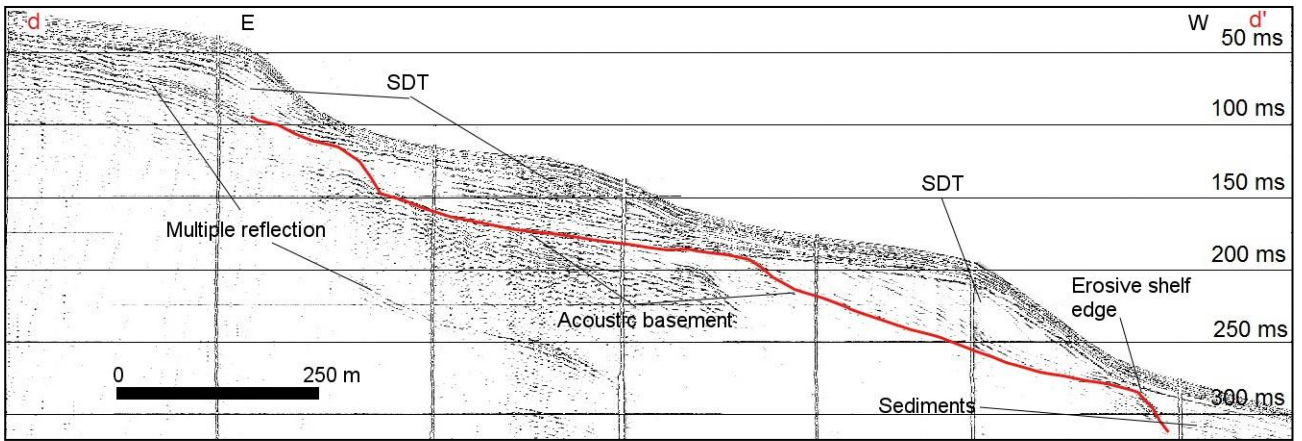
Figure 6.10 *Sparker seismic reflection profile showing the erosive edge and the SDT lying above the shelf. Location of the seismic profile in figure 6.9.*
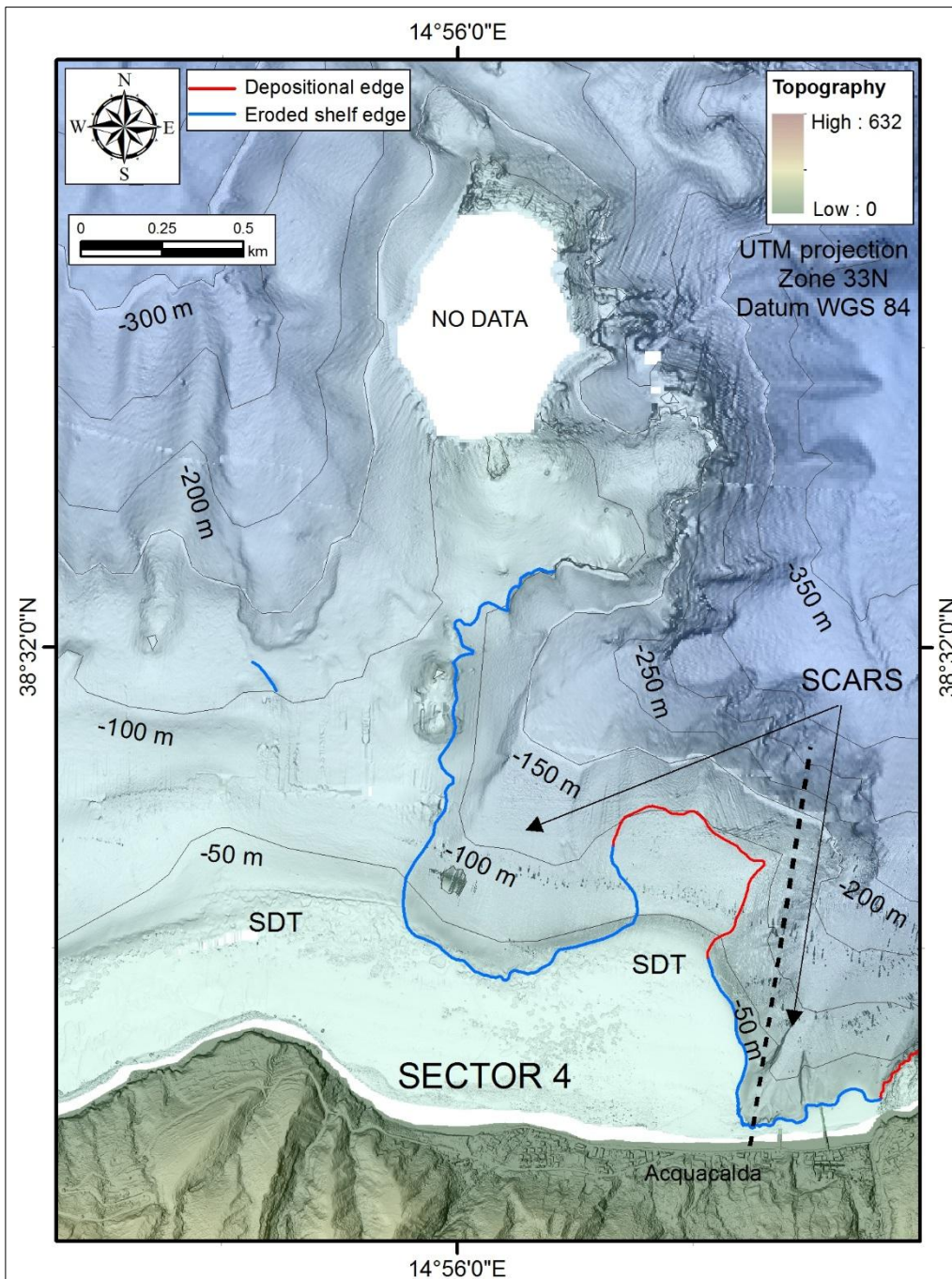
Figure 6.11 *Shaded relief map of the northernmost portion of shelf sector 4 (equidistance of isobaths: 50 m). The black dashed line represents the northern limit of the shelf sector 4.*

BANCO DEL BAGNO BANK

Banco del Bagno is a sub-rounded feature around 1.3 km wide, coalescing with the western shelf of Lipari through a saddle around 100 m deep (Figure 6.12). A flat rocky outcrop rises in the center of the bank reaching -35 m depth and exhibiting a tongue-like shape (Figure 6.12). All around the outcrop, the seafloor is smooth, suggesting the occurrence of a sedimentary cover; seismic profiles show, in fact, an overlying SDT having a depositional shelf break at roughly -60/-65 m depth (Figure 6.13). The shelf is around 260 to 700 m wide with respect to the central, rocky

outcrop at the top of Banco del Bagno (Figure 6.12 and Table 6.1). The erosive shelf edge depth varies from -85 m to -119 m, being mostly around -95/-105 m.
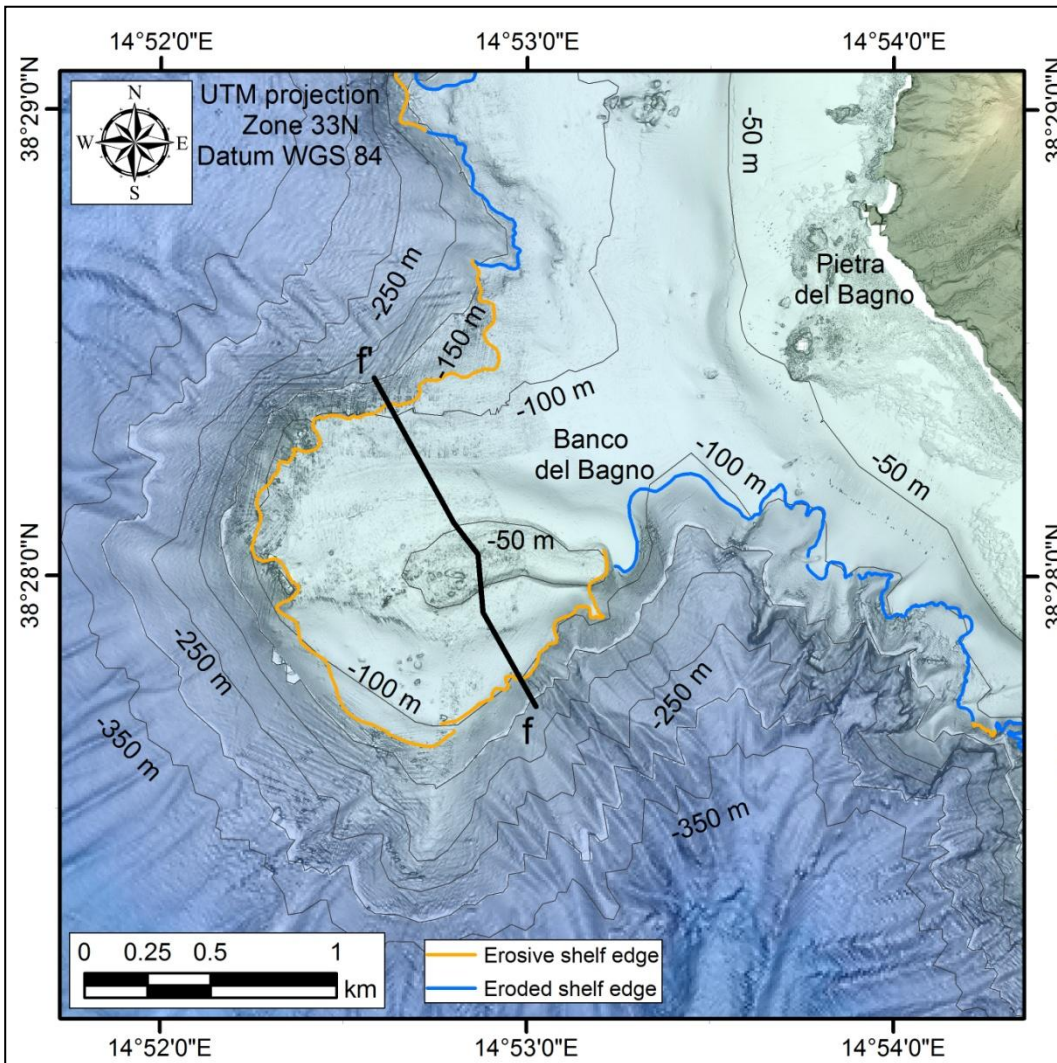
Figure 6.12 *Shaded relief of Banco del Bagno bank (equidistance of isobaths: 50 m).The seismic profile ff' is shown in figure 6.13.*
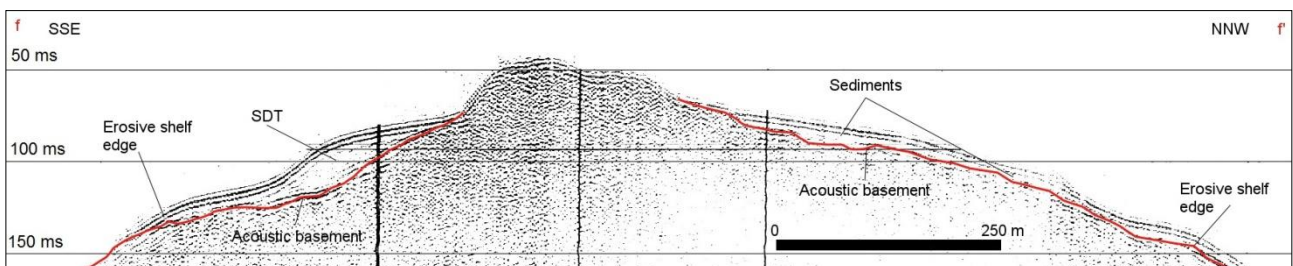
Figure 6.13 *Sparker seismic reflection profile acquired across Banco del Bagno bank showing the erosive edge and the SDT lying above the shelf. Location of the seismic profile in figure 6.12.*

	Max. Erosive edge depth	Max. shelf width
Sector 2	169	845
Sector 3	128	750
Sector 4 TC	178	1515
Sector 4 MM	182	2048
Sector 4 CV	156	2100
Banco del Bagno	119	700

Table 6.1 *Erosive edge depth and shelf width maximum values measured for the insular shelf around Lipari Island (not observed in sector 1).TC: Timpone Carrubbo; MM: Monte Mazzacaruso; CV: Chiesa Vecchia.*

6.2 Discussion

6.2.1 GEOLOGICAL IMPLICATIONS OF INSULAR SHELVES DISTRIBUTION AROUND LIPARI

The morphology and the evolution of the shelf surrounding Lipari Island results from the marine erosion acting on the flanks of volcanic edifices of different ages and for varying lengths of time. As already observed (Romagnoli et al., 2013b), at Lipari wider shelves with deeper edges are generally located offshore the oldest volcanic edifices, attesting for an overall increase of the shelf width with the amount of time the corresponding volcanic units have been exposed to wave action (Menard, 1983; Llanes, et al., 2009; Quartau et al., 2010).

Similarly to Salina (see Manuscript I, Chapter 5), at Lipari we recognize narrow, intermediate and wide shelves among those sectors where the original shelf width is preserved (in orange in figures 6.3a, 6.5a, 6.7a, 6.9, 6.12). This division excludes the sector 1, surrounded in its northern part by a narrow and shallow erosive surface possibly representing the present-day shore platform, similarly to what observed by Romagnoli et al. (2012) around the Vulcanello lava platform. This is in agreement with the fact that this sector is carved in the latest volcanic products of the island (EE9, 8.7 ka – AD 1220, figure 6.1). The irregular shoreline and the pristine submarine lava flow morphologies visible offshore, provide a further evidence of the very young age of this sector. Offshore the Capo Rosso domes, instead, the wide semicircular area with a smooth morphology suggests the occurrence of a thick SDT, likely resulting from the erosion of the soft pumiceous succession recognized onshore (Forni et al., 2013). Its width (c. 550 m) might attest the presence of an underlying shelf on which the sediments rest, likely resulting from the erosion of the older Capo Rosso domes (EE8b, 24-20 ka). However, the lack of seismic profiles does not allow to verify this and to measure the shelf width or depth of the possible erosive edge that should be buried beneath the sedimentary cover, so this sector has not been considered in the Discussion.

Narrow shelves

Shelves of relatively narrow width (Figures 6.5a and 6.5b) have been recognized in sector 3 offshore Castello (EE8a, 27-24 ka) and Falcone (EE7, 43-40 ka) domes (Figures 6.5a and 6.5b), being carved in products of this age or slightly older. A strong difference in terms of shelf width is noticeable between the southeastern (offshore the Falcone domes, around 460 m wide) and the

southwestern shelf of sector 3 (offshore the Pt. di Perciato domes, 750 m wide; Figures 6.5a and 6.5b), both carved in the EE7 products. As suggested by the strongly uneven morphology of the shelf in plan view, mass wasting processes looks more efficient on the southeastern shelf sector in eroding the submarine flank of the island. Most of the scars are developed in correspondence of the subaerial drainage marking the limits between the several, overlapping small domes (belonging to EE7 and EE8) located on the southeastern side of Lipari. These features likely promoted the formation of a dense drainage network also offshore (Figure 6.5a), which in turn would have amplified the shelf dismantling, decreasing its original edge depth (and/or width), as also pointed out along the eastern sector of Salina Island (see Manuscript I).

Intermediate shelves

The shelf width around the Monterosa volcanic edifices (EE4, 119-114 ka), ranges from c. 400 m to c. 845 m (Figures 6.3a and 6.3b), being wider with respect to that carved around the EE7/8 domes, in agreement with the width-age model (Menard, 1983). However, the erosive edge depth along the northern and eastern side of the promontory (around -110/-131 m, respectively) is comparable to that of sector 3 where the younger EE7/8 domes are located. The erosive edge is deeper offshore the southern side, where it reaches a maximum depth of -159 m, although in most of its extension the shelf is eroded (Figure 6.3a). The occurrence of a deep erosive edge and of two superimposed SDTs lying on it (Figures 6.3a and 6.4) suggest a possible subsidence that affected this portion of the shelf.

Wide shelves

The occurrence of the widest and deepest shelf areas offshore the sector 4 is in accordance with the age and stratigraphy of the volcanic products exposed onshore. This sector, in fact, results from the interaction of different volcanic phases connected to the formation of the "older volcanoes" and "western volcanoes" first, overlapped by the EE3 to EE7 products, that partly covered the older products (Forni et al., 2013). The coastline and the shelf morphologies reflects that interaction and complexity.

The shelf areas offshore Timpone Carrubbo (TC) and Monte Mazzacaruso (MM) are among the widest at Lipari (being from c. 1500 m to 2000 m wide, Figures 6.7a, 6.7b and 6.8), in agreement with the inferred old age of the volcanic edifices found onshore. The sub-rounded shape of this shelf might outline their paleo-morphology, indicating their possible original extent prior to erosion. The erosive shelf edge depth (-180 m and -182 m respectively (Figures 6.7a, 6.7b, 6.8 and 6.9) suggests that these shelf sectors were subsided after the formation of the shelf, and/or the shelf may refer to early products, being older in age than these volcanic edifices.

The widest shelf of Lipari (c. 2100 m) occurs offshore the Chiesa Vecchia (CV) volcano, also belonging to the EE2. Also this portion of the shelf likely suffered subsidence, since the erosive shelf edge reaches at maximum -156 m. As suggested by the sub-rounded shape of the deepest portion of the shelf offshore CV volcano (Figure 6.9), this shelf area might reflect the original extension of the early volcanic center before being largely eroded to form the present shelf. The eroded remnants of early volcanic centers have been similarly recognized offshore the nearby SE sector of Salina (chapter 5, Manuscript I). Evidence of offshore volcanic activity are also

represented by the shallow rounded bank located offshore Le Puntazze and by the profusion of submerged cones in the northern Lipari offshore (Romagnoli et al., 2012).

6.3 The vertical mobility of Lipari

The vertical displacement affecting the shelf sectors of Lipari are estimated using the same method adopted for Salina (see Manuscript III, chapter 5). The erosive shelf edge depth in the different sectors have been related with the eustatic sea-level peaks from the Bintanja et al. (2005)'s curve, vertically displaced by the amount of uplift deduced from the elevation of MIS 5.5 terrace. According to the elevation of the MIS 5.5 terrace at Lipari (43-45 m) and taking into account a regional value of +6 (+/-3) m for the eustatic sea-level in the Last Interglacial (Lambeck et al., 2004), we calculated here a displacement of 39 m due to the uplift trend (Table 5.2), instead of 44 m adopted for Salina, where the same terrace is at 50 m a.s.l. (see Manuscript III, chapter 5). Nevertheless, since terraces older than MIS5 were not recognized on the flanks of Lipari (Lucchi et al., 2013b), where the MIS 7.3 (221 ka) raised terrace is possibly not formed/preserved, any estimate of previous vertical movements (before MIS 5.5, i.e. before 124 ka) cannot be estimated here as modeled for Salina. However, evidence of subsidence possibly occurred during the earlier stage of development of Lipari, come from the shelf sectors offshore the western coastline of the island, as suggested by the occurrence of erosive shelf edges deeper than c. -125 m. According to the age estimated for the subaerial volcanic edifices at Lipari, we tried to match the relative sea-level curve with the height/depth of paleo-sea level markers as we did for Salina, bearing in mind all the limitations associated to our method (see Manuscript III, chapter 5).

In the case of Lipari, the shelves carved in the Timpone Carrubbo (TC) and Monte Mazzacaruso (MM) flanks, having the deepest erosive edge (-178/-182) are tentatively related to the paleo-sea level during MIS 12 (465 ka) or MIS 10 (356 ka). In the later case, their estimated net displacement should be 96 m for TC and 100 m for MM, corresponding to a time-averaged subsidence trend of 0.41-0.43 m/ka for the time interval between the MIS 10 (356 ka) and the MIS 5 (124 ka). Conversely, if the shelves formation is firstly attributed to the MIS 12 (465 ka), the average subsidence rates are 0.24 m/ka for TC and 0.28 m/ka for MM (Table 5.2). Actually, the age of the TC and MM volcanic edifices is unknown (Forni et al., 2013, Figure 4.4). Regarding the edifices of CV and Monterosa, on the base of their age (Figures 4.4, 6.1 and Table 6.2) and of the shallower erosive edge (-156 m and -159 m, respectively) with respect TC and MM, we consider MIS 10 (356 ka) or MIS 8 (272 ka) as possibly related to their initial formation. In the first case, the net displacements suffered by the shelf are 74 m and 77 m respectively, yielding an average subsidence trend of 0.32-0.33 m/ka for the time interval between the MIS 10 (356 ka) and the MIS 5 (124 ka). If related to the MIS 8, the net displacements should be of 93 m for CV and 96 m for Monterosa, yielding a related subsidence rate of 0.63-0.65 m/ka respectively (Table 5.2). However, considering the age of the products of Monterosa (119-114 ka), we also tentatively related the initial formation of this shelf area to the MIS 6 (138 ka). The obtained displacement would be -37 m and the average subsidence rate for the time interval between the MIS 6 and the MIS 5 is 2.64 m/ka (Table 6.2).

Insular shelf	Age of volcanic units (ka)	Present Depth (m)	Depth Before Uplift (m)	Related Paleo-s.l. (at -10 m)	Sea level (m) at formation	Vertical Displacement (m)	Subsidence Rate(m/ka)
		(h)	(D5.5)	(d)	(E)	D (h+d-E)	
Timp. Carrubbo	Unknown	-178	-217	-207	-126 (465 ka, MIS12)	-81	0.24(124-452ka)
"		"	"	"	-111 (356 ka, MIS10)	-96	0.41(124-356ka)
"		"	"	"	-92 (272 ka, MIS8)	-115	0.77(124-272ka)
Mazzacaruso	Unknown	-182	-221	-211	-126 (465 ka, MIS12)	-95	0.28(124-452ka)
"		"	"	"	-111 (356 ka, MIS10)	-100	0.43(124-356ka)
"		"	"	"	-92 (272 ka, MIS8)	-119	0.80(124-272ka)
Chiesa Vecchia	267-188	-156	-195	-185	-111 (356 ka, MIS10)	-74	0.32(124-356ka)
"		"	"	"	-92 (272 ka, MIS8)	-93	0.63(124-272ka)
Monterosa	119-114	-159	-198	-188	-111 (356 ka, MIS10)	-77	0.33(124-356ka)
"		"	"	"	-92 (272 ka, MIS8)	-96	0.65(124-272ka)
		-131	-170	-160	-123 (138 ka, MIS6)	-37	2.64(124-138ka)

Table 6.2 *Displacement amounts and rates relative to the insular shelves around Lipari Island.*

6.3.1 THE EARLIER EVOLUTIONARY STAGES OF LIPARI

The analysis of the geomorphic parameters of the insular shelves (shelf width and depth of the erosive edge) around Lipari allowed us to propose a relative age attribution for the volcanic centers on which the shelves formed.

Considering a homogeneous subsidence process before the Last Interglacial, we propose that the shelves offshore TC and MM volcanoes are the eroded remnants of the earlier volcanic stages of these edifices, that can be considered as among the oldest at Lipari and possibly contemporaneous to the oldest centers of Salina (Pizzo Corvo and Monte Fossa delle Felci south, see Manuscript III). This evolutionary model is in agreement with that previously proposed by Forni et al., (2013) based on onshore studies. By attributing the formation of the shelves around TC and MM to the MIS 12 (465 ka), the obtained average subsidence trend (0.24-0.28 m/ka) is similar to that estimated for Salina (0.39-0.56 m/ka, see Manuscript III). This relative chronological attribution is in agreement with the width of the shelf offshore TC and MM, being amongst the widest at Lipari and likely affected by the same amount of subsidence. A further evidence supporting this similar evolution is that these volcanic edifices are aligned NW-SE, as Fossa Felci South and the nearby flat-topped cone located offshore the SE coastline of Salina (see Manuscripts I and III), whose development is associated to the MIS 12 (465 ka). These structures, in fact, follow the NNW-SSE oriented volcanic belt striking along the Tindari-Letojanni regional fault system as other volcanic features active during the early stages of development of the Aeolian Archipelago

(Romagnoli et al., 1989). By taking into account a subsidence rate similar to that of TC and MM (0.35 m/ka, Table 5.2), we also infer that the shelf offshore CV was firstly carved during MIS 10 (356 ka), predating the volcanic activity onshore. This stage of evolution might be related to the early development of the sector offshore CV, as previously inferred on the base of the shelf morphology and width (see section 5.3.2).

A comparable average subsidence trend (0.33 m/ka, Table 6.2) is obtained if the initial formation of the shelf offshore the southern coastline of Monterosa is attributed to the MIS 10 (356 ka). Although the attribution to MIS 6 (138 ka) and MIS 8 (272 ka) would better fit the age of the volcanic products onland (119-114 ka), the related average subsidence rates (2.64 m/ka and 0.65 m/ka respectively, Table 6.2) are considered too high and possibly not realistic over the long term, if compared to the inferred subsidence trend of the other sectors of Lipari. Therefore, we suggest that the early volcanic activity of Monterosa was probably centered here, and occurred before the EE4. The sub-rounded morphology of the shelf (Figure 6.3a) and its greater width (c. 845 m), further support our inference. Conversely, the erosive edge depth of the northern and eastern shelf sectors is in the range of the sea level occurred during MIS 2 (22 ka).

The erosive shelf edge depth offshore the Falcone domes (-120 m) and P. di Perciato (-128 m) is compatible with their age and the sea-level depth during LGM (-120 m, Rohling et al., 2014), suggesting a tectonic stability or slight uplift for these shelf sectors, in agreement with the uplift trend calculated for the island (0.34 m/ka) on the base of the current elevation of the MIS 5 terraces (Lucchi et al., 2013). Conversely, the shallower shelf edge depth (-95 m) offshore the Castello domes, may suggest the occurrence of local vertical movements. The vertical mobility of a single volcanic edifice due to local volcanic inflation and deflation processes, in fact, might be very high (Lajoie, 1986), although onland there is no evidence of recent volcanic activity in the area that might justify vertical displacements of this sector. Further investigation are needed to verify this.

The erosive shelf edge depth highlights an overall stability or uplift of Banco del Bagno. Although physically connected to the shelf offshore MM, its sub-rounded morphology suggests that it is an isolated submerged eruptive center, presently not active and partially eroded during the LGM, as evidenced by the erosive shelf edge depth. Considering that the uplift trend in the Aeolian Archipelago started around 125 ka, the erosive shelf edge depth suggests that this feature may be younger than the MIS 5.

6.4 Conclusions

The study of the morphological characteristics (width and erosive edge depth) of the insular shelf surrounding Lipari allowed us to better constrain the geological evolution of the earlier portion of the volcanic edifice and to infer a similar vertical behavior to that proposed for Salina Island (see Manuscript III, chapter 5). In particular, a possible early subsidence for the island of Lipari, that was likely active since at least until 465 ka (MIS 12) to (or before) the Last Interglacial, is proposed, having similar average rates as at Salina, highlighting that the vertical mobility trend in the central Aeolian sector is likely driven by regional tectonic processes.

6.5 Insular shelves around Vulcano Island

Similarly to the islands of Salina and Lipari, Vulcano results from the activity of overlapping volcanic edifices (De Astis et al., 2013; see Chapter 4). However, the distribution of the volcanic edifices is less complex with respect the other islands, being mostly formed by the products of the Primordial Vulcano, Monti Lentia and La Fossa Cone (LFC hereafter). At Vulcano, the shelf has been divided in four sectors on the base of the shelf characteristics and of the distribution of the main volcanic edifices onshore (Figure 6.14).
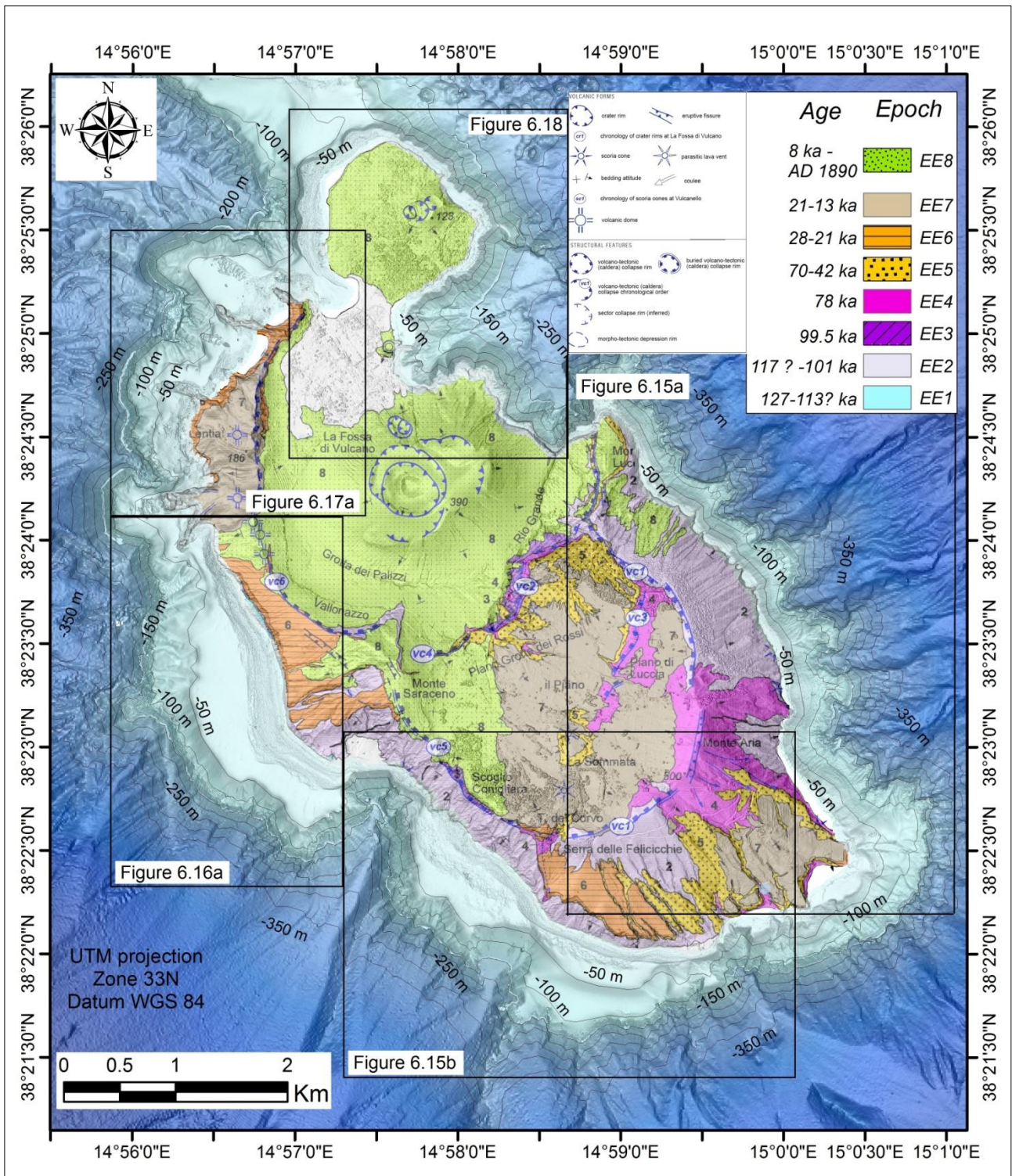
Figure 6.14 *Simplified geological map of Vulcano (modified after De Astis et al., 2013) merged on the DEM of the island and the multibeam bathymetry of the submarine shallow areas. The black boxes locate the shelf sectors represented in figures 6.15a, 6.15b, 6.16a,6.17a and 6.18.*

SECTOR 1

This sector runs along the eastern, southern and the southwestern coastline of Vulcano from Punta Luccia to Punta del Rosario (Figures 6.15a and 6.15b). It is carved in the products of the Primordial Vulcano stratocone belonging to the EE2 (117-101 ka, Figure 6.14).

The shelf offshore the eastern side of Vulcano (from Punta Luccia to Punta Bandiera, Figure 6.15a) has an irregular shape, with small-scale (few tens of meters wide) and medium-scale (few hundred of meters wide) scars that contribute to create a strongly uneven shelf morphology (Figure 6.15a). The shelf is mostly sediment-starved and furrowed, on its top, by channelized features, in continuity with the subaerial drainage. The shelf width varies from c. 230 m to c. 680 m, being progressively wider to the south (Figures 6.15a and 6.15c). From Punta Bandiera to Faro Nuovo, along the southern flank of Vulcano, the shelf widens to some hundreds m (up to c. 870 m), being then interrupted by the wide scar offshore Faro Nuovo (Figures 6.15b and 6.15c). From Faro Nuovo to Punta del Rosario, the shelf exhibits a convex shape interrupted by incised by a 600 m-wide headwall scars. Its width increases up to a maximum value of 925 m (Figures 6.15b and 6.15c). As for the erosive shelf edge depth, offshore the eastern and southern flank of Vulcano it is constantly around -110/-125 m, apart from few portions (mostly offshore Punta Bandiera and in the south-western area) where it is slightly deeper, reaching at maximum c. -150 m (Figures 6.15a and 6.15c).

Despite the lack of seismic profiles, from the bathymetric appearance the eastern and the southeastern shelves appear almost devoid of sediments, exhibiting only small deposits trending parallel to the coastline on the inner shelf down to -10/-15 m (Figure 6.15a). Conversely, from Faro Nuovo to Punta del Mortaro the sedimentary cover looks organized in two superimposed SDTs (Figure 6.15b) having a depositional break at roughly -40/-45 m and -90/-95 m. Their thickness cannot be measured due to the lack of seismic profiles in the area. To the north of Punta del Mortaro only a single SDT is visible, exhibiting a depositional break at roughly -40/-50 m (Figure 6.15a).
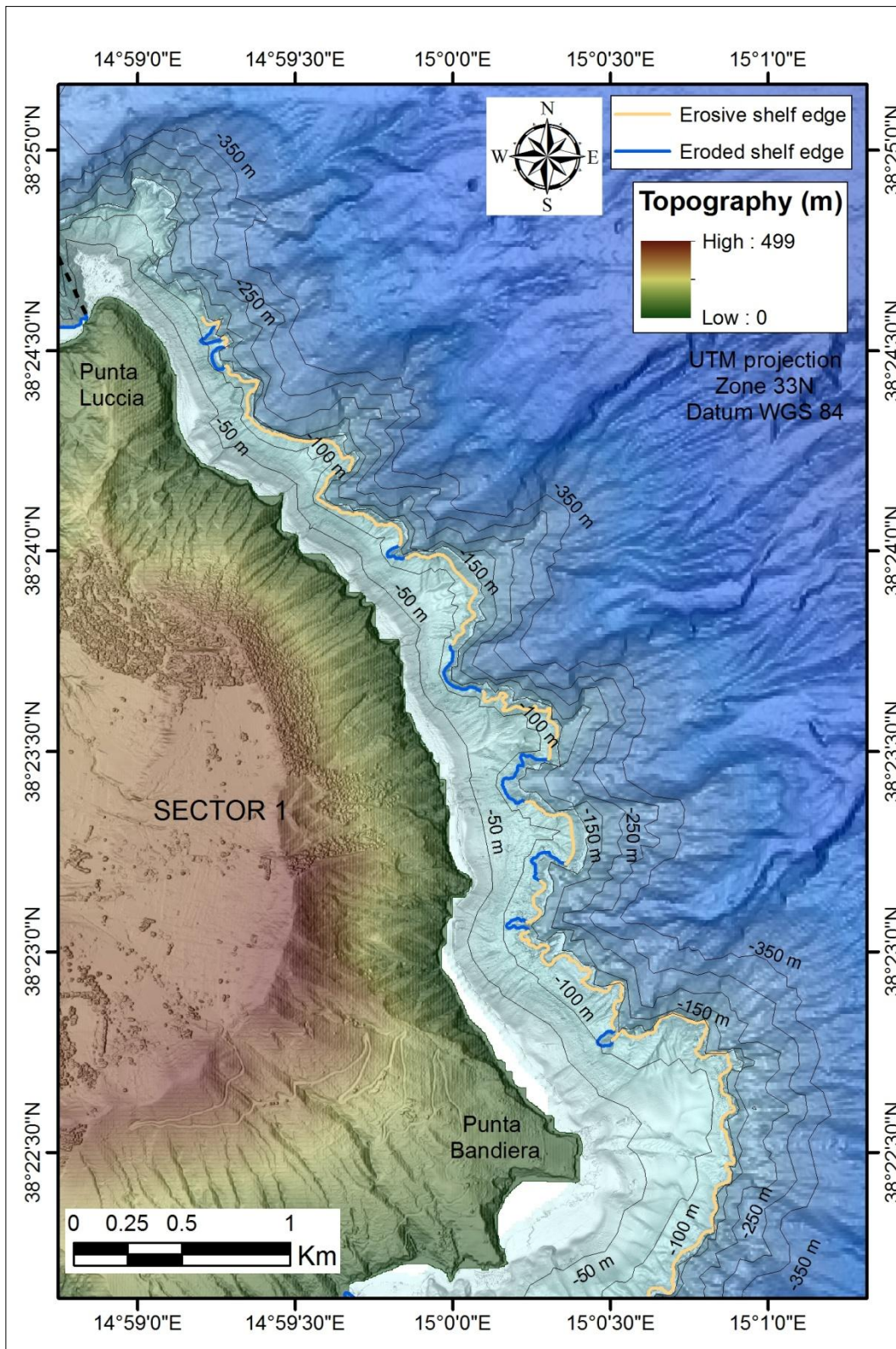
Figure 6.15a. *Shaded relief map representing the easternmost portion of shelf sector 1. The black dashed line represents the eastern limit of the shelf sector 1.*
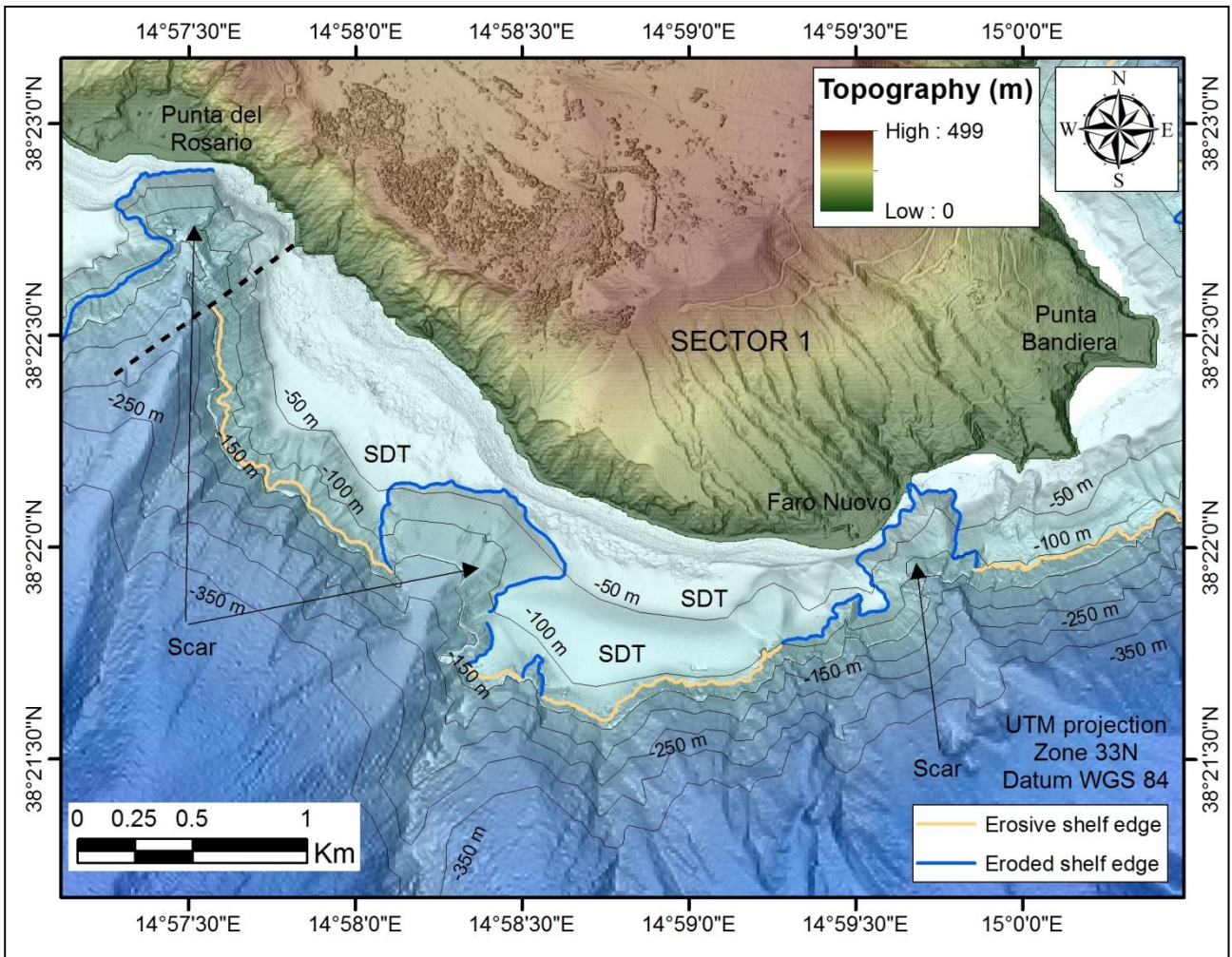
Figure 6.15b. *Shaded relief map representing the southernmost portion of shelf sector 1. The black dashed line represents the western limit of the shelf sector 1.*
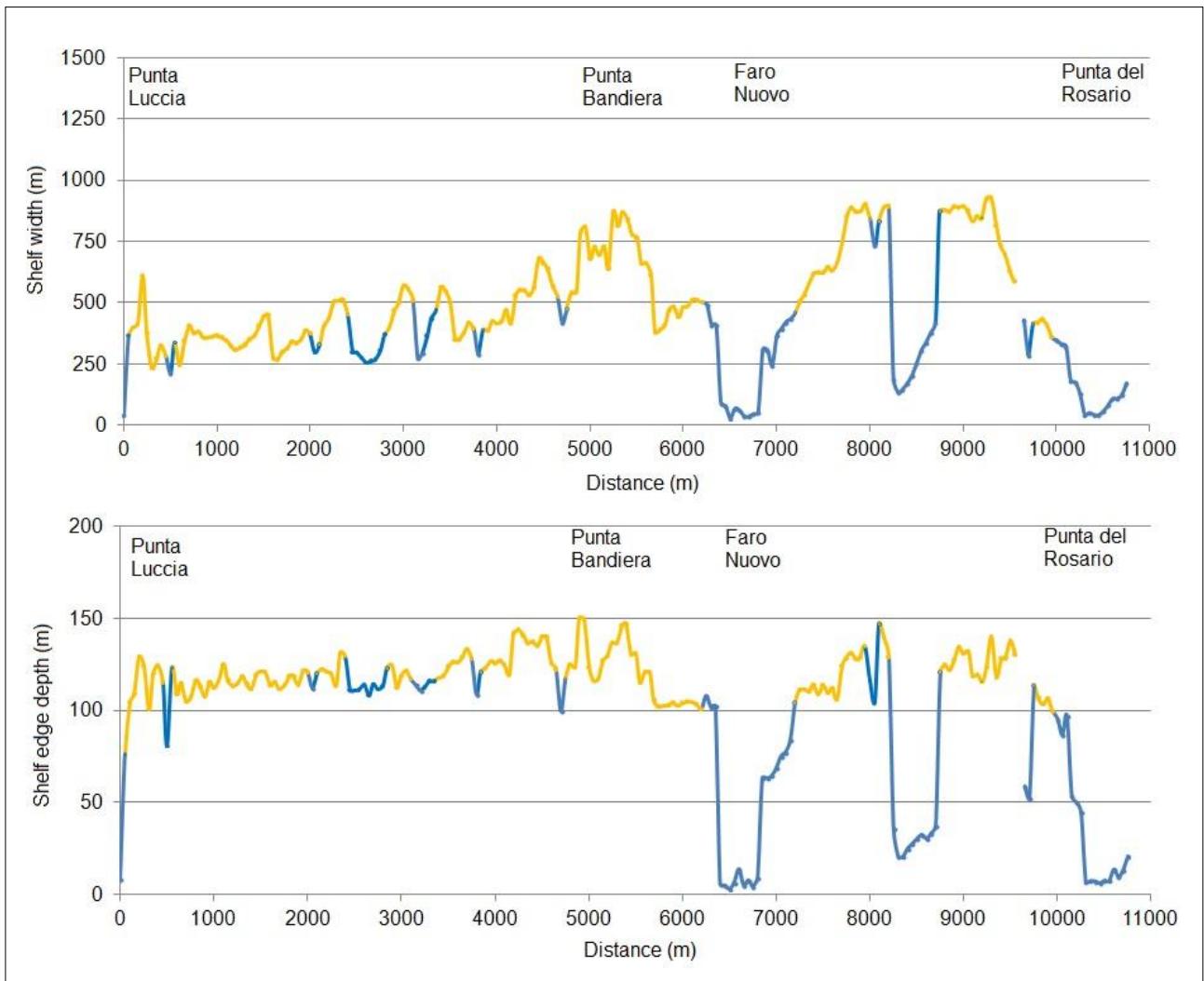
Figure 6.15c. *Graphs showing the shelf width and shelf edge depth for shelf sector 1.*

SECTOR 2

This sector runs aside the Capo Secco eccentric lava cone from Punta del Rosario to Punta del Capo Secco (Figure 6.16a). The shelf is carved in the thick succession of lava flows belonging to EE1, partly overlapped by the EE2 "Primordial Vulcano" products and by the EE6 pyroclastic successions (Figure 6.14). This sector of the shelf has a semicircular shape, with a shelf width gradually increasing in the central part (where it ranges from c. 900 to up to c. 1367 m, (Figures 6.16a and 6.16b), while in the southernmost part it is dissected by a wide (up to c. 900 m) scar offshore Punta Conigliara (Figures 6.16a and 6.16b). The shelf edge depth is very constant along the whole sector, ranging from c.-100 m to -128 m (Figures 6.16a and 6.16b). The shelf is covered by a single main SDT, with a depositional edge located roughly at -40/-45 m (Figure 6.16a).
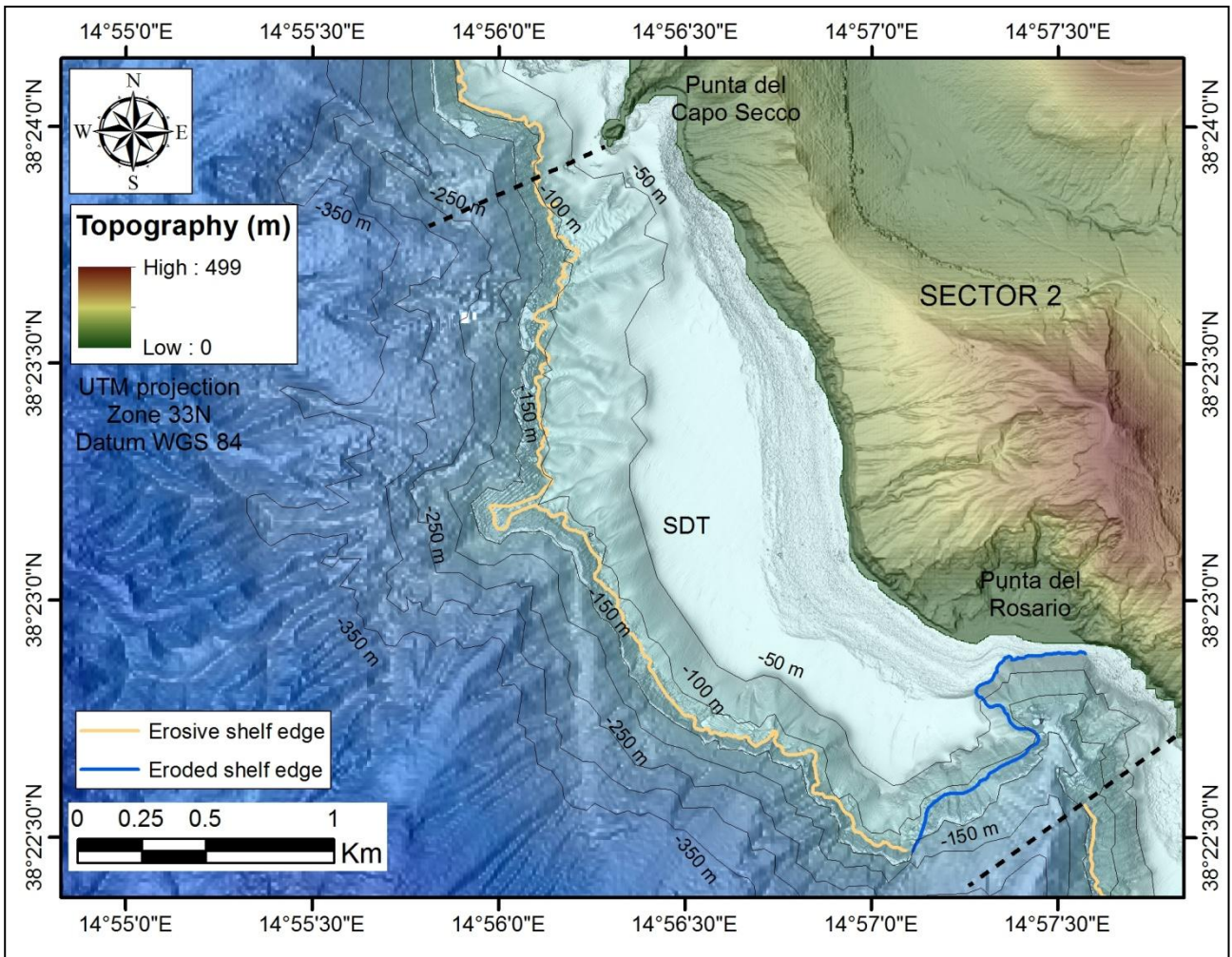
Figure 6.16a. Shaded relief map representing shelf sector 2. The black dashed lines represents the limits of the shelf sector 2.
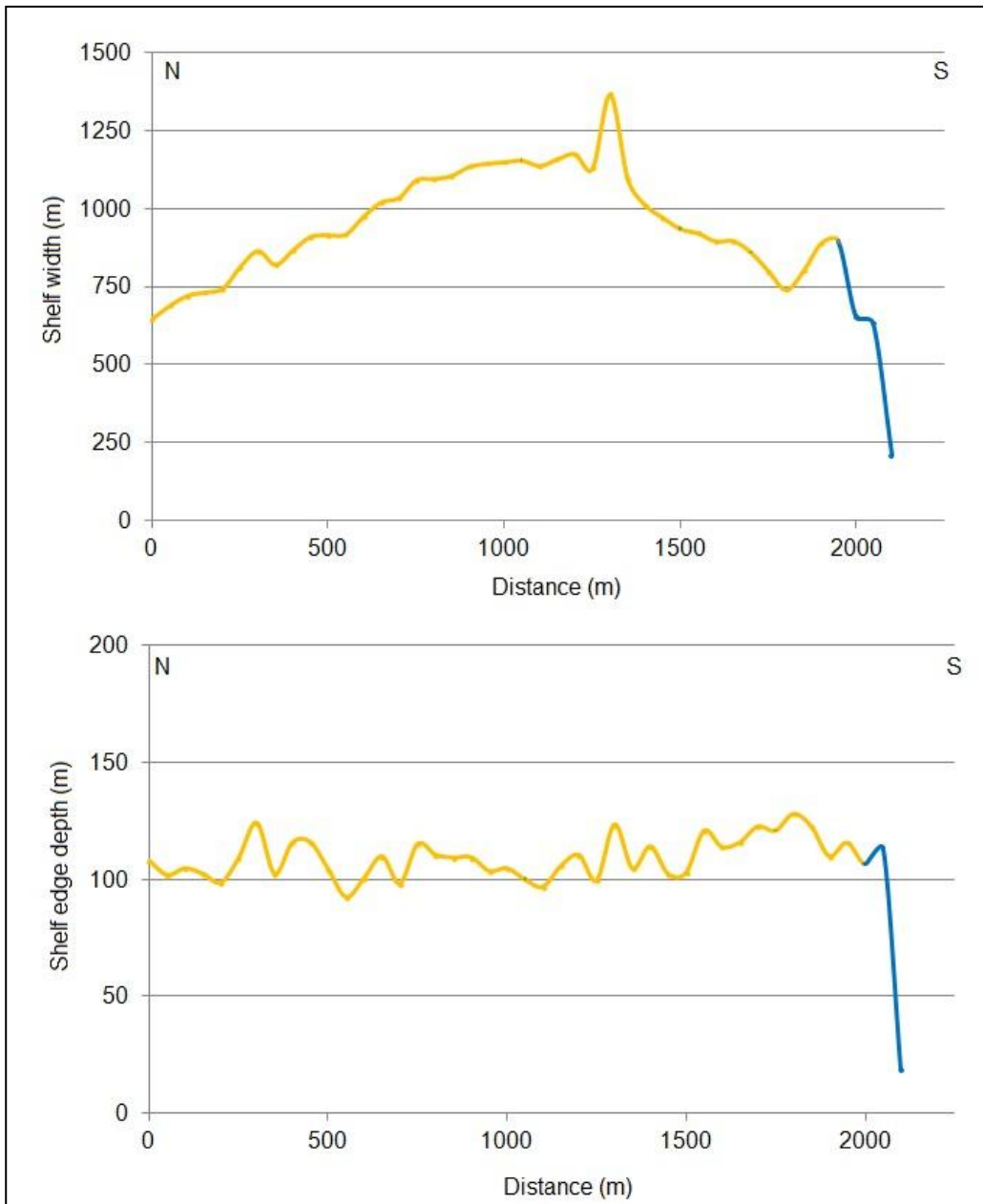
Figure 6.16b. Graphs showing the shelf width and shelf edge depth for shelf sector 2.

SECTOR 3

This sector runs along the northwestern side of the island from Scoglio di Capo Secco to Punta Cala del Formaggio (Figure 6.17a). The strongly irregular coastline is carved in the products of the EE2 overlapped by younger EE6, EE7 and EE8 (Monte Lentia lava domes products, Figure 6.14). The shelf is locally deeply eroded by mass wasting processes reaching the shallow water areas and causing a very variable shelf width along this sector (Figure 6.17a). The scar headwalls dissect the shelf in three main sub-rounded portions that reflect the morphology of the Monte Lentia domes onshore (Figure 6.17a). The shelf offshore the southernmost domes (from Scoglio di Capo Secco to Punta del Monaco) is up c. 800 m wide, while to the north (offshore Cala del Formaggio) the width increases up to c. 1260 m (Figures 6.17a and 6.17b). The erosive shelf edge depth is similar along the entire sector, being generally from -74 m to -104 m (Figures 6.17a and 6.17b). The inner shelf

147

is characterized by an E-W elongated rocky outcrops developed down to -35/-45 m depth, likely representing the seaward continuation of subaerial *coulées* from the nearby Monti Lentia (Romagnoli et al., 2013b, Figure 6.17a). They are characterized by distinctive lobate outlines, low relief and rugged surface texture. Sediments are sparse in this shelf sector, in particular in the southernmost portion where mass wasting processes likely prevent the formation of a uniform sedimentary cover. Nevertheless, the widest portion of the shelf offshore Cala Formaggio is covered by a thick SDT exhibiting a depositional edge at -45 m (Figure 6.17a).
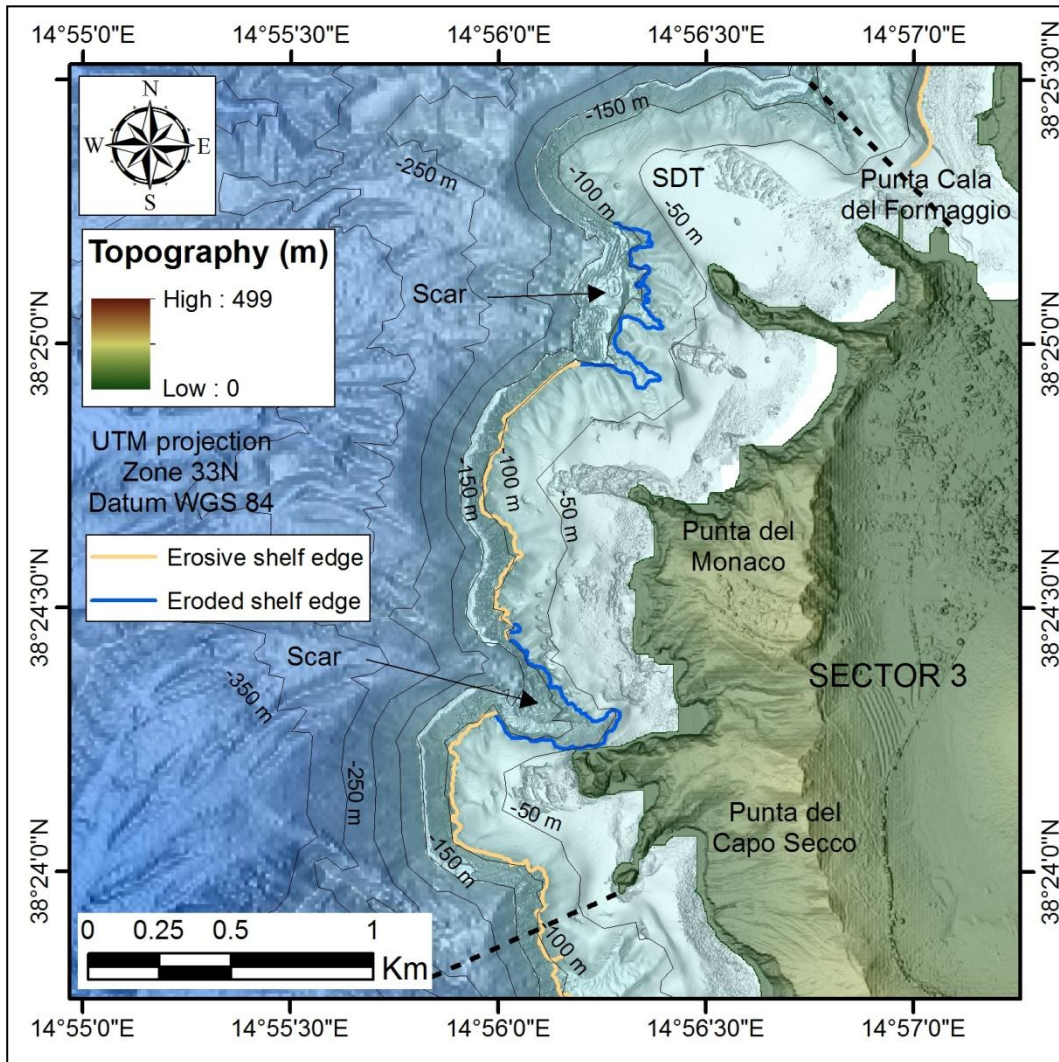
Figure 6.17a. *Shaded relief map representing the easternmost portion of shelf sector 3. The black dashed lines represents the limits of the shelf sector 3.*
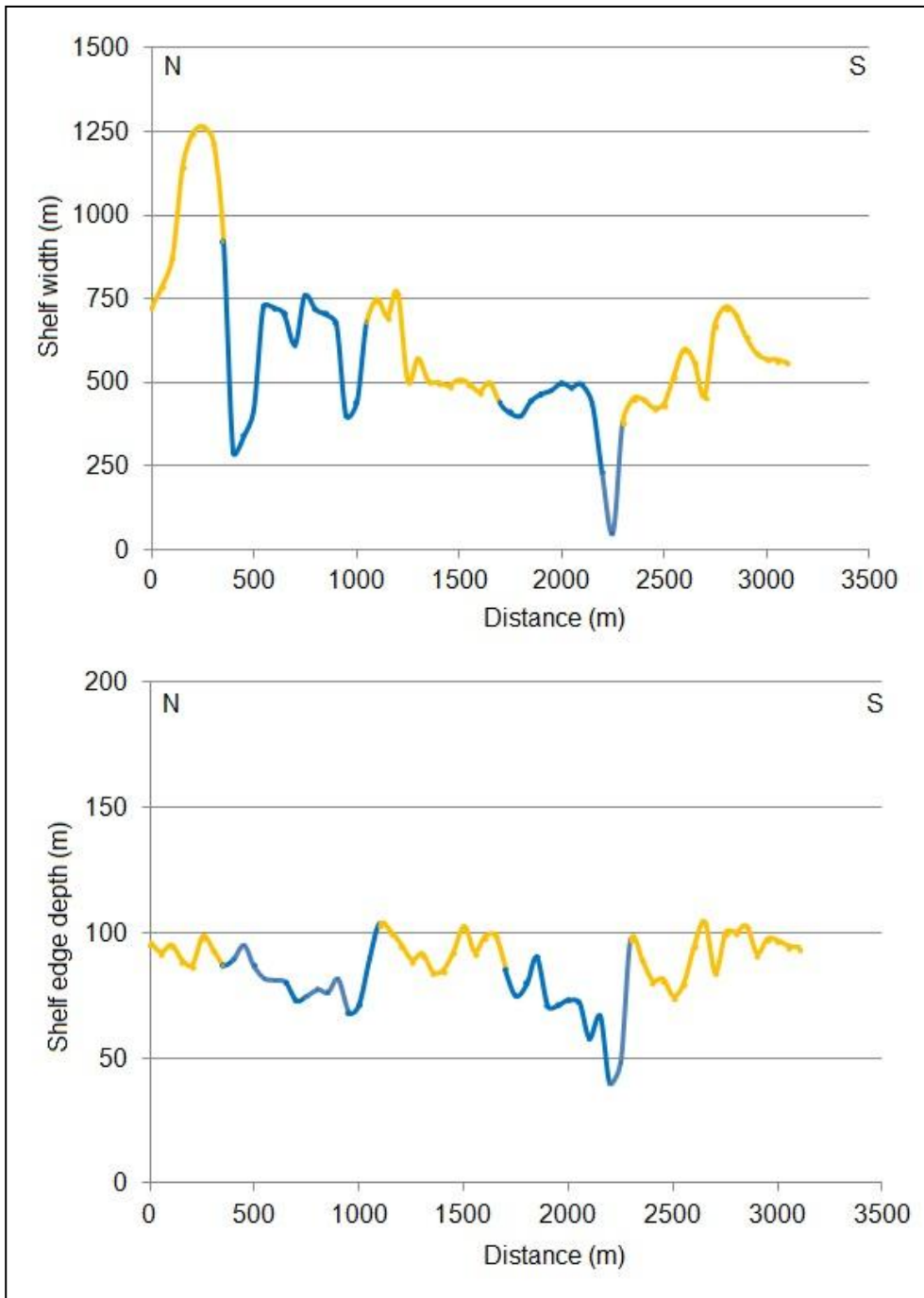
Figure 6.17b. *Graphs showing the shelf width and shelf edge depth for shelf sector 3.*

SECTOR 4

This sector runs aside the Vulcanello composite cone and the northeastern border of La Fossa Cone to Punta Luccia (Figure 6.18), i.e. in correspondence of the products of the youngest volcanic activity of Vulcano island (Figure 6.14). No insular shelf is observed here, but a narrow, sediment-starved shore platform (Figure 6.18) develops down to a maximum depth of 30 m all around Vulcanello (Romagnoli et al., 2013). The same characteristics have been recognized offshore sector 1 at Lipari (see chapter 6.1.1). The age of the products erupted onshore (8ka-AD1890, De Astis et al., 2013) is similar to those erupted at Lipari (8ka-AD1220, Forni et al., 2013), suggesting a

149

common evolution of these sectors. A submarine network of erosive scars and channels affects instead the easternmost portion of this sector (Figure 6.18).
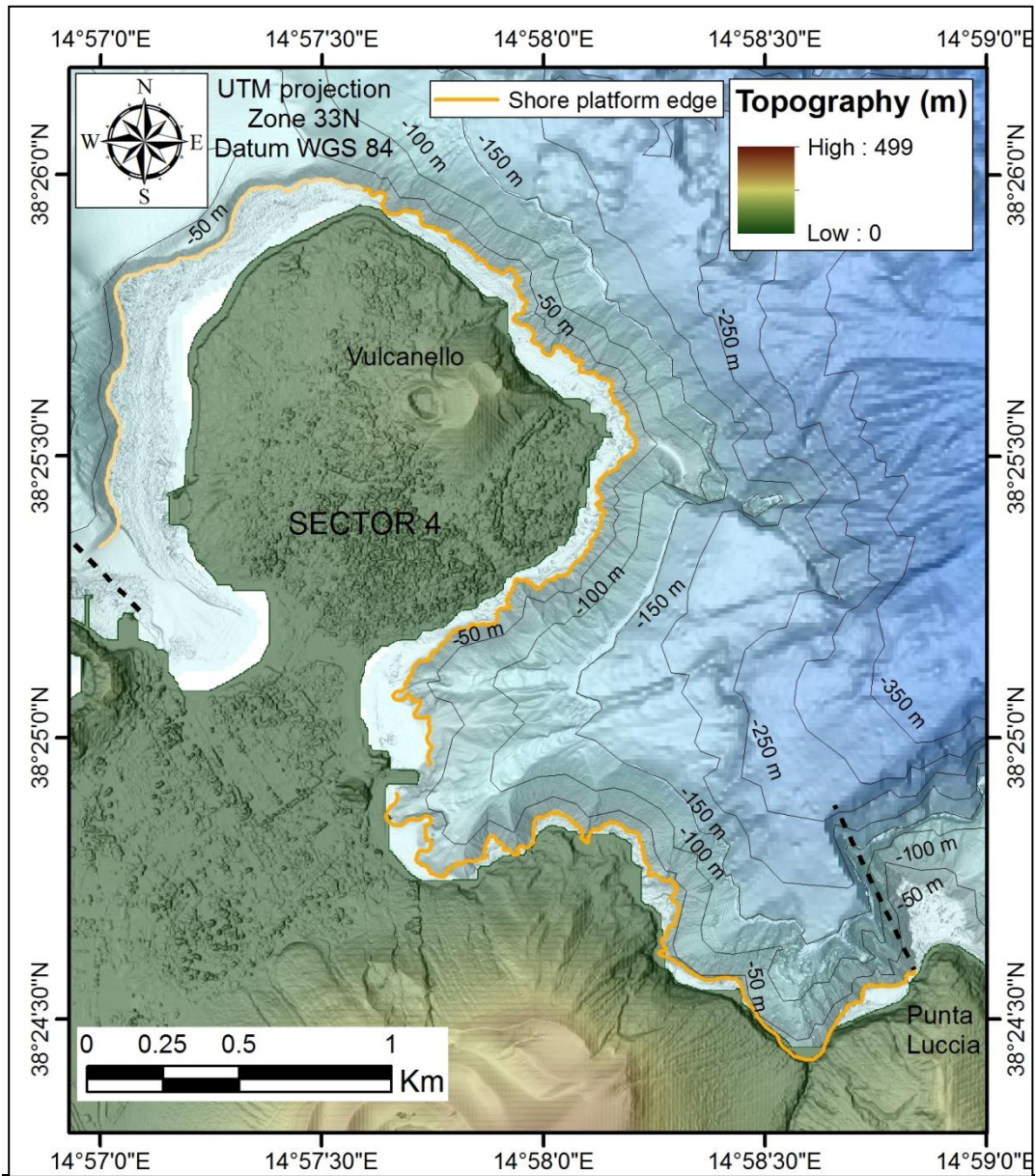
Figure 6.18. *Shaded relief map representing the easternmost portion of shelf sector 4. The black dashed lines represents the limits of the shelf sector 4.*

6.6 The evolution of the shelf around Vulcano

The island of Vulcano is surrounded by relatively narrow shelves (up to c. 1370 m wide, but mostly narrower than 1000 m) compared to that of Salina and Lipari (up to 2100 m wide), in accordance with the younger age of the products onshore. On the base of the occurrence of a well-developed insular shelf offshore the Capo Secco, this latter was already inferred to be the oldest volcanic center of the island (Romagnoli et al., 1989 e 2013; De Astis et al., 2006). Similar value of shelf

widths are observed also off Faro Nuovo and Punta Bandiera, that likely represent the trace (presently submerged) of other eccentric volcanic centres, predating the formation of Primordial Vulcano.

Romagnoli (2013) also inferred the occurrence of an earlier stage of volcanic activity offshore Cala del Formaggio on the base of an "anomalously" wide shelf (up to over 1200 m wide) with respect to a shelf width/age model and compared to the young age of the products cropping out onshore, possibly associated to a "rhyolitic phase" older than the emplacement of the Lentia Domes products. In this work, the systematic analysis of the geomorphic parameters of the shelf highlights the occurrence of a shelf offshore Punta Cala del Formaggio with an erosive edge depth between -74 m and -104 m, likely due to later lava progradation onto an early formed shelf. In fact, post-erosional lava flows can overflow the coast and partly or completely fill the accommodation space created in shallow water by past erosion, creating a "rejuvenated shelf", as observed in some shelf sectors offshore Pico island in the Azores Archipelago (Quartau et al., 2015b).

The shelf edge depth at Vulcano, being mostly c. -100/-125 m, records the sea-level depth during the MIS 2 (Romagnoli et al. 2013). Very small portions of the island exhibit a locally deeper erosive edge located at -135/-145 m, attesting for possible subsidence processes, likely in correspondence with older volcanic centres. However, due the relatively young age of Vulcano it is difficult to verify if this subsidence can be somehow related to the inferred subsidence trend reconstructed in the Central Aeolian Archipelago on the base of deeper shelves as active before MIS 5 (section 6.1.3 and Manuscript III, chapter 5).

7. INSULAR SHELVES IN THE AZORES ARCHIPELAGO: MORPHO-ACOUSTIC CHARACTERIZATION, CONTROLLING FACTORS AND IMPLICATIONS FOR SANTA MARIA ISLAND GEOLOGICAL EVOLUTION

7.1 Santa Maria Island: Manuscript IV

In this study we combined high-resolution bathymetric data and an extensive single-channel seismic dataset with detailed onshore geological field studies performed on Santa Maria Island (Azores Archipelago) to better understand the connection between the onshore and the offshore domains. By analysing the geomorphic parameters of the shelf (shelf width and erosive edge depth) and relating the morphology of the outcrops found on the shelf with those onshore, we provide a simplified geological map of the offshore. Moreover, we studied how varied wave influence, oceanographic/climatic regime and sediment supply influence the development and the distribution of the sedimentary bodies on the shelves. The finding of clear relationships could improve our comprehension on the factors controlling the formation and evolution of such sediments in other high-energy, wave-dominated shelves.

"The interplay between volcanic, tectonic, erosive and sedimentary processes on volcanic islands shelves"

Authors:
- **Alessandro Ricchi** (University of Bologna, Bologna – Italy)
- **Rui Quartau** (Instituto Hidrográfico, Divisão de Geologia Marinha);
  (Universidade de Lisboa, Instituto Geofisico Infante Dom Luiz, Instituto Dom Luiz, Faculdade de Ciências da Universidade de Lisboa, Lisbon, Portugal).
- **Ricardo Ramalho** (University of Bristol, UK)
- **Claudia Romagnoli** (University of Bologna, Bologna – Italy);
  (Istituto di Geologia Ambientale e Geoingegneria, Consiglio Nazione delle Ricerche, Rome – Italy).
- **Daniele Casalbore** (University of Rome – "La Sapienza", Rome – Italy);
  (Istituto di Geologia Ambientale e Geoingegneria, Consiglio Nazione delle Ricerche, Rome – Italy).

Status: in preparation.

VOLCANIC, EROSIONAL, DEPOSITIONAL, TECTONIC AND MASS-WASTING PROCESSES AT SANTA MARIA INSULAR SHELF (AZORES ARCHIPELAGO).

ABSTRACT

Volcanic Ocean islands are often surrounded by shallow and low gradient regions (insular shelves), which can occupy an area bigger than the subaerial part of the islands. These shelves are mainly the result of wave erosion of the subaerial flanks of the islands as sea level fluctuates during glacial and interglacial periods. A detailed mapping of such shelves is useful because their morphology records the original shape of the subaerial islands and their evolution. Correlating the information provided by the onshore studies with the submerged domain is, therefore, fundamental to increase our knowledge regarding the evolution of such islands. Santa Maria Island in the Azores Archipelago is a 6 Ma old ocean-island volcano surrounded by a 135 km^2 shelf, characterized by an history of subsidence, followed by uplift from 3.5 Ma. By analyzing the geomorphic parameters of the insular shelf (such as the shelf width and the erosive edge depth), the island's history of vertical movements and by relating the morphology of the outcrops found on the shelf with those onshore, we integrated the evolutionary history of Santa Maria with particular focus on its earlier stages of growth. Our study provide a simplified geological map of the offshore in which we inferred that the outer part of the northern shelf is carved on units older than the oldest volcanic sequences exposed onland; the western and southern shelves are almost entirely carved in the products of the oldest shield volcano (Anjos Volcanic Complex), while the eastern shelf is the youngest in formation, being related to units of the Pico Alto volcanic complex. We also discussed distribution of sediments on the shelf. High wave energy concomitant with sea level drops contributed to the transport of older sequences offshore, which were ultimately lost to the slopes of the island. Presently, wide shelves contribute to waves reaching the cliffs with less energy, resulting in less sediment produced to fill such large accommodation spaces. The shelf edges around Santa Maria have several small scours, probably the head of a submarine drainage of the slopes of the island. On the southern and eastern shelves, these mass-wasting features are mostly controlled by tectonics since the extension of faults and lineaments can be followed from onshore to the shelf edge. On the northern shelf mass-wasting appears to be correlated with presence of unstable sediments on the shelf edge that triggered the landsliding.

INTRODUCTION

The subaerial and submarine morphology of volcanic islands results from the interplay between volcanic, tectonic, erosive and depositional processes acting at different time-scales (Ramalho et al., 2013; Casalbore et al., 2015; Casalbore, 2018; Lebas et al., 2018; Quartau et al., 2018a;). These processes and their influence on the geomorphology are very well known for the subaerial portions of volcanic islands (Thouret, 1999). However, volcanic islands are mostly developed beneath the sea; hence the study of their submarine areas can provide much more information than the subaerial parts, which constitute only the "tip of iceberg" (e.g., Romagnoli et al., 2013;

Chiocci et al., 2013; Quartau and Mitchell, 2013; Quartau et al., 2015a). Most part of submarine studies were mainly addressed to reconstruct large-scale instability processes that commonly affect the flank of these edifices (Mitchell et al., 2002; Ohler et al., 2008; Casalbore et al., 2011). On the contrary, less attention has been paid on the impact of volcanism, erosion, tectonics, time-variant sediment supply and climatic/oceanographic conditions on the surrounding shelf and the link with the geology onshore. Only in the last decade, a growing number of nearshore marine surveys performed with high-resolution multibeam and seismic reflection systems revealed the importance of insular shelf studies to obtain a more detailed picture of the geological history of volcanic islands (Romagnoli et al., 2013; Quartau et al., 2012, 2014, 2015 and 2016; Romagnoli et al., 2018; Casalbore et al., 2018). Insular shelves surrounding volcanic islands are, in fact, representative of their original extension during glacial maxima, thus playing a potential role for palaeo-morphological and relative age reconstructions as well as for evaluating the vertical mobility of such areas. Geomorphic parameters such as the shelf edge depth and shelf width, as well as the morphology of the submerged lava flows or rocky outcrops, provide useful insights concerning the original morphology of the volcanic edifices, and the occurrence of older or younger than expected volcanic activity not recorded onshore.

In this study, we combined high-resolution bathymetric data and an extensive single-channel seismic dataset with detailed onshore geological field studies performed on Santa Maria Island (Azores Archipelago) to better understand the connection between the onshore and the offshore domain. Inferences on the contribution of tectonics, wave regime, volcanism, erosion and sediment supply in shaping the insular shelf are provided. Moreover, through the analysis and comparison of the shelf width, edge depth and morphology for each sector of the island, an evolutionary model for the submerged portion of Santa Maria is derived, integrating that already proposed for the island by Ramalho et al. (2017).

2. GEOLOGICAL SETTING

2.1 THE AZORES ARCHIPELAGO

The Azores Archipelago is located in the North Atlantic Ocean, across the Mid Atlantic Ridge (MAR in Fig. 1) separating the westernmost group of islands from the central and easternmost groups. Volcanism here results from the interaction between the triple junction of the Eurasian, Nubian and American lithospheric plates and a hotspot (Lourenço et al., 1998; Gente et al., 2003, Miranda et al., 2017). The complex interaction between the seafloor spreading forces driven by the Mid Atlantic Ridge and the right-transtensional movements associated with the Nubian/Eurasian plate's boundary dominates the area (Hipólito et al., 2013; Marques et al., 2013; Madeira et al., 2015). Santa Maria sits on a roughly triangular shaped area located between the Nubian/European plate boundary (the active Terceira Rift, TR in Fig. 1) and the presently inactive East Azores Fracture Zone (EAFZ in Fig. 1), most likely already outside the influence of the Nubian/European plate boundary (Miranda et al., 2018).

Being under an oceanic regime, the coastlines of the Azores Archipelago are frequently subjected to high wave energy. Waves in the Azores have average significant height (H_s) between 2.5 m and 3.1 m mainly from NW (29%), W (24%) and N (16%) (Quartau et al., 2012). Moreover,

84 violent storms are quite frequent, striking the archipelago, on average, every seven years
85 (Andrade et al., 2008) with maximum wave height greater than 20 m (Rusu and Guedes Soares,
86 2012).
87
88 *2.2 GEOLOGY OF SANTA MARIA ISLAND*
89 Santa Maria rises from -2500 m and it is considered the oldest of the Azores Archipelago, since it
90 has emerged from the sea c. 6 Ma ago (Ramalho et al., 2017). The eastern (leeward) side of the
91 island exhibits a rugged morphology, culminating in the Pico Alto high (587 m in elevation, Fig. 2).
92 The coastline is made of up to 250-300 m high plunging cliffs, randomly displaying wave-cut
93 notches at varying elevations. On the contrary, the western (windward) side has a typical staircase
94 morphology due to the occurrence of a number of raised marine terraces from 7 m to 200 m in
95 height (Ramalho et al., 2017).
96   Offshore, Santa Maria is surrounded by a wide insular shelf, in particular along the northern
97 coastal sector (up to 8 km wide), in contrasts with narrower shelves at the western, southern and
98 eastern sides (~2 km). Five sets of submerged marine terraces have been recognized on the shelf
99 (Ricchi et al., 2018), reflecting the interplay between the island's vertical movements and sea-level
100 fluctuations.
101   The volcanic history of Santa Maria is the result of the activity of different overlapping
102 volcanoes, interrupted by relative long periods of quiescence (Ramalho et al., 2017). The products
103 of the Cabrestantes and Porto Formations on the westernmost side of the island (Fig. 2), emplaced
104 by surtseyan and strombolian activity, witness the first emergence of the island c. 6 Ma ago. The
105 products of the Anjos Volcanic Complex are widespread in central and western island,
106 representing the remnants of large shield volcano formed between 5.8 Ma and 5.3 Ma (Fig. 2). The
107 following 1 Ma was mostly characterized by marine erosion that caused the partial dismantling,
108 and possibly submersion of the previously formed shield volcano. Simultaneously, low-volume
109 submarine volcanism mainly focused on the eastern portion of the island, culminated in the
110 emplacement of the Touril Volcano-sedimentary Complex (Fig. 2). This period also saw the onset
111 of a subsidence trend (c. 100 m/Myr on average) that lasted until 3.5 Ma and is reflected by the
112 numerous passage zones of Pico Alto and Anjos lava deltas and the transgressive sequences of
113 Touril complex showing a deeping-up sequence (Ramalho et al., 2017). Widespread volcanic
114 activity begun c. 4.1 Ma promoting the re-emergence of the island edifice. The products of the
115 Pico Alto volcanic complex (Fig. 2) correspond to the lateral growth of the edifice due to lava delta
116 progradation over Touril marine sediments and the eroded remains of the Anjos edifice.
117 Subsidence reversed into uplift at 3.5 Ma (estimated at c. 59 m/Myr from 3.5 to 2.14 Ma, 42
118 m/Myr from 2.14 to present, Ricchi et al., 2018), as attested by the occurrence of marine terraces
119 on the western side of the island (Ramalho et al., 2017) and offshore. Although the last stage of
120 the island evolution is considered mainly erosional, from 3.2 to 2.8 Ma a low volume magmatic
121 and hydromagmatic activity led to the formation of the cones of the Feteiras Formation (Fig. 2).
122   Tectonics is expressed onshore by the main NW–SE-, N-S and NE–SW-trending faults (Fig. 2,
123 Madeira et al., 2015) that partly influenced the development of the subaerial terraces. Some of
124 these faults have been also recognized offshore, affecting the distribution of the submerged
125 terraces on the shelf (Ricchi et al., 2018). Moreover, Zbyszewski and Ferreira (1960) and

126 Serralheiro et al. (1987) reported a large set of N 045° and N 150° striking dikes located mostly in
127 the SW and NE portion of the island (Fig. 2), being likely contemporaneous to the main building
128 stages of the island.
129
130 *3.MATERIAL AND METHODS*
131
132 *3.1 DATA ACQUISITION AND PROCESSING*
133 The mapping of the insular shelf around Santa Maria Island has been carried out onboard the R/V
134 Arquipélago from 24th August to 15th September 2016 in the scope of PLATMAR project
135 (*Development of volcanic island shelves: insights from Sta. Maria Island and implications on hazard*
136 *assessment, habitat mapping and marine aggregates management"*). The survey included the
137 acquisition of multibeam bathymetry and single-channel seismic profiles (boomer) between c. -20
138 m and c. -250 m (Fig. 3). Further details of the geometry acquisition and equipment are reported
139 by Ricchi et al. (2018). The subaerial DTM is generated from a 1/5000 scale digital altimetric
140 database with a resolution of 5 m. The integrated analysis of the multibeam bathymetry and
141 subaerial topography has been mainly used to study the morphology of the shelf and to map the
142 volcanic, structural, erosional and depositional features, comparing with those of the
143 corresponding onshore sectors. The shelf width and the erosive edge depth values in each sector
144 were determined from the seismic profiles collected perpendicular to the coastlines (Fig. 3) and
145 reported in graphs in order to constrain its variability along the shelf. Since later mass wasting of
146 the shelf edge can cause a landward shift of that feature, we always took into account in our
147 interpretation the maximum depth values, which represent the original depth at which waves cut
148 the island subaerial flanks.
149   Seismic reflection profiles were recorded using an AA200 boomer plate (300 Hz to 6.5 KHz, -6
150 dB), applying a shooting rate between 250 ms and 500 ms, while the recording length was
151 comprised between 240 ms and 490 ms, depending on the water depth. The initial .TRA format
152 has been converted into SEG-Y in order to process the seismic profiles using the IXBLUE DELPH
153 SEISMIC INTERPRETATION software v4.0. The analysis of seismic reflection profiles allowed
154 mapping the distribution and thickness of the unconsolidated sediments lying on the shelf of Santa
155 Maria Island. For time/depth conversion we used a sound velocity of 1500 m/s in the water
156 column and 1800 m/s inside the sediments. Sound velocity is based on data for coarse sands of
157 Hamilton and Bachman (1982), which in the Azorean shelves are the dominant grain-size (Quartau
158 et al., 2012; 2015b) .In each seismic profile we picked two reflectors corresponding to the seafloor
159 and, where present, the bottom of the sedimentary cover, respectively.
160
161 *4. THE INSULAR SHELF AROUND SANTA MARIA ISLAND*
162
163 *4.1 NORTHERN SHELF SECTOR*
164 This sector is located offshore the northern coast of the island from Ponta do Norte to Baía do Mar
165 da Barca (Fig. 4a). The ENE-WSW oriented coastline has a strongly irregular profile characterized
166 by embayments and promontories. From Ponta do Norte to Ponta dos Frades sea cliffs are steep,
167 up to 200 m high, and were cut in the products of the Anjos Volcanic Complex at the base,

156

168 overlapped by those of Touril Volcano-sedimentary and Pico Alto Volcanic Complex (see Fig. 2).
169 From Ponta dos Frades to Baía do Mar da Barca, cliffs are entirely carved in the products of the
170 Anjos Volcanic Complex and their height progressively decreases westwards to ~20-30 m. The
171 entire shelf has a rough trapezoidal shape and shows a different morphology between the eastern
172 and the western sides, similarly to the asymmetric topography of the island. To the east of Baía da
173 Cré the shelf width varies between 6 km and 8 km, while to west is narrower being c. 4 km wide
174 (not considering the sector where the submarine cone of Baixa do Ambrósio is located, Figs. 4a
175 and 4b). The maximum depth of the erosive shelf edge in this sector is c.-170 m on the
176 northwestern portion (off Baía do Mar da Barca, Figs. 4a and profile aa' Fig. 5), then it slowly
177 decreases to a maximum value of -156 m the east (Fig. 4a and 4b). Here lower values can be found
178 (c.-115 m) in correspondence of scars affecting the shelf edge.

179   To the west of Baía da Cré rocky outcrops have been recognized down to 80-100 m depth,
180 being mostly located in the inner to middle shelf, while to the east the entire shelf is dominated by
181 rocky outcrops with sub-conical and articulated morphological highs. A total of 17 sub-conical
182 structures were recognized from c. -70 m to c. -120 m on this shelf sector. These positive
183 morphological features show a random arrangement on the shelf and exhibit different size and
184 morphology. We mostly recognized single cones, with circular to elliptical morphology, a basal
185 diameter from c. 250 m to c. 1 km and height comprised between c. 20 m and c. 40 m. Other
186 cones, located on the easternmost portion of this shelf sector (Fig. 4a), are flat-topped and show a
187 sub-circular morphology (c. 600 m in diameter, around 15 m high), with a sharp conical feature in
188 the centre, or show a ring-like morphology with an internal depressed area covered by sediments.
189 A larger cone (Baixa do Ambrosìo, 1.3 km in diameter and about 130 m high) has been identified
190 on the westernmost portion of this shelf sector. This is a pillow cone whose flanks are cut by
191 marine terraces located at different depths (Ricchi et al., 2018).

192   Sharp linear escarpments, ranging in heights from c.10 m to c.30 m, dissect the portion of the
193 inner shelf located to the west of Baía da Cré in three compartmented blocks (Fig. 4a). These
194 lineaments, 2 to 2.7 km long, can be followed from shallow water down to -100 m, where they
195 apparently disappear in an area characterized by an overall smooth morphology. Offshore
196 continuation of these lineaments are possibly represented by a sharp escarpment that dissects a
197 rocky outcrop located to the south of Baixa do Ambrosio at c.-130/-170 m (extension of AjL in Fig.
198 4a) and by a narrow gully head, located offshore the Anjos Fault at -135 m (extension of CF in Fig.
199 4a). To the east, another lineament (Raposo Fault, RF in Fig. 4a) can be also apparently followed
200 offshore in a linear escarpment c. 2 km long, down to -50 m.

201   Ricchi et al. (2018) identified on the northern shelf a sequence of submerged marine terraces
202 with their inner margin located at approximately -40/-50 m, -70/-80 m, -85/-90 m, -100/-110 m
203 and -120/-140 m. Terrace width vary between 0.4 km and 0.9 km and their distribution is also
204 conditioned by the sharp morphological difference between the NE and NW area of the shelf and
205 by the linear escarpments, which apparently controlled the distribution of the shallower terraces.

206   Sediments are mostly restricted to the outer shelf in the NW area and in-between the rocky
207 outcrops in the NE area (Fig. 6). Deposits are normally very thin (mostly between 0 and 2 m, Fig.
208 6), being locally thicker (up to 14 m) on local depocenters (e.g., in a NW-SE oriented small basin,

157

209 located offshore Baia da Cré, and in the ENE-WSW oriented basin bordered by two sub-vertical
210 escarpments offshore Ponta do Norte, Figs. 4a, 7a and 7b).

211

212 *4.2 WESTERN SHELF SECTOR*
213 This sector is located offshore the western coast of the island from Baía do Mar da Barca to Ilhéu
214 da Vila (Fig. 8a). The coastline is NNW-SSE oriented with sub-vertical sea cliffs up to 75 m high,
215 entirely carved in the subaerial lava flows and pyroclastic succession of the Anjos Volcanic
216 Complex (Fig. 2). The shelf runs parallel to the coastline and is generally rocky down to c. -50/-70
217 m. Offshore Campo Grande a WNW-ESE trending strip around 1.7 km long and c. 150 m wide
218 separates the shelf in two parts characterized by different width (c.1 km to the north, c.2 km to
219 the south). In this sector the erosive shelf edge is generally at -100/-110 m along the northern
220 portion, whilst in the central and southernmost part its depth increases to -135/-147 m (Figs. 8a,
221 8b and profile dd' in Fig. 9). However, offshore Ponta do Poção the shelf edge has also been locally
222 affected by mass wasting, shallowing its depth up to -50 m.

223   The lineament located offshore Campo Grande exhibits an arc-shaped escarpment dissected by
224 a set of WNW-ESE and WSW-ENE dikes (Zbyszewsky and Ferreira, 1960) and the Campo Grande
225 fault (CgF in Fig. 8a, Madeira et al., 2015).

226   Marine terraces are also present in this sector of the shelf, despite not the all set (Ricchi et al.,
227 2018). Terrace width (< 200 m) is much smaller than in the northern shelf.

228   Sediments are almost absent on the western shelf. Some scattered patches have been
229 recognized at -100/-120 m and inside the WNW-ESE oriented lineament offshore Campo Grande
230 (Fig. 6). Here the thickness is less than 5 m in the narrower portion, but increase up to c. 10 m at
231 the shelf edge.

232

233 *4.3 SOUTHERN SHELF SECTOR*
234 This sector is located offshore the southern coast of the island from Ilhéu da Vila to Ponta do
235 Castelo (Fig. 10a). In the western-most portion (to Ponta da Marvão) the coastline is very irregular
236 in plan-view, with cliffs mostly formed by lava flows and pyroclastic products of the Anjos Volcanic
237 complex (Fig. 2). From Ponta da Marvão to Ponta do Malbusca, the coastline has a arcuate shape
238 due to the occurrence of a 5 km-wide bay (Praia Formosa Bay, Fig. 10a), bounded by up to 200 m-
239 high, sub-vertical sea cliffs. These are cut in a sequence comprising the Anjos Volcanic Complex
240 lava flows at the base, overlapped by marine sediments and submarine/subaerial volcanic
241 products of both the Touril and the Pico Alto Volcanic Complexes (Fig. 2). From Ponta da Malbusca
242 to Ponta do Castelo the coastline is made of steep cliffs, carved on the Touril and Pico Alto
243 sequences (Fig. 2).

244   The southern shelf has an irregular morphology, with its edge showing a configuration that
245 roughly mimics the coastline. The westernmost portion of the shelf is around 2 km wide, up to the
246 eastern end of Praia Formosa Bay, after which it is reduced to c.0.7 km offshore Ponta da
247 Malbusca. Eastwards it enlarges again, increasing to up to 2.6 km in width offshore Ponta do
248 Castelo, at the SE edge of the sector (Figs. 10a and 10b). The depth of the erosive shelf edge varies
249 accordingly. South of Ilhéu da Vila it is -135/-140 m; moving eastwards to Praia Formosa Bay it is -
250 80/-90 m, while it is in the range -50/-90 m to Ponta da Malbusca. Then the shelf edge depth

158

251 progressively increases to maximum value of -142 m offshore Ponta do Castelo (Figs. 10a, 10b and
252 profile ee' in Fig. 11).

253   A dense network of NNW-SSE and NNE-SSW trending lineaments, 0.5 km to 2 km long and with
254 escarpments up to 15 m high, dissect the shelf from the coastline down to its edge, creating a
255 succession of rocky structural high interspersed by sediment-covered depressed areas (Figs. 6, 10a
256 and 12). The most evident features are located offshore Vila do Porto, Praia Formosa Bay and
257 Ponta da Malbusca, also having a clear expression onshore (Fig. 10a). Other lineaments show an
258 orientation similar to the dikes recognized onland by Zbyszewsky and Ferreira (1960), (Fig. 10a).
259 Some lineaments appears to control the location of small scars affecting the outer shelf. The
260 distribution of the sediments and their thickness is highly variable being from <6 m (offshore Ilhéu
261 da Vila) up to 15-20 m (offshore Praia Formosa Bay, Figs. 6, 12 and 13). Here the sediments cover
262 most of the shelf, while offshore Ilhéu da Vila and from Ponta do Malbusca to Ponta do Castelo
263 the sediments are situated only on the outer shelf with a gradually increasing thickness towards
264 the shelf edge (Fig. 6).

265

266 *4.4 EASTERN SHELF SECTOR*
267 This sector is located offshore the eastern coast of the island from Ponta do Castelo to Ponta do
268 Norte. The coast is very irregular in plan-view, being characterized by several embayments and
269 promontories, with steep cliffs carved in the submarine and subaerial products of the Pico Alto
270 Volcanic Complex (Fig. 2). The NNW-SSE oriented shelf, runs parallel to the coastline and is c. 1 to
271 c. 2 km wide, being wider offshore Ponta do Castelete and São Lourenço bay (Figs 14a and 14b).
272 The erosive shelf edge depth mostly varying between -90 m and -110 m, apart from areas where it
273 shallows to -50 m, where it is incised by gullies (Figs. 14a and 14b). Rocky outcrops are frequently
274 extended down to the shelf edge, where in places they forms fin-like structures up to few tens of
275 meter high (Figs. 14a and 15a). Besides some small indentations affecting the shelf edge, the
276 eastern sector exhibits only an evident headwall scar that dissects the shelf at c. -70 m offshore
277 Pontinha, in front of a concave cliff on the coast (Fig. 14a).

278   Along the eastern shelf sector the sediments fill some depressions bordered by rocky outcrops
279 and cover the shelf down to c. -70 m, showing a thickness variable from 2 to 15 m (Fig. 6). The
280 southernmost and most extensive sediment accumulation, lying offshore Pontinha (Fig. 6), has an
281 inner prograding geometry (Fig. 15b).

282

283 *5. DISCUSSION*

284

285 *5.1 SEDIMENT DISTRIBUTION ON THE SHELF*
286 On reefless volcanic islands the production of sediments reaching the coast largely depends on the
287 volcanic activity (for instance explosive volcanism produces much more sediments than effusive
288 volcanism), the occurrence of a well-developed subaerial drainage system, wet climate stimulating
289 the subaerial erosion, and high wave energy promoting coastal erosion (Krastel et al., 2001;
290 Ramalho et al., 2013; Quartau et al., 2018a). In particular, on small, oceanic reefless volcanic
291 islands (like Santa Maria), sediment is produced mainly through the retreat of coastal cliffs by
292 wave erosion (Quartau et al., 2012). Thus, on these islands, sediments that result from cliff erosion

159

293 accumulate in the inner shelf and are transported offshore during storms. They tend to fill the
294 accommodation space on the shelf by forming deposits such as the submerged depositional
295 terraces (SDTs hereafter) recognized on the shelf of other volcanic islands (such as in the Aeolian
296 archipelago, see Chiocci & Romagnoli, 2004).

297 At Santa Maria, part of the southern and the northern shelf sectors and the entire eastern shelf
298 sector are backed by high cliffs (up to c. 200-250 m high) belonging to the Touril and Pico Alto
299 volcanic complexes (the youngest volcanic products of Santa Maria, Fig. 2). Moreover, the eastern
300 portion of the island shows a drainage system onshore (Fig. 2). Conversely, the northwestern and
301 the western portions exhibits low cliffs and the subaerial drainage is almost absent. Accordingly,
302 the shelf offshore the western and the northwestern flanks of the island is sediment-starved (see
303 Fig. 6). Most of the sedimentary cover here is on the outer shelf and it is very thin (c. 2 m thick).
304 The shelf sectors backed up by higher cliffs exhibits a wider sedimentary cover. However,
305 sediments account for less than 50 % of the seafloor and are mostly located on the outer shelf. On
306 the nearshore areas the sedimentary cover is thicker, but sediments are mostly accommodated on
307 small fault-controlled basins and offshore stream mouths surrounded by a rocky seafloor (Fig. 6).
308 The fact that nearshore areas are mostly rocky, despite sediments are produced from cliff erosion
309 is puzzling. The Azores archipelago is considered an energetic environment in terms of winds and
310 wave action (Andrade et al., 2008; Quartau et al., 2012; Rusu and Guedes Soares, 2012). Several
311 studies showed that storms are able to produce storm-induced downwelling currents that
312 transport sediments from shallow to deeper areas of the shelf. (Field and Roy, 1984; Tsutsui et al.,
313 1987; Nittrouer and Wright, 1994; Myrow and Southard, 1996; Hernández-Molina et al., 2000;
314 Chiocci and Romagnoli, 2004; Meireles et al., 2013). This sediment distribution pattern is also seen
315 in other islands of the Azores archipelago such as Faial and Pico (Quartau et al., 2012; Quartau et
316 al., 2015b;) This effect is higher on the NW, W and SW shelf sectors because the cliffs are smaller
317 (so less sediment production) but also because these areas are more exposed to the dominant
318 waves. Sediments of the southern and eastern shelf sectors, being on the leeward side of the
319 island are less transported offshore and occur at shallower depths (from -35/-40 m).

320 The shelf around Santa Maria lacks thick sedimentary bodies as those recognized on the
321 Aeolian and Azores archipelagos, where some portions of the shelf are covered by up to 30-40 m
322 thick volcaniclastic sequences (Chiocci & Romagnoli, 2004; Quartau et al., 2012; Casalbore et al.,
323 2017). Being Santa Maria much older and eroded for a longer period of time should not the shelf
324 have thicker deposits? We believe that the thin sediment cover in Santa Maria can be explained by
325 two reasons:

326 1. The weal potential for preservation of depositional sequences in the shelves of volcanic
327 islands. Due to the strong wave regime, sediments tend to be transported offshore. As sea
328 levels falls most of the sediments are transported below the shelf edge, leaving the shelves
329 empty. This cycle goes on and on every time the sea level falls preventing the accumulation
330 of depositional sequences as can be seen on continental shelves (Quartau et al., 2012).

331 2. As shelves widen, not only the space of accommodation increases, but the energy reaching
332 the coastline decreases due to wave attenuation over the shelves (Quartau et al., 2010).
333 Thus, the lower sediment production by cliff retreat and the higher accommodation space
334 explains the thin cover around Santa Maria shelf.

335

336   Only on places where faults and lineaments are present the shelf is covered by thicker deposits.
337 On the western shelf, the only sedimentary body on the inner shelf is recognized offshore Campo
338 Grande (Fig. 6), where the sediment deposition is likely controlled by a sharp tectonic lineament
339 displacing the shelf and creating a depressed area. Likewise, on the northern shelf sector the
340 sedimentary bodies recognized offshore Baia da Cré (up to 12 m thick, Figs. 6 and 7b) and Ponta
341 do Pesqueiro Alto (up to 8 m thick, Fig. 6) are the only ones present on the inner shelf. The
342 depressions created by the seaward extension of NW-SE striking faults (Figs. 4a and 7b) allowed
343 sediments to be deposited and stored. Another sedimentary body that has likely been formed due
344 to local tectonic activity is that recognized offshore Ponta do Norte (Fig. 6). The structural setting
345 of this small basin, with sharp escarpments bordering the sedimentary body, suggests the
346 occurrence of two fault segments that controls the sediment infilling (Fig. 7a). The distribution of
347 the sedimentary bodies in the southern shelf sector also looks partly controlled by tectonic
348 lineaments connected to the faults and dikes recognized onshore, as it occurs offshore Vila do
349 Porto and Ponta do Malbusca (Fig. 6 and 10). Similarly, on the eastern shelf sector, sediments fill
350 depressions and small basins interspersed by rocky outcrops. However, a tectonic control can only
351 be inferred here, since evident lineaments cutting the shelf were not recognized.

352

353 *5.2 MASS WASTING PROCESSES*
354 The subaerial and submerged flanks of volcanic islands are frequently dominated by large-scale
355 sector collapses scars as observed in the Hawaii (Moore et al., 1994), Canaries (Masson et al.,
356 2002), La Reunion (Oehler et al., 2008), Aeolian Archipelago (Romagnoli et al., 2009a and 2009b),
357 Aleutians (Montanaro and Beget, 2011) and Madeira island (Quartau et al., 2018a). At Santa Maria
358 large-scale instability features are absent, similarly to what was recently observed in other
359 Azorean, with exception of Pico Island islands (Casalbore et al., 2015; Chiocci et al., 2013; Costa et
360 al., 2014; Costa et al., 2015; Quartau et al., 2012; 2013; 2014; 2015b;). Local instability processes
361 were identified at the edge of the insular shelf surrounding Santa Maria Island, even if they are
362 mostly concentrated on the northern and southern sectors. The biggest scars are located along the
363 NE shelf edge, between the areas offshore Ponta do Norte and Baía da Cré and exhibit a wide
364 semicircular shape (Fig. 5). Several gully heads, with an elongated shape, are also found at the
365 southern shelf edge, between the areas offshore Vila do Porto and Ponta do Marvão (Fig. 10).
366 These morphological differences might be related to the processes responsible for the formations
367 of the scars. Along the edge of the NE shelf sector, the distribution of the scars is apparently
368 controlled by the distribution of the eroded cones and the rocky outcrops (Figs. 4a and 6). The
369 areas among the cones/outcrops are more erodible, thus representing a possible lithological
370 weakness, and a preferential pathway for sediment reworking. Despite the wide northern shelf
371 preventing the direct stream discharge on the outer shelf and upper slope, during lowstands the
372 shelf around the island was mostly exposed, and sedimentary flows might have reached the steep
373 upper slopes of the islands, carving the head of those "proto-gullies".
374   Conversely, eruptive cones are absent along the southern shelf sector, where the elongated
375 morphology of the scars seem to reflect NE-SW striking structural weakness zones, related to the
376 faults that extend to the south of the island and affect the shelf inducing localized erosion (Fig.

377 10). The same structural control might be inferred for the formation of the narrow scar located at
378 the shelf edge offshore Ponta dos Frades, in the northern shelf sector (Fig. 4a), being probably the
379 continuation of the faults recognized onshore (Madeira et al., 2015) and on the inner shelf (Ricchi
380 et al., 2018). A similar feature can be found on the eastern shelf sector where a likely fault-
381 controlled basin (see Figs. 6 and 14a) coincides with the scar of shelf edge landslide.

382 Hampton et al. (1996) and Locat and Lee. (2002) suggested several mechanisms for landslide
383 triggering. In the case of Santa Maria, it appears that on the southern and eastern shelves, these
384 mass-wasting processes are mostly controlled by tectonics (i.e., earthquakes). On the northern
385 shelf sector, tectonics appears to play a smaller role. On these sites it is more likely that the
386 accumulation of incohesive sediments near the shelf edge might trigger those landslides as
387 suggested by Mazuel et al. (2016) and Quartau et al. (2012; 2018a) promoting shelf edge retreat.
388 On the western, probably due to the scarcity of sediments there are no significant scars.

389

390 *5.3 NEW INSIGHTS ON THE EVOLUTION OF SANTA MARIA ISLAND*

391

392 Here we discuss the evolution of the shelf, based on the analysis of its morphologic parameters
393 (erosive shelf edge depth, shelf width, and morphology, Table 1) and relation with outcropping
394 volcanic units. Generally, on volcanic islands a correspondence between the shelf width and the
395 age of the volcanic products outcropping onland, is found (Menard, 1983). The width/age
396 relationship is associated to the fact that the shelf width increases with increasing time as
397 shorelines retreat with prolonged exposure to marine erosion (Quartau et al., 2010, 2012, 2014;
398 Romagnoli, 2013; Romagnoli et al., 2018). At Santa Maria this relationship can better be observed
399 between the two width/age extremes, the northern shelf (up to c. 8 km), likely carved in the c. 5.8
400 Ma-old Anjos volcanic products, and the eastern shelf (2.3 km), carved in the c. 4.1-3.5 Ma old
401 products of the Pico Alto volcanic Complex (Fig. 2). However, the western shelf shows a
402 dramatically lower width (up to c. 2 km) with respect the northern one (up to c. 8 km), despite
403 both sectors are carved in the Anjos volcanic product and are exposed to the same dominant
404 winds (from W and NW). Remarkably, the western sector shelf is generally narrower than the
405 southern one (2.6 km, also carved in the Anjos volcanic units) and similar to that of the eastern
406 sector (2.3 km). This apparent incongruence can be explained by the paleogeography of the island
407 in its earlier stages of growth. The western side of the subaerial island is an uplifted shelf that, at
408 the onset of the uplift (3.5 Ma), was entirely submerged (Fig. 16) as suggested by presently
409 exposed subaerial marine terraces (Ramalho et al., 2017; Ricchi et al., 2018). The width of the
410 western shelf, if measured from the coastline of 3.5 Ma BP (Fig. 16) is c. 5.5 km in the widest
411 portion.

412 The analysis of the shelf edge depth might also help us in our reconstruction. The erosive shelf
413 edge depth is related to sea level coeval to the shelf formation; therefore this morphological
414 feature can be used as a marker of palaeo sea-level, to assess subsequent vertical movements
415 affecting the volcanic edifice (Quartau et al. 2014; 2016, Romagnoli et al., 2018). Since glacial
416 eustatic sea level never reached depths over -125 m in the last 3.5 Ma (Bintanja and Van de Wal,
417 2008; De Boer et al., 2010), so any shelf sector that is presently located below this depth should
418 have experienced subsidence (Quartau et al., 2014; 2015; 2018b; Romagnoli et al., 2018). At Santa

419 Maria, affected by early subsidence processes that later reversed into uplift (Ramalho et al., 2017),
420 the portions of the shelf exhibiting the deepest erosive edges can be considered the oldest since
421 they underwent the largest submergence after formation, as observed at Salina in the Aeolian
422 Islands (Romagnoli et al., 2018). According to the history of vertical movements reconstructed for
423 Santa Maria (Ramalho et al., 2017; Ricchi et al., 2018), the northwestern shelf sector, being the
424 deepest of all (erosive shelf edge depth at -170 m, Figs. 5a and 5b), can be thus considered the
425 oldest in formation. Deep (>-127 m) shelf edges have been also identified along the central and
426 eastern portion of the northern sector and offshore the western sectors of the island. However, in
427 these shelf sectors the maximum edge depth is -156 m and -147 m respectively (Figs. 4a, 4b, 8a,
428 8b, and 9), indicating that they suffered less subsidence than the northwestern shelf. Being carved
429 in the products of the Anjos Volcanic Complex (Figs. 2 and 17) these shelf sectors might be
430 younger with respect the northwestern portion of the shelf. Along the southern portion, the shelf
431 exhibits a more complex morphology and the shelf edge depth has a strongly irregular trend
432 reaching around -90/-100 m and being locally at -50/-60 m (Figs. 9a and 9b). The deeper shelf edge
433 offshore Ilhéu da Vila and Ponta do Castelo (-135/-142 m see Fig. 9a and 9b) is in agreement with
434 the inferred subsidence processes experienced by the island and the relatively old age of this shelf
435 sector. The depth of the shelf edge (c. -142 m) is comparable to the maximum depth along the
436 western sector (-147 m, Figs. 8a and 8b), suggesting that the south-eastern portion of Santa Maria
437 could be as old as the western portion of the island. The sharp decrease in shelf width and edge
438 depth just east of Ponta do Castelo, in the southern sector, and east of Ponta do Norte in the
439 northern sector (Figs. 4a and 14a) might be related to the occurrence of the limit between the
440 products belonging to the older Touril and Anjos Volcanic Complexes respectively and younger
441 Pico Alto Volcanic Complex (Fig. 17). We can infer that the relatively shallow depth of the edge
442 (maximum depth c. -100 m, Figs. 14a and 14b) is due to younger age of the shelf, which was likely
443 carved at the end of the subsidence trend, i.e. about 3.5 Ma. The association of the eastern shelf
444 sector to the Pico Alto products is also supported by the occurrence of the eroded foresets at the
445 shelf edge (Fig. 15a), which mimics the steeply dipping foresets units of lava fed deltas extended
446 from the passage zone (located at c. 130 m in elevation) to the sea-level (Ramalho et al., 2017).
447 When looking at the morphology of the NW inner shelf we see that there are, from Baía do Mar da
448 Barca to Baía da Cré, a ~3 km wide belt of flat rocky outcrops (Figs. 4a and 8a), very similar to
449 those that we see on the western shelf, so most likely carved on Anjos Volcanic Complex. We
450 believe that offshore those rocky outcrops lies also an older part of the island, probably older than
451 the products of the Anjos Volcanic Complex. This limit cannot be followed much eastwards by the
452 profusion of cones recognized in this portion of the shelf. Although the cones cannot be directly
453 linked with any past volcanic activity due to the lack of dating, they might be considered the
454 remnants of larger edifices, eroded during subsequent sea-level changes, as attested by the sub-
455 rounded morphology of the shelf around the cones (Fig. 4a) and the evidence of erosion on their
456 flanks. We believe these cones belong to the Anjos Volcanic Complex and are covering a "proto-
457 Santa Maria island" (Fig. 17) that consists on the of the outer northern shelf. The fact that all the
458 northern shelf east of Baixa do Ambrosio is at maximum depths of -156 m might be explained by
459 the progradation of Anjos to the north shallowing the edge of this older part of the island. The
460 occurrence of an older volcanic edifice offshore the northern portion of the island has already

163

461 been inferred by Ramalho et al. (2017). In our reconstruction the pillow cone of Baixa do Ambrósio
462 is not associated to any of the volcanic complex making up Santa Maria Island. The lack of dated
463 samples does not allowed us to make any inference regarding its earlier growth. The depth of its
464 top (c. -50 m) suggests that probably it is younger with respect the rest of the northern shelf
465 sector; otherwise it would be a flat-topped cone. On its flanks, Ricchi et al. (2018) recognized a set
466 of submerged marine terraces from -70/-80 m to -120/-140 m. The shallowest terraces located at -
467 70/-80 m are also the oldest and were likely carved at least since 866 ka (Ricchi et al., 2018),
468 suggesting that the cone can slightly older than this age.
469
470 *CONCLUSIONS*
471
472 The morphologic analysis of the shelf surrounding Santa Maria Island complemented with the
473 known geological historical of the subaerial island allowed us to improve our understanding of the
474 island's evolution and the processes which have shaped its shallow submerged portions.
475 The shelves surrounding Santa Maria are sediment starved. A little more than 50% of the shelf is
476 rocky and sediment thickness is on average less than 2 m. The few depocenters up to 14 m thick
477 are fault-controlled-basins. The lack of thicker and older deposits that should have accumulated by
478 erosion of the subaerial flanks of the island are related with the high wave energy in the Azores
479 and the ciclicity of sea level changes. High wave energy tend to transport sediments offshore and
480 during sea level falls the sediments that normally accumulate on the shelf are swept offshore until
481 they are lost to the slopes when they cross the shelf edge. In the present-day since shelves are
482 wide, waves attenuate when crossing them and attack with smaller energy the cliffs. Not only few
483 sediments are produced but also the high accommodation space (wide shelves) prevents having
484 thicker deposits as found on other Azorean islands.
485 Small mass-wasting features were found on the shelf edge of Santa Maria. These are mostly
486 restricted to the northern and southern shelves, with only one evident scar on the eastern shelf.
487 However, different processes appear to be responsible for such features. On the southern and
488 eastern shelf sectors, tectonics controls the mass-wasting processes, with faults extending to the
489 offshore and reaching the shelf break. On the northern and western shelves, accumulation of
490 unconsolidated sediments near the edge are probably the triggering factor.
491 Based on the analysis of the shelf geomorphic features (shelf width, erosive shelf edge depth and
492 morphology) and the volcanic sequences outcropping on the island, we were able to extend those
493 sequences to the shelf. We suggest that given the wide extension of the northern shelf, its outer
494 part belongs to an older and undated volcanic sequence of Santa Maria that predated the
495 Cabrestantes and Porto Formations. Most of the mid-to inner northern shelf, western and
496 southern shelf is probably carved on the products of Anjos Volcanic Complex, while the eastern
497 shelf results from erosion of the products of Pico Alto Volcanic Complex. The present-day narrow
498 width of the western shelf, when compared with the more protected to wave erosion southern
499 and eastern shelves can be explained by the uplift mechanism that raised part of the western shelf
500 changing a ~5.5 km wide shelf into a ~2 km wide one.
501
502

503 *REFERENCES*

504

505 Andrade, C., Trigo, R.M., Freitas, M.C., Gallego, M.C., Borges, P., Ramos, A.M., 2008. Comparing
506 historic records of storm frequency and the North Atlantic Oscillation (NAO) chronology for the
507 Azores region. The Holocene 18, 745-754.

508 Bintanja, R., van de Wal, R.S., 2008. North American ice-sheet dynamics and the onset of 100,000-
509 year glacial cycles. Nature 454 (7206), 869–872. https://doi.org/10.1038/ nature07158.

510

511 Casalbore, D., Chiocci, F.L., Scarascia Mugnozza, G., Tommasi, P., Sposato, A., 2011. Flash-flood
512 hyperpycnal flows generating shallow-water landslides at Fiumara mouths in Western Messina
513 Straits (Italy). Mar. Geophys. Res. 32, 257e271.

514

515 Casalbore, D.; Bosman, A.; Romagnoli, C.; Chiocci, F.L., 2014 Large-scale seafloor waveforms on the
516 flanks of insular volcanoes (Aeolian Archipelago, Italy), with inferences about their origin. Mar.
517 Geol., 355, 318–329.

518

519 Casalbore, D., Romagnoli, C., Pimentel, A., Quartau, R., Casas, D., Ercilla, G., Hipólito, A., Sposato,
520 A., Chiocci, F.L., 2015. Volcanic, tectonic and mass-wasting processes offshore Terceira Island
521 (Azores) revealed by high-resolution seafloor mapping. Bull. Volc. 77, 1-19.

522 Casalbore, D.; Falese, F.; Martorelli, E.; Romagnoli, C.; Chiocci, F.L. 2017a. Submarine depositional
523 terraces in the Tyrrhenian Sea as a proxy for paleo-sea level reconstruction: Problems and
524 perspective. Quat. Int., 439, 169–180.

525

526 Casalbore, D., 2018. Volcanic Islands and Seamounts, in: Micallef, A., Krastel, S., Savini, A. (Eds.),
527 Submarine Geomorphology. Springer International Publishing, Cham, pp. 333-347.

528 Casalbore, D., Romagnoli, C., Adami, C., Bosman, A., Falese, F., Ricchi, A., Chiocci, F., 2018.
529 Submarine Depositional Terraces at Salina Island (Southern Tyrrhenian Sea) and Implications on
530 the Late-Quaternary Evolution of the Insular Shelf. Geosciences 8, 20.

531 Chiocci, F.L., D'Angelo, S., Romagnoli, C., 2004. Atlas of Submerged Depositional Terraces Along
532 the Italian Coasts. In: Memorie Descrittive della Carta Geologica d'Italia, vol. 58.

533

534 Chiocci, F.L., Romagnoli, C., Casalbore, D., Sposato, A., Martorelli, E., Alonso, B., Casas, D., Conte,
535 A.M., Di Bella, L., Ercilla, G., Estrada, F., Falese, F., Farran, M., Forleo, V., Frezza, V., Hipolito, A.,
536 Lebani, A., Maisto, F., Pacheco, Pimentel, J.A., Quartau, R., Roque, C., Sampaio, I., Santoro, P.C.,
537 Tempera, F., 2013. Bathymorphological setting of Terceira island (Azores) after the FAIVI cruise.
538 Journal of Maps 9, 590e595.

539

540 De Boer, B., Van De Wal, R.S.W., Bintanja, R., Lourens, L.J., Tuenter, E., 2010. Cenozoic global ice-
541 volume and temperature simulations with 1-D ice-sheet models forced by benthic 18O records.
542 Ann. Glaciol. 51 (55), 23–33.

544 Field, M.E., Roy, P.S., 1984. Offshore transport and sand-body formation: evidence from a steep,
545 high energy shoreface, southeastern Australia. J. Sediment. Petrol. 54 (4), 1292–1302.

547 Gaspar, J. L., Queiroz, G., Ferreira, T., Medeiros, A. R., Goulart, C. & Medeiros, J. 2015. Earthquakes
548 and volcanic eruptions in the Azores Region: geodynamic implications from major historical events
549 and instrumental seismicity. In: Gaspar, J. L., Guest, J. E., Duncan, A. M., Barriga, F. J. A. S. &
550 Chester, D. K. (eds) Volcanic Geology of Sa˜o Miguel Island (Azores Archipelago). Geological
551 Society, London, Memoirs, 44, 33–49, http://doi.org/10. 1144/M44.4.

553 Gente, P., Dyment, J., Maia, M., and Goslin, J., 2003, Interaction between the Mid-Atlantic Ridge
554 and the Azores hotspot during the last 85 Myr: Emplacement and rifting of the hot spot–derived
555 plateaus: Geochemistry Geophysics Geosystems, v. 4, no. 10, p. 8514, doi: 10 .1029
556 /2003GC000527 .

558 Hernández-Molina, F.J., Fernández-Salas, L.M., Lobo, F., Somoza, L., Díaz-del-Río, A., Dias, J.M.,
559 2000. The infralittoral prograding wedge: a new large-scale progradational sedimentary body in
560 shallow marine environments. Geo-Mar. Lett. 20, 109–117.

562 Hampton, M. A., H. J. Lee, and J. Locat (1996), Submarine landslides, Rev. Geophys., 34, 33–59,
563 doi:10.1029/95RG03287.

565 Hipólito, A., Madeira, J., Carmo, R., and Gaspar, J.L., 2013, Neotectonics of Graciosa Island
566 (Azores): A contribution to seismic hazard assessment of a volcanic area in a complex geodynamic
567 setting: Annals of Geophysics, v. 56, no. 6, p. S0677.

569 Krastel, S., Schmincke, H.-U., Jacobs, C.L., 2001. Formation of submarine canyons on the flanks of
570 the Canary Islands. Geo Mar. Lett. 20, 160–167.

572 Lebas, E., Friant, A.L., Deplus, C., Voogd, B., 2018. Understanding the Evolution of an Oceanic
573 Intraplate Volcano From Seismic Reflection Data: A New Model for La Réunion, Indian Ocean. J.
574 Geophys. Res. Solid Earth 123, 1035-1059.

575 Locat, J., and H. J. Lee (2002), Submarine landslides: Advances and challenges, Can. Geotech. J.,
576 39(1), 193–212, doi:10.1139/t01-089.

578 Lourenço, N., Miranda, J.M., Luís, J.F., Ribeiro, A., Victor, L.M., Madeira, J., Needham, H., 1998.
579 Morpho-tectonic analysis of the Azores Volcanic Plateau from a new bathymetric compilation of
580 the area. Mar. Geophys. Res. 20 (3), 141–156.

581

582   Madeira, J., Brum da Silveira, A., Hipólito, A., and Carmo, R., 2015, Active tectonics along the

583   Eurasia-Nubia boundary: Data from the central and eastern Azores Islands, *in* Gaspar, J.L., Guest,

584   J.E., Duncan, A.M.

585

586   Marques, F.O., Catalão, J.C., DeMets, C., Costa, A.C.G., and Hildenbrand, A., 2013, GPS and

587   tectonic evidence for a diffuse plate boundary at the Azores triple junction: Earth and Planetary

588   Science Letters, v. 381, p. 177–187, doi: 10 .1016 /j .epsl .2013 .08 .051.

589

590   Masson, D.G., Watts, A.B., Gee, M.J.R., Urgeles, R., Mitchell, N.C., Le Bas, T.P., Canals, M., 2002.

591   Slope failures on the flanks of the western Canary Islands. Earth Sci. Rev. 57 (1–2), 1–35.

592

593   Mazuel, A., Sisavath, E., Babonneau, N., Jorry, S.J., Bachèlery, P., Delacourt, C., 2016. Turbidity

594   current activity along the flanks of a volcanic edifice: the Mafate volcaniclastic complex, La

595   Réunion Island, Indian Ocean. Sediment. Geol.335, 34–50.

596

597   Meireles, R., Quartau, R., Ramalho, R.S., Rebelo, A.C., Madeira, J., Zanon, V., Ávila, S.P., 2013.

598   Depositional processes on oceanic island shelves – evidence from storm-generated Neogene

599   deposits from the mid-North Atlantic. Sedimentology 60, 1769–1785.

600

601   Menard, H.W., 1983. Insular erosion, isostasy, and subsidence. Science 220, 913–918.

602

603   Miranda, J.M., Luís, J.F., Lourenço, N., 2018. The geophysical architecture of the Azores from

604   magnetic data. In: Küppers, U., Beier, C. (Eds.), Volcanoes of the Azores. Active Volcanoes of the

605   World Springer Verlag, Berlin, pp. 89–100.

606

607   Mitchell, N.C., Dade, W.B., Masson, D.G., 2003. Erosion of the submarine flanks of the Canary

608   Islands. J. Geophys. Res. 108 (3–1–3–11).

609

610   Montanaro C, Beget J (2011) Volcano collapse along the Aleutian Ridge (western Aleutian Arc). 734

611   Nat Haz Earth Sys Sci 11:715–730.

612

613   Myrow, P.M. and Southard, J.B. (1996) Tempestite deposition. J. Sed. Res., 66, 875–887.

614

615   Oehler JF, Lénat JF, Labazuy P (2008). Growth and collapse of the Reunion Island volcanoes. Bull

616   Volcanol 70:717–742.

617

618   Piper, D.J.W., Normark, W.R., 2009. Processes that initiate turbidity currents and their influence on

619   turbidites: a marine geology perspective. J. Sediment. Res.79, 347–362.

620

621   Quartau, R., Tempera, F., Mitchell, N.C., Pinheiro, L.M., Duarte, H., Brito, P.O., Bates, R., Monteiro,

622   J.H., 2012. Morphology of the Faial Island shelf (Azores): The interplay between volcanic,

623 erosional, depositional, tectonic and mass-wasting processes. Geochem. Geophys. Geosyst., 13,
624 Q04012, doi:10.1029/2011GC003987.

625 Quartau, R., Mitchell, N.C., 2013. Comment on "Reconstructing the architectural evolution of
626 volcanic islands from combined K/Ar, morphologic, tectonic, and magnetic data: The Faial Island
627 example (Azores)" by Hildenbrand et al. (2012) [J. Volcanol. Geotherm. Res. 241-242 (2012) 39-
628 48]. J. Volcanol. Geotherm. Res. 255, 124-126.

629 Quartau, R., Hipólito, A., Romagnoli, C., Casalbore, D., Madeira, J., Tempera, F., Roque, C., Chiocci,
630 F.L., 2014. The morphology of insular shelves as a key for understanding the geological evolution
631 of volcanic islands: Insights from Terceira Island (Azores). Geochem. Geophys. Geosyst. 15, 1801–
632 1826.

633 Quartau, R., Madeira, J., Mitchell, N.C., Tempera, F., Silva, P.F., Brandão, F., 2015a. The insular
634 shelves of the Faial-Pico Ridge: a morphological record of its geologic evolution (Azores
635 archipelago). Geochem. Geophys. Geosyst. 16, 1401–1420.

636 Quartau, R., Hipólito, A., Mitchell, N.C., Gaspar, J.L., Brandão, F., 2015b. Comment on
637 "Construction and destruction of a volcanic island developed inside an oceanic rift: Graciosa
638 Island, Terceira Rift, Azores" by Sibrant et al. (2014) and proposal of a new model for Graciosa
639 geological evolution [J. Volcanol. Geotherm. Res. 284 (2014) 32-45]. J. Volcanol. Geotherm. Res.
640 303, 146-156.

641 Quartau, R., Madeira, J., Mitchell, N.C., Tempera, F., Silva, P.F., Brandão, F., 2016. Reply to
642 comment by Marques et al. on "The insular shelves of the Faial-Pico Ridge (Azores archipelago): A
643 morphological record of its evolution". Geochem. Geophys. Geosyst. 17, 633-641.

644 Quartau, R., Ramalho, R.S., Madeira, J., Santos, R., Rodrigues, A., Roque, C., Carrara, G., Brum da
645 Silveira, A., 2018. Gravitational, erosional and depositional processes on volcanic ocean islands:
646 Insights from the submarine morphology of Madeira archipelago. Earth Planet. Sci. Lett. 482, 288-
647 299.

648 Ramalho, R.S., Quartau, R., Trenhaile, A.S., Mitchell, N.C., Woodroffe, C.D., Ávila, S.P., 2013.
649 Coastal evolution on volcanic oceanic islands: A complex interplay between volcanism, erosion,
650 sedimentation, sea-level change and biogenic production. Earth-Sci. Rev. 127, 140-170.

651 Ramalho, R.S., Helffrich, G., Madeira, J., Cosca, M., Thomas, C., Quartau, R., Hipólito, A., Rovere,
652 A., Hearty, P.J., Ávila, S.P., 2017. Emergence and evolution of Santa Maria Island (Azores)—The
653 conundrum of uplifted islands revisited. Geol. Soc. Am. Bull. 129, 372-390.

654 Ricchi, A., Quartau, R., Ramalho, R.S., Romagnoli, C., Casalbore, D., Ventura da Cruz, J., Fradique,
655 C., Vinhas, A., 2018. Marine terraces development on reefless volcanic islands: new insights from
656 high-resolution marine geophysical data offshore Santa Maria Island (Azores Archipelago). Mar.
657 Geol. 406, 42-56.

658 Romagnoli, C., 2013. Characteristics and morphological evolution of the Aeolian volcanoes from
659 the study of submarine portions, in: Lucchi, F., Peccerillo, A., Keller, J., Tranne, C.A., Rossi, P.L.
660 (Eds.), Geological Society, London, Memoirs, 37, pp. 13-26.

661 Romagnoli C, Casalbore D, Chiocci FL, Bosman A (2009a). Offshore evidence of large-scale lateral
662 collapses on the eastern flank of Stromboli, Italy, due to structurally controlled, bilateral flank
663 instability. Mar Geol 262:1–13.
664
665 Romagnoli C, Kokelaar P, Casalbore D, Chiocci FL (2009b). Lateral collapses and active sedimentary
666 processes on the northwestern flank of Stromboli volcano, Italy. Mar Geol 265:101–119.
667
668 Romagnoli, C., Casalbore, D., Bortoluzzi, G., Bosman, A., Chiocci, F.L., D'Oriano, F., Gamberi, F., Ligi,
669 M., Marani, M., 2013a. Bathy-morphological setting of the Aeolian islands. In: Lucchi, F., Peccerillo,
670 A., Keller, J., Tranne, C.A., Rossi, P.L. (Eds.), The Aeolian Islands Volcanoes. Geological Society,
671 London, Memoirs 37. pp. 27–36.
672
673 Romagnoli, C., Casalbore, D., Ricchi, A., Lucchi, F., Quartau, R., Bosman, A., Tranne, C.A., Chiocci,
674 F.L., 2018. Morpho-bathymetric and seismo-stratigraphic analysis of the insular shelf of Salina
675 (Aeolian archipelago) to unveil its Late-Quaternary geological evolution. Mar. Geol. 395, 133-151.

676 Rusu, L., Guedes Soares, C., 2012. Wave energy assessments in the Azores islands. Renew. Energy
677 45, 183-196.

678 Serralheiro, A., Alves, C.A.M., Forjaz, V.H., Rodrigues, B., 1987. Carta Vulcanológica dos Açores.
679 Ilha de Santa Maria na escala 1/15 000 (folhas 1 e 2). Serviço Regional de Protecção Civil dos
680 Açores, Universidade dos Açores and Centro de Vulcanologia.
681
682 Sibrant, A.L.R., Hildenbrand, A., Marques, F.O., Costa, A.C.G., 2015. Volcano-tectonic evolution of
683 the Santa Maria Island (Azores): implications for paleostress evolution at the western Eurasia–
684 Nubia plate boundary. J. Volcanol. Geotherm. Res. 291, 49–62.
685
686 Thouret, J.C., 1999. Volcanic geomorphology-an overview. Earth-Sci. Rev. 47, 95-131.

687 Tsutsui, B., Campbell, J.F. and Coulbourn, W.T. (1987) Storm-generated, episodic sediment
688 movements off Kahe Point, Oahu, Hawaii. Mar. Geol., 76, 281–299.
689

690 Zbyszewski, G., Ferreira, O.V., 1960. Carta geológica de Portugal, Ilha de Santa Maria (Açores),
691 scale 1:50 000. Serviços Geológicos de Portugal.
692
693
694
695
696
697
698
699
700
701
702
703
704
705
706
707
708
709
710
711
712
713
714
715
716
717
718
719
720
721

FIGURES
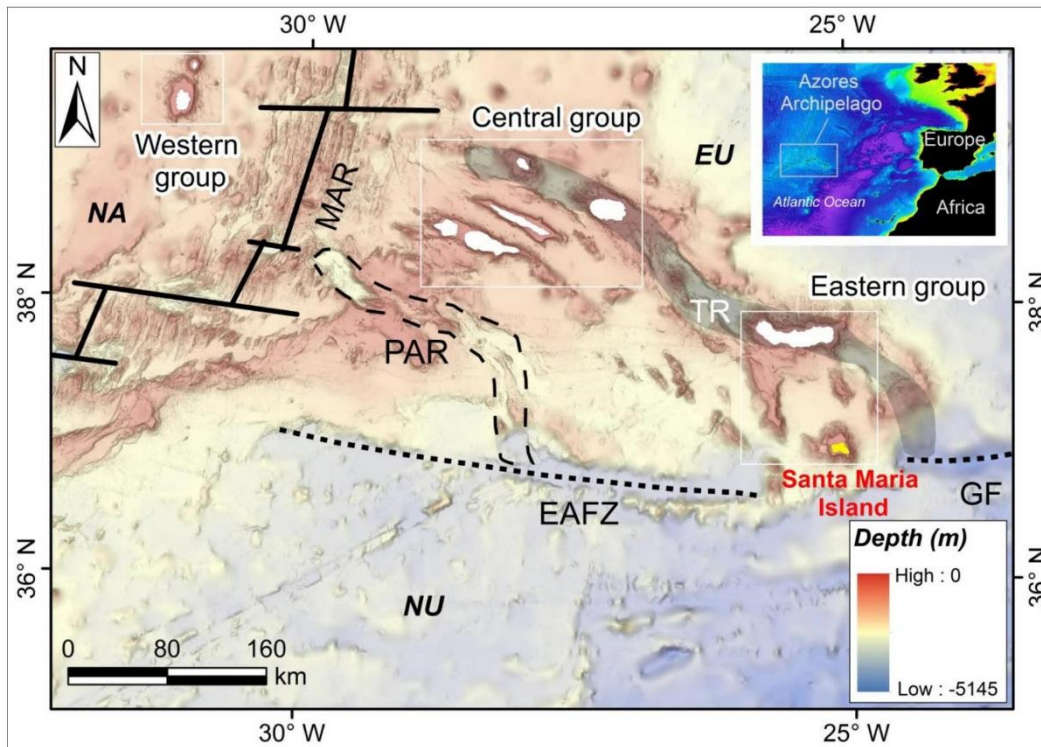
Fig. 1

Shaded relief map depicting the geodynamic setting of the Azores Archipelago. The upper right inset exhibits the location of the Azores islands within the North Atlantic Ocean. Tectonic structures: MAR – Mid Atlantic Ridge; EAFZ – East Azores Fracture Zone; GF – Gloria Fault; PAR – Prince Alice Rift; TR – Terceira Rift; EU – European Plate; NA – North America Plate; NU – Nubian Plate; Santa Maria Island is highlighted in yellow. Solid lines corresponds to major structures or faults while dashed lines represents the inferred structures or faults. The grey shaded area evidence the right-lateral transtensional shear zone of the Terceira Rift main structure. The bathymetry is derived from the EMODNET web portal (http://portal.emodnet-bathymetry.eu), tectonic structures adapted from Miranda et al. (2018).

737
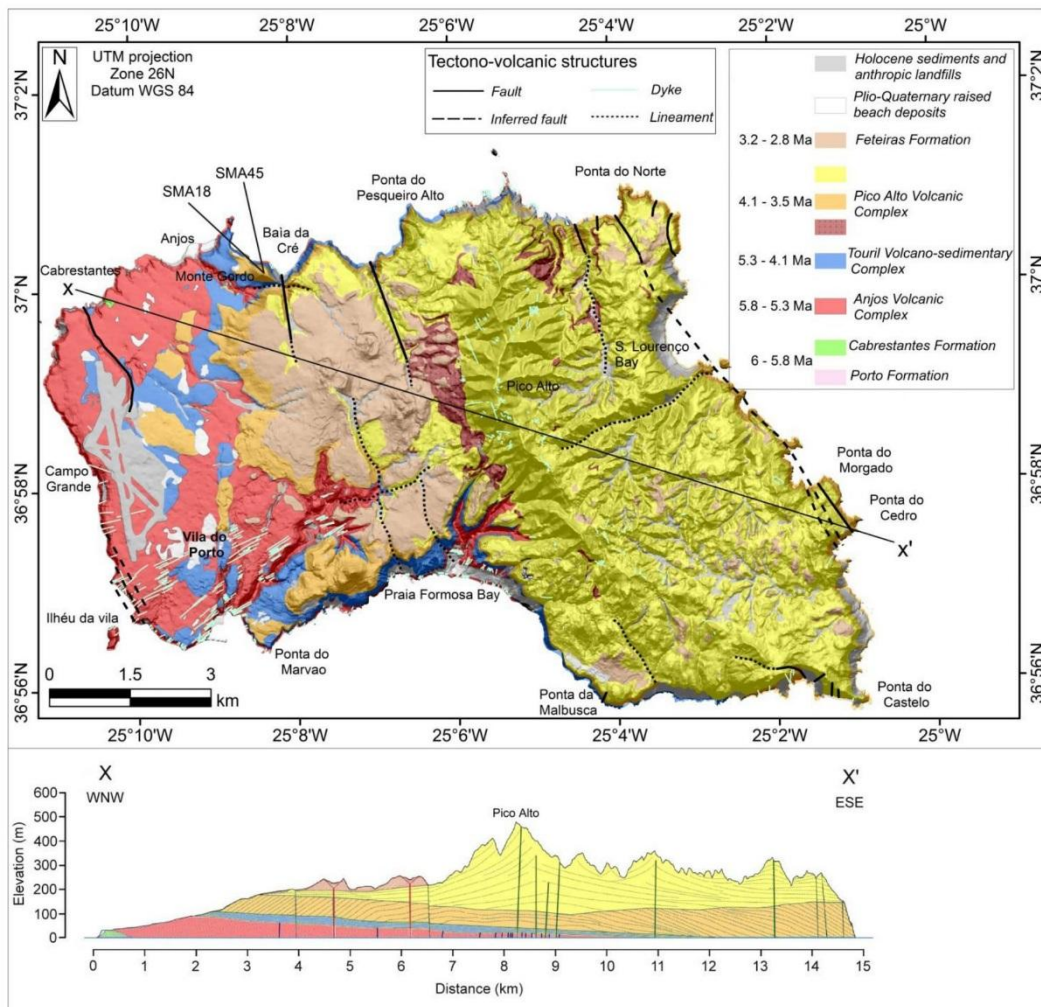
Fig. 2

a. Geological map of Santa Maria, merged on a shaded relief DEM of the Island generated from 1/5000 scale digital altimetric database. **b.** WNW-ENE oriented cross section showing the main geological formations of Santa Maria. (Modified after Ramalho et al., 2017).

742

743
744

745   *Fig. 3*
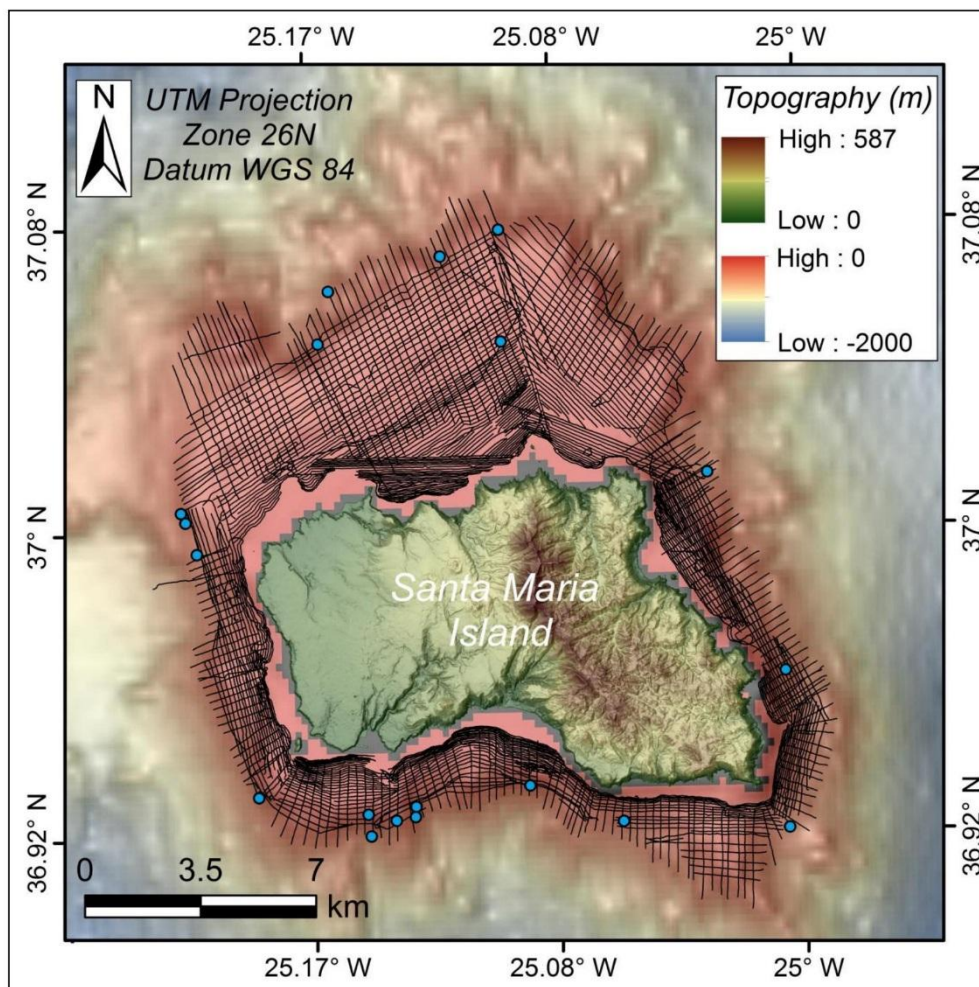
746   Dataset acquired during the PLATMAR 2016 oceanographic survey. The black lines represent the
747   survey track lines followed to acquire the seismic reflection profiles and the multibeam
748   bathymetric dataset. Pale blue dots represent the location of the Sound Velocity Profiles (SVP)
749   collected during the survey. The DEM of the island is generated from 1/5000 scale digital altimetric
750   database, while the bathymetry (c. 200 m resolution) was derived from the EMODNET web portal
751   (http://portal.emodnet-bathymetry.eu).

752

173
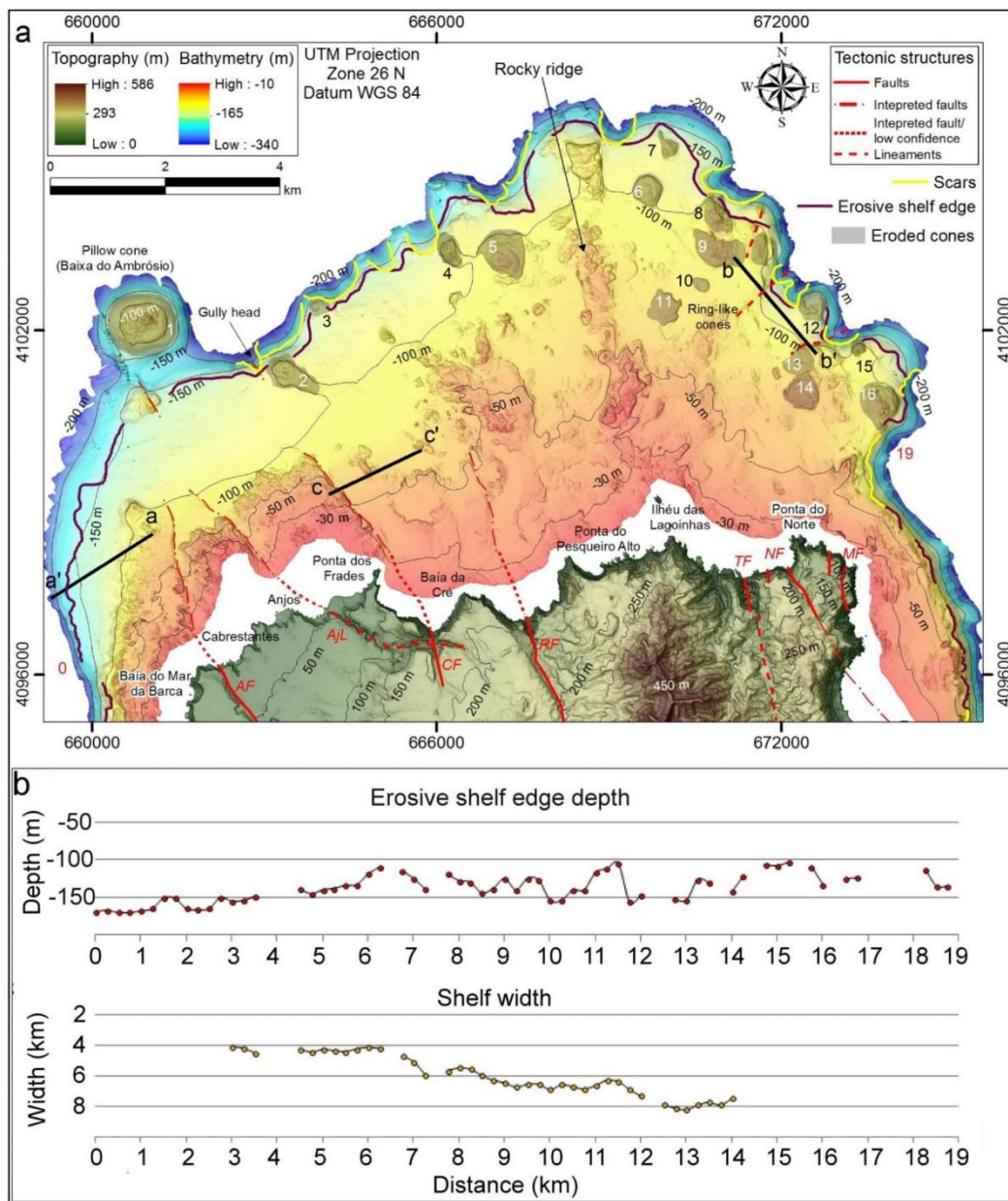
Fig. 4
Shaded relief map of the northern shelf sector **(a)** and graphs showing the shelf width and the erosive edge depth **(b)**. In (a) the black lines represent the location of the seismic profiles shown in figures 5, 7a and 7b. AF – Aeroporto Fault; AjF – Anjos Fault; CR – Cré Fault; RF – Raposo Fault; TF – Tanagarete Fault; NF – Norte Fault; MF – Massapês Fault.
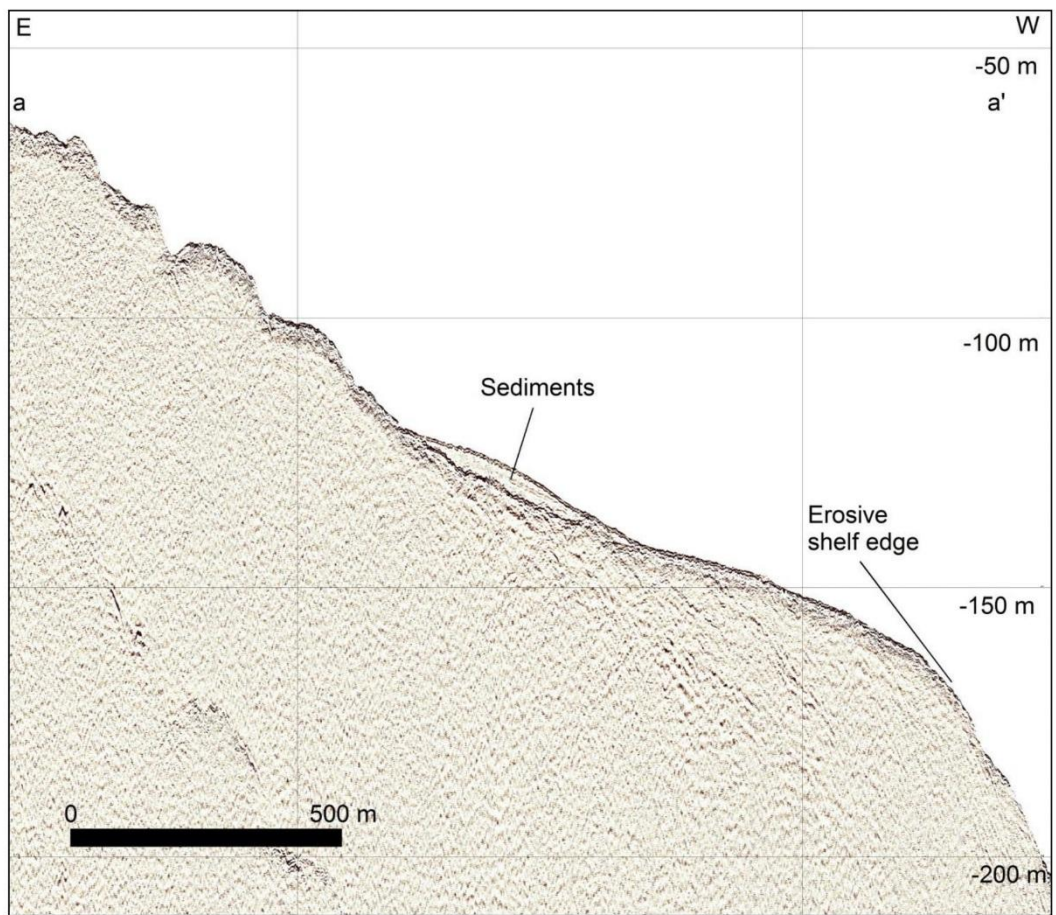
761
762
763 *Fig. 5*
764 Boomer seismic reflection profile collected across the northern shelf sector showing the erosive
765 edge depth and the sediments lying above the shelf. Location of the seismic profiles in Fig. 4.
766
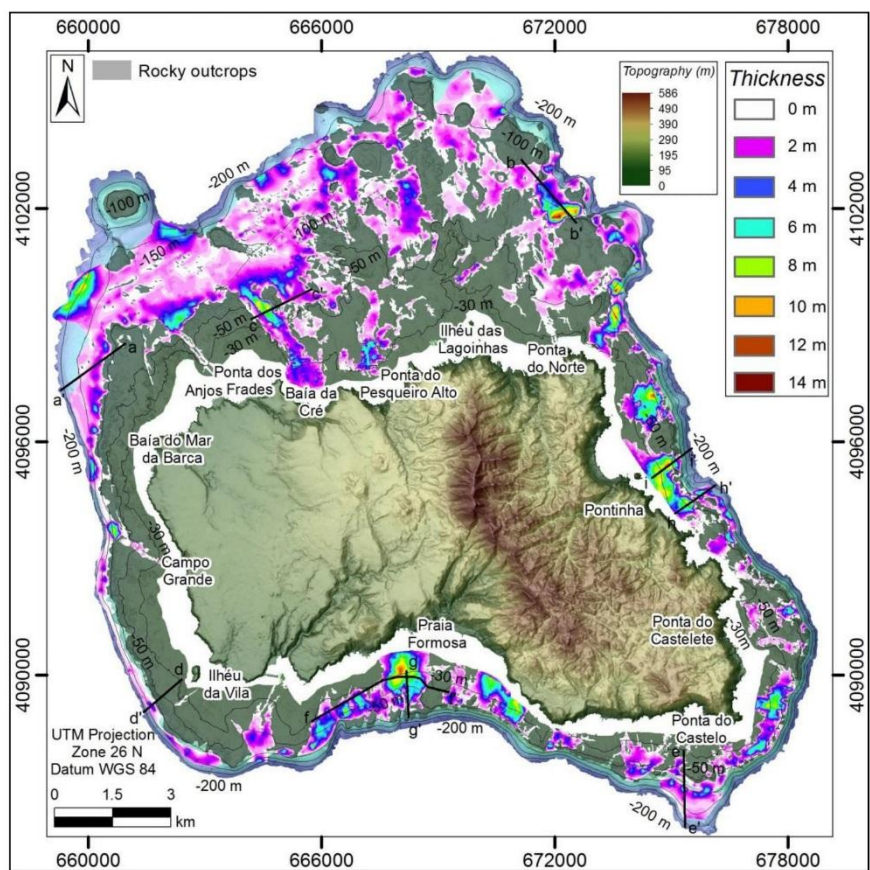
Fig. 6

Shaded relief map showing the distribution of the rocky outcrops and the sediments thickness on the shelf around Santa Maria Island.
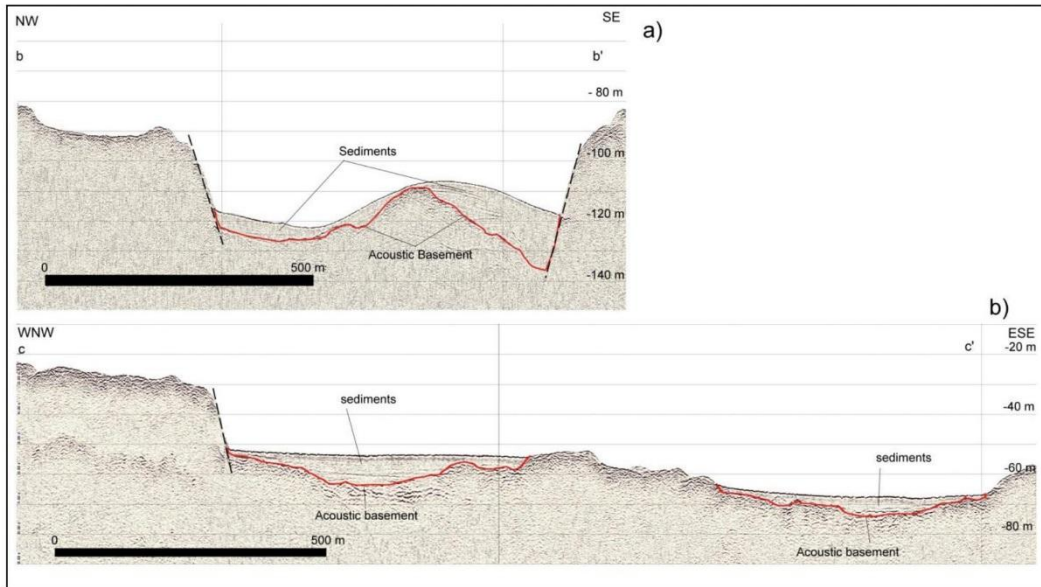
773
774
775 *Fig. 7*
776 Boomer seismic reflection profiles collected across the northern shelf sector showing the
777 sediments lying above the shelf. The black dashed lines represent possible faults. Location of the
778 seismic profiles in Fig. 4.
779

780
781
Fig. 8
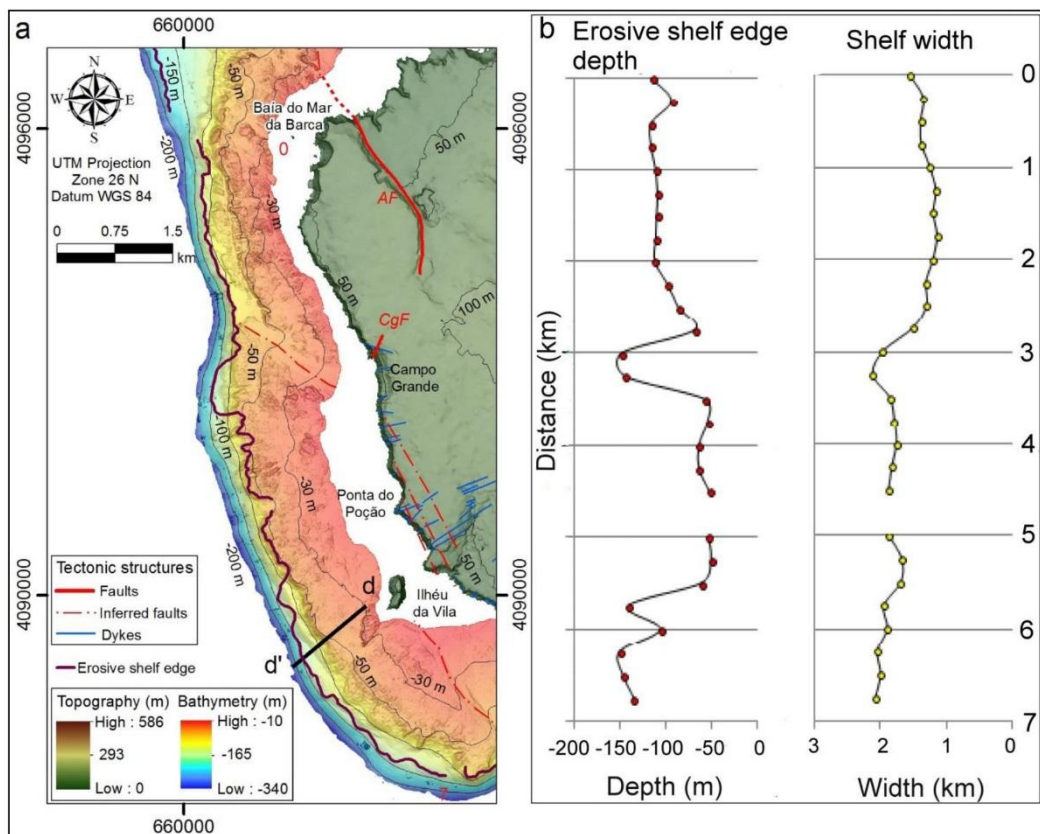
Shaded relief map of the western shelf sector **(a)** and graphs showing the shelf width and the erosive edge depth **(b)**. In (a) the black lines represent the location of the seismic profile shown in figure 9. AF – Aeroporto Fault; CgF – Campo Grande Fault.

786
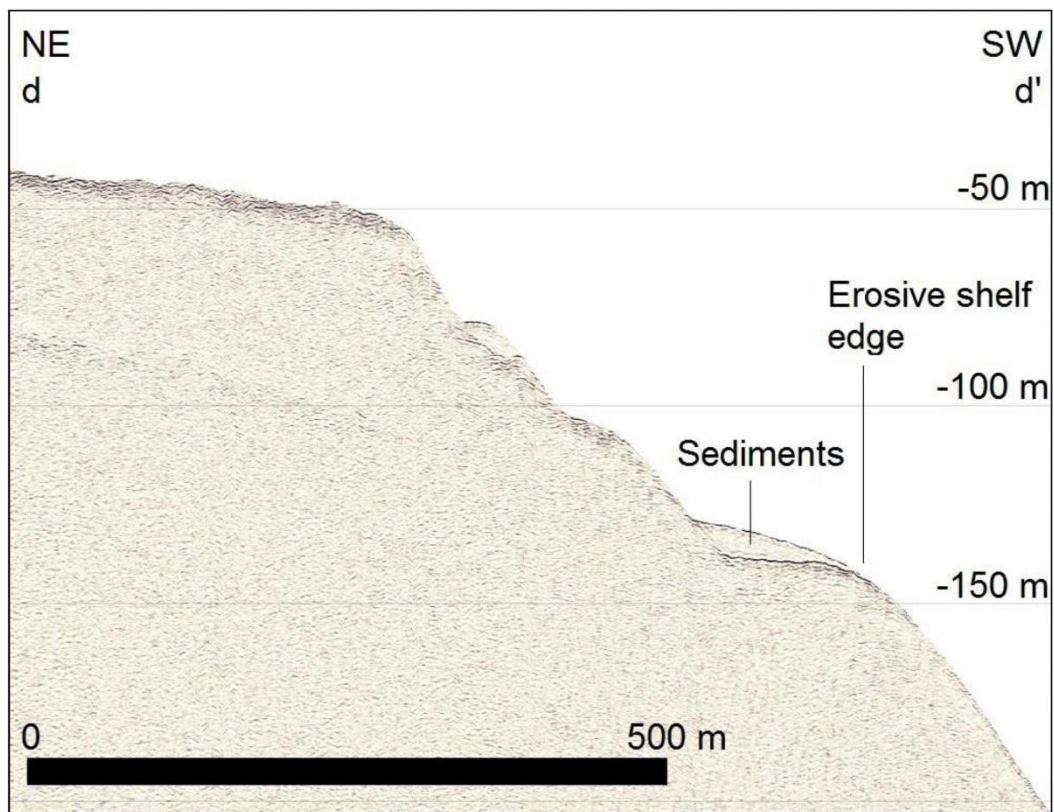
787
788
789 *Fig. 9*
790 Boomer seismic reflection profile collected across the western shelf sector showing the erosive
791 edge depth and the sediments lying above the shelf. Location of the seismic profiles in Fig. 8.
792

793
794
795 *Fig. 10*
796 Shaded relief map of the southern shelf sector **(a)** and graphs showing the shelf width and the
797 erosive edge depth **(b)**. In (a) the black lines represent the location of the seismic profiles shown in
798 figures 11, 12 and 13.
799

800
801

802 *Fig. 11*

803 Boomer seismic reflection profile collected across the southern shelf sector showing the erosive
804 edge depth and the sediments lying above the shelf. Location of the seismic profiles in Fig. 10.

805

806
807

808 *Fig. 12*
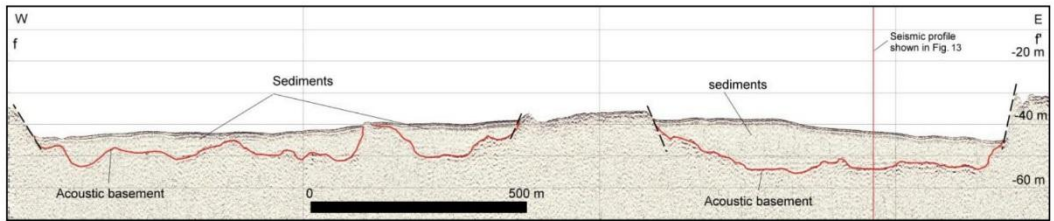
809 Boomer seismic reflection profile collected across the southern shelf sector showing the
810 sediments lying above the shelf. The black dashed lines represent possible faults. Location of the
811 seismic profiles in Fig. 10.

812

815   *Fig. 13*

816   Boomer seismic reflection profile collected across the southern shelf sector showing the erosive
817   edge depth and the sediments lying above the shelf. Location of the seismic profiles in Fig. 10. This
818   profiles intersects the profile shown in Fig. 12 in correspondence of the red vertical line.

819

820
821
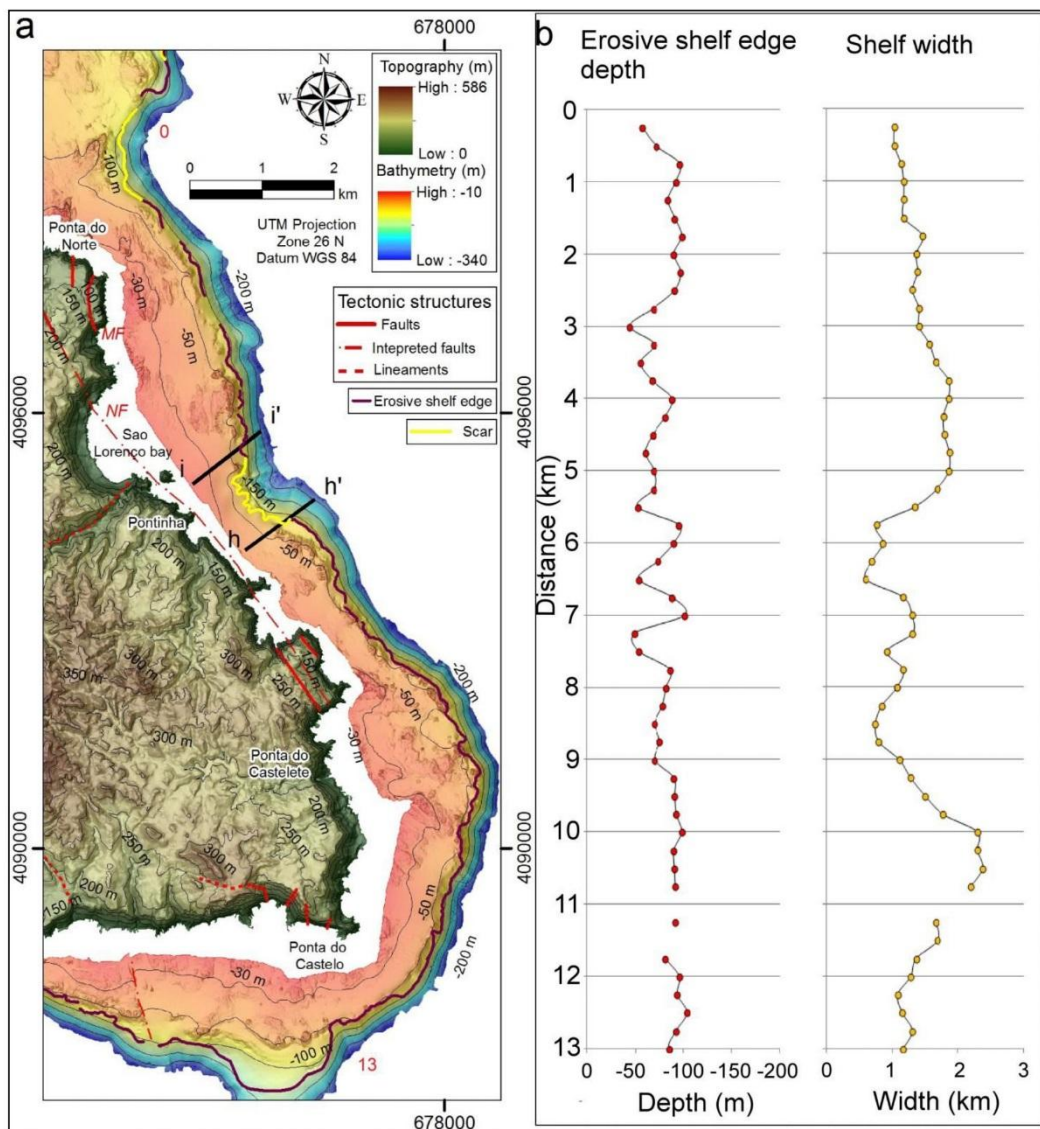
822 *Fig. 14*
823 Shaded relief map of the eastern shelf sector **(a)** and graphs showing the shelf width and the
824 erosive edge depth **(b)**. In (a) the black lines represent the location of the seismic profiles shown in
825 figures 15a and 15b. NF – Norte Fault; MF – Massapês Fault.
826

827
828
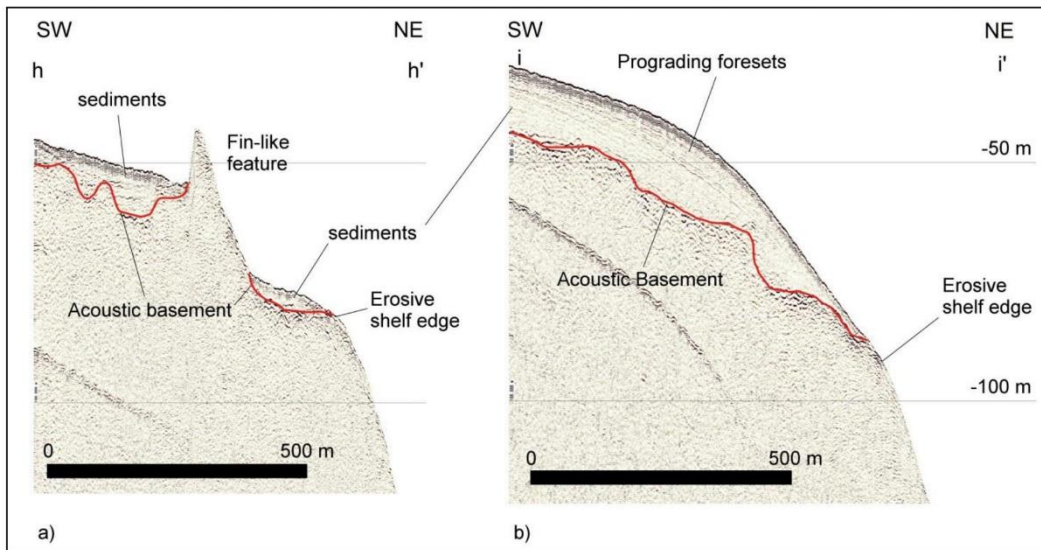
829   *Fig. 15*
830   Boomer seismic reflection profile collected across the eastern shelf sector showing the erosive
831   edge depth and the sediments lying above the shelf. Location of the seismic profiles in Fig. 14.
832

UTM projection
Zone 26N
Datum WGS 84

0   2.5   5
km
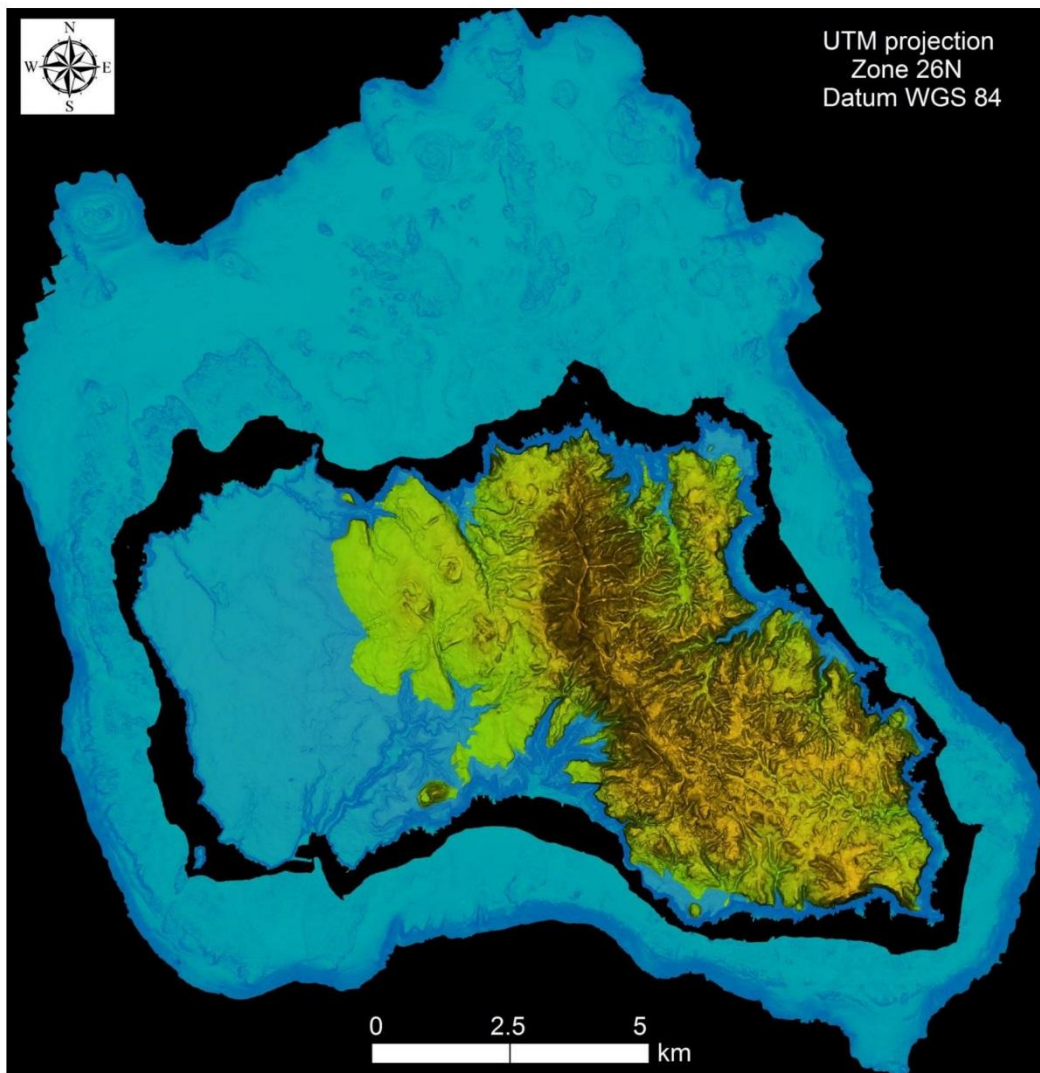
Fig. 16
Possible flooding scenario of Santa Maria Island at the onset of the uplift tend 3.5 Ma ago.
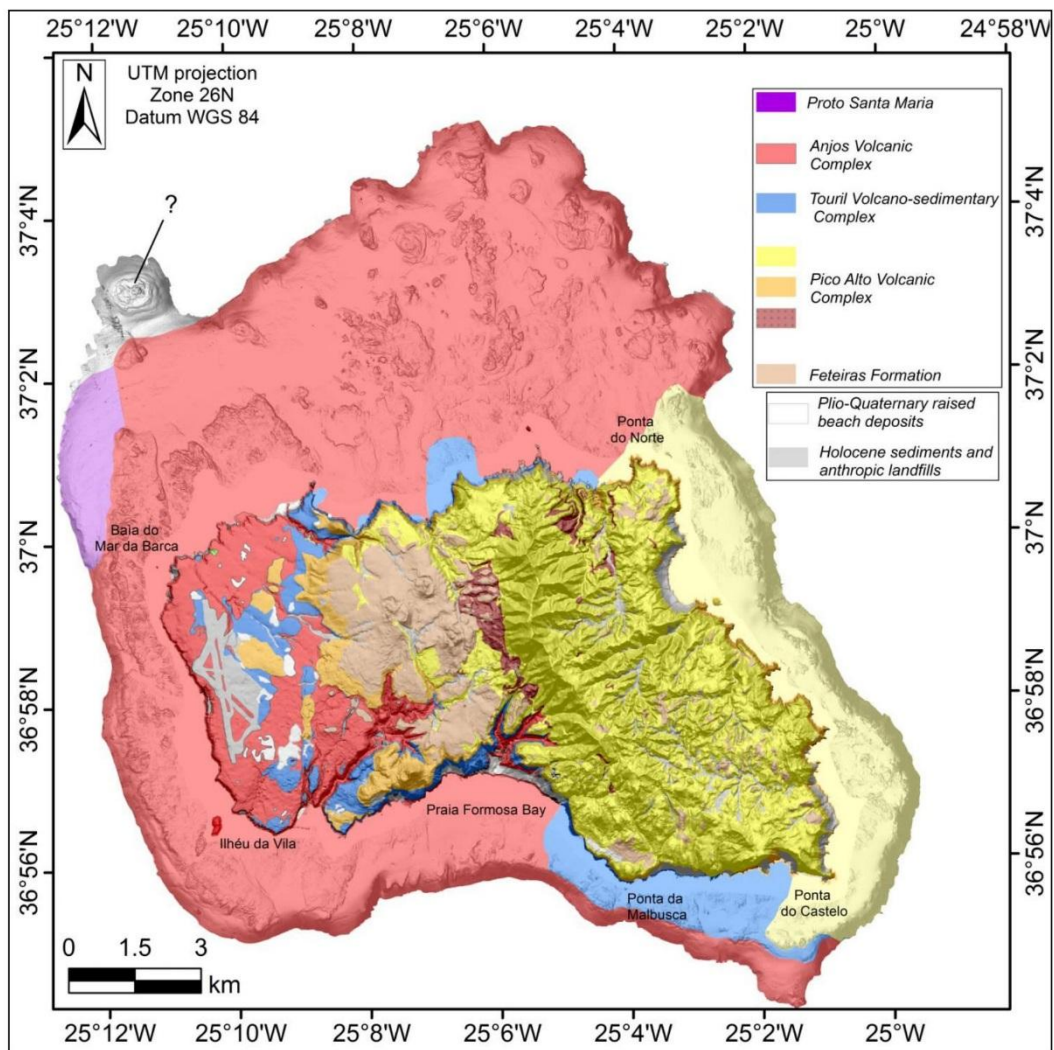
Fig. 17

Shaded relief map of the shelf around Santa Maria merged with the geological map of the Island, showing the inferred offshore continuation of the volcanic complexes recognized onshore by Ramalho et al. (2017).

Northern sector		Western sector		Southern sector		Eastern sector	
Edge depth	Shelf width	Edge depth	Shelf width	Edge depth	Shelf width	Edge depth	Shelf Width
-169				-114	2.04		
-167		-114.09	1.56	-131	2.25	-57	1.03
-170		-93	1.35	-140	2.45	-71	1.03
-170		-115	1.39	-135	2.495	-96	1.13
-168		-115	1.38	-126	2.44	-92	1.17
-165		-110	1.25	-128	2.365	-84	1.17
-151		-108	1.16	-76	2.26	-91	1.17
-151		-109	1.2	-103	2.04	-98	1.455
-165		-110	1.14	-82	1.9	-90	1.36
-166		-111	1.2	-78	1.94	-97	1.38
-165		-97	1.31	-88	1.9	-91	1.305
-150		-85	1.3	-101	2.045	-69	1.4
-155	4.134	-68	1.51	-73	1.9	-44	1.4
-154	4.236	-147	1.96	-98	1.92	-69	1.56
-149	4.51	-143	2.12	-96	1.79	-55	1.66
		-56	1.86	-119	1.95	-67	1.86
		-54	1.79	-75	1.4	-88	1.86
		-63	1.76	-96	1.275	-81	1.78
-139	4.26	-63	1.83	-78	1.705	-68	1.795
-145	4.49	-52	1.88	-110	1.91	-60	1.87
-140	4.31			-113	1.91	-69	1.865
-138	4.38	-53	1.88	-99	1.77	-69	1.68
-134	4.45	-50	1.68	-97	2.205	-52	1.34
-133	4.275	-60	1.69	-83	2.12	-95	0.77
-119	4.175	-140	1.95	-89	2.04	-90	0.86
-110	4.25	-105	1.9	-50	1.95	-73	0.695
		-147	2.05	-89	2.01	-53	0.595
-115	4.74	-146	2	-53	1.87	-88	1.165
-125	5.1	-134	2.08	-54	1.92	-101	1.295
-139	5.93			-63	1.82	-49	1.305
				-60	1.85	-53	0.92
-119	5.68			-62	1.05	-86	1.165
-128	5.5			-59	0.79	-82	1.07
-130	5.58			-78	0.87	-78	0.845
-144	5.99			-43	0.77	-70	0.745
-138	6.3			-94	1.015	-75	0.795
-125	6.45			-95	1	-70	1.105
-140	6.73			-86	0.93	-90	1.275
-125	6.56			-74	0.9	-91	1.495
-127	6.55			-80	0.7	-92.5	1.765
-154	6.89			-50	0.59	-98	2.295
-154	6.59			-59	0.68	-90	2.295
-140	6.7			-67	0.93	-90.5	2.374
-140	6.86			-67	1.1	-91.4	2.195
-117	6.63			-92	1.245		
-112	6.3			-92	1.25	-91.5	1.66
-105	6.37			-101	1.365		1.685
-156	6.9			-111	1.55	-80.7	1.36
-147	7.3			-97	1.49	-95.6	1.275
				-90	1.55	-93.6	1.08
	7.87			-100	1.65	-103.5	1.15
-152	8.1			-106	1.68	-92.5	1.3
-154	8.2			-133	2	-85	1.16
-126	7.9			-142	2.4	-104	
-131	7.72			-126	2.61		
	7.9			-124	2.46		
-142	7.47			-118	2.1		
-122				-123	1.94		
-107							
-108							
-103							
-109							
-133							
-125							
-124							
-113							
-135							
-135							

843

Table 1.

845 Shelf width (in km) and erosive edge depth (in m) values measured on the northern, western, southern and eastern shelf sectors of Santa Maria. In red the values representing the max width/edge depth in each sector.

8. SEA LEVEL FLUCTUATIONS VS VERTICAL MOBILITY AT SANTA MARIA ISLAND

8.1 Santa Maria Island: Manuscript V

The study carried out at Santa Maria focuses on the long-term generation and preservation of both submerged and raised marine terraces along the shelf and coast of a slowly uplifting volcanic island, and discusses which factors control the formation of such coastal morphologies. Our work exploits a very high-resolution marine geophysics dataset on the shelf of this island, to provide an integrated onshore/offshore analysis on the formation of marine terraces.

Taking into account the occurrence of raised marine terraces on the island (previously reported by Ramalho et al., 2017), we correlated the formation of the different raised and submerged terraces with relative sea-level changes. By considering and discussing the complex interplay between glacio-eustatic sea-level fluctuations, and the island vertical motion trends, we also propose a possible timeframe for the formation of the terraces, with presently raised marine terraces mostly formed from ~3.5 Ma to ~1 Ma, and submerged terraces formed from ~1 Ma to the Last Glacial Maximum.

My contribution to this paper covers the whole range of activities associated to a scientific research: I joined the scientific team during the PLATMAR cruise around Santa Maria to collect the dataset, which I successively processed (seismic profiles) at the Instituto Hidrografico in Lisbon. Being the first author I wrote a first draft of the manuscript, completed with the support of all the authors.

"*Marine terrace development on reefless volcanic islands: new insights from high-resolution geophysical data offshore Santa Maria Island (Azores Archipelago)*"

Authors:
- **Alessandro Ricchi** (University of Bologna, Bologna – Italy)
- **Rui Quartau** (Instituto Hidrográfico, Divisão de Geologia Marinha);
  (Universidade de Lisboa, Instituto Geofisico Infante Dom Luiz, Instituto Dom Luiz, Faculdade de Ciências da Universidade de Lisboa, Lisbon, Portugal).
- **Ricardo Ramalho** (University of Bristol, UK)
- **Claudia Romagnoli** (University of Bologna, Bologna – Italy);
  (Istituto di Geologia Ambientale e Geoingegneria, Consiglio Nazione delle Ricerche, Rome – Italy).
- **Daniele Casalbore** (University of Rome – "La Sapienza", Rome – Italy);
  (Istituto di Geologia Ambientale e Geoingegneria, Consiglio Nazione delle Ricerche, Rome – Italy).
- **João Ventura da Cruz** (Instituto Hidrográfico, Divisão de Geologia Marinha, Lisbon – Portugal)
- **Catarina Fradique** (Instituto Hidrográfico, Divisão de Geologia Marinha, Lisbon – Portugal)

- **André Vinhas** (Instituto Hidrográfico, Divisão de Geologia Marinha, Lisbon – Portugal)
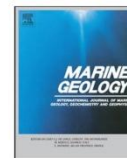
Marine terrace development on reefless volcanic islands: New insights from high-resolution marine geophysical data offshore Santa Maria Island (Azores Archipelago)

Alessandro Ricchi[a,*], Rui Quartau[b,c], Ricardo S. Ramalho[c,d,e], Claudia Romagnoli[a], Daniele Casalbore[f,g], João Ventura da Cruz[b], Catarina Fradique[b], André Vinhas[b]

[a] University of Bologna, Dip. Scienze Biologiche, Geologiche e Ambientali, Bologna, Italy
[b] Instituto Hidrográfico, Divisão de Geologia Marinha, Lisboa, Portugal
[c] Instituto Dom Luiz, Faculdade de Ciências, Universidade de Lisboa, Lisboa, Portugal
[d] School of Earth Sciences, University of Bristol, Bristol, UK
[e] Lamont-Doherty Earth Observatory at Columbia University, Palisades, NY, USA
[f] Sapienza Università di Roma, Dipartimento Scienze della Terra, Roma, Italy
[g] Istituto di Geologia Ambientale e Geoingegneria, Consiglio Nazionale delle Ricerche, Area della Ricerca, Roma, Italy

ARTICLE INFO

ABSTRACT

Submerged marine terraces are relict coastal erosional landforms now underwater due to rising sea level and/or land subsidence. Using as case study the shelf around Santa Maria Island (North Atlantic Ocean), we intend to advance our knowledge on the formation and preservation of these features on reefless volcanic islands. Santa Maria is an ideal place to study their combined generation, since it displays a sequence of subaerial and sub-merged marine terraces (the latter not studied before), distributed between 7/230 m in elevation, and −40/−140 m in depth, respectively. Based on some geological constraints, we investigated a possible correlation between the formation of the different terraces with known sea-level changes. Our results suggest that the spatial distribution of marine terraces at Santa Maria depends on the complex interplay between glacio-eustatic sea-level fluctuations, the island's vertical motion trends, the morphology of the shelf, and the intensity of marine erosion. Subaerial terraces probably developed from ~3.5 Ma to ~1 Ma following a fortuitous conjugation of optimal exposure to energetic waves and a suitable arrangement/lithology of the stratigraphic units promoting easier erosion. Their preservation was likely promoted by the uplift trend the island experienced in the last 3.5 Ma, which was rapid enough to prevent their destruction by subsequent highstands. The submerged terraces, presumably all younger than ~1 Ma, were largely influenced by shelf gradient, leading to more developed and preserved terraces in wider and low-gradient sectors. Displacement by active faults also conditioned the for-mation and further development of both subaerial and submerged terraces, with tectonic activity documented for the 0.693 Ma–2.7 Ma period.

1. Introduction

Relative sea-level changes have left unambiguous morphologies in the geological record, as attested by the presence of coastal notches (e.g. Ferranti et al., 2006; Trenhaile, 2015), marine terraces (e.g. Zazo et al., 2002; Pedoja et al., 2014) and beach rocks (e.g. Mauz et al., 2015). In submarine settings the effects of glacio-eustatic sea-level changes can be witnessed by markers such as the shelf breaks on insular shelves (Quartau et al., 2014) or depositional features formed below storm-wave base (e.g. submarine prograding wedges; Casalbore et al.,

2017 and references therein). Marine terraces are frequently referred to as excellent tracers of palaeo sea-level (Pirazzoli et al., 1993) and they can be used to discern the vertical movements affecting the coastline (Campbell, 1986; Ferranti et al., 2006; Zazo et al., 2007). This approach has been successfully applied to study the history of uplifting volcanic islands (see Lucchi et al., 2007; Lucchi, 2009 and Ramalho et al., 2017) where vertical deformations usually operate at varied timescales (De Guidi and Monaco, 2009; Ramalho et al., 2013). Most studies so far did not integrate the offshore information (Quartau and Mitchell, 2013; Quartau et al., 2015), and when they did, mostly focused on oceanic

islands surrounded by coral reefs (Coulbourn et al., 1974; Blanchon and Jones, 1995; Faichney et al., 2010). To date, only few studies have looked closely at submerged terraces on reefless volcanic islands or at seamounts (Passaro et al., 2011; Schwartz et al., 2018) and consequently little is known about the factors that control the generation and timing of submerged terraces in these settings.

Santa Maria is the southeastern-most and oldest island of the Azores Archipelago in the Atlantic Ocean, with a history of intermittent volcanism spanning between approximately 6 to 2.8 Ma (Sibrant et al., 2015; Ramalho et al., 2017). Its subaerial evolution is now well constrained (Serralheiro et al., 1987; Serralheiro, 2003; Ávila et al., 2008; Sibrant et al., 2015; Ramalho et al., 2017) and so is the history of vertical movements affecting the island edifice. Based on several volcanic, erosional, and sedimentary relative sea-level markers found onshore, Ramalho et al. (2017) inferred that Santa Maria was subjected to over 200 m of subsidence from emergence at 6 Ma until 3.5 Ma BP (at average ~100 m/m.yr), after which the island experienced an uplift trend at a slower pace (~60 m/m.yr on average) until recent times. Additionally, Ramalho et al. (2017) reported a sequence of subaerial marine terraces at elevations ranging between 7–11 m and 210–230 m, formed during the post-erosional stage of the island. In this paper, the analysis of newly acquired high-resolution multibeam bathymetry and seismic profiles reveal a sequence of submerged marine terraces extending to the shelf edge. This makes Santa Maria an ideal case study to employ a combined onshore/offshore approach to investigate the generation of subaerial and submerged marine terraces and their likely timing of formation in relation to the island's vertical motion history. Based on one dated subaerial terrace and a dated passage zone between subaerial and submarine lava flows (which were used as "anchor" points), we also present a possible correlation between each subaerial and submerged terrace identified on the island and their respective possible time of formation, as extracted from published eustatic curves. The case study of Santa Maria therefore will improve our understanding of the controlling mechanisms of marine terrace formation and preservation at reefless volcanic islands, and more generally in other settings.

2. Geological background

The Azores Archipelago consists of a group of nine volcanic islands in the mid-North Atlantic, located around the triple junction between the North American, Eurasian and Nubian lithospheric plates (Fig. 1). The Eastern (São Miguel and Santa Maria) and Central group of islands (Terceira, Graciosa, São Jorge, Pico, and Faial Islands) are located on a roughly triangular-shaped area between the Terceira Rift (TR in Fig. 1) and the inactive East Azores Fracture Zone (EAFZ in Fig. 1) on the eastern side of the Mid-Atlantic Ridge (MAR in Fig. 1; Lourenço et al., 1998; Gente et al., 2003; Miranda et al., 2018). This complex volcano-tectonic structure is the result of a right-transtensional shear zone that links the MAR with the Gloria Fault (GF) (Hipólito et al., 2013; Lourenço et al., 1998; Marques et al., 2013). Santa Maria Island is considered now outside the influence of such wide structure after a ridge-jump, occurred at ~4 Ma, from the incipient Princess Alice Rift (PAR in Fig. 1) to the present-day Terceira Rift (Miranda et al., 2018).

Santa Maria was the first island in the Azores Archipelago to emerge above sea level, at approximately 6 Ma (Ramalho et al., 2017). The present-day edifice rises from the −2500 m isobath to a summit at 587 m (Pico Alto, Fig. 2). The emergent stage of island building corresponds to the Cabrestantes and Porto Formations, which crop out on the western side of the island (age ~ 6 Ma, Fig. 2a). Then, a subaerial shield volcano was formed about 5.8–5.3 Ma, which consolidated the island edifice (Anjos Volcanic Complex, Fig. 2a). During the following ~1 Ma, volcanic activity waned, leading to a partial or complete dismantling of the shield volcano and to marine deposition synchronous with occasional, low-volume submarine volcanism (Touril Volcano-sedimentary Complex, Fig. 2a). This stage is considered as mainly

erosional and occurred alongside a significant subsidence trend, which further contributed to the planation and possibly complete submergence of the island edifice (Ramalho et al., 2017). At ~4.1 Ma, however, renewed volcanic activity, which culminated in the creation of the Pico Alto Volcanic Complex (Fig. 2a), caused the edifice to re-emerge, as attested by the vertical succession of submarine and subaerial volcanic products. At ~3.5 Ma subsidence reversed into uplift, as attested by the presence of raised submarine volcanic sequences and a succession of subaerial marine terraces on the western (windward) side (Ramalho et al., 2017), arranged in a typical staircase morphology. Conversely, the eastern (leeward) side is characterized by a rugged morphology, featuring high plunging cliffs (up to 250–300 m in elevation) with occasional wave-cut notches at varying elevations. A last stage of volcanism (3.2–2.8 Ma) created the Feteiras Formation (Fig. 2a), but this activity did not reverse the dominantly erosional trend the island has experienced in the last 3.5 Ma (Ramalho et al., 2017).

In terms of tectonics, Santa Maria is mainly dominated by NW–SE-, N-S and NE–SW-trending extensional faults (Madeira et al., 2015), as attested by the existence of main morphological lineaments in the subaerial topography that displace some of the subaerial terraces (Fig. 2a; Madeira et al., 2015). Numerous dikes, contemporaneous with the two main shield building stages, striking N 045° and N 150° have also been reported (Zbyszewski and Ferreira, 1960; Serralheiro et al., 1987) (Fig. 2a).

In the Azores Archipelago the wave regime is dominated by waves impacting the coastline from the NW (29%), W (24%) and N (16%), with average significant heights (H_s) ranging between 2.5 m and 3 m (Quartau et al., 2012). Storminess in the Azores is high, and the archipelago is struck by severe storms, at least once every seven years (Andrade et al., 2008) that are able to produce maximum wave heights up to 20 m (Rusu and Guedes Soares, 2012). The Azores is subjected to semidiurnal regular tides and the annual mean tidal range in Santa Maria Island is about 1,44 m (Instituto Hidrográfico, 2000).

3. Data and methods

3.1. Marine geophysical data acquisition

High-resolution multibeam bathymetric and seismic reflection data were collected around Santa Maria between −20 m and −250 m onboard the R/V *Arquipélago* from 24th August to 15th September 2016. High-resolution multibeam bathymetry was collected mostly parallel to the isobaths along overlapping track lines, relying on DGPS with OMNISTAR corrections for positioning and using a pole-mounted Kongsberg EM2040C™ system (operating frequency range of 200–400 kHz and angular coverage of 130°). Sound velocity profiles (SVP, yellow dots, Fig. 3) were regularly collected during the survey. Data were processed using Caris Hips & Sips 9.0 software to produce high-resolution digital elevation models (DEMs) with variable cells size depending on the water depth (1 m for shallow water to 8 m at ~250 m).

A total of 2008 km of high-resolution seismic profiles (Fig. 3) was also acquired between −25 m and −300 m using an Applied Acoustic Engineering AA 200 Boomer™ plate and a receiver array consisted of a single-channel streamer with 8 hydrophones. Most of the seismic profiles were acquired using 100/200 J of output energy, depending on the water depth. Seismic survey lines parallel to bathymetry have line spacing varying with depth (between 20 and 200 m), whilst seismic lines perpendicular to the coastline were regularly spaced at ~250 m.

3.2. Terrace mapping

Multibeam bathymetry and seismic profiles were combined with an existing onshore topographical model (generated from a 1:5000 scale digital altimetric database) in a GIS environment, allowing for
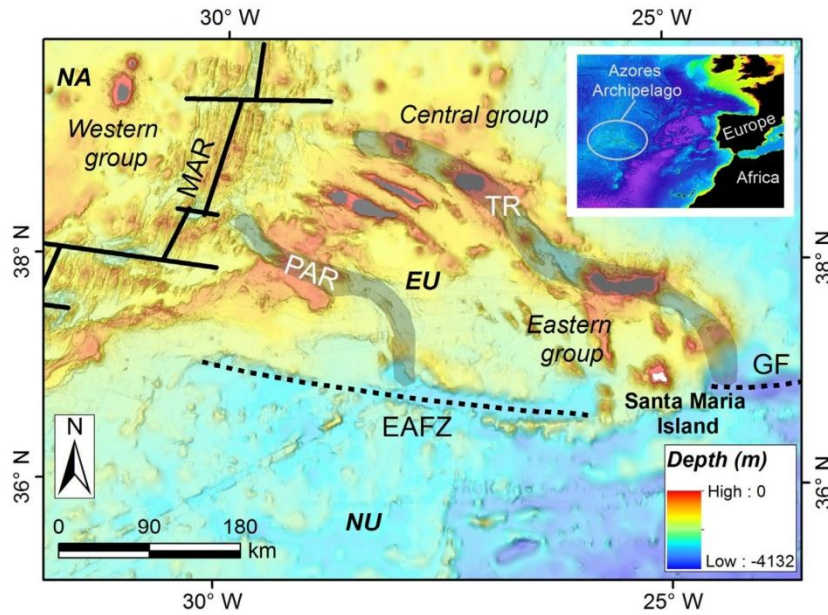
191

Fig. 1. Shaded relief map illustrating the geodynamic setting of the islands (western, central and eastern groups) in the Azores Archipelago (islands in grey, Santa Maria Island in white) and how they straddle the triple junction between the North American (NA), Eurasian (EU) and Nubian (NU) lithospheric plates. MAR: Mid-Atlantic Ridge; PAR: Princess Alice Rift; EAFZ: Eastern Azores Fracture Zone; TR: Terceira Rift; GF: Gloria Fault. The top-right inset shows the geographical setting of the Azores Archipelago within the Northern Atlantic Ocean. Grey shading represents the deformation zone of Terceira rift and of the inactive Princess Alice Rift.

The bathymetry is derived from the EMODNET web portal (http://portal.emodnet-bathymetry.eu), tectonic structures adapted from Miranda et al. (2018).

integrated onshore/offshore geomorphological analysis. Using this database, we mapped the erosive shelf edge and the submerged terraces on the shelf. Specifically, we mapped (where possible) the inner margin of each terrace (Fig. 4, also named "shoreline angle"), which provides an estimation of the shoreline position at the time it was formed, within an error of few meters (Firth et al., 1996; Trenhaile, 2002; Antonioli et al., 2003). Where the shelf and overlying terraces are covered by sediment, we used seismic profiles to measure their extension and edge depth. In such cases a sound velocity of 1800 m/s was adopted for the time/velocity conversion for sediments, which on the Azorean mid/outer shelves often correspond to sands (Quartau et al., 2012).

The mapped shelf was divided into four sectors (north, west, south, east), based on their orientation to the wave climate, their distinctive morphology and the distribution of submerged terraces (Figs. 5, 7–10; 3 and 8 on the Electronic supplementary material, hereafter ESM). To consider the island vertical movements, we always took into account the maximum values of the shelf edge depths for each sector, since later retrogressive erosion might have affected its depth, making it shallower in places. Mean values of the terrace width were calculated from bathymetric profiles plotted every 250 m perpendicular to the coastline and/or the shelf edge (Fig. 8ESM). The width of the subaerial terraces was also measured using topographic profiles (Fig. 8ESM and Table 3ESM) to obtain average values, assuming that it corresponds to the distance from one palaeoshoreline to the one immediately above or below.

3.3. Estimate of the age of subaerial and submerged marine terraces

The uplift rates of Santa Maria were calculated using two dated subaerial markers, together with published sea-level curves. Considering the time period under analysis (almost 4 Ma) we merged the Bintanja and van de Wal's (2008) curve, which has a very good resolution and covers 3 Ma, with a curve having a lower resolution (De Boer et al., 2010) for periods after 3 Ma (Fig. 6).

The subaerial marine terrace at 90 m above sea level (a.s.l.; dated at 2.15 ± 0.03 Ma, Ramalho et al., 2017) and the maximum highstand between 2.12 Ma and 2.18 Ma (−0.47 m at 2.134 Ma) were used as reference markers to calculate the possible uplift rate, assuming that during that period this terrace was uplifted from −0.47 m to 90 m a.s.l. Using this methodology, we obtained an average uplift rate of 42.4 m/m.yr (0.042 mm/yr). The passage zone between subaerial and submarine lava flows of the effusive lava deltas of Monte Gordo (Fig. 2a) was chosen as another reference sea-level marker to calculate an earlier uplift trend. This feature, that marks very accurately the position of sea level at the moment of the eruption (e.g. Cas and Wright, 1987; Porębski and Gradziński, 1990; Ramalho et al., 2010a, 2010b, 2010c; Ramalho, 2011; Meireles et al., 2013), is located at 190 m a.s.l. and its timing of formation is constrained by two $^{40}Ar/^{39}Ar$ analyses (SMA 18 and SMA 45 samples collected in the submarine lava flows below the passage zone) yielding ages of 3.63 ± 0.09 and 3.71 ± 0.08 Ma (see Ramalho et al., 2017). Although the formation of this lava delta did not occur, necessarily, during a highstand, the temporally nearest highstand provides a minimum value for the inferred vertical displacement experienced by this marker, which constitutes the highest datable sea-level indicator in Santa Maria (Ramalho et al., 2017). The average age of the marker is 3.67 Ma, which falls between two highstands in our composite curve. Therefore, we used the nearest and highest highstand (dated as 3.704 Ma, at 6.4 m above present sea-level) to calculate the average uplift rate, which is approximately 59 m/m.yr (0.059 mm/yr). The result is an uplift rate that progressively slowed down with time, in agreement with the current elevation of the Marine Isotope Stage (MIS) 5e raised terrace (7–11 m a.s.l.), which attests to a substantial vertical stability, or to very small uplift, on Santa Maria Island in the last 125 ka.

The composite sea-level curve, based on the literature, has been modified according to the obtained uplift rates (Fig. 6), in order to infer the possible age of formation of the mapped marine terraces. Accordingly, we tentatively matched all the stands (including highstands, stillstands and lowstands) and all the passing sea-level cycles (rises and falls) with the current terrace elevation/depth (see Section 4.3). We assumed that subaerial and submerged marine terraces could be multi-generational, i.e. their geometry could result from the action of several stillstands, as well as sea-level passages. We are, in fact, aware of the inherent errors of using one sea-level curve in detriment of another
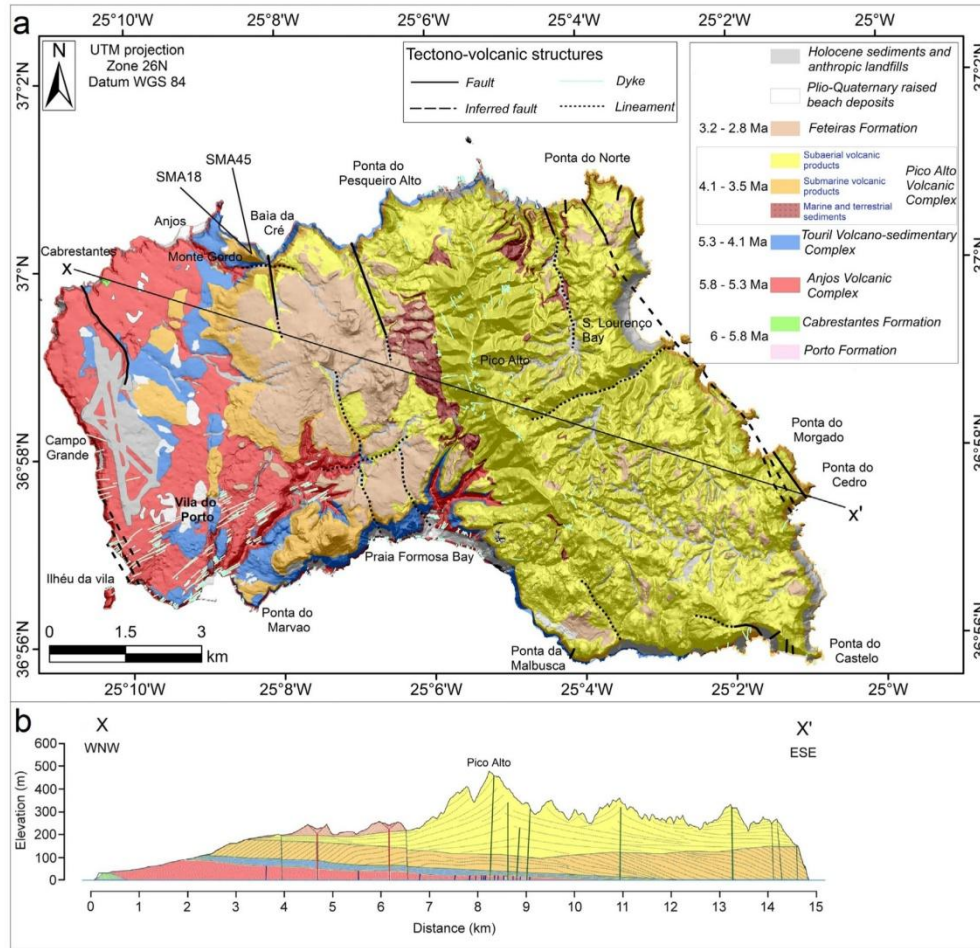
Fig. 2. (a) Geological map of Santa Maria Island, and (b) WNW–ESE oriented cross-section. Underlying digital elevation model (DEM) is generated from a 1/5000 scale digital altimetric database. Note that the Porto Fm and Lower Pico Alto volcanic complex are not visible on the map/section at this scale. SMA 18 and SMA 45: samples collected in the submarine lava flows below the passage zone of Monte Gordo (see the text for further details).
Modified after Ramalho et al. (2017).

(Caputo, 2007) and also that uplift rates have possibly changed through time in the period of our reconstruction (Ramalho et al., 2010b). Although a confident correlation between a particular terrace and a single sea-level stand is impossible, the establishment of a probable time frame for its likely formation can be proposed. Moreover, we also took into account the time that waves eventually would take to carve the terraces at a specific depth, within a ± 5 m uncertainty (i.e., we considered for the calculations the timing that sea was 5 m above and below the level of the terrace) (see Table 1ESM).

4. Results

4.1. The insular shelf around Santa Maria Island

The northern sector of the shelf (Fig. 7) has a rough trapezoidal shape, being widest in front of Ilhéu das Lagoinhas (~8 km) and narrower westwards (~4.5 km). The northwestern-most tip of the shelf is characterized by an oval-shaped, 200 m-high conical structure (Baixa

do Ambrósio) that likely represents the remnants of an old pillow-lava cone. Other concentric structures, probably corresponding to truncated cinder/scoria cones of the Cabrestantes and Porto Formations, and of the Anjos Volcanic Complex have been also identified, mostly on the easternmost portion from −120 m to −30 m. The westernmost portion of the inner shelf is divided into three rocky blocks by sharp and linear escarpments (2 to 2.5 km long, Fig. 7) that are, apparently, the seaward expression of tectonic lineaments recognized on land (Aeroporto, Anjos and Baía da Cré faults in Figs. 2 and 7). The shelf edge depth is constantly below −125 m with maximum depths of ~ −170 m to NW off Baía do Mar da Barca (Fig. 7).

The western sector of the shelf is generally characterized by a rocky surface with almost no sediment cover. A WNW-ESE lineament located offshore Campo Grande (possible fault, Fig. 8), separates the shelf into two parts characterized by different widths (~1 km to the north, ~2 km to the south). In this sector the erosive shelf edge has been significantly affected by mass wasting; where preserved, its depth varies between −100/−110 m and −135/−145 m (Fig. 8).
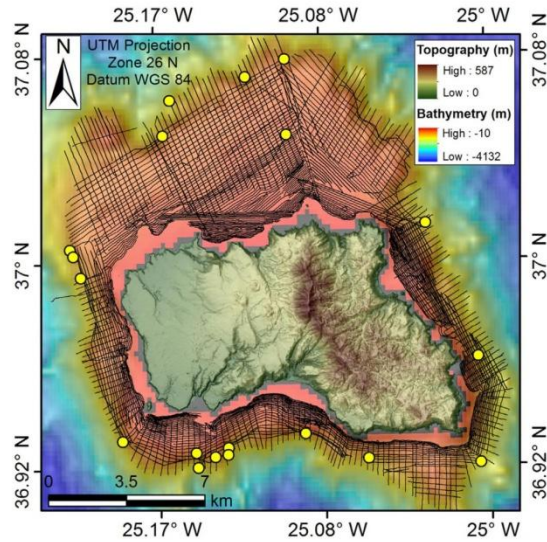
Fig. 3. Dataset used for this study, showing the seismic reflection profiles acquired during the PLATMAR cruise. The multibeam survey covered the area shown by the seismic grid. Yellow dots represent location of sound speed profiles collected during the multibeam survey. Bathymetry shown in this figure (~200 m resolution) was derived from the EMODNET web portal (http://portal.emodnet-bathymetry.eu); topography was constructed from a 1/5000 scale digital altimetric database. (For interpretation of the references to colour in this figure legend, the reader is referred to the web version of this article.)

The southern shelf sector has an irregular morphology, since more preserved and wider portions of the shelf alternate with narrower areas affected by gully heads (Fig. 9). Accordingly, the shelf width varies from ~0.7 km to up to ~2.5 km and the edge depth from −80/−90 m to a maximum value of −142 m (Fig. 9). Sharp NNE-SSW oriented

lineaments cut the shelf, often defining rocky structural highs, which are bordered by more depressed areas covered by sediments (Fig. 9).

The eastern sector of the shelf is from ~1 to ~2 km wide, with the erosive shelf edge located at a fairly constant depth, varying mostly between −90 m and −110 m (Fig. 10). Some portions of the outer shelf are affected by landslides which contributed to a decline in the shelf width and the depth of its edge. The morphology of the shelf is generally rough and thus associated with rocky outcrops alternating with patchy sedimentary cover, similar to the southern sector.

4.2. Submerged marine terraces

Five sets of marine terraces, with their inner margins located approximately at −40/−50 m, −70/−80 m, −85/−90 m, −100/−110 m and −120/−140 m were identified on the shelf around Santa Maria (Figs. 7 to 14 and 1ESM to 7ESM).

4.2.1. Terrace at −40/−50 m

This terrace is marked by an inner margin generally located between −40 m and −50 m (black line in Figs. 7–10, 12–14, and 4ESM–7ESM), whilst the outer edge depth varies between −50 m and −60 m. Overall, this terrace exhibits a patchy distribution on the northern sector and is narrow (~400 m, Fig. 7 and Table 2ESM) when compared to other terraces and to the shelf extent in the north. This terrace is ~200 m wide along the western shelf sector (Table 3ESM) extending to ~300 m and ~400 m, respectively, along the southern and the eastern shelf sectors; it is wider than the remaining terraces on the western, southern and eastern shelf sectors (Figs. 9, 10, 16 and Table 2ESM). The terrace is laterally discontinuous as it is interrupted by tectonic lineaments in the northern and western shelf sectors (respectively offshore Baía do Mar da Barca-Baía da Cré and Campo Grande, Figs. 7 and 8) and is compartmentalized by rocky blocks in the southern and eastern sectors (Figs. 9 and 10).

4.2.2. Terrace at −70/−80 m

The terrace with an inner edge located at −70/−80 m is evident in almost the entire northern shelf sector and on the summit of the pillow cone of Baixa do Ambrósio (blue line in Figs. 7–10, 12–14 and 2ESM,
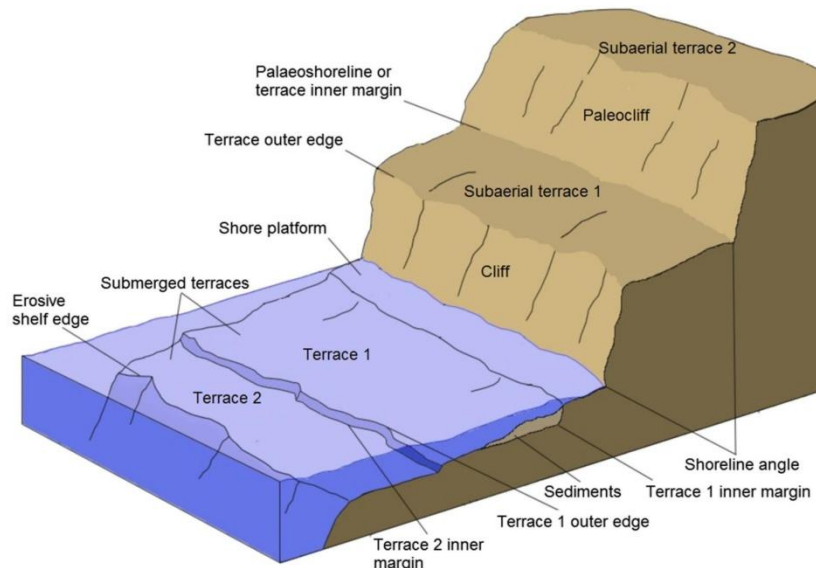
Fig. 4. Sketch showing the morphologic elements considered in this work.
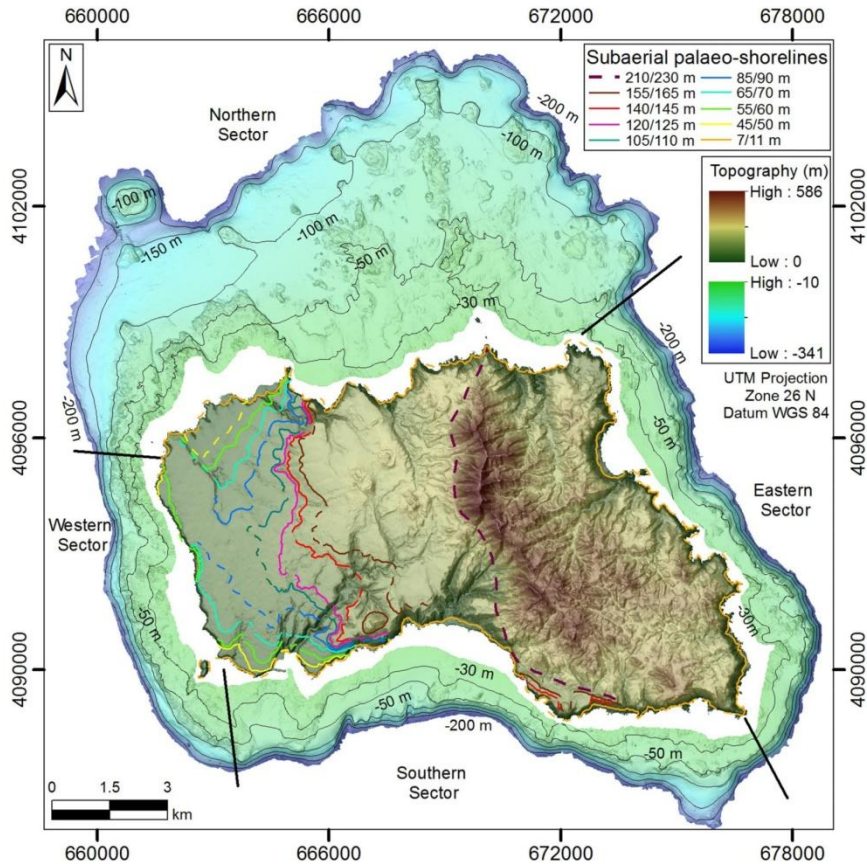
Fig. 5. Shaded relief map of the subaerial part of Santa Maria Island (1:5000 scale, digital altimetric database from Secretaria Regional do Turismo e Transportes of the Azores Government) and surrounding shelf (derived from the multibeam bathymetry). Black lines represent the limits of the Northern, Western, Southern and Eastern sectors described in the text. Colored solid and dashed lines represent the location of the evident and inferred inner margins of subaerial marine terraces. (For interpretation of the references to colour in this figure legend, the reader is referred to the web version of this article.)
Modified after Ramalho et al. (2017).

4ESM–7ESM). This terrace is up to ~2 km wide (average width of ~880 m, Table 2ESM) along the easternmost portion of the northern shelf. To the west (corresponding to the rocky blocks offshore Ponta dos Frades, Fig. 7) its expression is markedly reduced, having the same discontinuous nature as the terrace at −40/−50 m. Despite being less extensive and being partly eroded by small landslides, the same terrace is evident on the western shelf sector to the north of the WNW-ESE trending tectonic lineament offshore Campo Grande (average width of 100 m, Fig. 8 and Table 2ESM). South of this lineament it is almost absent. Along the southern shelf sector, this terrace is interrupted by tectonic lineaments, being mainly developed offshore Ponta do Castelo (~300 m wide, Fig. 9). Here the average width is about 90 m (Table 2ESM). Along the eastern shelf sector, the terrace occurs discontinuously (Fig. 10) and is ~100 m wide on average (Table 2ESM).

4.2.3. Terrace at −85/−90 m

This terrace has an inner edge located at −85/−90 m (yellow line in Figs. 7, 9, 10, 1ESM, 4ESM–7ESM) being wider in the northern shelf sector (Fig. 7), where it can attain widths of ~1 km (over 500 m on average, Table 2ESM). Along the rocky outcrops offshore Ponta dos Frades, it is also interrupted (like the two previous terraces) by

lineaments. Apart from the northern shelf sector, this terrace is also preserved in places along the southern sector (average width of 50 m, Table 2ESM), where it is also partly interrupted by tectonic lineaments (Fig. 9). Along the eastern sector it occurs sporadically with an average width of 50 m (Fig. 10 and Table 2ESM).

4.2.4. Terrace at −100/−110 m

This terrace has an inner edge located at −100/−110 m (purple line in Figs. 7–9, 11–13, 2ESM, 4ESM–6ESM) and the greatest width along the northern sector (average 800 m, Table 2ESM), which progressively decreases from west to east. This terrace has also been detected around Baixa do Ambrósio, even if it is narrower (commonly < 50 m) (Fig. 7). The inner edge also appears to be affected by the faults seen offshore Anjos and Baía da Cré (Fig. 7), although less distinctively when compared with other terraces. Along the western and southern shelf sectors the same terrace is observed in narrow strips where the shelf edge is deeper (Figs. 8, 9, and 4ESM–6ESM) and has average widths of 70 m and 50 m, respectively (Table 2ESM). In these sectors, several landslide scars make the terrace laterally discontinuous (Figs. 8 and 9). This terrace is not present on the eastern shelf sector (Fig. 10).
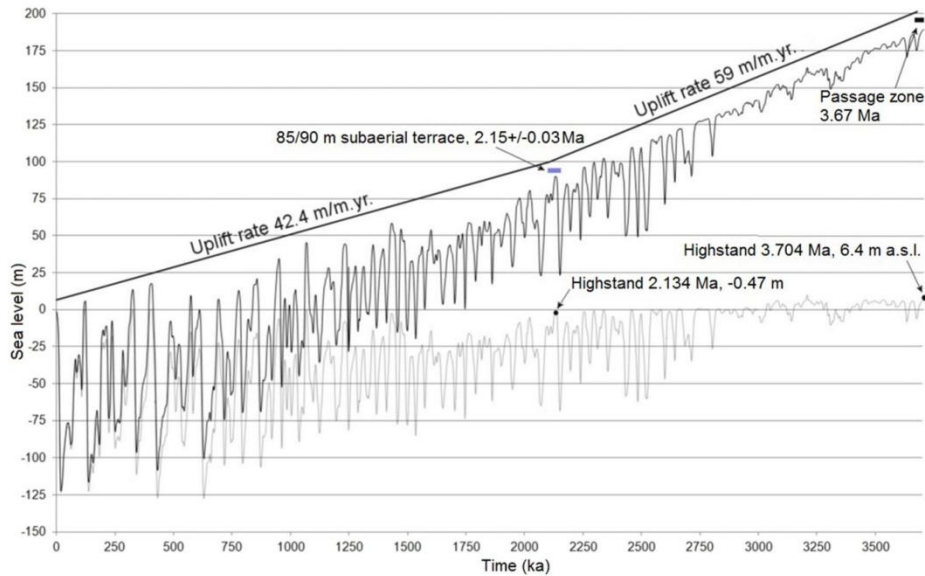
Fig. 6. Uplift trend of Santa Maria Island reconstructed on the base of a dated subaerial marine terrace (the short blue line represent its current elevation) and a passage zone between subaerial and submarine lava flows (the short black line represent its current elevation). In grey, the composite sea-level curve of Bintanja and van de Wal (2008) and De Boer et al. (2010). In black, the same sea-level curve modified according to the adopted uplift rates (see text for details). The black dots on the grey curve represent the highstands considered in our calculations. (For interpretation of the references to colour in this figure legend, the reader is referred to the web version of this article.)

4.2.5. Terrace at −120/−140 m

This is the deepest submerged terrace identified on the shelf, with the inner edge located between −120 and −140 m (red line in Figs. 7–9, 11, 13, 1ESM, 2ESM, 4ESM–6ESM). Along the eastern and central portions of the northern shelf sector it is characterized by a patchy distribution, whilst to the west it widens (offshore Anjos to Baía do Mar da Barca in Fig. 7), being characterized by a sub-horizontal surface and an evident inner edge (Fig. 1ESM). This submerged terrace has also been detected at Baixa do Ambrósio (Fig. 7). In the northern sector it has an average width of 300 m (Table 2ESM), whereas it is marked by narrow and discontinuous strips (average widths of ~100 m) affected by small-scale landslide scars on the western shelf sector (Fig. 8). Along the southern shelf sector, it is almost absent apart from a sub-horizontal surface, with an inner edge at ~ −120 m. The terrace has an average width of ~130 m (Table 2ESM) whilst its maximum width is ~300 m offshore Ponta do Castelo (Figs. 9 and 13). This terrace is also absent along the eastern sector (Figs. 10 and 14).

4.3. Correlation of marine terraces with sea-level oscillations

Following the approach described in Section 3.3, and taking into account the associated limitations and uncertainties, a possible time-frame for the formation of each marine terrace is here proposed (Fig. 15). It was assumed that the subaerial terraces were preserved when uplift quickly carried them above the level of wave action (see Trenhaile, 2002, 2014). Because of uplift, only the most recent sea-level stands could be responsible for the formation of the submerged terraces. The results of our reconstruction (Fig. 15) imply that the uppermost subaerial terrace (210/230 m a.s.l.) recognized by Ramalho et al. (2017) has no match with sea-level stands younger than 3.5 Ma. This is largely a modelling artifact given that we anchored the formation of the Pico Alto lava deltas to a particular highstand at 3.704 Ma. Moreover, the 210/230 m terrace was marked by Ramalho et al. (2017) with a high uncertainty because its morphologic imprint on the island is not

clearly recognizable. Given these limitations, we will focus our analysis on terraces that are located below the passage zone of Pico Alto's lava deltas (at approximately 200 m). These terraces can be found down to 45/50 m in elevation, after which the island is cliff-bounded, with no visible terraces excepting the 7–11 m terrace, which is preserved in places (see Fig. 5). Accordingly, we propose that the subaerial marine terraces (with the exception of the lowest and highest) were formed between 3.436 Ma to 1.065 Ma BP (Fig. 15 and Table 1ESM). The lowest subaerial terrace (7–11 m), despite being exclusively attributed to MIS 5e by Ramalho et al. (2017) on the basis of existing sedimentary deposits, according to our model could have been formed and subsequently modified from 1.749 Ma to 121 ka (a period of 1.628 m.yr, Table 1ESM). Our reconstructions also suggest that, on account of the reduction of uplift trend but also because of the gradual increase in the amplitude of the sea-level oscillations, as well as a decrease in their frequency, from 2.8 Ma to the present, the possible age interval during which sea level was able to carve and modify these terraces also increased (Fig. 15). Using the same approach, the formation and subsequent development of the submerged terraces probably took place in various stages between 1.122 Ma and 12.1 ka, with the deepest submerged terrace (−120/−140 m) being only affected by the lowstand at 19.8 ka (MIS 2; Table 1ESM).

A parameter to consider in these reconstructions is also the effective time that sea level was at a particular elevation to form a terrace (within a ± 5 m uncertainty; see Table 1ESM). This is different from the possible age interval during which sea level passed through each terrace elevation i.e., considering also the combined effects of uplift and glacio-eustatic oscillations. Whilst the possible age interval for the formation of a terrace provides us with a maximum and minimum age for that terrace, the effective time quantifies the actual amount of time sea level spent at that particular elevation. This information provides the total amount of time a terrace was effectively exposed to active wave erosion during all the cycles included within the possible age interval. For instance, the effective time during which sea level was at the elevation of
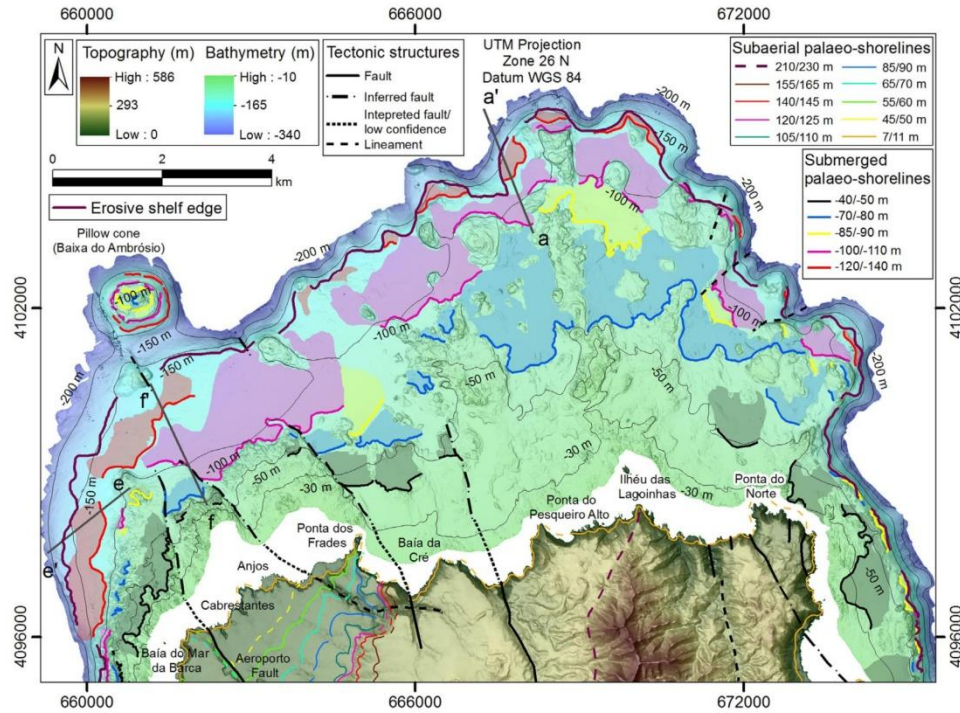
196

Fig. 7. Shaded relief map with the recognized terraces on the northern shelf sector. Colored lines offshore correspond to the inner edge of each terrace, whilst the respective colored adjacent areas to their extension. Colored lines onshore correspond to the inner edge of the raised terraces. The seismic profile aa′ is shown in Fig. 11 and seismic profiles ee′ and ff′ are respectively shown in Figs. 1ESM and 2ESM. (For interpretation of the references to colour in this figure legend, the reader is referred to the web version of this article.)

the inner margin of the 45/50 m raised terrace (305 k.yr) is estimated to be similar to that of the 155/165 m terrace (318.7 k.yr) although the possible age interval for their formation is very different (respectively 1.460 m.yr, i.e. between 2.525 Ma and 1.065 Ma, and 373 k.yr, i.e. between 3.436 Ma and 3.063 Ma, Table 1ESM).

5. Discussion

Several geological and oceanographic factors – such as uplift/subsidence rates, local changes in wave regime, shelf gradients, differential resistance to erosion, amplitude of sea-level oscillations and stillstand duration – influence the formation and preservation of marine terraces (Trenhaile, 2002, 2014; Ramalho et al., 2013). It is thus difficult to isolate, in quantitative terms, the contribution of each of these factors in controlling the spatial distribution of the observed terraces.

Our correlation between the present-day position of marine terraces and relative sea level for the last 3.5 Ma allowed us to suggest a likely timing (or age interval) of formation for each subaerial and submerged terrace. Despite the many sources of uncertainty in this approach – such as uncertainties in the adopted eustatic curve (particularly before the last 3 Ma) and in uplift rates, along with the fact that we did not incorporate any effects of glacio-isostatic adjustment –it constitutes a first-order approximation from which useful insights can be derived concerning the generation, destruction, and preservation of marine terraces along an uplifting landmass, throughout a considerable period of time (3.5 m.yr) and under the effects of multiple glacio-eustatic cycles. This integrated onshore/offshore approach has been rarely adopted but constitutes the basis for a more complete, holistic comprehension of how long-term relative sea-level change interacts with

landmasses to form distinctive coastal and nearshore morphologies such as subaerial and submerged terrace staircases.

5.1. Subaerial terraces

According to Ramalho et al. (2017), the interplay between exposure to the dominant wave direction (from the western quadrant, i.e. the windward side) and a favorable lithological/stratigraphical framework (i.e. the softer Touril sequence and the gently dipping contacts between this units and underlying Anjos and overlying Pico Alto volcanic edifices) in the western half of Santa Maria, enhanced coastal retreat and formed a wide and gently-sloping terraced morphology, under the combined action of uplift and glacio-isostatic oscillations. We agree with this model, which offers a simple-enough explanation for the island asymmetry, being in tune with the local lithological, structural, and oceanographic conditions. Our analysis, however, suggests that the effective time of formation is also an important factor contributing to the generation of the terraced morphology in this part of the island, and to the greater width of the terraces now located between 50 m and 120 m in elevation.

Our reconstructions suggest that subaerial terraces at Santa Maria are most probably polygenic because uplift rates were low enough to expose each terrace to the passage of several sea-levels (Fig. 15). As such, these terraces were affected by wave erosion during multiple cycles of rising and falling sea level (Fig. 15, Table 1ESM). According to our calculations, the effective time that each terrace was exposed to wave erosion with passing sea level spans from ~140 to ~319 k.yr, much more than the average duration of a single highstand or stillstand. A possible relationship exists between terrace width and effective time,

197

Fig. 8. Shaded relief map with the recognized terraces on the western shelf sector. Legend is the same as in Fig. 7. The seismic profile bb′ is shown in Fig. 12. (For interpretation of the references to color in this figure, the reader is referred to the web version of this article.)

e.g. wider terraces were subjected to marine erosion for longer time periods. The plot between terrace width vs effective time shown in Fig. 16 (see also Tables 1ESM and 3ESM) suggests a positive correlation between these two parameters, with terrace width increasing proportionally to the effective time they have been exposed to sea level. Notable exceptions to this trend include the 105–110 m and 155–165 m terraces, which are considered outliers for different reasons. The 105–110 m terrace coincides with the bulk of the softer Touril sequence (allowing for enhanced coastal retreat in a shorter period of time) and therefore it is not surprising it deviates from this relationship. Why the 155–165 m terrace is relatively narrow despite the fact it was probably exposed for a longer effective time (Table 3ESM) is more difficult to explain. However, a possible explanation lies in the fact that this terrace, being one of the oldest, has suffered considerable topographic decay since its formation.

A peculiar fact about Santa Maria is that it does not exhibit any well-developed raised marine terraces below 45–50 m in elevation, with the exception of the 7–11 m terrace, attributed to MIS 5e (Ramalho et al., 2013; Ávila et al., 2015; Ramalho et al., 2017). In between these elevations, only rare and poorly-developed wavecut notches can be observed (Ramalho et al., 2017). In our view, the combined effect of two factors might have contributed to this absence. One is related to the fact that in the last 1 m.yr the frequency of the glacio-eustatic oscillations started to be dominated by the longer 100 k.yr (Miller et al., 2005), reducing the effective time for erosion at each elevation over this whole period, as highstands/stillstands were fewer when compared to the Late Pliocene and Early- to Mid-Pleistocene. During the latter period, the amplitude of glacio eustatic oscillations was lower and their frequency was dominated by the 41 k.yr cycles, implying more frequent passages of sea level at each elevation (resulting in longer effective times for erosion). The second effect could be related to a slowdown in uplift rates – perhaps a slowdown even more dramatic than we modelled in Fig. 15 – during which terrace preservation would be significantly inhibited, with erosion at each subsequent highstand erasing previous terraces and contributing to the maintenance of steep plunging cliffs. This reduction in uplift rates is, in fact, supported by the position of MIS 5e deposits and notches, which indicate a relative sea-level at 7–11 m, a position just slightly above the expected elevation for MIS 5e in the area (Bintanja and van de Wal, 2008). Our reconstructions suggest that the 7–11 m erosive surface is probably polygenic, notwithstanding the fact that MIS 5e deposits can be found resting on this surface (Callapez and Soares, 2000; Ávila et al., 2008; Ávila et al., 2015; Ramalho et al., 2017). Fig. 15 shows that in the last 1.7 m.yr multiple stillstands could

Fig. 9. Shaded relief map with the recognized terraces on the southern shelf sector. Legend is the same as in Fig. 7. The seismic profile cc′ is shown in Fig. 13. (For interpretation of the references to color in this figure, the reader is referred to the web version of this article.)
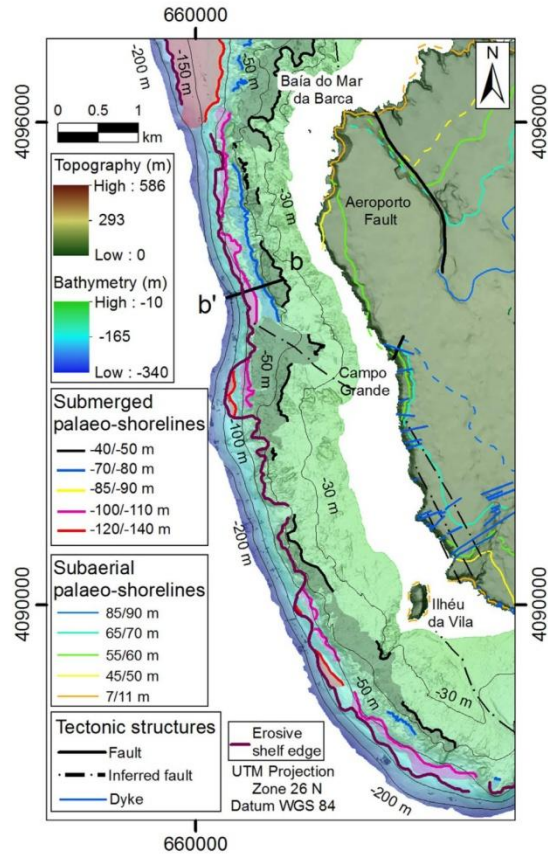
Fig. 10. Shaded relief map with the recognized terraces on the eastern shelf sector. Legend is the same as in Fig. 7. The seismic profile dd′ is shown in Fig. 14. (For interpretation of the references to color in this figure, the reader is referred to the web version of this article.)
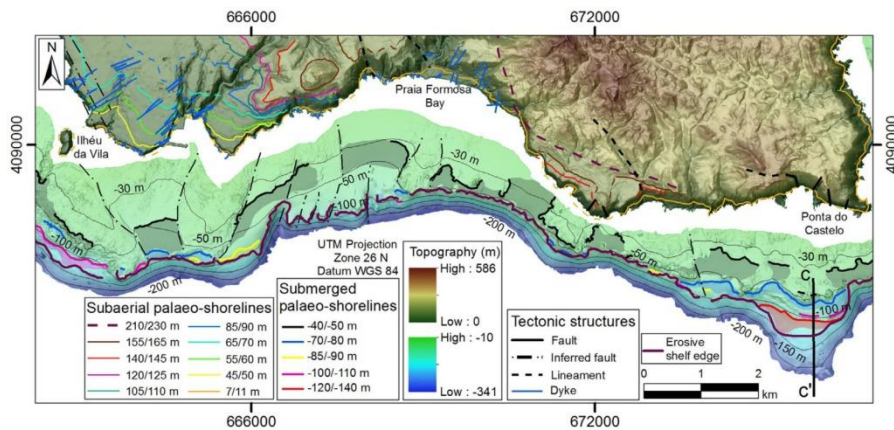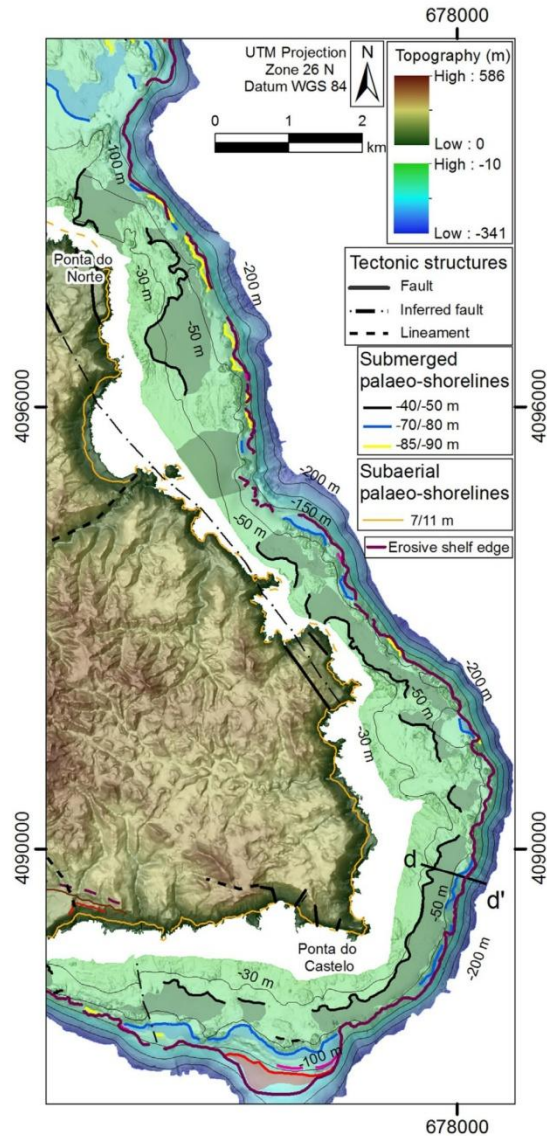
have effectively contributed to the erosion of such a surface, although this terrace had maintained a significant morphological and depositional imprint by the Last Interglacial. This highstand was thus responsible for planating even further an already existing terrace (carved during previous cycles), being also responsible for the deposition of fossiliferous beach deposits that can nowadays be found preserved at several sites along this palaeo-shoreline.

5.2. Submerged terraces

The distribution and characteristics of the submerged terraces likely result from the interaction of several factors, which contributed to their formation and preservation or destruction, depending on their position. Particularly, the width of the submerged terraces is thought to be controlled by the carved lithology, shelf gradients, water depth at the time of formation, frequency and amplitude of relative sea-level changes (Trenhaile, 2014).

Our data show that submerged terraces (except for the shallowest terrace at $-40/-50$) are much wider and better preserved in the northern shelf sector than in the other sectors. Moreover, this shelf sector is the only one exhibiting the complete set of submerged marine terraces. This situation can be explained by the low shelf gradients characterizing the northern shelf, which likely allowed for the development of much wider terraces, despite the greater wave attenuation induced by the lower gradients (Trenhaile, 2014). Lithological and structural factors probably also contributed to a greater width of terraces in this sector. The profusion of softer pyroclastic structures due to numerous cinder/scoria cones, for instance, may have allowed faster marine erosion and enhanced coastal retreat, resulting in wider terraces. Differently, the poor development or even absence of deeper terraces on the other shelf sectors (Table 2ESM) could be related to the steeper pre-existing shelf gradients on harder effusive substrates, which precluded the development and preservation of wide terraces. Previous studies (e.g. Anderson et al., 1999; Trenhaile, 2014) suggested, in fact, that terrace destruction due to marine erosion during rapidly rising sea levels (such as during glacial terminations) is more effective when shelf gradients are steeper. In addition, it should be considered that deeper terraces could have been erased by retrogressive (landward) erosion of the shelf edge by small-scale mass wasting, as suggested by the morphology of the shelf edge along the western, southern and eastern sectors (Figs. 8, 9 and 10). Effectively, along the western and southern sectors, the deepest terraces are only present where the shelf edge is preserved in deeper waters. In the eastern sector only shallow- and mid-terraces are present, because the shelf edge is always shallower than -100 m. Due to its geological structure – composed of eastward-dipping steep foresets of pillow lavas and hyaloclastites of the Pico Alto Volcanic Complex – this sector of the shelf is more prone to landsliding and therefore terraces are less likely to be preserved, particularly at greater depths (Ramalho et al., 2013; Ramalho et al., 2017).

We have also verified the possible relationship between submerged terrace width vs effective time of erosion (Fig. 16 and Table 2ESM). The data distribution is more scattered than for subaerial terrace, even if a slightly positive correlation can be visually observed in the plots. This larger scatter can be related to the fact that submerged terraces have been affected by more cycles of erosional modification during subsequent periods of rising and falling sea level, being thus characterized by a less distinctive shape than subaerial terraces (Trenhaile, 2014). Unsurprisingly, due to uplift (even if very slow) and increasing eustatic amplitudes in the Late Quaternary, the $-40/-50$ m terrace is generally the widest, except for the northern sector (Figs. 15 and 16). This surface is polygenic, and results from recurrent erosion over a greater time period than other submerged terraces (Fig. 15 and Table 2ESM). Conversely, we do not have a simple explanation for its lower width in the northern shelf sector with respect to the deeper terraces; perhaps the lithology where this terrace was carved was harder in the northern sector. More generally, it is also difficult to explain the similar range of width observed for this terrace in the different sectors, unless to imagine that the controlling factors for its genesis (shelf gradients, water depths and so on) or their interplay were quite constant around Santa Maria at the time of its formation.

5.3. Tectonic control on marine terraces

Faulting at Santa Maria clearly affects the subaerial terraces from
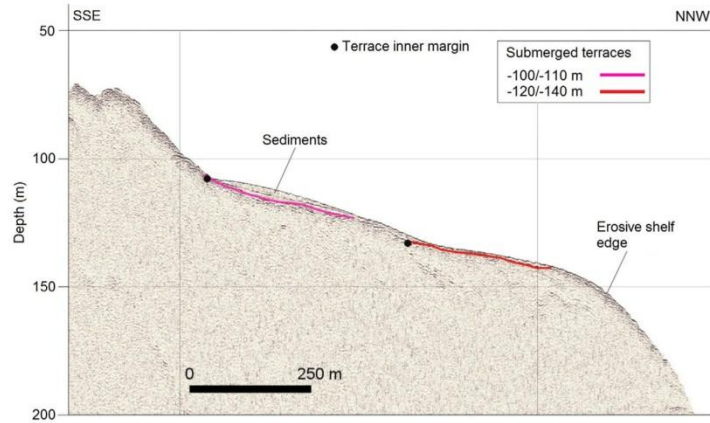
Fig. 11. Boomer seismic profile aa′ showing the shelf morphology off the northern sector of Santa Maria. Location of the seismic profile in Fig. 7. (For interpretation of the references to color in this figure, the reader is referred to the web version of this article.)
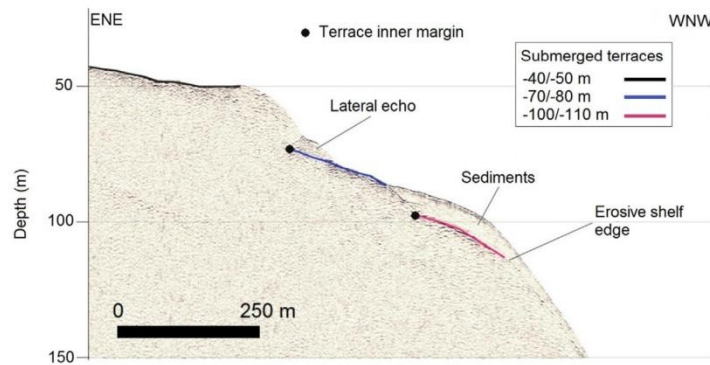
Fig. 12. Boomer seismic profile bb′ showing the shelf morphology off the western sector of Santa Maria. Location of the seismic profile in Fig. 8. (For interpretation of the references to color in this figure, the reader is referred to the web version of this article.)
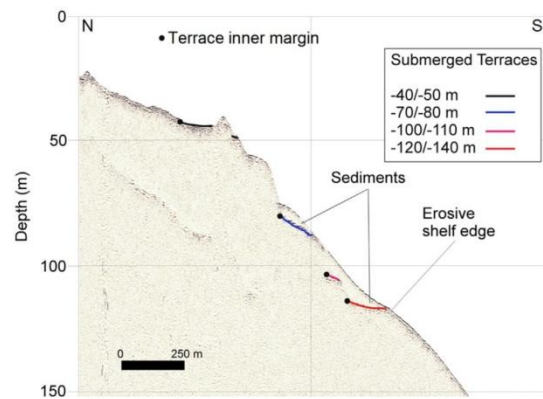
Fig. 13. Boomer seismic profile cc′ showing the shelf morphology off the southern shelf sector of Santa Maria. Location of the seismic profile in Fig. 9. (For interpretation of the references to color in this figure, the reader is referred to the web version of this article.)
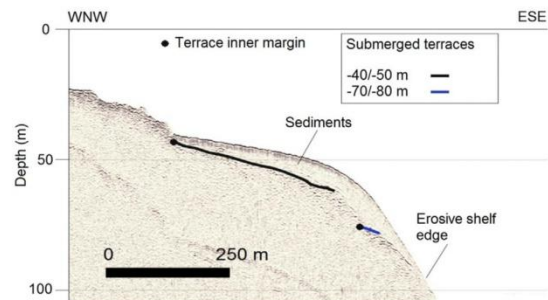
Fig. 14. Boomer seismic profile dd′ showing the shelf morphology off the eastern shelf sector of Santa Maria. Location of the seismic profile in Fig. 10. (For interpretation of the references to color in this figure, the reader is referred to the web version of this article.)

the shallowest one up to at least the 85/90 m terrace, which means that these faults could have been activated sometime after ~2.7 Ma. However, this might have started before, but due to the subaerial erosion and sediment covering of the faults it is impossible to verify. Since the faults also affect the distribution and geometry of the submerged

200
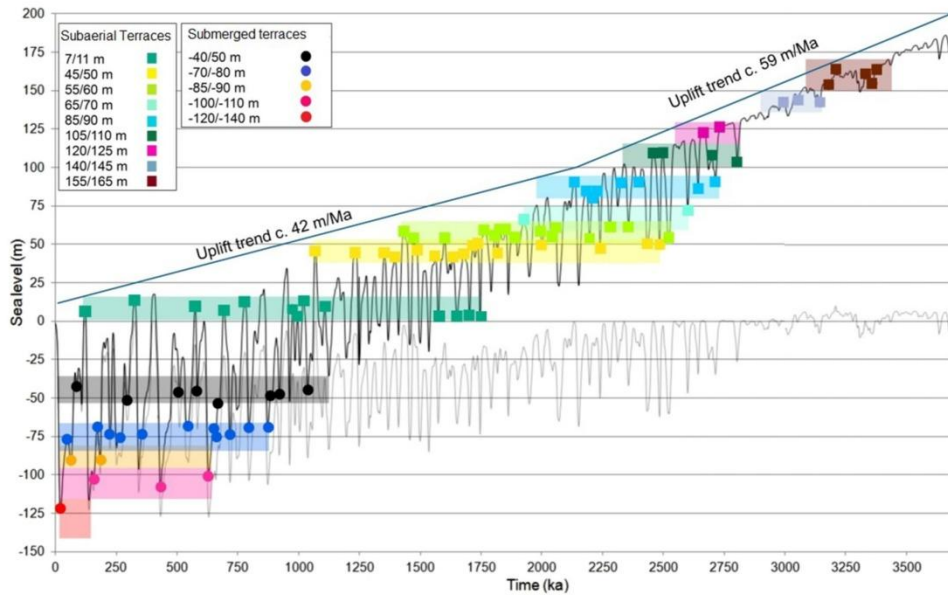
Fig. 15. Tentative correlation between the terraces and their possible timing of formation and subsequent modification within eustatic sea-level oscillations. Colored horizontal bars represent the admissible time interval during which each terrace might have been carved by marine erosion according to sea-level fluctuations and island uplift. The vertical width of each bar represents the elevation range of the terrace ± 5 m (see the text for details). The dots/squares with different colors represent sea-level highstands, lowstands or other stillstands within the respective time frame for each terrace. (For interpretation of the references to color in this figure, the reader is referred to the web version of this article.)

terraces (at least down to the −85/−90 m terrace), according to our model these faults might have been active up to at least 693 ka ago, or 15 ka at the latest. In detail, on the northern shelf sector the shallowest terrace (−40/−50 m), together with the −70/−80 m and −85/ −90 m terraces, are all affected by several NW–SE faults, located between Baía do Mar da Barca and Baía da Cré (see Fig. 7). These faults extend inland, where they displace the subaerial terraces up to 90 m in elevation, as with the "Aeroporto fault", or at Baía da Cré. The tectonic structure in this sector suggests a compartmentalization of the volcanic edifice in grabens and semi-grabens, where blocks with a relative downthrown movement experienced greater degrees of coastal retreat, allowing also for the formation of depocenters where marine sedimentation occurred. A similar situation can be observed along the deepest part of the shelf at the southern sector (Fig. 9). Here, terrace geometry and distribution are somewhat controlled by several tectonic lineaments (roughly oriented NNE–SSW) that may either correspond to faults, or to dikes that served as limiting barriers to erosion and sedimentation. The NW-SE lineament offshore Campo Grande, in the western shelf sector (Fig. 8), also limits the −70/−80 m terrace to the south of this lineament. These features show that local vertical tectonics played an important role in the development of submerged marine terraces, a role that needs further investigation. However, these local effects do not influence the overall depth ranges of marine terraces.

5.4. Terrace formation and preservation

As far as we know, Santa Maria is the only reefless volcanic island that has submerged terraces mapped with high detail. Most of the studies about terraces on volcanic islands are from reefal settings and are almost exclusively off Hawaii (e.g., Campbell, 1986; Faichney et al., 2010). Terraces in reef settings are mostly constructional in origin and hence they are of little utility for a comparison with our study. Nevertheless, some inferences can be made based on modelling of

erosional terraces (Trenhaile, 2002, 2014) and the geological record of raised and submerged terraces in other settings.

Raised terraces in Santa Maria are moderately well preserved despite their relatively old age (3.436–1.065 Ma). However, terraces developed on islands and on relatively narrow landmasses tend to be better preserved because the length of the streams is limited and so is the erosion of the landscape (Anderson et al., 1999). Two contrasting hypotheses regarding the formation/preservation of the terraces have been found in the literature. According to Pedoja et al. (2014) coastal staircase sequences are present mainly in areas where apparent uplift rates are very low to moderate, because sea level must remain stationary long enough to allow for the formation of these features. Their compilation of subaerial terraces in hotspot settings shows that these occur on islands with average uplift rates of 0.01 mm/yr. However, modelling by Trenhaile (2002, 2014) suggest that only rapid uplift rates are able to preserve terraces, otherwise these are removed by erosion and cliff retreat during periods following high, interglacial sea level. Trenhaile (2014) considers 0.02 mm/yr as slow uplift rates and 0.1 mm/yr as fast. Our data agree with the model presented by Trenhaile (2014). In fact, estimated uplift rates for Santa Maria (0.042/ 0.059 mm/yr) fall between those two values of Trenhaile (2014), which might explain why the terraces are relatively well preserved.

As for submerged terraces, modelling by Trenhaile (2014) suggests that very narrow terraces form on uplifting coasts (Fig. 6 of Trenhaile, 2014). According to this author, this is because submerged terraces are preferentially formed during lowstands and are subsequently modified (or even eliminated) during periods of rising and falling sea as they are uplifted. Our observations support, however, the preservation of different orders of submerged terraces on the shelf of Santa Maria. Not surprisingly, the average width (Table 3ESM) of the submerged terraces of Santa Maria is smaller (normally < 200 m if we exclude the northern sector) than the width of the subaerial terraces (300–500 m). A likely explanation lies in the fact, already discussed above, that submerged

201
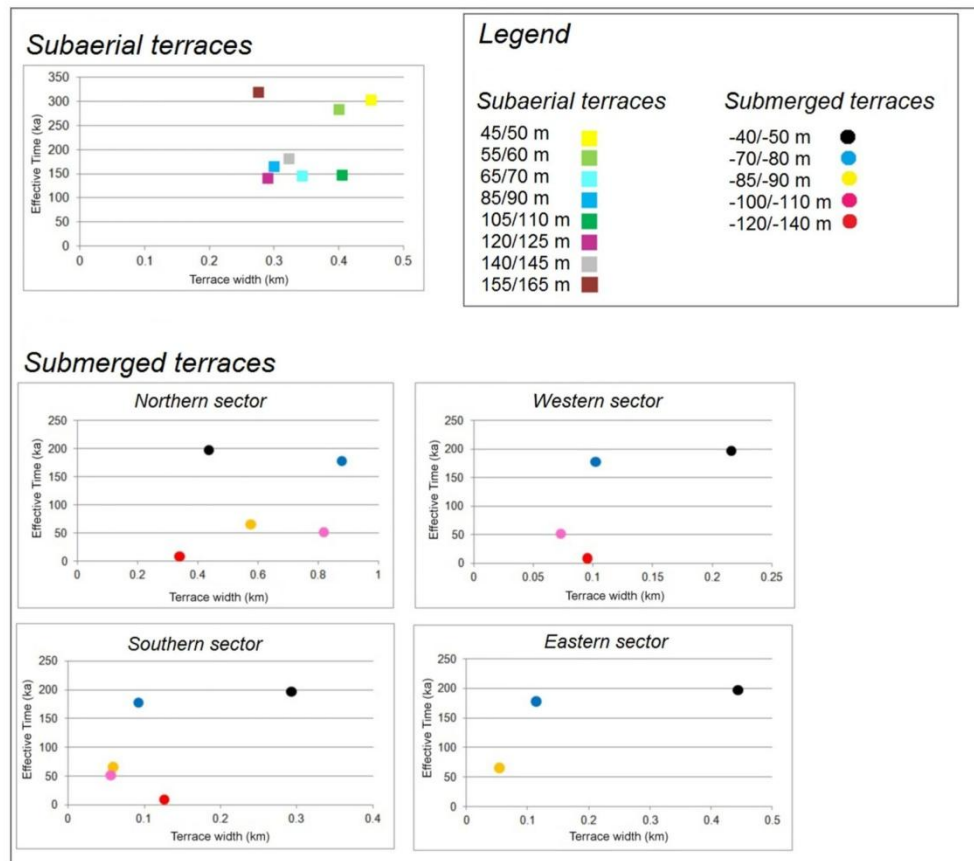
Fig. 16. Plot of the width of the subaerial and submerged marine terraces for each shelf sector against the effective time that sea level was at their vertical position (these graphs were based on the measurement of the width of the terraces along several profiles drawn in Fig. 8ESM). Note that the horizontal scale is different among shelf sectors.

terraces here bear the strong imprint of sea-level changes with much higher amplitude and lower frequency in the late Quaternary than the raised terraces formed in early-middle Quaternary (Fig. 15). According to Trenhaile (2014) the scale of sea-level oscillations has an important effect on shelf width, which increases with increasing eustatic amplitude on uplifting landmasses. The fact that submarine terraces are systematically eroded by passing sea level as the shelf widens, also contributes to a final morphology in which clearly preserved terraces are apparently not as wide as subaerial terraces.

6. Conclusions

In this study we analyzed for the first time the possible correlation between the formation of the subaerial and submerged terraces with known sea-level changes, on a reefless volcanic island setting. Our approach, including the integration of newly available high-resolution marine geophysical data with detailed onshore field studies, allowed us to:

- recognize five sets of submerged marine terraces located at different depths.
- better estimate the uplift rates for Santa Maria island, using two dated raised, subaerial palaeoshorelines and a composite sea level

curve. Those rates were used to determine the possible age interval of formation of subaerial and submerged marine terraces, ranging from 3.436 Ma to 12.1 ka BP, being formed and later modified by more than one passage of sea level.

- analyze the controlling factors on the submerged marine terraces distribution. On low gradient, and consequently wider shelves, terraces are more easily carved/preserved. Conversely, steeper shelf gradients facilitate the erosion of upper and older terraces by younger and deeper terraces in uplifting areas.
- better constrain the faulting activity at least to the 0.693–2.7 Ma period, based on the offset experienced by subaerial and submerged terraces. Activity could have been more prolonged in time, but degradation of the subaerial terraces and lack of clear evidence on the submerged ones does not allow us to extend further that period.
- propose an original and consistent reconstruction for the marine terraces formation at Santa Maria, notwithstanding the complex interplay between glacio-eustatic oscillations, marine erosion, and island uplift.

Supplementary data to this article can be found online at https://doi.org/10.1016/j.margeo.2018.09.002.

Acknowledgments

References

Anderson, R.S., Densmore, A.L., Ellis, M.A., 1999. The generation and degradation of marine terraces. Basin Res. 11, 7–19. https://doi.org/10.1046/j.1365-2117.1999.00085.x.

Andrade, C., Trigo, R.M., Freitas, M.C., Gallego, M.C., Borges, P., Ramos, A.M., 2008. Comparing historic records of storm frequency and the North Atlantic Oscillation (NAO) chronology for the Azores region. The Holocene 18 (5), 745–754. https://doi.org/10.1177/0959683608091794.

Antonioli, F., Kershaw, S., Rust, D., Verrubbi, V., 2003. Holocene sea-level change in Sicily and its implications for tectonic models: new data from the Taormina area, northeast Sicily. Mar. Geol. 3293, 1–19.

Ávila, S.P., Madeira, P., Da Silva, C.M., Cachão, M., Landau, B., Quartau, R., Martins, A.M., 2008. Local disappearance of bivalves in the Azores during the last glaciation. J. Quat. Sci. 23 (8), 777–785.

Ávila, S.P., Melo, C., Silva, L., Ramalho, R.S., Quartau, R., Hipólito, A., Cordeiro, R., Rebelo, A.C., Madeira, P., Rovere, A., Hearty, P.J., 2015. A review of the MIS 5e highstand deposits from Santa Maria Island (Azores, NE Atlantic): palaeobiodiversity, palaeoecology and palaeobiogeography. Quat. Sci. Rev. 114, 126–148. https://doi.org/10.1016/j.quascirev.2015.02.012.

Bintanja, R., van de Wal, R.S., 2008. North American ice-sheet dynamics and the onset of 100,000-year glacial cycles. Nature 454 (7206), 869–872. https://doi.org/10.1038/nature07158.

Blanchon, P., Jones, B., 1995. Marine-planation terraces on the shelf around Grand Cayman - a result of stepped Holocene sea-level rise. J. Coast. Res. 11 (1), 1–33 (PubMed PMID: WOS: A1995QG34200001).

Callapez, P., Soares, A.F., 2000. Late Quaternary marine mollusks from Santa Maria (Azores); paleoecologic and paleobiogeographic considerations. Ciências Terra (UNL) 14, 313–322.

Campbell, J.F., 1986. Subsidence rates for the Southeastern Hawaiian Islands determined from submerged terraces. Geo-Mar. Lett. 6 (3), 139–146.

Caputo, R., 2007. Sea-level curves: perplexities of an end-user in morphotectonic applications. Glob. Planet. Chang. 57 (3–4), 417–423.

Cas, R., Wright, J., 1987. Volcanic Successions. Modern and Ancient: A Geological Approach to Processes, Products and Successions. Chapman & Hall, London. https://doi.org/10.1007/978-94-009-3167-1. (528 pp.).

Casalbore, D., Falese, F., Martorelli, E., Romagnoli, C., Chiocci, F.L., 2017. Submarine depositional terraces in the Tyrrhenian Sea as a proxy for paleo-sea level reconstruction: problems and perspective. Quat. Int. 439, 169–180. https://doi.org/10.1016/j.quaint. 2016.07.051.

Coulbourn, W.T., Campbell, J.F., Moberly, R., 1974. Hawaiian submarine terraces, canyons and quaternary history evaluated by seismic-reflection profiling. Mar. Geol. 17, 215–234.

De Boer, B., Van De Wal, R.S.W., Bintanja, R., Lourens, L.J., Tuenter, E., 2010. Cenozoic global ice-volume and temperature simulations with 1-D ice-sheet models forced by benthic 18O records. Ann. Glaciol. 51 (55), 23–33.

De Guidi, G., Monaco, C., 2009. Late Holocene vertical deformation along the coast of Pantelleria (Sicily Channel, Italy). Quat. Int. 206, 158–165.

Faichney, I.D.E., Webster, J.M., Clague, D.A., Paduan, J.B., Fullager, P.D., 2010. Unraveling the tilting history of the submerged reefs surrounding Oahu and the Maui-Nui Complex, Hawaii. Geochem. Geophys. Geosyst. 11 (7), Q07002.

Ferranti, L., Antonioli, F., Mauz, B., Amorosi, A., Dai, Pra G., Mastronuzzi, G., Monaco, C., Orrù, P., Pappalardo, M., Radtke, U., Renda, P., Romano, P., Sansò, P., Verrubbi, V., 2006. Markers of the last interglacial sea-level high stand along the coast of Italy: tectonic implications. Quat. Int. 145–146, 30–54.

Firth, C., Stewart, I., McGuire, W.J., Kershaw, S., Vita-Finzi, C., 1996. Coastal elevation changes in eastern Sicily: implications for volcano instability at Mount Etna. In: McGuire, W.J., Jones, A.P., Neuberg, J. (Eds.), Volcano Instability on the Earth and Other Planets. Geol. Soc. London Spec. Publ., vol. 80. pp. 57–74.

Gente, P., Dyment, J., Maía, M., Goslin, J., 2003. Interaction between the Mid-Atlantic Ridge and the Azores hotspot during the last 85 Myr: emplacement and rifting of the hot spot-derived plateaus. Geochem. Geophys. Geosyst. 4 (10), 8514.

Hipólito, A., Madeira, J., Carmo, R., Gaspar, J.L., 2013. Neotectonics of Graciosa Island (Azores): a contribution to seismic hazard assessment of a volcanic area in a complex geodynamic setting. Ann. Geophys. 56 (6), S0677.

Instituto Hidrográfico (Ed.), 2000. Arquipélago dos Açores, 2nd edn. Roteiro da Costa de Portugal Instituto Hidrográfico, Lisboa.

Lourenço, N., Miranda, J.M., Luís, J.F., Ribeiro, A., Victor, L.M., Madeira, J., Needham, H., 1998. Morpho-tectonic analysis of the Azores Volcanic Plateau from a new bathymetric compilation of the area. Mar. Geophys. Res. 20 (3), 141–156.

Lucchi, F., 2009. Late-Quaternary marine terrace deposits as tools for wide-scale correlation of unconformity-bounded units in the volcanic Aeolian archipelago (southern Italy). Sediment. Geol. 216, 158–178.

Lucchi, F., Tranne, C.A., Calanchi, N., Rossi, P.L., 2007. Late Quaternary deformation history of the volcanic edifice of Panarea (Aeolian Arc). Bull. Volcanol. 69, 239–257.

Madeira, J., Brum da Silveira, A., Hipólito, A., Carmo, R., 2015. Chapter 3. Active tectonics in the central and eastern Azores islands along the Eurasia-Nubia boundary: a review. Geol. Soc. Lond. Mem. 44 (1), 15–32. https://doi.org/10.1144/M44.3.

Marques, F.O., Catalão, J.C., DeMets, C., Costa, A.C.G., Hildenbrand, A., 2013. GPS and tectonic evidence for a diffuse plate boundary at the Azores Triple Junction. Earth Planet. Sci. Lett. 381, 177–187.

Mauz, B., Vacchi, M., Green, A., Hoffmann, G., Cooper, A., 2015. Beachrock: a tool for reconstructing relative sea level in the far-field. Mar. Geol. 362, 1–16. https://doi.org/10.1016/j.margeo.2015.01.009.

Meireles, R.P., Quartau, R., Ramalho, R.S., Rebelo, A.C., Madeira, J., Zanon, V., Ávila, S.P., 2013. Depositional processes on oceanic island shelves—evidence from storm-generated Neogene deposits from the mid-North Atlantic. Sedimentology 60 (7), 1769–1785. https://doi.org/10.1111/sed.12055.

Miller, K., Kominz, M., Browning, J., Wright, J., Mountain, G., Katz, M., Sugarman, P., Cramer, B., Christie-Blick, N., Pekar, S., 2005. The Phanerozoic record of global sea-level change. Science 310 (5752), 1293–1298. https://doi.org/10.1126/science.1116412.

Miranda, J.M., Luís, J.F., Lourenço, N., 2018. The geophysical architecture of the Azores from magnetic data. In: Küppers, U., Beier, C. (Eds.), Volcanoes of the Azores. Active Volcanoes of the World Springer Verlag, Berlin, pp. 89–100.

Passaro, S., Ferranti, L., de Alteriis, G., 2011. The use of high-resolution elevation histograms for mapping submerged terraces: tests from the Eastern Tyrrhenian Sea and the Eastern Atlantic Ocean. Quat. Int. 232 (1–2), 238–249.

Pedoja, K., Husson, L., Johnson, M.E., Melnick, D., Witt, C., Pochat, S., Nexer, M., Delcaillau, B., Pinegina, T., Poprawski, Y., Authemayou, C., Elliot, M., Regard, V., Garestier, F., 2014. Coastal staircase sequences reflecting sea-level oscillations and tectonic uplift during the Quaternary and Neogene. Earth-Sci. Rev. 132, 13–38.

Pirazzoli, P.A., Radtke, U., Hantoro, W.S., Jouannic, C., Hoang, C.T., Causse, C., et al., 1993. A one million-year-long sequence of marine terraces on Sumba Island, Indonesia. Mar. Geol. 109 (3), 221–236.

Porębski, S., Gradziński, R., 1990. Lava-fed Gilbert type delta in the Polonez Cove Formation (Lower Oligocene), King George Island, West Antarctica. In: Colella, A., Prior, D. (Eds.), Coarse Grained Deltas. International Association of Sedimentologists Special Publication 10pp. 333–351. https://doi.org/10.1002/9781444303858.ch19.

Quartau, R., Mitchell, N.C., 2013. Comment on "Reconstructing the architectural evolution of volcanic islands from combined K/Ar, morphologic, tectonic, and magnetic data: the Faial Island example (Azores)" by Hildenbrand et al. (2012). [J. Volcanol. Geotherm. Res. 241-242 (2012) 39-48]. J. Volcanol. Geotherm. Res. 255, 124–126.

Quartau, R., Tempera, F., Mitchell, N.C., Pinheiro, L.M., Duarte, H., Brito, P.O., Bates, R., Monteiro, J.H., 2012. Morphology of the Faial Island shelf (Azores): the interplay between volcanic, erosional, depositional, tectonic and mass-wasting processes. Geochem. Geophys. Geosyst. 13, Q04012. https://doi.org/10.1029/2011GC003987.

Quartau, R., Hipólito, A., Romagnoli, C., Casalbore, D., Madeira, J., Tempera, F., Roque, C., Chiocci, F.L., 2014. The morphology of insular shelves as a key for understanding the geological evolution of volcanic islands: insights from Terceira Island (Azores). Geochem. Geophys. Geosyst. 15, 1801–1826.

Quartau, R., Madeira, J., Mitchell, N.C., Tempera, F., Silva, P.F., Brandao, F., 2015. The insular shelves of the Faial-Pico Ridge (Azores archipelago): a morphological record of its evolution. Geochem. Geophys. Geosyst. 16, 1401–1420.

Ramalho, R.S., 2011. Building the Cape Verde Islands, 1st ed. Springer, Berlin. https://doi.org/10.1007/978-3-642-19103-9. (207 pp.).

Ramalho, R.S., Helffrich, G., Schmidt, D.N., Vance, D., 2010a. Tracers of uplift and subsidence in the Cape Verde Archipelago. J. Geol. Soc. Lond. 167 (3), 519–538. https://doi.org/10.1144/0016-76492009-056.

Ramalho, R.S., Helffrich, G., Cosca, M., Vance, D., Hoffmann, D., Schmidt, D.N., 2010b. Episodic swell growth inferred from variable uplift of the Cape Verde hotspot islands. Nat. Geosci. 3 (11), 774–777. https://doi.org/10.1038/ngeo982.

Ramalho, R.S., Helffrich, G., Cosca, M., Vance, D., Hoffmann, D., Schmidt, D.N., 2010c. Vertical movements of ocean island volcanoes: insights from a stationary plate environment. Mar. Geol. 275, 84–95. https://doi.org/10.1016/j.margeo.2010.04.009.

Ramalho, R.S., Quartau, R., Trenhaile, A.S., Mitchell, N.C., Woodroffe, C.D., Ávila, S.P., 2013. Coastal evolution on volcanic oceanic islands: a complex interplay between volcanism, erosion, sedimentation, sea-level change and biogenic production. Earth Sci. Rev. 127, 140–170.

Ramalho, R.S., Helffrich, G., Madeira, J., Cosca, M., Thomas, C., Quartau, R., Hipólito, A., Rovere, A., Hearty, P., Ávila, S.P., 2017. Emergence and evolution of Santa Maria Island (Azores) – the conundrum of uplifted islands revisited. Geol. Soc. Am. Bull. 129, 2017. https://doi.org/10.1130/B31538.1.

Rusu, L., Guedes Soares, C., 2012. Wave energy assessments in the Azores islands. Renew. Energy 45, 183–196.

Schwartz, D.M., Soule, S.A., Wanless, V.D., Jones, M.R., 2018. Identification of erosional terraces on seamounts: implications for interisland connectivity and subsidence in the Galápagos Archipelago. Front. Earth Sci. 6, 88. https://doi.org/10.3389/feart.2018.00088.

Serralheiro, A., 2003. A geologia da ilha de Santa Maria, Açores. Açoreana 10 (1), 141–192.

Serralheiro, A., Alves, C.A.M., Forjaz, V.H., Rodrigues, B., 1987. Carta Vulcanológica dos Açores. Ilha de Santa Maria na escala 1/15 000 (folhas 1 e 2). Serviço Regional de

Protecção Civil dos Açores, Universidade dos Açores and Centro de Vulcanologia.

Sibrant, A.L.R., Hildenbrand, A., Marques, F.O., Costa, A.C.G., 2015. Volcano-tectonic evolution of the Santa Maria Island (Azores): implications for paleostress evolution at the western Eurasia–Nubia plate boundary. J. Volcanol. Geotherm. Res. 291, 49–62.

Trenhaile, A.S., 2002. Modeling the development of marine terraces on tectonically mobile rock coasts. Mar. Geol. 185, 341–361.

Trenhaile, A.S., 2014. Modelling the effect of Pliocene–Quaternary changes in sea level on stable and tectonically active land masses. Earth Surf. Process. Landf. 39, 1221–1235. https://doi.org/10.1002/esp.3574.

Trenhaile, A.S., 2015. Coastal notches: their morphology, formation, and function. Earth Sci. Rev. 150, 285–304. https://doi.org/10.1016/j.earscirev.2015.08.003.

Zazo, C., Goy, J.L., Hillaire-Marcel, C., Gillot, P.Y., Soler, V., González, J.Á., Ghaleb, B., 2002. Raised marine sequences of Lanzarote and Fuerteventura revisited - a re-appraisal of relative sea-level changes and vertical movements in the eastern Canary Islands during the Quaternary. Quat. Sci. Rev. 21 (18–19), 2019–2046. https://doi.org/10.1016/S0277-3791(02)00009-4.

Zazo, C., Goy, J.L., Dabrio, C.J., Soler, V., Hillaire-Marcel, C., Ghaleb, B., et al., 2007. Quaternary marine terraces on Sal Island (Cape Verde archipelago). Quat. Sci. Rev. 26 (7–8), 876–893.

Zbyszewski, G., Ferreira, O.V., 1960. Carta geológica de Portugal, Ilha de Santa Maria (Açores), scale 1:50 000. Serviços Geológicos de Portugal.

204

9. FACTORS CONTROLLING SHELVES FORMATION AND EVOLUTION: A COMPARISON BETWEEN THE AEOLIAN AND THE AZORES

The detailed analysis of the insular shelves surrounding the islands of the Central Aeolian archipelago and Santa Maria Island in the Azores allowed us to investigate the processes that control their formation and evolution, and to compare the related effects on islands characterized by markedly different age, geodynamic and oceanographic contexts. The morphological characteristics of the shelves around the central Aeolian sector and Santa Maria are typical of insular shelves formed by marine erosive processes, located in reefless areas. Wave erosion, along with subaerial erosion, is the most powerful agent promoting the destruction of volcanic islands' flanks and the coastline retreat. Combined with sea-level changes (due to eustatic fluctuations occurring during the Pliocene and Quaternary and to vertical crustal movements), wave erosion may affect (and be recorded within) a large range of depth/heights. Nevertheless, several other factors, such as the different time of exposure to marine erosion, the degree of wave exposure, active tectonics and mass wasting, post-erosional volcanism and varied geological resistance to erosion, can interplay in a complex manner and influence the final morphology of insular shelves. In this chapter the effects of these processes are discussed and compared, taking the shelves of the central Aeolian sector and Santa Maria Island as case studies.

TIME OF EXPOSURE TO MARINE EROSION

Overall, by comparing the studied shelves with the subaerial portions of the islands forming the central Aeolian sector and Santa Maria, a good correspondence between the shelf width and the age of the volcanic edifices onshore is commonly observed, as pointed out for other volcanic islands such as the Canaries (Menard, 1983; Mitchell et al., 2003; Llanes et al., 2009), Antilles (Le Friant et al., 2004), Faial, Pico and Terceira in the Azores (Quartau et al., 2010, 2012, 2015b; Casalbore et al., 2015) and other Aeolian Islands (Romagnoli, 2013). At Salina, the widest shelves located offshore the W, the NE and the SE sectors are associated to the oldest volcanic edifices of Pizzo Corvo, Pizzo Capo and Monte Fossa delle Felci (Lucchi et al., 2013a; Manuscript I) or to some early centers not exposed onland. At Lipari, the widest shelf sector mostly runs along the western coastline, offshore the "older volcanoes" and "the western volcanoes" recognized by Forni et al. (2013) as the oldest of the island, and in a small sector around the Monte Rosa volcano in the eastern part (Romagnoli et al., 2013a). Likewise, the widest shelves recognized around Vulcano are located offshore the now almost entirely dismantled Capo Secco lava cone, referred as the first site of subaerial activity of the island (De Astis et al., 2013; Romagnoli et al., 2013b). At Santa Maria, the widest northern shelf (c. 8 km wide) is carved on the flanks of the oldest (now partly dismantled) stratovolcano of the island, belonging to the Anjos Volcanic complex (Ramalho et al., 2017). In this thesis, the relationship between shelf width, erosive edge depth and age of the related volcanic units (where available) has been investigated with more detail. In particular, at Salina the northwestern (sector 4 in Table 9.1) and the southeastern (Sector 7 in Table 9.1) shelf sectors are characterized by wide (1730 m and 1690 m, respectively) and deep (-141 m and -212 m, respectively) shelves, compared with the age of the products outcropping onshore (244 ka and

160 ka, respectively) and considering the history of vertical movements of the island (see Manuscript II). These evidences are explained with the occurrence of early volcanic centers, presently partly dismantled, whose products are no more exposed onland and that likely predate the volcanic activity onshore (see Manuscrtipt I, chapter 5.1). The age of these eruptive centres is unknown due to the lack of rock samples for dating, however by correlating the erosive edge depth with the sea-level curve of Rohling et al. (2014) and assuming a steady state of subsidence they have been associated to the MIS 10 (356 ka, northwestern sector) and MIS 12 (465 ka, southeastern sector, see Manuscript II, chapter 5.2). Likewise, at Santa Maria by correlating the erosive edge depth with the relative sea-leve curve and taking into account the vertical mobility of the island, the deep shelf area found on the northwestern sector has been tentatively associated to an early center that predates the volcanic activity onshore (Proto-Santa Maria island, see Manuscript IV). The wide shelf (c. 8 Km) of the northeastern sector, being slightly shallower, has been instead related to the initial volcanic activity of the Anjos stratovolcano (see Chapter 7).

By comparing the width of the shelves surrounding Santa Maria with those in the central Aeolian islands, the former (and older) appear much larger, indicating the role exerted by the time of exposure to marine erosive processes and sea-level fluctuations (see below and chapters 5 and 7). Accordingly, the widest shelf sectors observed off the oldest portions of the central Aeolian sector is c. 2 km wide (Lipari and Salina), that is a minimum value for shelf width in Santa Maria, where some shelf sectors exhibit a width of c. 8 km (Table 9.1). The erosion rates estimated for Santa Maria and the Aeolians are then obtained by dividing the maximum shelf width for the age of the products exposed on land. This method, adopted by several authors (see Quartau et al., 2012; Romagnoli and Jacobsson, 2015 and references therein), provides a rough estimate of cliff recession rate, since several factors may cause an overestimation or underestimation of the real amount of shelf widening/cliff retreat. Measures have been carried out considering only the maximum shelf width because a sector affected by mass wasting, exhibits a shelf that is narrower due to a process that is not related to wave erosion (see Chapter 3).

Santa Maria			
	Age (Ma)	Shelf width (m)	Erosion rate (mm/yr)
N sector	5.8	8200	1.41
W sector	5.8	5000	0.86
E sector	4.1	2360	0.58
S sector	5.8	2610	0.45
Salina			
	Age (ka)	Shelf width (m)	Erosion rate (mm/yr)
Sector 2	465	2048	4.40
Sector 4	356(244)	1730	4.86 (7.09)
Sector 5	244	750	3.07
Sector 7	465 (160)	1690	3.63 (10.56)
Sector 6	160	720	4.5
Sector 3	70	960	13.71
Sector 1	70	650	9.28
Lipari			
	Age (ka)	Shelf width (m)	Erosion rate (mm/yr)
Timp. Carrubbo	465 (?)	1515	3.26
M.Mazzacaruso	465 (?)	2048	4.40
Chiesa Vecchia	356(188)	2115	5.94 (11.25)
SE sector	43	463	10.77
SW sector	43	862	20.04
NEsec. CapoRosso	27	560	20.74
NEsec. RoccheRosse	1.4	227	162.1
Vulcano			
	Age (ka)	Shelf width (m)	Erosion rate (mm/yr)
Capo Secco	c.127	1367	10.76

Table 9.1. *Time averaged shelf erosion rates estimated for the studied islands, obtained by considering the age of the volcanic units onshore (in black) or the inferred age of the offshore portions (in red). See Manuscript I, II and IV for details and references for absolute ages.*

If we compare the time-averaged shelf erosion rates obtained for the Central Aeolian sector and at Santa Maria (Table 9.1), based on the age of related products onland (that is a minimum age), average erosion rates appear one order of magnitude higher in the central Aeolian islands, being from c. 3 to c. 11 mm/yr against 0.4-1.4 mm/yr obtained for Santa Maria (Table 9.1). Remarkably, the erosion rates in the Aeolians are of the same order of magnitude of those calculated for Faial and Terceira in the Azores (12-20 mm/yr, Quartau et al., 2015a) whose ages are comprised

between c. 120-400 ka. The erosion rates calculated for Santa Maria are instead similar to those of older volcanic islands as the Canary (0.6 mm/yr), the reefless Hawaiians (1.7 mm/yr, Menard, 1983, 1986) and Lord Howe island, Australia (1.7 mm/yr, Dickinson, 2004). Erosion rates appear thus dependent on the period of detection, being higher in the short term, and this tendency is probably associated to the episodic nature of cliff recession (Quartau et al., 2010).

In the short-term, Romagnoli and Jakobsson (2015) described the effects of marine erosion on cliff recession in the newly formed island of Surtsey (Iceland) emerged in the North Atlantic in 1963, and compared them with other young volcanic islands characterized by surtseyan (phreatomagmatic) activity. They found that during syn-eruptive stages, or shortly after the end of the eruption (i.e. first months/years), erosion rates are very high, ranging from c. 10 to more than c. 100 m/yr, while they are lower (from some metres per year to less than 1 m) on longer time range (decades). However, these estimate refer to present shore platforms, and cannot take into account the contribution of sea-level fluctuations.

Conversely, wave attenuation induced by shore platforms or insular shelves appear to play an important role if long periods of time are considered: in fact, as the shelf become wider and gently-sloping, the increasing effect of wave attenuation reduces the energy of marine erosion, resulting in slower rates of cliff recession. As a consequence, erosion rates appear lower for islands surrounded by wider shelves (Trenhaile, 2000), like Santa Maria, and this may cause the relationship between time and shelf widening to be not-linear and long term (Mitchell et al., 2003; Llanes et al., 2009; Quartau et al., 2010). The Aeolian Islands are relatively young compared with Santa Maria and other oceanic islands, therefore they are far from that "state of equilibrium" (Trenhaile, 2000; Quartau et al., 2010), as demonstrated by their higher rates. Nevertheless, it is likely that the relatively high (compared to Santa Maria) uplift rate of the Aoelian Islands in the last 127 ka and the active volcanism, are actively opposing the shoreline erosion, helping the islands to survive the erosive processes.

DEGREE OF WAVE EXPOSURE

Wave erosion is also strongly influenced by the exposure to dominant winds, which is considered a first-order controlling factor on the effectiveness of marine erosion processes (Llanes, 2009; Quartau et al., 2010; Romagnoli and Jakobsson, 2015). The intensity of marine erosion and the rate of shorelines retreat are linked to wave energy parameters (Trenhaile, 1987, 2000, 2001). Normally, insular shelves carved in volcanic products of similar age are wider if located offshore the windward side of the island (Quartau et al., 2010; 2014 Romagnoli et al., 2013 and Manuscript I), i.e. more exposed to the energy of the waves, as observed at Prince Edward Island in the Indian Ocean (Mitchell et al., 2003), Madeira in the Atlantic (Brum da Silveira et al., 2010b), and the Hawai'i in the Pacific (Menard, 1986), Gomera in the Canary Islands (Llanes et al., 2009). Furthermore, the Azores islands are located in a more energetic environment (the Atlantic Ocean) with respect to the Aeolian archipelago (Mediterranean Sea), and they are struck by more severe and frequent storms (maximum H_s up to c. 20 m vs 6 m, respectively; Cicala, 2000; Andrade et al., 2008; Rusu and Guedes Soares, 2012). In the Azores, in fact, c. 70% of the most energetic waves comes from north, west and northwest (Andrade et al., 2008). The fetch exposition is also higher in the Azores (more than 1000 nautical miles for the westernmost sectors) with respect to

the Aeolian islands (c. 300 nautical miles). Accordingly, the widest shelf sectors are commonly located off the northern and western side of the islands (Quartau et al., 2012, 2014, 2015b). In this work (Chapter 7, Manuscript IV) it is proposed that, due to the effects of northwestern stronger winds, the southern shelf sector at Santa Maria is narrower with respect to the northern one, despite being both carved in the same volcanic products (Anjos Volcanic Complex).

The effects of wave exposure on shelf width has also been locally observed in the Aeolian Islands, despite the milder meteo-marine conditions with respect to the Atlantic. In the Southern Tyrrhenian Sea, stronger winds and major storms usually come from the west and northwest direction. Nevertheless, this relationship is not always straightforward, since other factors, such as the occurrence of eccentric eroded cones, might influence the shelf width independently from the exposure to dominant winds and the waves energy (see for instance in the southeastern portion of Salina, that is a sheltered sector with respect to westerly winds). For instance, the marked difference in width off the eastern side of Pizzo Capo at Salina, has been partly related to the slightly different age of the erupted products (see Manuscript I).

ISLANDS VERTICAL MOBILITY AND RELATIVE SEA-LEVEL FLUCTUATIONS

As indicated in Chapters 6 and 8, volcanic islands are normally affected by vertical movements. Most of the oceanic volcanic islands are subjected to long term subsidence due to flexural loading (Walcott, 1970; Watts and ten Brinck, 1989), age-driven plate cooling (Stein and Stein, 1992) and hot spot swell decay (Morgan et al., 1995; Ramalho, 2011), while hotspot swell growth, far field effects of surface loading by other islands, vicinity to active plate margins, erosional unloading and mass wasting might be responsible for islands' uplift (McNutt and Menard, 1978; Melosh, 1978; Grigg and Jones, 1997; Rubin et al., 2000; Menendez et al., 2008; McMurtry et al., 2010; Madeira et al., 2010; Ramalho et al., 2010a,b,c; Ramalho, 2011). Uplift can also be a common process in the evolution of a volcanic island. Long-lived islands (over 10 Ma old) such as Sal, Boa Vista, Maio and Fuerteventura in the Atlantic Ocean, survived marine erosive processes because of the uplift (and wave attenuation effects, as discussed above)(Zazo et al., 2002; Dyhr and Holm, 2010; Ramalho et al., 2010 a, b;). Santa Maria is in such an age range. The uplift trend is considered to have almost doubled its area (Quartau et al., 2016), opposing to the effects of coastline retreat.

The effects of the islands vertical mobility on the development of insular shelves are still debated (Marques et al., 2016; Quartau et al., 2016), although many authors agree that subsidence affects the width of the shelves (Menard, 1983; Ramalho et al., 2013, 2017; Quartau et al., 2014; Trenhaile, 2014) and its effect can cause overestimation when measuring the waves erosion rates. Quartau et al. (2018b) quantitatively assessed the contribution of subsidence to shelf widening by comparing the present width of real cross-shore profiles with modeled profiles at Faial and Pico islands (Azores archipelago), revealing that subsidence might increase the shelf width up to 2.5 times. Because of subsidence, the nearshore water depth increases and consequently wave attenuation decreases, promoting the migration of the breaker zone close to the shore. Therefore, the wave energy at the cliff toe increases, boosting the shoreline retreat (Trenhaile, 2014). Moreover, subsidence may bring the erosive shelf edge below the maximum depth reached by the sea-level during lowstands. In such cases the erosive shelf edge is more protected from the erosion accomplished in the intertidal zone during the successive lowstand

209

stages, promoting shelf widening (Quartau et al., 2018b). The effects of subsidence and uplift on the shelf width are invariably connected with relative sea-level fluctuations. In particular, the amplitude of sea-level changes (local or global) has a profound effect on insular shelves development because of its impact on marine erosion. Generally, large eustatic variations (as those occurring since c. 1 Ma, Bintanja et al., 2005; Bintanja and van de Wal, 2008) promote the formation of wide and deep shelves. The islands of the central Aeolian sector are all younger than 450 ka, therefore they suffered only Late Quaternary (high-amplitude) sea-level fluctuations. Conversely, the shelf around Santa Maria was initially carved during low-amplitude sea-level fluctuations conditions (until 1 Ma ago), when the marine erosion probably started forming the presently wide shelf surrounding the island. Despite being difficult to quantitatively assess how the low-amplitude fluctuations affected the wave erosion rates during the first stages of development of the island, it is proposed that the rate of shelf widening around Santa Maria sharply increased 1 Ma ago (Chapter 8, Manuscript V). Since the last 1 Ma, in fact, the amplitude of the eustatic sea-level cycles remained almost constant (Bintanja et al., 2005; Bintanja and van de Wal, 2008; Rohling et al., 2014), a condition that promoted the formation of wide and gently sloping shelves and the achievement of a state of static equilibrium in the studied areas. The increased wave erosion due to high-amplitude sea-level fluctuations might have been partly compensated by the increased wave attenuation and slower coastline erosion due to uplift of the island (Trenhaile, 1989, 2001).

The islands studied in this project have been affected by early subsidence changing to uplift during their geological evolution. In the central Aeolian sector, the rates of uplift have been calculated by Lucchi (2009), Lucchi et al. (2013a, b) on the base of subaerial, raised marine terraces, while the subsidence trend was inferred taking into account the insular shelf edges by Lucchi et al. (in press; Chapter 6). An uplift of 0.34/0.36 m/ka, active since the Last Interglacial, has been estimated, while subsidence was likely active before (at least since the MIS 12) at a rate of 0.39/0.56 m/ka at Salina and 0.24/0.28 m/ka at Lipari (see chapter 6). Santa Maria has been affected by early subsidence at an average rate of c. 0.1 m/ka from 5.5 to 3.5 Ma, which then turned into uplift with a progressively decreasing rate of 0.059/0.042 m/ka (Ramalho et al., 2017; chapter 8)(Table 9.2). This complex vertical behavior results in the setting of the studied insular shelves. The relatively high subsidence rate of Salina and Lipari might have boosted the shelf widening, and likely partly explain the higher shelf erosive rates in the central Aeolian sector.
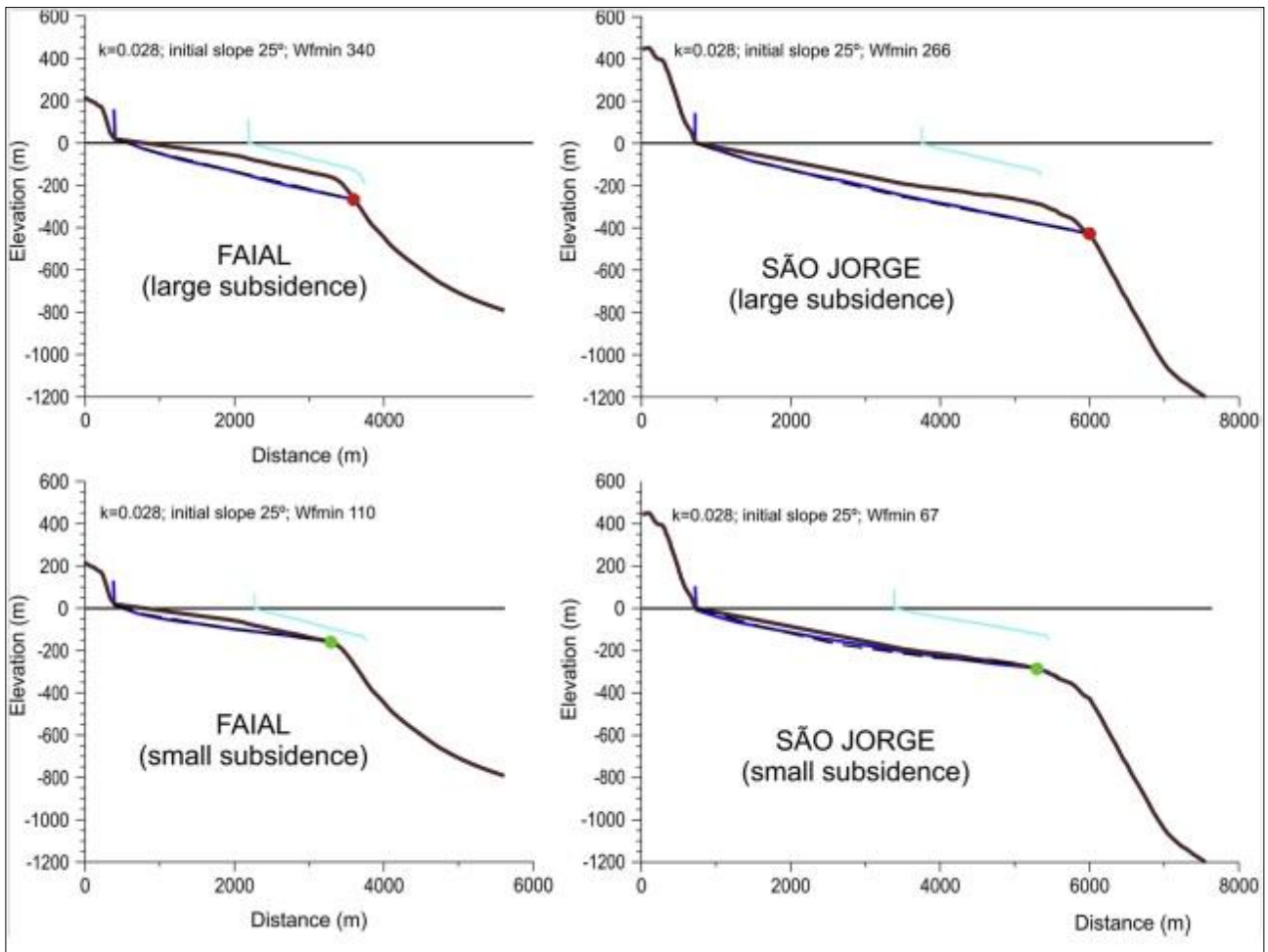
Fig. 9.1 *Simulated cross-shore shelf profiles. In brown the present day profile, in dark blue and in light blue the same profile with and without subsidence respectively (Modified after Quartau et al., 2018b).*

	Uplift (m/ka)	Period		Subsidence (m/ka)	Period
Salina	*0.36**	MIS 5.5 - present		*0.39/0.56*	MIS 12 (?) - MIS 5.5
Lipari	*0.34**	MIS 5.5 - present		*0.24/0.28*	MIS 12 (?) – MIS 5.5
S. Maria	*0.059*	3.5 - 2.15 Ma		*0.1**	6 (?) – 3.5 Ma
	0.042	2.15Ma - present			

Table 9.2 *Average uplift and subsidence rates derived from literature (with asterisk: Lucchi et al., 2013b; Ramalho et al., 2017) and calcaluted for Salina, Lipari and Santa Maria Islands.*

TECTONICS AND MASS WASTING

Active or inherited volcano-tectonic structures resulting from either regional or local tectonic/volcanic stresses might influence the coastal and shelf morphology. Erosion rates might be influenced by active or inactive tectonic structures such as faults and dikes that may have effects on the geometry of coastal and marine areas (Ramalho et al., 2013). Tectonic lineaments represent weakness features that promote differential erosion, while faults slips might trigger mass wasting processes affecting the shelf width and the depth of the shelf edge. Regional and

local structural controls have been recognized both in the Azores (Madeira at al., 2015) and in the Aeolian Archipelago (Ventura et al., 2013). Long-terms and large-scale deformation due to the geodynamic setting of both archipelagoes are reflected, for instance, in vertical movements affecting the islands in opposite direction (uplift/subsidence; Lucchi et al., 2007b; Lucchi, 2009; Ramalho et al., 2017). At the local scale, fault activity might superimpose on the regional tectonic trends. At Santa Maria, several faults observed onshore (Madeira et al., 2015) are developed also on the surrounding shelf, affecting the morphology of the subaerial and submerged portions of the islands and the marine terraces distribution and width (see the western shelf of Santa Maria, Fig. 8 in Manuscript V, chapter 8). In the southern shelf sector, tectonic lineaments apparently promoted the development of scars that, in turn, contributed to the shelf narrowing (Figure 9 in Manuscript V, chapter 8). Conversely, in the central Aeolian sector the effects of faulting activity on the development of the shelf is less evident, although it appears to locally induce mass wasting or tectonic subsidence (see chapters 4 and 5).

Mass wasting at different scales contributes significantly to shelf and subaerial island dismantling that, in turn, would amplify the erosion of the coastlines, due to retrogressive erosion. Moreover, the removal of the gently-sloping surface of the shelf reduces the wave attenuation. The subaerial and submerged flanks of volcanic islands are frequently dominated by large-scale sector collapses, as observed in the Hawaii (Moore et al., 1994), Canaries (Masson et al., 2002), La Reunion (Oehler et al., 2008), Stromboli in the Aeolian Archipelago (Romagnoli et al., 2009a and 2009b), Aleutians (Montanaro and Beget, 2011) and Madeira island (Quartau et al., 2018b). However, at Santa Maria and in the Central Aeolian sector large-scale instability features are not observed. Insular shelves here are instead affected by local erosion at the outer edge (Chiocci and Casalbore, 2017).

At Santa Maria, erosive scars located at or close to the shelf edge do not exhibit any direct connection with the subaerial drainage system in the present high-stand condition, therefore the risk of shelf retreat due to gullies and canyons is much lower when compared to the Aeolian Archipelago. Here, offshore the eastern side of Salina, the eastern side of Lipari and the western and eastern sides of Vulcano (see Manuscript I and chapter 6) some portions of the shelf are poorly developed and dissected by scars converging in larger channels at deeper depths. This, along with the connection with the subaerial drainage system, promotes the erosion of the shelf and the transport of the eroded material from the onshore to the offshore.

POST-EROSIONAL VOLCANISM

Volcanism controls the islands growth and can change the coastlines and shelves rapidly and dramatically, depending on its nature (Ramalho et al., 2013). Although most of the volcanic activity inducing the island growth is concentrated in the first phases of the island evolution (Schmidt & Schmincke, 2000), on most volcanic islands, episodes of post-erosional volcanism may occur, rejuvenating the island morphology after long periods of quiescence. In the case post-erosional volcanism occurs after a period of erosion of the islands flanks, the geometry of the newly erupted units is conditioned by the topography assumed by the volcanic edifice (Clague and Darlymple, 1987; Carracedo, 1999; Schiminke, 2004; Ramalho, 2011). For instance, complex coastal morphologies may be common on edifices affected by post-erosional volcanism (Quartau

et al., 2015b). If abundant, lava flows may partially or completely fill the accommodation space carved by erosion, narrowing the original shelf width, leading eventually to underestimate the shelf erosive rates (Quartau et al., 2015b).

At Santa Maria the last subaerial volcanic activity occurred 2.8 Ma ago (Ramalho et al., 2017). However, Ramalho et al. (in preparation) recognized a likely recent submerged tuff ring on the northern shelf at -80 m. Nevertheless, apart from this local manifestation of post-erosional volcanism, young lava flows reaching the submarine areas that might have reduced the shelf width were not recognized, hence the is no evidence of rejuvenation on the shelf around Santa Maria. In the central Aeolian sector, instead, some late volcanism occurred at Salina, Lipari and Vulcano (De Astis et al., 2013; Forni et al., 2013; Lucchi et al., 2013a, b). However, only offshore Punta Cala del Formaggio on the western shelf of Vulcano (see Figure 6.16a in chapter 6) evidence of rejuvenation have been recognized. Differently from what has been observed at Pico Island (Quartau et al., 2015b), the few "fresh" lava flows recognized on most of the shelves in the Central Aeolian sector do not affect the shelf width nor the erosive edge depth. Nevertheless, several volcanic progradations during the lifetime of the islands were possibly not recorded on the shelf, because of the effect of wave erosion accomplished at different elevation in response to glacio-eustatic sea-leve fluctuations and islands' vertical movments.

LITHOLOGY CONTROL AND SEDIMENT DISTRIBUTION ON THE SHELF

The lithology and structure of the eroded rocks influence the mechanical properties of the coastlines and their resistance to marine erosion, so adjacent shelf sectors might have different widths due to their different lithology. Different erosion rates may thus occur over times and space scales (Trenhaile, 2011, see also discussion on "time of exposure to marine erosion"). Pyroclastic products are commonly more easily eroded with respect to lavas, and less resistant materials (like unconsolidated tephra or thin and fractured lavas) are especially eroded during the syn-eruptive stages or shortly after the end of their emission (Romagnoli and Jakobsson, 2015). The geological formations of Santa Maria and the central Aeolian islands have different lithologies (Lucchi 2009, Lucchi et al., 2013a, b; Forni et al., 2013; De Astis et al., 2013) and sensitivity to marine erosion (Ramalho et al., 2017), however it is difficult to identify shelf sectors whose width is clearly influenced by different types of material. This is because we commonly lack the direct evidence of this information in submerged areas, and we can just infer their possible lithology from the adjacent subaerial volcanic units. The Aeolian Islands are made of volcanic products associated to a subduction zone, while the Azorean islands are made of product connected to a transtensional regime. The different chemical composition of these products affects also the production of sediments. In fact, the volcanic succession of the Aeolians are essentially acid in nature, i. e. more easily erodible with respect the basaltic lava flows that dominate in the Azores and Santa Maria Island.

The sediment distribution is highly variable on the shelves of the Central Aeolian sector and Santa Maria, also reflecting their marked morphological differences and wave/currents regime. Overall, the sediments exhibit a sparse distribution at Santa Maria, with few depositional bodies up to 14 m thick, mostly developed inside depressed areas such as fault-controlled basins.

213

Therefore, the shelf around Santa Maria lacks thick sedimentary bodies with an inner prograding geometry (SDTs) as those recognized in other Azores islands like Faial and Pico, where they are up to 40/50 m thick (Quartau et al., 2012, 2015b) and on shallow-water areas in the Aeolian Archipelago, where some portion of the shelf are covered by up to 30 m-thick volcaniclastic sequences (Chiocci & Romagnoli, 2004; Casalbore et al., 2017a). This difference might be partly related to the stronger wave regime at Santa Maria with respect to the Aeolian Islands. However, the higher waves energy is in part balanced by the wider shelf of Santa Maria with respect the Aeolian Islands, which cause higher wave attenuation, i.e. lower erosion rates. Moreover, in the Azores the wave energy is the same all around the islands, hence from this point of view the sediment production should be similar. Therefore, we might infer that the thicker deposits found on the shelves of the Central Aeolian, Faial and Pico Islands are probably due to the occurrence of narrower shelves, which promote the accumulation of the sediments, rather than their dispersal as it likely occurs on the wide shelf around Santa Maria.

Nevertheless, by comparing Santa Maria with other Azorean islands characterized by the same wave regime, like Faial and Pico, it looks that other factors might also control the sediment distribution. The most striking difference between Santa Maria and the mentioned Azorean islands (and the Aeolian islands) is the age of the volcanism. At a first glance one should expect that older island should exhibit shelves covered by thicker sedimentary bodies, resulting from long lasting erosive processes. Nevertheless, we should take into account that as the sea-level drops, sediments are transported to the slope, leaving the shelf almost depleted (Quartau et al., 2012; Casalbore et al., 2017a). Only the sediments located at the shelf edge eventually survive if the shelf edge is located below the maximum depth reached during the glacial stage. These sediments are normally replaced during the following phase of sea-level rise and high-stand, as observed at Salina (see Manuscripts I and II) where three different order of SDTs have been recognized, associated to the present high-stand phase (near shore terraces) and sea-level rise (mid-shelf terraces). Therefore, it can be expected that each glacial-interglacial cycle may produce, if sediment is available, a set of sedimentary bodies that should be almost completely dismantled during the following phase of sea-level fall. If the amount of sediments produced by the erosion of the islands flanks and reworked during the phase of sea-level rise and high-stand is high, compared to the areal extent of the shelf, sediments might create thick sedimentary bodies like the SDTs found in the Aeolian islands, Faial and Pico. In the case of Santa Maria, which exhibits the widest shelf among the mentioned islands due to its older age, the amount of sediments delivered to the shelf is not enough to cover the entire shelf.

Besides the creation of accommodation on the shelf due to relative sea-level changes, the type of volcanism may also influence the sediments production. Unlike the Aeolian, Faial and Pico Islands, where active explosive volcanism produced easily erodible products that can be carried on the shelf by wave erosion (Lucchi et al., 2013a; Forni et al., 2013; Madeira and Brum da Silveira, 2003), at Santa Maria the volcanism is considered extint (Ramalho et al., 2017). In the central Aeolian sector, soft geological formations are frequently intercalated by hard and less erodible sequences, and differential erosion rates might produce local effects. For instance, at Lipari, the pumiceous successions outcropping along the northeastern sector of the island (Forni et al., 2013) have been mostly dismantled and possibly deposited offshore, creating the thick sedimentary

214

terraced body located offshore Capo Rosso (see SDTs in Figure 6.1, Chapter 6). Likewise, at Salina the up to 30 m thick sedimentary cover laying on the western shelf sector at Salina island (see Manuscript I), likely results from the erosion of the Pollara products (mostly pyroclastic successions) occurred between 30 and 15.6 ka (see Lucchi et al., 2013 for details). Along the eastern shelf sector of Salina (see Figure 11 in Manuscript I), the occurrence of soft materials likely promoted the formation of a dense drainage system onshore that filled the shelf offshore, narrowing this feature. At Santa Maria we recognize an evident influence of the lithological differences on the shelf development. The softer Touril sequence and the gently dipping contacts between this unit and the underlying Anjos and overlying Pico Alto volcanic units represent a favorable lithological/stratigraphical framework that, along with the exposure to dominant wave direction, boosted the coastal retreat and formed a wide terraced morphology here (Ramalho et al., 2017). Likewise, the greater width of the marine terraces on the northern shelf sector is probably due to the profusion of soft pyroclastic structures and cinder/scoria cones, which promoted higher erosion rates (see Manuscript V). However, due to uplift, these products are mostly not affected by wave erosion (see Figure 2 of Manuscript V), implying that only few sediments are delivered to the shelf. Finally, the Aeolian Islands are made of volcanic products associated to a subduction zone, while the Azorean islands are made of product connected to a spreading volcanic ridge. The different chemical composition of these products, affects also the production of sediments. In fact the volcanic succession of the Aeolians are essentially acid in nature, i. e. more easily erodible with respect the basaltic lava flows that mostly forms the Azores and Santa Maria Island.

An important factor that may influence the sediments production, is climate. For instance at Montserrat Island the final stage of the island evolution caused an almost complete dismantling of the subaerial edifice, with c. 65% of the extruded material deposited in the offshore (Le Friant et al., 2004). This high erosion rate might be related to the tropical climate of the island, which promotes the erosion of volcanic successions, unlike the temperate climate of the Azores and the Aeolian islands. The islands of Faial and Pico are characterized by higher precipitation regime with respect Santa Maria (c. 2000 mm/yr vs 1000 mm/yr of Santa Maria, Climate atlas, 2012) which results in higher sediment production due to subaerial erosion. This effect is likely hampered by the fact that Santa Maria suffered intense erosive processes in the past that heavily eroded the island, as attested by its low altitude (max 587 m above sea-level) if compared with Faial (max 1043 m above sea-level) and Pico (max 2351 m above sea-level). On the contrary, the annual precipitation regime of the Aeolian Islands is lower, being around 600 mm/yr (Cicala, 2000). As such we expect a lower sediment discharge in the Aeolian Islands, in contrast with the occurrence of thick sedimentary bodies on the shelf. The lower sediment production due to subaerial erosion here is possibly balanced by, as mentioned before, the higher erosive rates and the occurrence of narrower shelves.

The availability of thick deposits on the shelves of the Central Aeolian sector allowed detailed studies on their depositonal characteristics and stratigraphic architecture. At Salina and Lipari Casalbore et al. (2016, 2018) grouped the SDTs found on the shelf in three orders on the base of their rollover depth (depositional edge). The SDTs edge varies between -10 and -30 m (near shore terrace), -40 and -90 m (mid-shelf terrace) and, -130/-160 m (shelf edge terrace). Each of these

deposits is associated to different sea-level stands, the near-shore terraces being related to the modern sea-level highstand. The mid-shelf terraces of Salina and Lipari exhibit aggradation rather than progradation, in agreement with a formation during the sea-level rise (see Casalbore et al., 2016, 2018; and Manuscript II). At Santa Maria, only few thicker sedimentary bodies exhibit an evident inner prograding geometry and a depositional edge. These are located along the eastern and southern shelf sector of the island (Fig. 6, Manuscript IV). Their rollover depth is invariably located from -40 to -50 m, being similar to that of the mid-shelf terraces recognized at Salina and Lipari, formed during sea-level rise conditions. However, a correlation with Santa Maria cannot be done since in the Tyrrhenian Sea the storm base level is shallower with respect to the Atlantic Ocean (Lobo et al., 2005; Quartau et al., 2010, 2014; Mitchell et al., 2012; Casalbore et al., 2017). The lack of internal reflector also suggests no subaerial erosion, thus formation after 6.5 ka when sea-level rose to its maximum level in the Azores (Bintanja and van de Wal, 2008) so that, despite the deeper edge depth, these wedges can be related to the present high-stand phase (unless older deposits have been preserved in protected depocenters, as for instance, the tectonically controlled depressions found on the northern and southern shelf sectors).

10. CONCLUSIONS AND FUTURE WORK

The main results of this Ph.D project offer an improved understanding of the geologic evolution of the studied volcanic islands, resulting from the adoption of an integrated approach involving field geological studies and marine geophysical data. For each volcanic island under study we analyzed and compared the morphometric parameters of the insular shelves and we discussed the factors controlling the shelves formation and evolution. Overall, the history of the earlier stages of growth of these islands is now better constrained, integrating what was previously known. Summarizing,

- ✓ this study allowed to associate the larger shelves to the oldest volcanic centers onshore and to document the occurrence of submerged volcanic centers that predates the onshore volcanism at Salina, Lipari and possibly at Santa Maria.
- ✓ Although the shelf width-age relationship has been documented in the studied areas, it is not straightforward, since "abnormally wide" shelves may occur due to different waves exposure and early volcanism not documented onshore. Narrower than-expected shelves occur if coastal rejuvenation and different submarine erosion of the edges affected the shelf.
- ✓ The erosive shelf edge depth-age relationship represents an important tool to reconstruct the vertical mobility trend of volcanic islands. In fact, it allowed to identify the shelf sectors affected by subsidence processes and to calculate the vertical mobility trend of the islands. Our reconstructions consider the occurrence of a continuous and constant subsidence and uplift trends in the Central Aeolian Sector and at Santa Maria, recorded by the erosive shelf edge depth, the submerged and subaerial marine terraces located at different depth/elevation. In the Aeolians we calculated a constant subsidence rate before the Last Interglacial by matching the insular shelf edge depth with the subaerial terraces found onshore. This rate has been used as a relative dating tool to associate the older portion of Salina and Lipari to a specific sea-level peak, outlining an early emergence for the islands, at around 430 ka. At Santa Maria, by matching the newly discovered submerged marine terraces with those previously recognized onshore, we were able to better constrain the uplift rate of the island and to relatively date the terraces. Moreover, the analysis of the shelf width and erosive edge depth allowed to integrate the evolutionary model of the island, by inferring the occurrence of an older phase of volcanic activity (Proto-Santa Maria) presently largely dismantled and not document onshore.

Due to the fact that the studied islands are affected by different meteo-marine conditions and sit in different geo-dynamic settings, the comparison of the obtained results allowed to discuss in a broader perspective the role of different controlling factors of shelves evolution, highlighting the main differences and similarities between the Azores and the Aeolian archipelagos.

- ✓ Remarkably, the erosion rates of the shelf in the Aeolians are one order of magnitude larger of those of Santa Maria. As the shelf become wider and gently-sloping, the increasing effect of wave attenuation reduces the energy of marine erosion, resulting in a slower rates of cliff recession. As a consequence, erosion rates are lower for islands

surrounded by wider shelves like Santa Maria, causing the relationship between time and shelf widening to be not-linear. Erosion rates appear thus dependent on the period of detection, being higher in the short term.

✓ The subsidence and uplift trend that affected the studied islands might have influenced the development of the shelves. The early subsidence trend possibly boosted the shelf widening, with a greater effect in the Aeolians, where the estimated subsidence trend is higher. Because of its effect of the shelf width, the subsidence affects the erosive rates, which may result overestimated with respect to stable coastal sectors.

✓ The effects of subsidence and uplift on the shelf width are invariably connected with relative sea-level fluctuations. The amplitude of sea-level changes has a profound effect on insular shelves development because of its impact on wave erosion. Differently from Santa Maria, the islands of the central Aeolian sector are all younger than 450 ka, therefore they suffered only high-amplitude sea-level fluctuations. Since 1 Ma the amplitude of the eustatic sea-level cycles remained almost constant, a condition that promoted the formation of wide and gently sloping shelves and the achievement of a state of static equilibrium. The increased wave erosion might have been partly compensated by the increased wave attenuation and slower coastline erosion.

✓ On most volcanic islands episodes of post-erosional volcanism may occur, rejuvenating the island morphology after long periods of quiescence. Apart from local manifestation of post-erosional volcanism, young lava flows reaching the submarine areas were recognized only at a local scale at Vulcano island. However, episodes of volcanic progradation during the lifetime of the islands were possibly not recorded on the shelf, causing an underestimation of the shelf erosive rates.

✓ Interestingly, it appears that older islands tend to have much less sediments on their shelves. Overall, the sediments exhibit a sparse distribution at Santa Maria with respect the shallow-water areas in the Aeolian Archipelago (and in younger Azorean islands like Faial and Pico). This difference has been related to the higher accommodation space of the shelves around Santa Maria. Moreover, since young islands are normally characterized by a more immature erosion than older islands, they produce more sediments due to subaerial erosion, enhancing the formation of thicker deposits. The different depth distribution of the sedimentary bodies has been instead related to the higher wave regime of the Azores, which promote the formation of the present-day highstand deposits only.

Apart from the scientific interest driving this study, there is also an important contribution from the **socio-economic** point of view. This project is particularly relevant for volcanic archipelagos (in Europe: Aeolian, Azores, Madeira, Canary, etc.) and for the population living there. The societal importance of this study is two-fold since these islands are the site of: (ii) their bordering shelves are shallow-water reservoirs of sediments and the seat of biological communities (both important resources for the insular economies, respectively for dredging and fishing); (iii) insular shelves protects the coastlines disconnecting the submerged canyons from the subaerial drainage. However, where absent, submarine landslides and associated tsunamis may occur close to the shorelines, representing a source of hazard.

Although the results of this Ph.D thesis contributed to better understand the evolution of these complex systems, several aspects still remains poorly constrained and need further research. The amount of studies that could be carried out is wide, since the systematic study of the shallow water portion surrounding volcanic islands only began in the recent past. In particular, the following steps might boost the research in the field:

- Modeling the formation and development of insular shelves. This would require to date rocks at the preserved shelf edges (i.e. the shelf portions that did not suffered for landsliding) in order to understand when shelves started to be incised. This goal is extremely difficult to achieve, but it would provide more precise shelves erosion rates.
- To improve measurements of the currents on the shelf in order to better understand the relation between wave climate and offshore transport of the sediments that form the SDT's.
- For the Aeolian Archipelago: further geophysical surveys with the aim of collecting a more closely spaced dataset of seismic profiles. This would allow to better investigate the stratigraphic relationship of the sedimentary bodies, to produce maps exhibiting their distribution and thickness and to study their inner geometry, in order to better relate their formation to the sea-level stands.

  Archeological and instrumental (GPS) data indicate that the southern portion of Lipari Island is subsiding for the last 2100 yr at a rate up to c.11 mm/yr (Anzidei et al., 2016). The geological markers studied in this thesis witness an opposite vertical behavior for this island. Therefore, a comparison between the geological and the geophysical/archeological data would be of great interest to shed light on the current vertical mobility trend of the island.
- For Santa Maria it would be useful to date the subaerial and submarine terraces. By integrating the dating with modelling of wave erosion it would be possible to better calibrate the models of terrace formation and shelf development.

REFERENCES

Ablay, G., Hurlimann, M., 2000. Evolution of the north flank of Tenerife by recurrent giant landslides. J. Volcanol. Geotherm. Res. 103, 135–159.

Ali, M. Y., Watts, A. B., & Hill, I. (2003). A seismic reflection profile study of lithospheric flexure in the vicinity of the Cape Verde Islands. Journal of Geophysical Research (Solid Earth),108(B5), 2239–2263.

Andrade, C., Trigo, R.M., Freitas, M.C., Gallego, M.C., Borges, P., Ramos, A.M., 2008. Comparing historic records of storm frequency and the North Atlantic Oscillation (NAO) chronology for the Azores region. The Holocene 18 (5), 745–754. https://doi. org/10.1177/0959683608091794.

Argnani, A., Serpelloni, E. and Bonazzi, C., 2007. Pattern of deformation around the central Aeolian Islands: evidence from multichannel seismics and GPS data. Terra Nova, 19, 371–323.

Ávila, S.P., Madeira, P., da Silva, C.M., Cachão, M., Landau, B., Quartau, R., Frias Martins, A.M., 2008a. Local disappearance of bivalves in the Azores during the last glaciation. J. Quat. Sci. 23 (8), 777–785.

Babonneau, N., Delacourt, C., Cancouët, R., Sisavath, E., Bachèlery, P., Mazuel, A., Jorry, S.J., Deschamps, A., Ammann, J., Villeneuve, N., 2013. Direct sediment transfer from land to deep-sea: insights into shallow multibeam bathymetry at La Réunion Island. Mar. Geol.346, 47–57.

Bárcenas, P.; Lobo, F.J.; Macías, J.; Fernández-Salas, L.M.; López-González, N.; Díaz del Río, V. Submarine deltaic geometries linked to steep, mountainous drainage basins in the northern shelf of the Alboran Sea: Filling the gaps in the spectrum of deltaic deposition. Geomorphology **2015**, 232, 125–144.

Barone, A., Fabbri, A., Rossi, S. and Sartori, R., 1982. Geological structure and evolution of the marine areas adjacent to the Calabrian arc. Earth Evol. Sci., 3, 207–221.

Barriga, F.J.A.S., and Chester, D.K., eds., Volcanic Geology of São Miguel Island (Azores Archipelago): Geological Society of London Memoir 44, p. 15–32.

Beccaluva, L., Rossi, P. L. & Serri, G. 1982. Neogene to recent volcanism of the Southern Tyrrhenian–Sicilian area: implications for the geodynamic evolution of the Calabrian Arc. Earth Evolution Sciences, 3, 222–238.

Beccaluva, L., Gabbianelli, G., Lucchini, F., Rossi, P. L. & Savelli, C. 1985. Petrology and K/Ar ages of volcanics dredged from the Aeolian seamounts: implications for geodynamic evolution of the Southern Tyrrhenian basin. Earth and Planetary Science Letters, 74, 187–208.

Bintanja R, van de Wal RSW, Oerlemans J. 2005. Modelled atmospheric temperatures and global sea levels the past million years. Nature 437: 125-128.

Bintanja, R., van de Wal, R.S., 2008. North American ice-sheet dynamics and the onset of 100,000-year glacial cycles. Nature 454 (7206), 869–872. https://doi.org/10.1038/ nature07158.

Bortoluzzi, G., Ligi, M. et al. 2010. Interactions between volcanism and tectonics in the Western Aeolian sector, Southern Tyrrhenian Sea. Geophysical Journal International, 183, 64–78.

Bosman, A., Casalbore, D., Anzidei, M., Muccini, F., Carmisciano, C., Chiocci, F.L., 2015. The first ultra-high resolution digital Terrain model of the shallow-water sector around Lipari Island (Aeolian Islands, Italy). Annals of Geophysics 58 (2). http://dx.doi.org/10.4401/ag-6746.

Brum da Silveira, A., Madeira, J., Ramalho, R., Fonseca, P., Rodrigues, C., Prada, S., 2010b. Carta Geológica da Ilha da Madeira na Escala 1:50.000, Folhas A e B. Secretaria Regional do Ambiente e Recursos Naturais e Universidade da Madeira. ISBN978-972-98405-1-7. 2 sheets at the 1:50,000 scale.

Calanchi, N., Romagnoli, C.&Rossi, P. L. 1995. Morphostructural features and some petrochemical data from the submerged area around Alicudi and Filicudi volcanic islands (Aeolian Arc, southern Tyrrhenian Sea). Marine Geology, 123, 215–238.

Calanchi, N., Lucchi, F., Pirazzoli, P., Romagnoli, C., Tranne, C.A., Radtke, U., Reyss, J.L., Rossi, P.L., 2002. Late-Quaternary and recent relative sea-level changes and vertical displacements at Lipari (Aeolian Islands). J. Quat. Sci. 17 (5–6), 459–467.

Calarco, M., 2011. Integrated analysis of the submarine volcanic structures offshore Pantelleria, Ph.D thesis. Dep. of Earth Sci., Univ. of Rome La Sapienza, Italy.

Calhoun, R.S., Fletcher, C.H. and Harney, J.N. (2002) A budget of marine and terrigenous sediments, Hanalei Bay, Kauai, Hawaiian islands. Sed. Geol., 150, 61–87.

Carracedo, J., 1999. Growth, structure, instability and collapse of Canarian volcanoes and comparisons with Hawaiian volcanoes. J. Volcanol. Geotherm. Res. 94 (1–4), 1–19.

Casalbore, D., Romagnoli, C., Chiocci, F., Frezza, V., 2010. Morphosedimentary characteristics of the volcanic apron around Stromboli volcano. Mar. Geol. 269 (3–4), 132–148.

Casalbore, D.; Bosman, A.; Romagnoli, C.; Chiocci, F.L., 2014 Large-scale seafloor waveforms on the flanks of insular volcanoes (Aeolian Archipelago, Italy), with inferences about their origin. Mar. Geol., 355, 318–329.

Casalbore, D.; Romagnoli, C.; Pimentel, A.; Quartau, R.; Casas, D.; Ercilla, G.; Hipolito, A.; Sposato, A.; Chiocci, F.L., 2015. Volcanic, tectonic andmass-wasting processes offshore Terceira island (Azores) revealed by high-resolution seafloor mapping. Bull. Volcanol., 77.

Casalbore, D., Bosman, A., Romagnoli, C., Chiocci, F.L., 2016a. Morphological map of Salina offshore (Southern Tyrrhenian Sea). J. Maps 12 (5), 725–730. http://dx.doi.org/10.1080/17445647.2015.1070300.

Casalbore, D.; Falese, F.; Martorelli, E.; Romagnoli, C.; Chiocci, F.L. 2017a. Submarine depositional terraces in the Tyrrhenian Sea as a proxy for paleo-sea level reconstruction: Problems and perspective. Quat. Int., 439, 169–180.

Chiarabba, C., De Gori, P., Speranza, F., 2008. The southern Tyrrhenian subductionzone: deep geometry, magmatism and Plio-Pleistocene evolution. Earth Planet.Sci. Lett. 268, 408–423, http://dx.doi.org/10.1016/j.epsl.2008.01.036.

Chiocci, F.L., 2004. Distorsioni nella forma dei TDS rilevati dai profili sismici e ripristino delle corrette geometrie (migrazione). In: Chiocci, F.L., D'Angelo, S., Romagnoli, C. (Eds.), Atlante dei Terrazzi Deposizionali Sommersi Lungo le Coste Italiane, Memorie Descrittive della Carta Geologica d'Italia, vol. 58, pp. 161e170.

Chiocci, F.L., Orlando, L., 1996. Lowstand terraces on Tyrrhenian Sea steep continental slopes. Marine Geology 134, 127e143.

Chiocci, F.L., Romagnoli, C., 2004. Terrazzi deposizionali sommersi nelle Isole Eolie. In: Chiocci, F.L., D'Angelo, S., Romagnoli, C. (Eds.), Atlante dei Terrazzi Deposizionali Sommersi Lungo le Coste Italiane, Memorie Descrittive della Carta Geologica d'Italia, vol. 58, pp. 81e114.

Chiocci, F.L., D'Angelo, S., Romagnoli, C., 2004. Atlas of Submerged Depositional Terraces Along the Italian Coasts. In: Memorie Descrittive della Carta Geologica d'Italia, vol. 58.

Chiocci, F.L., Romagnoli, C., Casalbore, D., Sposato, A., Martorelli, E., Alonso, B., Casas, D., Conte, A.M., Di Bella, L., Ercilla, G., Estrada, F., Falese, F., Farran, M., Forleo, V., Frezza, V., Hipolito, A., Lebani, A., Maisto, F., Pacheco, Pimentel, J.A., Quartau, R., Roque, C., Sampaio, I., Santoro, P.C., Tempera, F., 2013. Bathymorphological setting of Terceira island (Azores) after the FAIVI cruise. Journal of Maps 9, 590e595.

Chiocci, F.L.; Casalbore, D. Unexpected fast rate of morphological evolution of geologically-active continental margins during Quaternary: Examples from selected areas in the Italian seas. Mar. Pet. Geol. 2017, 82, 154–162.

Cicala, A., 2000. Guida alla meteorologia delle Isole Eolie. In: Natali, A. (Ed.), Comune di Lipari, Lipari, Italy.

Clague, D., Dalrymple, G., 1987. The Hawaiian-Emperor volcanic chain. Part I. Geologic evolution. Volcanism in Hawaii. U.S. Geological Survey Professional Paper, vol. 1, pp. 5–54.

Clague, D. A. & Moore, J. G. 2002. The proximal part of the giant submarine Wailau landslide, Molofai, Hawaii. Journal of Volcanology and Geothermal Research, 113, 259–287.

Climate Atlas. 2012. *Climate atlas of the archipelagos of the Canary Islands, Madeira and the Azores*. The Meteorological State Agency of Spain and the Institute of Meteorology, Portugal. http://www.meteo.pt/export/sites/default/bin/docs/tecnicos/Atlas__Climatico_ilhas.pdf

Coombs, M. L., D. A. Clague, G. F. Moore, and B. L. Cousens (2004), Growth and collapse of Waianae volcano, Hawaii, as revealed by exploration of its submarine flanks, Geochem. Geophys. Geosyst., 5, Q08006, doi:10.1029/2004GC000717.

Dalca AV, Ferrier KL, Mitrovica JX, Perron JT, Milne GA, Creveling JR. On postglacial sea level—III. Incorporating sediment redistribution. Geophys J Int. 2013; 194:45–60.

De Astis, G., La Volpe, L., Peccerillo, A., Civetta, L., 1997. Volcanological and petrological evolution of the Vulcano Island (Aeolian Arc, Southern Tyrrhenian Sea). Journal of Geophysical Research 102, 8021–8050.

De Astis, G., Ventura, G., Vilardo, G., 2003. Geodynamic significance of the Aeolian volcanism (Southern Tyrrhenian Sea, Italy) in light of structural, seismological and geochemical data. Tectonics 22 (4), 1040–1057.

De Astis, G., Lucchi, F., Tranne, C.A., 2006b. The Aeolian volcanic district: volcanism and magmatism. Acta Vulcanologica 18 (1–2), 79–104.

De Astis, G., Lucchi, F., Dellino, P., La Volpe, L., Tranne, C.A., Frezzotti, M.L., et al. (2013). Geology, volcanic history and petrology of Vulcano (central Aeolian archipelago). In F. Lucchi, A. Peccerillo, J. Keller, Tranne CA, & P.L. Rossi (a cura di), The Aeolian Islands volcanoes (pp. 281-349). THe Geological Society, London, Memoirs.

De Boer, B., Van De Wal, R.S.W., Bintanja, R., Lourens, L.J., Tuenter, E., 2010. Cenozoic global ice-volume and temperature simulations with 1-D ice-sheet models forced by benthic 18O records. Ann. Glaciol. 51 (55), 23–33.

De Guidi, G., Monaco, C., 2009. Late Holocene vertical deformation along the coast of Pantelleria Island (Sicily Channel, Italy). Quat. Int. 206, 158–165.

Detrick, R., & Crough, T. (1978). Island subsidence, hot spots, and lithospheric thinning. Journal of Geophysical Research (Solid Earth), 83(B3), 1236–1244.

De Ritis, R., Ventura, G. & Chiappini, M. Aeromagnetic anomalies reveal hidden tectonic and volcanic structures in the central sector of the Aeolian Islands, southern Tyrrhenian Sea, Italy. Journal of Geophysical Research, 112, B10105, doi: 10.1029/2006JB004639.

Dickson, M. E. (2004), The development of talus slopes around Lord Howe island and implications for the history of island planation, Aust. Geogr., 35(2), 223–238.

Dura T, Engelhart SE, Vacchi M, Horton BP, Kopp RE, PeltierWR, Bradley S. The role of holocene relative sea-level change in preserving records of subduction zone earthquakes. Curr Clim Chang Rep. 2016:1–15.

Dutton A, Carlson AE, Long AJ, Milne GA, Clark PU, DeConto R, Horton BP, Rahmstorf S, Raymo ME. Sea-level rise due to polar ice-sheet mass loss during past warm periods. Science. 2015;349: aaa4019.

Dyhr, C., Holm, P., 2010. A volcanological and geochemical investigation of Boa Vista, Cape Verde Islands; 40Ar/39Ar geochronology and field constraints. Journal of Volcanology and Geothermal Research 189 (1–2), 19–32.

Faccenna, C., Funiciello, F., Giardini, D., Lucente, P., 2001. Episodic back-arc extensionduring restricted mantle convection in the Central Mediterranean. Earth Planet.Sci. Lett. 187, 105–116.

Ferranti, L., Antonioli, F., Mauz, B., Amorosi, A., Dai, Pra G., Mastronuzzi, G., Monaco, C., Orrù, P., Pappalardo, M., Radtke, U., Renda, P., Romano, P., Sansò, P., Verrubbi, V., 2006. Markers of the last interglacial sea-level high stand along the coast of Italy: tectonic implications. Quat. Int. 145–146, 30–54.

Field, M.E., Roy, P.S., 1984. Offshore transport and sand-body formation: evidence from a steep, high energy shoreface, southeastern Australia. J. Sediment. Petrol. 54 (4), 1292–1302.

Filmer, P., McNutt, M., Webb, H., & Dixon, D. (1994). Volcanism and archipelagic aprons in the Marquesas and Hawaiian Islands. Marine Geophysical Researches, 16(5), 385–406.

Fletcher, C., Bochicchio, C., Conger, C., Engels, M., Feirstein, E., Frazer, N., Glenn, C., Grigg, R., Grossman, E., Harney, J., et al., 2008. Geology of Hawaii reefs. In: Riegl, B., Dodge, R. (Eds.), Coral Reefs of the USA, vol. 1. Springer Verlag, pp. 435–487.

F. Forni, F. Lucchi, A. Peccerillo, C. A. Tranne, P. L. Rossi and M. L. Frezzotti, 2013. Stratigraphy and geological evolution of the Lipari volcanic complex (central Aeolian archipelago). Geological Society, London, Memoirs, 37, 213-279, 2013, https://doi.org/10.1144/M37.10

Gabbianelli, G., Romagnoli, C., Rossi, P. & Calanchi, N. 1993. Marine geology of the Panarea-Stromboli area (Aeolian Archipelago, Southeastern Tyrrhenian Sea). Acta Vulcanologica, 3, 11–20.

Gente, P., Dyment, J., Maia, M., and Goslin, J., 2003, Interaction between the Mid-Atlantic Ridge and the Azores hotspot during the last 85 Myr: Emplacement and rifting of the hot spot–derived plateaus: Geochemistry Geophysics Geosystems, v. 4, no. 10, p. 8514, doi: 10 .1029 /2003GC000527 .

Gornitz V (2005) Eustasy. In: Encycl Coast Sci Springer, pp 439–442.

Grigg, R., & Jones, A. (1997). Uplift caused by lithospheric flexure in the Hawaiian Archipelago as revealed by elevated coral deposit. Marine Geology,141(1–4), 11–25.

Hay C, Mitrovica JX, Gomez N, Creveling JR, Austermann J, Kopp RR. The sea-level fingerprints of ice-sheet collapse during interglacial periods. Quat Sci Rev. 2014;87:60.

Hernández-Molina, F.J., Fernández-Salas, L.M., Lobo, F., Somoza, L., Díaz-del-Río, A., Dias, J.M., 2000. The infralittoral prograding wedge: a new large-scale progradational sedimentary body in shallow marine environments. Geo-Mar. Lett. 20, 109–117.

Hipólito, A., Madeira, J., Carmo, R., and Gaspar, J.L., 2013, Neotectonics of Graciosa Island (Azores): A contribution to seismic hazard assessment of a volcanic area in a complex geodynamic setting: Annals of Geophysics, v. 56, no. 6, p. S0677.

Keller, J., 1980. The island of Salina. Rend. Soc. Ital. Mineral. Petrol. 36, 489–524.

Kelsey HM, Bockheim JG. Coastal landscape evolution as a function of eustasy and surface uplift rate, Cascadia margin, southern Oregon. Geol Soc Am Bull. 1994;106:840–54.

Kennedy, D. M., C. D. Woodroffe, B. G. Jones, M. E. Dickson, and C. V. G. Phipps (2002), Carbonate sedimentation on subtropical shelves around Lord Howe Island and Balls Pyramid, Southwest Pacific, Mar. Geol., 188(3–4), 333–349.

Kopp RE, Hay CC, Little CM, Mitrovica JX (2015) Geographic variability of sea-level change. Curr Clim Chang Reports 1:192– 204 69.

Krastel, S., Schmincke, H.-U., Jacobs, C.L., 2001. Formation of submarine canyons on the flanks of the Canary Islands. Geo Mar. Lett. 20, 160–167.

Lajoie KR. 1986. Coastal tectonics. In Usselman TM (ed). Studies in Geophysics – Active Tectonics. National Academy Press: Washington DC; 95–124.

Lambeck K. Volcanic loading and isostasy. In: Hopley D, editor. Encycl.Mod. Coral reefs Struct. Form process. Dordrecht: Springer Netherlands; 2011. p. 1140–2.

Laughton, A.S., and Whitmarsh, R.B., 1974, The Azores- Gibraltar plate boundary, *in* Kristjansson, L., ed., Geodynamics of Iceland and the North Atlantic Area: Dordrecht, Netherlands, D. Reidel Publishing Co., p. 63–81, doi: 10 .1007 /978 -94 -010 -2271 -2_5 .

Lebas, E., A. Le Friant, G. Boudon, S. F. L. Watt, P. J. Talling, N. Feuillet, C. Deplus, C. Berndt, and M. E. Vardy (2011), Multiple widespread landslides during the long-term evolution of a volcanic island: Insights from high-resolution seismic data, Montserrat, Lesser Antilles, Geochem. Geophys. Geosyst., 12, Q05006, doi:10.1029/2010GC003451.

Leat, P.T., Tate, A.J., Tappin, D.R., Day, S.J., Owen, M.J., 2010. Growth and mass wast-ing of volcanic centers in the northern South Sandwich arc, South Atlantic, revealed by new multibeam mapping. Mar. Geol.275, 110–126.

Le Friant, A., Harford, C.L., Deplus, C., Boudon, G., Sparks, R.S.J., Herd, R.A., Komorowski, J.C., 2004. Geomorphological evolution of Montserrat (West Indies): importance of flank collapse and erosional processes. J. Geol. Soc. Lond. 161, 147–160.

Le Friant, A., E. Lebas, V. Clement, G. Boudon, C. Deplus, B. de Voogd, and P. Bachelery (2011), A new model for the evolution of La Reunion volcanic complex from complete marine geophysical surveys, Geophys. Res. Lett., 38, L09312, doi:10.1029/2011GL047489.

Llanes, P., Herrera, R., Gomez, M., Munoz, A., Acosta, J., Uchupi, E., 2009. Geological evolution of the volcanic island La Gomera, Canary Islands, from analysis of its geomorphology. Mar. Geol. 264, 123–139.

Lobo, F.J.; Fernandez-Salas, L.M.; Hernandez-Molina, F.J.; Gonzalez, R.; Dias, J.M.A.; Díaz del Río, V.; Somoza, L. Holocene, 2005. Highstand deposits in the Gulf of Cadiz, SW Iberian Peninsula: A high-resolution record of environmental changes. Mar. Geol., 219, 119–141.

Lourenço, N., Miranda, J.M., Luís, J.F., Ribeiro, A., Victor, L.M., Madeira, J., and Needham, H., 1998, Morphotectonic analysis of the Azores Volcanic Plateau from a new bathymetric compilation of the area: Marine Geophysical Researches, v. 20, no. 3, p. 141–156, doi: 10 .1023 /A: 1004505401547 .

Lucchi, F., 2009. Late-Quaternary marine terrace deposits as tools for wide-scale correlation of unconformity-bounded units in the volcanic Aeolian archipelago (southern Italy). Sediment. Geol. 216, 158–178.

Lucchi, F., Tranne, C.A., Calanchi, N., Rossi, P.L., 2004. Late Quaternary fossil shorelines in the Aeolian Islands (Southern Tyrrhenian Sea): evaluation of long-term vertical displacements. In: Antonioli, F., Monaco, C. (Eds.), Contribution From the Study of Ancient Shorelines to Understanding the Recent Vertical Motions. Field Trip Across the Messina Straits Quaternaria Nova, Il Calamo Editore, Roma, Italy, VIII, pp. 115–137.

Lucchi, F., Tranne, C. A., Calanchi, N. & Rossi, P. L. , 2007b. Late Quaternary deformation history of the volcanic edifice of Panarea (Aeolian Arc). Bulletin of Volcanology, 69, 239–257.

Lucchi, F., Gertisser, R., Keller, J., Forni, F., De Astis, G., Tranne, C.A., 2013a. Eruptive history and magmatic evolution of the island of Salina (central Aeolian archipelago). In: Lucchi, F., Peccerillo, A., Keller, J., Tranne, C.A., Rossi, P.L. (Eds.), The Aeolian Islands Volcanoes. Geological Society, London, Memoirs 37. pp. 155–211.

Lucchi, F., Keller, J., Tranne, C.A., 2013b. Regional stratigraphic correlations across the Aeolian archipelago (southern Italy). In: Lucchi, F., Peccerillo, A., Keller, J., Tranne, C.A., Rossi, P.L. (Eds.), The Aeolian Islands Volcanoes. Geological Society, London, Memoirs 37. pp. 55–81.

Luís, J.F., and Miranda, J.M., 2008, Reevaluation of magnetic chrons in the North Atlantic between 35°N and 47°N: Implications for the formation of the Azores triple junction and associated plateau: Journal of Geophysical Research–Solid Earth (1978–2012), v. 113, no. B10, p. B10105, doi: 10 .1029 /2007JB005573 .

Luís, J.F., Miranda, J.M., Galdeano, A., Patriat, P., Rossignol, J.C., and Mendes Victor, L.A., 1994, The Azores triple junction evolution since 10 Ma from an aeromagnetic survey of the Mid-Atlantic Ridge: Earth and Planetary Science Letters, v. 125, p. 439–459, doi: 10 .1016 /0012 -821X (94)90231 -3 .

Madeira, J., and Ribeiro, A., 1990, Geodynamic models for the Azores triple junction: A contribution from tectonics: Tectonophysics, v. 184, no. 3–4, p. 405–415, doi: 10 .1016 /0040 -1951 (90)90452 -E.

Madeira, J., Brum da Silveira, A., 2003. Active tectonics and first paleosismological results in Faial, Pico e S. Jorge islands (Azores, Portugal). Annals of Geophysics 46 (5), 733–761.

Madeira, J., Mata, J., Mourão, C., Brumda Silveira, A., Martins, S., Ramalho, R.S., Hoffmann, D., 2010. Volcano-stratigraphic and structural evolution of Brava Island (Cape Verde) from 40Ar/39Ar, U/Th and field constraints. J. Volcanol. Geotherm. Res. 196 (3–4), 219–235.

Madeira, J., Brum da Silveira, A., Hipólito, A., and Carmo, R., 2015, Active tectonics along the Eurasia-Nubia boundary: Data from the central and eastern Azores Islands, in Gaspar, J.L., Guest, J.E., Duncan, A.M.

Marques, F.O., Catalão, J.C., DeMets, C., Costa, A.C.G., and Hildenbrand, A., 2013, GPS and tectonic evidence for a diffuse plate boundary at the Azores triple junction: Earth and Planetary Science Letters, v. 381, p. 177–187, doi: 10 .1016 /j .epsl .2013 .08 .051.

Marques, F.O., Hildenbrand, A., Zanon, V., Boulesteix, T., 2016. Comment on "The insular shelves of the Faial–Pico Ridge (Azores archipelago): a morphologi-cal record of its evolution" by Quartau et al. (2015). https://doi .org /10 .1002 /2015GC005733. Geochem. Geophys. Geosyst.

Marriner N, Flaux C,Morhange C, Kaniewski D. Nile Delta's sinking past: quantifiable links with Holocene compaction and climatedriven changes in sediment supply? Geology. 2012;40:1083–6.

Masson, D.G., Watts, A.B., Gee, M.J.R., Urgeles, R., Mitchell, N.C., Le Bas, T.P., Canals, M., 2002. Slope failures on the flanks of the western Canary Islands. Earth Sci. Rev. 57 (1–2), 1–35.

Masson, D.G., Le Bas, T.P., Grevemeyer, I., Weinrebe, W., 2008. Flank collapse and large-scale landsliding in the Cape Verde Islands, off West Africa. Geochem. Geophys. Geosyst.9. https://doi.org/10.1029/2008GC001983.

Mauz, B., Vacchi, M., Green, A., Hoffmann, G., Cooper, A., 2015. Beachrock: a tool for reconstructing relative sea level in the far-field. Mar. Geol. 362, 1–16. https://doi. org/10.1016/j.margeo.2015.01.009.

Mazzuoli, R., Tortorici, L. & Ventura, G. 1995. Oblique rifting in Salina, Lipari and Vulcano Islands (Aeolian Islands, Southern Tyrrhenian Sea, Italy). Terra Nova, 7, 444–452.

McMurtry, G.M., Campbell, J., Fryer, G., Fietzke, J., 2010. Uplift of Oahu, Hawaii, during the past 500 ky as recorded by elevated reef deposits. Geology 38 (1), 27.

McNutt, M., Menard, H.W., 1978. Lithospheric flexure and uplifted atolls. J. Geophys. Res. Solid Earth 83 (B3), 1206–1212.

McNutt, M. (1988). Thermal and mechanical properties of the Cape Verde Rise. Journal of Geophysical Research (Solid Earth), 93(B4), 2784–2794.

Meireles, R., Quartau, R., Ramalho, R.S., Rebelo, A.C., Madeira, J., Zanon, V., Ávila, S.P., 2013. Depositional processes on oceanic island shelves – evidence from storm-generated Neogene deposits from the mid-North Atlantic. Sedimentology 60, 1769–1785.

Melosh, H., 1978. Dynamic support of the outer rise. Geophys. Res. Lett. 5 (5), 321–324.

Menard, H. (1973). Depth anomalies and the bobbing motion of drifting islands. Journal of Geophysical Research (Solid Earth),78(B3), 5128–5137.

Menard, H.W., 1983. Insular erosion, isostasy, and subsidence. Science 220, 913–918.

Menard, H., 1986. Islands.Scientific American Library.

Menendez, I., Silva, P.,Martin-Betancor, M., Perez-Torrado, F., Guillou, H., Scaillet, S., 2008. Fluvial dissection, isostatic uplift, and geomorphological evolution of volcanic islands (Gran Canaria, Canary Islands, Spain). Geomorphology 102 (1), 189–203.

Milankovitch, M., 1930. Mathematische Klimalehre und Astronomische Theorie der Klimaschwankungen. Handbuch der Klimatologie, Band I, Teil A. Gebruder Borntraeger, Berlin, 298 pp.

Miller KG, Kominz MA, Browning JV, Wright JD, Mountain GS, Katz ME, Sugarman PJ, Cramer BS, Christie-Blick N, Pekar SF. The Phanerozoic record of global sea-level change. Science. 2005; 310:1293–8.

Miranda, J.M., Luís, J.F., Lourenço, N., 2018. The geophysical architecture of the Azores from magnetic data. In: Küppers, U., Beier, C. (Eds.), Volcanoes of the Azores. Active Volcanoes of the World Springer Verlag, Berlin, pp. 89–100.

Mitchell, N.C., Dade, W.B., Masson, D.G., 2003. Erosion of the submarine flanks of the Canary Islands. J. Geophys. Res. 108 (3–1–3–11).

Mitchell, N.C., Beier, C., Rosin, P.L., Quartau, R., Tempera, F., 2008. Lava penetrating water: submarine lava flows around the coasts of Pico Island, Azores. Geochem. Geophys. Geosyst. 9 (3), Q03024.

Mitchell, N.C., Masselink, G., Huthnance, J.M., Fernández-Salas, L.M., Lobo, F.J., 2012. Depths of modern coastal sand clinoforms. J. Sediment. Res. 82, 469–481.

Montanaro C, Beget J (2011) Volcano collapse along the Aleutian Ridge (western Aleutian Arc). 734 Nat Haz Earth Sys Sci 11:715–730.

Morgan, J., Morgan, W., & Price, E. (1995). Hotspot melting generates both hotspot volcanism and a hotspot swell. Journal of Geophysical Research (Solid Earth), 100(B5), 8045–8062.

Norcross, Z.M., Fletcher, C.H., Merrifield, M., 2002. Annual and interannual changes on a reef-fringed pocket beach: Kailua Bay, Hawaii. Mar. Geol. 190 (3), 553–580.

Oehler JF, Lénat JF, Labazuy P (2008). Growth and collapse of the Reunion Island volcanoes. Bull Volcanol 70:717–742.

Ogston, A.S., Storlazzi, C.D., Field, M.E. and Presto, M.K. (2004) Sediment resuspension and transport patterns on a fringing reef flat, Molokai, Hawaii. Coral Reefs, 23, 559-569.

Parsons, B., & Sclater, J. (1977). An analysis of the variation of ocean floor bathymetry and heat flow with age. Journal of Geophysical Research (Solid Earth), 82(5), 803–827.

Pepe, F.; Bertotti, G.; Ferranti, L.; Sacchi, M.; Collura, A.M.; Passaro, S.; Sulli, A., 2014. Pattern and rate of post-20 ka vertical tectonic motion around the Capo Vaticano Promontory (W Calabria, Italy) based on offshore geomorphological indicators. Quat. Int., 322, 85–98.

Quartau, R., 2007. The insular shelf of Faial: morphological and sedimentary evolution. Universidade de Aveiro, Unpublished PhD Thesis. 301 pp. http://e-geo.ineti.pt/ edicoes_online/teses/rui_quartau/default.htm.

Quartau, R., Mitchell, N.C., 2013. Comment on "Reconstructing the architectural evolution of volcanic islands from combined K/Ar, morphologic, tectonic, and magnetic data: the Faial Island example (Azores)" by Hildenbrand et al. (2012) [J. Volcanol. Geotherm. Res. 241-242 (2012) 39-48]. J. Volcanol. Geotherm. Res.255, 124–126.

Quartau, R., Trenhaile, A.S., Mitchell, N.C., Tempera, F., 2010. Development of volcanic insular shelves: insights from observations and modelling of Faial Island in the Azores Archipelago. Mar. Geol. 275, 66–83.

Quartau, R., Tempera, F., Mitchell, N.C., Pinheiro, L.M., Duarte, H., Brito, P.O., Bates, R., Monteiro, J.H., 2012. Morphology of the Faial Island shelf (Azores): the interplay between volcanic, erosional, depositional, tectonic and mass-wasting processes. Geochem. Geophys. Geosyst. 13, Q04012. http://dx.doi.org/10.1029/ 2011GC003987.

Quartau, R., Hipolito, A., Romagnoli, C., Casalbore, D., Madeira, J., Tempera, F., Roque, C., Chiocci, F.L., 2014. The morphology of insular shelves as a key for understanding the geological evolution
230

of volcanic islands: insights from Terceira Island (Azores). Geochem. Geophys. Geosyst. 15, 1801–1826.

Quartau, R., Hipólito, A., Mitchell, N.C., Gaspar, J.R., Brandão, F., 2015a. "Construction and destruction of a volcanic island developed inside an oceanic rift: Graciosa Island, Terceira Rift, Azores" by Sibrant et al. (2014) and proposal of a new model for Graciosa geological evolution[J. Volcanol. Geotherm. Res. 284 (2014) 32-45]. J. Volcanol. Geotherm. Res. 303, 146-156.

Quartau, R., Madeira, J., Mitchell, N.C., Tempera, F., Silva, P.F., Brandão, F., 2015b. The insular shelves of the Faial-Pico Ridge: a morphological record of its geologic evolution (Azores archipelago). Geochem. Geophys. Geosyst.16, 1401–1420.

Quartau, R., Madeira, J., Mitchell, N.C., Tempera, F., Silva, P.F., Brandão, F., 2016. Reply to comment by Marques et al. on "The insular shelves of the Faial–Pico Ridge (Azores archipelago): a morphological record of its evolution". Geochem. Geo-phys. Geosyst.17, 633–641.

Quartau, R., Trenhaile, A., Ramalho, R.S., Mitchell, N.C., 2018b. The role of subsidence in shelf widening around ocean island volcanoes: Insights from observed morphology and modeling. Earth and Planetary Science Letters. https://doi.org/10.1016/j.epsl.2018.07.007.

Ramalho, R.S., 2011. Building the Cape Verde Islands, 1st ed. Springer, Berlin. https://doi.org/10.1007/978-3-642-19103-9. (207 pp.).

Ramalho, R.S., Helffrich, G., Schmidt, D.N., Vance, D., 2010a. Tracers of uplift and subsidence in the Cape Verde Archipelago. J. Geol. Soc. Lond. 167 (3), 519–538. https://doi.org/10.1144/0016-76492009-056.

Ramalho, R.S., Helffrich, G., Cosca, M., Vance, D., Hoffmann, D., Schmidt, D.N., 2010b. Episodic swell growth inferred from variable uplift of the Cape Verde hotspot islands. Nat. Geosci. 3 (11), 774–777. https://doi.org/10.1038/ngeo982.

Ramalho, R.S., Helffrich, G., Cosca, M., Vance, D., Hoffmann, D., Schmidt, D.N., 2010c. Vertical movements of ocean island volcanoes: insights from a stationary plate environment. Mar. Geol. 275, 84–95. https://doi.org/10.1016/j.margeo.2010.04.009.

Ramalho, R.S., Quartau, R., Trenhaile, A.S., Mitchell, N.C., Woodroffe, C.D., Ávila, S.P., 2013. Coastal evolution on volcanic oceanic islands: a complex interplay between volcanism, erosion, sedimentation, sea-level change and biogenic production. Earth Sci. Rev. 127, 140–170.

Ramalho, R.S., Heiffrich, G., Madeira, J., Cosca, M., Thomas, C., Quartau, R., Hipolito, A., Rovere, A., Hearthy, P.J., Avila, S.P., 2017. Emergence and evolution of Santa Maria Island (Azores) – the

conundrum of uplifted islands revisited. Geol. Soc. Am. Bull. 129 (3–4), 372–390. http://dx.doi.org/10.1130/B31538.1.

Raymo ME, Hearty P, Conto RD, O'Leary M, Dowsett HJ, Robinson MM. 2009. PLIOMAX: Pliocene maximum sea level project. *PAGES News* 17(2).

Rees, B., Detrick, R., & Coakley, B. (1993). Seismic stratigraphy of the Hawaiian flexural moat. Bulletin of the Geological Society of America, 105(2), 189–205.

Rohling, E.J., Foster, G.L., Grant, K.L., Marino, G., Roberts, A.P., Tamisiea, M.E., Williams, F., 2014. Sea-level and deep-sea-temperature variability over the past 5.3 milion years. Nature 508: 477-482.

Romagnoli, C. 1990. Caratterizzazione morfostrutturale e vulcanologica sottomarina delle isole Eolie (Tirreno meridionale): ipotesi di stadi evolutivi dei complessi. Unpublished PhD thesis, University of Bologna, Italy.

Romagnoli, C. 2004. Terrazzi deposizionali sommersi nell'isola di Linosa (Canale di Sicilia). Memorie descrittive della Carta Geologica d'Italia, 2004. 58, pp. 133-140.

Romagnoli, C., 2013. Characteristics and morphological evolution of the Aeolian volcanoes from the study of submarine portions. In: Lucchi, F., Peccerillo, A., Keller, J., Tranne, C.A., Rossi, P.L. (Eds.), The Aeolian Islands Volcanoes. Geological Society, London, Memoirs 37. pp. 13–26.

Romagnoli C, Casalbore D, Chiocci FL, Bosman A (2009a). Offshore evidence of large-scale lateral collapses on the eastern flank of Stromboli, Italy, due to structurally controlled, bilateral flank instability. Mar Geol 262:1–13.

Romagnoli C, Kokelaar P, Casalbore D, Chiocci FL (2009b). Lateral collapses and active sedimentary processes on the northwestern flank of Stromboli volcano, Italy. Mar Geol 265:101–119.

Romagnoli, C., Casalbore, D. & Chiocci, F. L. 2012. La Fossa Caldera breaching and submarine erosion (Vulcano island, Italy). Marine Geology, 303–306, 87–98, doi: 10.1016/j.margeo.2012.02.004.

Romagnoli, C., Casalbore, D., Bortoluzzi, G., Bosman, A., Chiocci, F.L., D'Oriano, F., Gamberi, F., Ligi, M., Marani, M., 2013a. Bathy-morphological setting of the Aeolian islands. In: Lucchi, F., Peccerillo, A., Keller, J., Tranne, C.A., Rossi, P.L. (Eds.), The Aeolian Islands Volcanoes. Geological Society, London, Memoirs 37. pp. 27–36.

Romagnoli, C., Casalbore, D., Bosman, A., Braga, R.&Chiocci, F. L. 2013b. Submarine structure of Vulcano volcano (Aeolian Islands) revealed by high-resolution bathymetry and seismo-acoustic data. Marine Geology, 338, 30–45.

Romagnoli, C.; Jakobsson, S.P. Post-eruptive morphological evolution of island volcanoes: Surtsey as a modern case study. Geomorphology 2015, 250, 384–396.

Romine, B.M., Fletcher, C.H., 2013. A summary of historical shoreline changes on beaches of Kauai, Oahu, and Maui, Hawaii. J. Coast. Res. 29 (3), 605–614.

Rovere A, Antonioli F, Bianchi CN (2015) Fixed biological indicators. In: Shennan I, Long AJ, Horton BP (eds) Handbook of sealevel research. Wiley Online Library, pp 268–280 Rubin, K.H., Fletcher, C.H., Sherman, C., 2000. Fossiliferous Lana'i deposits formed by multiple events rather than a single giant tsunami. Nature 408 (6813), 675–681.

Rovere A, Stocchi P, Vacchi M, (2016). Eustatic and Relative Sea-Level Changes. Curr. Clim. Change. Rep. DOI 10.1007/s40641-016-0045-7.

Rusu, L., Guedes Soares, C., 2012. Wave energy assessments in the Azores islands. Renew. Energy 45, 183–196.

Saint-Ange, F., Savoye, B., Michon, L., Bachelery, P., Deplus, C., De Voogd, B., Dyment, J., Le Drezen, E., Voisset,M., Le Friant, A., et al., 2011.Avolcaniclasticdeep-sea fanoff LaRéunion Island (Indian Ocean): gradualism versus catastrophism. Geology 39 (3), 271–274.

Schmidt, R., & Schmincke, H.-U. (2000). Seamounts and island building. In H. Sigurdsson, B. Houghton, S. McNutt, H. Rymer, & J. Stix (Eds.), Encyclopedia of volcanoes (pp. 383–402). USA: Academic Press.

Schmincke, H.-U. (2004). Volcanism (1st ed.). Berlin: Springer Verlag.

Schmincke, H.-U.,Weaver, P., Firth, J., Baraza, J., Bristow, J., Brunner, C., Carey, S., Coakley, B., Fuller, M., Funck, T., et al., 1995. Background, objectives, and principal results of drilling the clastic apron of Gran Canaria (VICAP). Proceedings of the Ocean Drilling Program, Initial Reports. College Station, TX (Ocean Drilling Program), vol. 157, pp. 11–25.

Scott, G., & Rotondo, G. (1983). A model to explain the differences between Pacific plate island-atoll types. Coral Reefs, 1(3), 139–150.

Searle, R., 1980, Tectonic pattern of the Azores spreading centre and triple junction: Earth and Planetary Science Letters, v. 51, no. 2, p. 415–434, doi: 10 .1016 /0012 -821X (80)90221 -6.

Serpelloni, E., Anzidei, M., Baldi, P., Casula, G., Galvani, A., 2005. Crustal velocityand strain-rate fields in Italy and surrounding regions: new results from theanalysis of permanent and non permanent GPS networks. Geophys. J. Int. 161,861–880.

Sisavath, E., Babonneau, N., Saint-Ange, F., Bachèlery, P., Jorry, S.J., Deplus, C., De Voogd, B., Savoye, B., 2011. Morphology and sedimentary architecture of a modern volcaniclastic turbidite system: the Cilaos fan, offshore La Réunion Island. Mar. Geol. 288 (1), 1–17.

Sleep, N. (1990). Hotspots and mantle plumes: Some phenomenology. Journal of Geophysical Research (Solid Earth), 95(B5), 6715–6736.

Southard, J.B., Stanley, D.J., 1976. Shelf-break processes and sedimentation. In: Stanley, D.J., Swift, D.J.P. (Eds.), Marine Sediment Transport and Environmental Management. John Wiley and Sons, New York, pp. 351–377.

Stein, C., & Stein, S. (1992). A model for the global variation in oceanic depth and heat flow with lithospheric age. Nature,359(6391), 123–129.

Törnqvist TE, Wallace DJ, Storms JEA, Wallinga J, Van Dam RL, Blaauw M, Derksen MS, Klerks CJW, Meijneken C, Snijders EMA. Mississippi Delta subsidence primarily caused by compaction of Holocene strata. Nat Geosci. 2008;1:173–6.

Trenhaile, A.S., 1987. The Geomorphology of Rock Coasts.Clarendon Press, Oxford, UK Oxford.

Trenhaile, A.S., 1989. Sea level oscillations and the development of rock coasts. Elsevier Oceanogr. Ser. 49, 271–295.

Trenhaile, A.S., 2000. Modeling the development of wave-cut shore platforms. Mar. Geol. 166 (1), 163–178.

Trenhaile, A.S., 2001. Modelling the Quaternary evolution of shore platforms and erosional continental shelves. Earth Surf. Process. Landf. 26 (10), 1103–1128.

Trenhaile, A.S., 2011. Cliffs and rock coasts. In: Wolanski, E., McLusky, D. (Eds.), Treatise on Estuarine and Coastal Science, vol. 3. Academic Press, Waltham, pp. 171–191.

Trenhaile, A.S., 2014. Modelling the effect of Pliocene–Quaternary changes in sea level on stable and tectonically active land masses. Earth Surf. Process. Landf. 39, 1221–1235. https://doi.org/10.1002/esp.3574.

Trenhaile, A.S., 2015. Coastal notches: their morphology, formation, and function. Earth Sci. Rev. 150, 285–304. https://doi.org/10.1016/j.earscirev.2015.08.003.
234

Tsutsui, B., Campbell, J.F. and Coulbourn, W.T. (1987) Storm-generated, episodic sediment movements off Kahe Point, Oahu, Hawaii. Mar. Geol., 76, 281–299.

Vacchi M, Rovere A, Zouros N, Desruelles S, Caron V, Firpo M. Spatial distribution of sea-level markers on Lesvos Island (NE Aegean Sea): evidence of differential relative sea-level changes and the neotectonic implications. Geomorphology. 2012;159-160:50–62.

Ventura, G. Kinematics of the Aeolian volcanism (Southern Tyrrhenian Sea) from geophysical and geological data. In The Aeolian Islands Volcanoes; Geological Society of London: London, UK, 2013; pp. 3–11.

Walcott, R. (1970). Flexure of the lithosphere at Hawaii. Tectonophysics,9(5), 435–446.

Watts, A., & Ten Brink, U. (1989). Crustal structure, flexure, and subsidence history of the Hawaiian Islands. Journal of Geophysical Research (Solid Earth), 94(B8), 10473–10500.

Zazo, C., Goy, J.L., Hillaire-Marcel, C., Gillot, P.Y., Soler, V., González, J.Á., Ghaleb, B., 2002. Raised marine sequences of Lanzarote and Fuerteventura revisited - a reappraisal of relative sea-level changes and vertical movements in the eastern Canary Islands during the Quaternary. Quat. Sci. Rev. 21 (18–19), 2019–2046. https://doi.org/10.1016/S0277-3791(02)00009-4.

ACKNOWLEDGEMENTS